Schweizerische Eidgenossenschaft
Confédération suisse
Confederazione Svizzera
Confederaziun svizra

Eidgenössisches Departement für Umwelt, Verkehr, Energie und Kommunikation UVEK
Département fédéral de l'environnement, des transports, de l'énergie et de la communication DETEC
Dipartimento federale dell'ambiente, dei trasporti, dell'energia e delle comunicazioni DATEC

Bundesamt für Strassen
Office fédéral des routes
Ufficio federale delle Strade

Design aids for the planning of TBM drives in squeezing ground

Entscheidungsgrundlagen und Hilfsmittel für die Planung von TBM-Vortrieben in druckhaftem Gebirge

Critères de décision et outils pour la planification de l'avancement au tunnelier dans des conditions de roches poussantes

ETH Zürich, Institut für Geotechnik, Professur für Untertagebau
Dr. Marco Ramoni
Prof. Dr. Georgios Anagnostou

Forschungsauftrag FGU 2007/005 auf Antrag der Fachgruppe Untertagebau (FGU)

Juli 2011 **1341**

Schweizerische Eidgenossenschaft
Confédération suisse
Confederazione Svizzera
Confederaziun svizra

Eidgenössisches Departement für Umwelt, Verkehr, Energie und Kommunikation UVEK
Département fédéral de l'environnement, des transports, de l'énergie et de la communication DETEC
Dipartimento federale dell'ambiente, dei trasporti, dell'energia e delle comunicazioni DATEC

Bundesamt für Strassen
Office fédéral des routes
Ufficio federale delle Strade

Design aids for the planning of TBM drives in squeezing ground

Entscheidungsgrundlagen und Hilfsmittel für die Planung von TBM-Vortrieben in druckhaftem Gebirge

Critères de décision et outils pour la planification de l'avancement au tunnelier dans des conditions de roches poussantes

ETH Zürich, Institut für Geotechnik, Professur für Untertagebau
Dr. Marco Ramoni
Prof. Dr. Georgios Anagnostou

Forschungsauftrag FGU 2007/005 auf Antrag der Fachgruppe Untertagebau (FGU)

Juli 2011 **1341**

Impressum

Forschungsstelle und Projektteam

Projektleitung
Prof. Dr. Georgios Anagnostou

Mitglieder
Dr. Marco Ramoni
Nikolaos Lavdas

Begleitkommission

Präsident
Felix Amberg

Mitglieder
François Bertholet
Martin Bosshard
Thomas Edelmann
Christian Gametter

Antragsteller

Fachgruppe Untertagebau (FGU)

Bezugsquelle

Das Dokument kann kostenlos von http://partnershop.vss.ch heruntergeladen werden.

Bevorzugte Zitierweise

Ramoni, M., Anagnostou, G., 2011. Design aids for the planning of TBM drives in squeezing ground. Research project FGU 2007/005 of the Swiss Federal Roads Office (FEDRO), Report 1341, Swiss Association of Road and Transportation Experts (VSS) Zurich.

Table of contents

Summary

Squeezing ground represents a challenging operating environment as it may slow down or obstruct TBM operation. Due to the geometrical constraints of the equipment, relatively small convergences of 10–20 cm may lead to considerable difficulties in the machine area (sticking of the cutter head, jamming of the shield) or in the back-up area (e.g., jamming of the back-up equipment, inadmissible convergences of the bored profile, damage to the tunnel support). Depending on the number and the length of the critical stretches, squeezing conditions may even call into question the financial viability or even the technical feasibility of a TBM drive.

Based upon case histories reported in the literature, Section 2 sets out firstly to give an overview of the specific problems of TBM tunnelling under squeezing conditions. The factors governing TBM performance are then analysed by means of a structured examination of the multiple interfaces and interactions between the ground, the tunnelling equipment (TBM and back-up) and the support. Furthermore, starting from the basic interactions, Section 2 provides a critical review of the technical options already existing or proposed for coping with squeezing ground in mechanized tunnelling.

Section 3 analyzes basic aspects of the interaction between the shield and the ground or tunnel support by means of computational results. From tunnelling practice, it is well-known that squeezing is a time-dependent process, which may take place over a period of days, weeks or months. Therefore, the risk of shield jamming depends essentially on the rapidness of ground deformation. For given geotechnical conditions and TBM characteristics, the load exerted by the ground upon the shield during continuous excavation depends on the gross TBM advance rate. During a break in operations, the ground pressure increases with time, thereby necessitating a higher thrust force in order to overcome shield skin friction and to restart the TBM. The investigations of Section 3 place emphasis on the effect of the gross advance rate and the effect of ground permeability on shield loading during regular TBM operation (the boring process including short standstills) and during a long standstill.

Section 4 discusses two application examples showing at the same time different methodical approaches applied assessing a TBM drive in squeezing ground. The first case history – the Uluabat Tunnel (Turkey) – mainly concerns the investigation of possible design measures aimed at reducing the risk of shield jamming. The second case history – the Faido Section of the Gotthard Base Tunnel (Switzerland) – deals with different types of tunnel support installed behind a gripper TBM.

Section 5 advances a number of theory-based decision aids, which will support rapid, initial assessments to be made of thrust force requirements. Based on numerical results, dimensionless design nomograms have been worked out that cover the relevant range of material constants, in situ stress and TBM characteristics. The nomograms make it possible to assess the feasibility of a TBM drive in a given geotechnical situation and to evaluate potential design measures or operational measures such as reductions in shield length, the installation of a higher thrust force, increases in the overcut or the lubrication of the shield surface, thus making a valuable contribution to the decision-making process. Furthermore, Section 5 includes a large amount of TBM technical data that is helpful in assessing the technical feasibility of such measures.

Finally, Section 6 addresses the key question of the ground pressure acting upon a segmental lining installed behind a single shielded TBM. Starting with a structured discussion of the influencing factors and their interactions, Section 6 investigates how the type, location and thickness of the backfilling play an important role with respect to the loading of a segmental lining. Furthermore, it advances a number of theory-based decision aids which cover the relevant range of ground parameters, initial stress, segmental lining and backfilling characteristics, thus supporting rapid initial assessments of the ground pressure acting upon a segmental lining and making a valuable contribution to the decision-making process.

Zusammenfassung

Druckhaftes Gebirge stellt für TBM eine anspruchsvolle Einsatzbedingung dar. Dadurch kann ein TBM-Vortrieb verlangsamt oder sogar blockiert werden. Aufgrund der geometrischen Randbedingungen der Vortriebseinrichtung können bereits relativ kleine Konvergenzen – in der Grossenordnung von 10–20 cm – zu erheblichen Schwierigkeiten für die TBM (Blockieren des Bohrkopfes, Verklemmen des Schildes) oder im rückwärtigen Bereich (Verklemmen des Nachläufers, Unterprofil, Beschädigung des Ausbaus) führen. Je nach Anzahl und Länge der kritischen Abschnitte können druckhafte Bedingungen die Wirtschaftlichkeit oder die technische Machbarkeit eines TBM-Vortriebs in Frage stellen.

Basierend auf Fallbeispielen aus der Literatur gibt das zweite Kapitel des vorliegenden Berichts zuerst einen Überblick über die spezifischen Probleme des Tunnelbaus mit TBM in druckhaftem Gebirge. Nachfolgend werden die Faktoren, welche die Bruttovortriebsleistung massgebend beeinflussen anhand einer strukturierten Untersuchung der vielfältigen Schnittstellen und Wechselwirkungen zwischen Gebirge, Vortriebseinrichtung (TBM und Nachläufer) und Ausbau analysiert. Darüber hinaus beschafft Kapitel 2 einen kritischen Überblick über die technischen Optionen, die für das Überwinden von druckhaften Verhältnissen mit einer TBM gängig sind oder vorgeschlagen wurden.

Das dritte Kapitel analysiert grundlegende Aspekte der Interaktion zwischen Gebirge und Schild sowie Gebirge und Ausbau mit Hilfe von Ergebnissen aus numerischen Untersuchungen. Von den praktischen Erfahrungen ist allgemein bekannt, dass druckhaftes Gebirge sich zeitabhängig verhält und somit die Konvergenzen über Tage, Wochen oder Monate kontinuierlich zunehmen können. Demzufolge hängt das Risiko eines Verklemmens des Schildes von der Schnelligkeit der Gebirgsverformungen ab. Für gegebene geotechnische Bedingungen und TBM-Eigenschaften hängt der Gebirgsdruck auf dem Schild einer regelmässig fortschreitender TBM von deren Bruttovortriebsleistung ab. Während eines Unterbruches des TBM-Betriebs steigt der Gebirgsdruck mit zunehmender Stillstandlänge. Gleichzeitig nimmt auch die für das Wiederaufnehmen des Vortriebs erforderliche Vorschubkraft zu, da eine höhere Reibung zwischen Gebirge und Schild zu überwinden ist. Kapitel 3 untersucht den Einfluss der Bruttovortriebsleistung und der Durchlässigkeit des Gebirges auf die Schildbelastung während regulärem TBM-Betrieb (Bohrprozess und kurze Stillstände) und langen Stillständen.

In viertem Kapitel werden zwei Anwendungsbeispiele und die dabei für die Beurteilung dieser TBM-Vortriebe in druckhaftem Gebirge verwendeten Vorgehensweisen vorgestellt. Das erste Fallbeispiel – der Uluabat Stollen (Türkei) – betrifft hauptsächlich die Untersuchung möglicher TBM-technologischer Massnahmen für die Reduktion des Risikos eines Verklemmens des Schildes. Das zweite Fallbeispiel – das Los Faido des Gotthard Basistunnels (Schweiz) – befasst sich mit verschiedenen Ausbautypen, die bei einem Gripper-TBM-Vortrieb verwendet werden können.

Das fünfte Kapitel enthält Hilfsmittel für die Entscheidungsfindung, welche die Berechnung der erforderlichen Vorschubkraft erlauben. Basierend auf numerischen Ergebnissen sind dimensionslose Nomogramme erarbeitet worden, welche die für die praktische Anwendung relevante Bandbreite der Materialparameter, des primären Spannungszustandes und der TBM-Eigenschaften abdecken. Die Nomogramme erlauben die Einschätzung der Machbarkeit eines TBM-Vortriebs in einer gegebenen geotechnischen Situation sowie die Beurteilung verschiedener technischer oder baubetrieblicher Massnahmen wie zum Beispiel eine Reduktion der Schildlänge, die Installation einer höheren Vorschubkraft, eine Vergrösserung des Überschnittes oder die Schmierung des Schildmantels. Kapitel 5 enthält auch eine Zusammenstellung technischer Daten von TBM, die bei der Beurteilung der Machbarkeit technischer Massnahmen hilfreich sein kann.

Das sechste Kapitel zeigt, dass Art, Ort und Dicke der Hinterfüllung eine wichtige Rolle in Bezug auf die Belastung eines Tübbingausbaus spielen. Kapitel 6 stellt auch Hilfsmittel für die Abschätzung des Gebirgsdrucks dar, der auf einen Tübbingausbau wirkt. Die erarbeiteten Nomogramme decken die für die praktische Anwendung relevante Bandbreite der Modellparameter: Materialkonstanten, primärer Spannungszustand, TBM-Charakteristiken sowie Eigenschaften der Tübbinge und der Hinterfüllung.

Résumé

L'excavation au tunnelier en conditions de roches poussantes est à l'heure actuelle toujours un défi de taille de par le risque élevé de diminution de la vitesse d'avancement ou de blocage du TBM. Même pour des convergences relativement faibles (10–20 cm), les contraintes géométriques imposées par l'équipement d'excavation peuvent conduire à des problèmes dans la zone du tunnelier (blocage de la tête de coupe ou du bouclier) ou dans celle du train suiveur (blocage du train suiveur, convergences inadmissibles, endommagement de soutènement du tunnel). Selon le nombre et la longueur des sections critiques où des conditions de roches poussantes sont attendues, la faisabilité économique ou technique d'une excavation au tunnelier peut être remise en question.

Le deuxième chapitre, basé sur une étude de cas issus de la littérature, donne tout d'abord un aperçu des problèmes spécifiques liés à l'excavation de tunnels au tunnelier dans des conditions de roches poussantes. Les facteurs influençant la performance du tunnelier sont ensuite analysés au moyen d'une investigation structurée des interfaces multiples et des interactions entre rocher, équipement (tunnelier et train suiveur) et soutènement. A la fin du chapitre est présentée une vue d'ensemble critique des moyens techniques existants ou en cours de développement qui permettent de diminuer les problèmes liés à une excavation mécanisée en milieu poussant.

Le troisième chapitre analyse les aspects fondamentaux de l'interaction entre bouclier, rocher et soutènement d'un tunnel par le biais de résultats obtenus par simulation numérique. L'expérience pratique montre que la convergence du profil d'un ouvrage excavé dans des roches poussantes peut se dérouler sur une période allant de quelques jours à plusieurs mois. Le risque de blocage du bouclier est donc fortement dépendant de la rapidité de déformation du massif rocheux. De la même manière, dans des conditions géotechniques connues et pour des caractéristiques du tunnelier données, la pression exercée par la roche sur le bouclier lors d'un avancement régulier dépend de la vitesse d'avancement brut. En cas d'arrêt de l'excavation, la pression de la roche augmente au cours du temps, induisant une augmentation de la poussée nécessaire à surmonter le frottement rocher-bouclier lors du redémarrage de la machine. Ce chapitre examine l'influence de deux paramètres – le taux d'avancement brut et la perméabilité de la roche – sur la pression exercée sur le bouclier dans une situation d'avancement régulier (excavation avec arrêts de courte durée) et en cas d'arrêt prolongé.

Le quatrième chapitre présente deux cas qui font l'objet d'une étude de faisabilité technique d'une excavation au tunnelier. Le premier cas – le tunnel d'Uluabat (Turquie) – est focalisé sur l'étude de mesures technologiques visant à diminuer le risque de blocage. Le deuxième cas – le lot Faido du tunnel de base du Gothard (Suisse) – traite différents types de soutènements qui peuvent être installés derrière un tunnelier avec grippeurs.

Le cinquième chapitre introduit des outils d'aide à la décision qui permettent d'estimer la force nécessaire à l'avancement de la machine. Sur la base de résultats numériques, des nomogrammes ont été élaborés en considérant l'entier de l'éventail des valeurs de constantes mécaniques du rocher, de contraintes in situ et de caractéristiques géométriques du tunnelier qui peuvent se présenter en pratique. Ces nomogrammes permettent d'évaluer la faisabilité de l'avancement pour une situation géotechnique donnée, ainsi que d'étudier d'influence des mesures techniques telles que la réduction de la longueur du bouclier, l'application d'une poussée d'excavation plus importante, l'augmentation de la surcoupe ou encore la lubrification de la surface de bouclier. Ce chapitre contient aussi un résumé des données techniques de tunneliers utile dans l'évaluation de la faisabilité de telles mesures.

Enfin, le sixième chapitre montre que le type, la location et l'épaisseur du remblaiement jouent un rôle important en ce qui concerne la pression de la roche exercée sur un anneau du voussoir. Des nomogrammes pour la détermination de cette pression sont proposés. Ces outils considèrent l'entier de la gamme des facteurs tels que les constantes mécaniques du rocher, l'état de contrainte initial ainsi que les caractéristiques du tunnelier, du voussoir et du remblaiement qui peuvent se présenter en pratique.

1 Introduction

In recent years, the need for new infrastructure to handle the intercity transportation of people and goods has steadily increased. The construction of such facilities often requires the excavation of long, deep tunnels such as the two base tunnels of the Alptransit Project in Switzerland (Kovári, 1995), the Brenner Base Tunnel between Austria and Italy (Bergmeister, 2007), the Lyon – Turin Tunnel between France and Italy (Nasri and Fauvel, 2005) or the Gibraltar Strait Tunnel between Spain and Morocco (Pliego, 2005). In many cases the cost of such projects can be reduced to a justifiable level only by utilizing TBMs, because they allow significant savings in construction time and costs (Gerstner and Vigl, 1996).

Due to alignment constraints and the uncertainties of geological exploration (which may be large, particularly for long, deep tunnels), it is not always possible to find a route that will avoid the problem of excavating in difficult geological zones with a sufficient degree of certainty (Robbins, 1992). The extent and frequency of the difficulties encountered can be decisive in terms of economical viability or even in terms of the technical feasibility of a TBM drive. This is particularly true where special measures are needed in order to accelerate the TBM drive or to free the TBM in case of jamming. In some cases of very great potential damage, a single event can cast the entire project into doubt. Minor setbacks may also become relevant if occurring frequently. The length and the number of critical stretches are very important in this respect. Short tunnel stretches with unfavourable but well-known geological conditions are not particularly risky for the economic success of a TBM drive (Kovári, 1986a), provided that adequate countermeasures are planned in advance.

TBM performance can be affected by geological conditions in a great variety of ways (Barla and Pelizza, 2000). In hard rock, for example, boreability problems may occur such as a low penetration rate or excessive wear of the cutting tools, necessitating frequent cutter changes and other maintenance work. Mixed face or blocky rock conditions may cause steering difficulties or severe vibration of the cutter head, leading to considerable wear or even damage. Major water inflows may reduce the efficiency of the mucking system or affect the installation of segmental linings.

Another group of difficulties is associated with a low strength or high deformability of the ground and these fall, in a wider sense, under the heading of "stability and deformation problems". A low strength ground, such as highly fractured or weathered rock, may lead to cave-ins ahead of the tunnel face or to blockage of the cutter head. In open-type TBMs difficulties with the support installation or the gripper positioning may also occur in the case of unstable excavation walls. It is particularly challenging to cross fault zones with soil-like material under high water pressures (Anagnostou and Kovári, 2005). When such a zone is suddenly encountered, water and loose material flows into the opening. Both the timely identification and the treatment of such zones may decrease the degree of TBM utilization considerably. On the other hand, when tunnelling through zones consisting of low stiffness ground, large long-term convergences of the opening may develop, destroying the tunnel support and, in extreme cases, completely closing the tunnel cross-section. Such, so-called "squeezing conditions" occur mostly in weak rocks (such as phyllites, schists, serpentinites and claystones) often in combination with a great depth of cover and a high pore pressure (Kovári, 1998; Vogelhuber et al., 2004).

Squeezing ground conditions may slow down or obstruct TBM operation (ITA, 2003) and sometimes even call into question the feasibility of a TBM drive. In fact, as described later in Section 2, there have occasionally been some very negative experiences (including complete loss of the TBM) in the past and this has often lead to TBM drives in squeezing ground being classified as generally too risky and therefore not feasible. However, between the borderline cases of a heavily squeezing ground and a non-problematic competent rock, a wide range of conditions exist which neither exclude a priori mechanized tunnelling nor allow it without careful consideration. These cases call for a well-founded, thorough investigation of the risks, the technical feasibility and the cost of TBM application. So it is not surprising that the question of TBM applicability in squeezing conditions has kept engineers busy for more than 30 years. First remarks can be found already in

Prader (1972), while more detailed conceptual considerations have been provided later by Lombardi (1981) and Robbins (1982). Other related works are, e.g., those of Kovári (1986a, 1986b), Amberg (1992), Gehring (1996), McCusker (1996) and Schubert (2000). As can be seen from recent publications (Downing et al., 2007; John and Schneider, 2007; Herrenknecht, 2010), the topic of the present report (which has five main sections) is particularly relevant today due to the increased economic importance of mechanized tunnelling associated with the demand for long deep tunnels.

Section 2 includes a qualitative discussion of the specific potential hazards as well as the complex interactions between the ground, the tunnelling equipment (TBM and back-up) and the support based upon both tunnelling experience and theoretical considerations. The peculiarities of the different TBM types are thereby highlighted and there is a brief description of the practical experience gained in mechanized tunnelling through squeezing ground. Furthermore, Section 2 deals with possible measures for coping with squeezing ground in TBM tunnelling with respect to TBM technology and tunnel support.

Section 3 investigates basic aspects of the interaction between the shield, the ground and the tunnel support by means of numerical investigations. This section also deals with the time-dependency of squeezing with particular emphasis placed on the risk of shield jamming and on some practical questions concerning mechanized tunnelling through water-bearing squeezing ground: the effects of the gross advance rate on shield loading as well as the increase in ground pressure during TBM standstills.

Section 4 shows different methodical approaches that can be applied in order to assess a TBM drive in squeezing ground by means of two application examples: the Uluabat Tunnel (Turkey) and the Faido Section of the Gotthard Base Tunnel (Switzerland).

Section 5 focuses on the risk of shield jamming and works out design aids that assist decision-making in the planning stage. The results of a comprehensive parametric study based upon numerical investigations and covering the relevant range of material constants, initial stress and TBM characteristics are presented in dimensionless nomograms that allow a quick preliminary assessment to be made of the thrust force required in order to overcome shield skin friction and avoid jamming of the shield. Using the nomograms it is also possible to evaluate the effects of potential design parameters and operational measures rapidly. Furthermore, Section 5 includes a large amount of TBM technical data that is helpful in assessing the technical feasibility of such measures.

Section 6 deals with a specific problem of shielded TBM tunnelling, namely the major hazard scenario of "overstressing of the segmental lining". By means of a structured discussion of the influencing factors and their interactions, Section 6 shows that the type, location and thickness of the backfilling play an important role in this respect. The key question of the ground pressure acting upon a segmental lining installed behind a single shielded TBM is also addressed, including a presentation – in the form of dimensionless design nomograms – of the results of a comprehensive parametric study. The nomograms cover the relevant range of ground parameters and initial stress, as well as different characteristics of the TBM, the segmental lining and the backfilling (type and location), and allow a quick preliminary assessment to be made of the loading of a segmental lining.

At this point, it should also be mentioned that the research findings have been reported on a continuous basis by means of publications in professional journals. The main publications are: Ramoni and Anagnostou (2010a, 2010b, 2011a, 2011b) and Ramoni et al. (2011).

2 Experiences and basic considerations

2.1 Introduction

The present section of the report presents a qualitative discussion of the complex interactions between ground, tunnelling equipment (TBM and back-up) and support based upon both tunnelling experience (Section 2.2) and theoretical considerations. Reference will be made to the peculiarities of the different TBM types and emphasis will be placed on the interfaces between the three essential system components: ground, tunnelling equipment and support (Section 2.3).

Over the last decade, considerable research and development efforts have been made with the goal of widening the range of applicability for TBMs in squeezing ground either by improving established TBM types (i.e., gripper, single or double shielded TBM) or by developing new construction methods involving alternative machine designs or deformable lining systems. Reference to these works will be made in Section 2.4, which – starting from the basic interactions discussed in Section 2.3 – deals with possible measures for coping with large ground deformations or high ground pressures in mechanized tunnelling.

2.2 Practical experience and specific problems

2.2.1 Introduction

According to Appendix I, which provides an overview of a comprehensive literature search on tunnelling experience involving TBMs under squeezing conditions, squeezing behaviour may become problematic at different distances behind the tunnel face. Therefore, the specific potential hazards concern both the machine area (sticking of the cutter head, jamming of the shield) and the back-up area (e.g., jamming of the back-up equipment, inadmissible convergences of the bored profile, damage to the tunnel support).

In addition to the difficulties that are directly caused by squeezing behaviour, adverse events such as clogging of the cutter head, insufficient bracing of the grippers or instabilities of the working face or the tunnel wall may also occur when boring through weak ground. Often it is difficult or even impossible to distinguish the different phenomena from each other. For example, when driving through poor quality ground it may remain uncertain if the ground pressure acting upon the TBM is due to squeezing or ravelling behaviour. Furthermore, in several cases a feedback between the different problems may be observed (Kovári, 1986a).

2.2.2 Magnitude of relevant deformations

Concerning the magnitude of the potentially problematic deformations, a marked difference exists between conventional and mechanized tunnelling. Due to the geometrical constraints imposed by the equipment, even convergences as small as 10–20 cm may lead to difficulties in the machine or in the back-up area of a TBM drive. So, for example, Andraskay (1986) suggests that deformations in the bored profile of up to 10 cm have to be taken into account a priori in the selection of the boring diameter, while Kovári (1986b) and Barla (2004) consider convergences exceeding 5 % or 2–3 % of the tunnel radius, respectively, as problematic. Of course, these figures must be seen as very rough estimates as they do not account for the spatial distribution of the deformation along the tunnel axis and, furthermore, suggest that the absolute magnitude of the "critical" convergence decreases with the tunnel diameter, which is not necessarily true. A convergence of 3–4 % does not present serious problems for a small diameter tunnel as it corresponds to a radial displacement of only a few centimetres. On the other hand, the values mentioned above indicate quite plainly the sensitivity of mechanized tunnelling to squeezing.

It should be noted that relatively moderate deformations of 10–20 cm, which may be problematic for a TBM (but could be easily dealt with by conventional tunnelling), are in no way limited to the typical squeezing formations of weak rocks such as phyllites, schists, serpentinites and claystones. Experience in some stretches of the Gotthard Base Tunnel (Switzerland) has shown that hard but highly fractured rocks may also exhibit relevant deformations and challenge TBM tunnelling, particularly if encountered at great depths.

2.2.3 The "time" factor

The case histories documented in the literature (Appendix I) indicate that interruptions of the TBM drive may be unfavourable in squeezing ground, i.e., that the "time" factor may play an important role. In several cases, the TBM did not become jammed until there was a slowdown or standstill in the TBM drive, which suggests that maintaining a high gross advance rate and reducing standstill times may have a positive effect. The Yacambú – Quibor Tunnel (Venezuela, gripper TBM, D = 4.80 m) may be mentioned as a first example. During the holiday break of Christmas 1979 TBM operation was interrupted in graphitic phyllites encountered at a depth of 350–400 m. Within 30 days the rock mass converged unexpectedly to such an extent that the bored profile was closed and the TBM together with the tunnel support were destroyed over a length of 250 m. During the excavation of the Nuovo Canale Val Viola (Italy, double shielded TBM, D = 3.60 m) the TBM became trapped because of squeezing ground (pelitic and phyllitic rock) during a one-week holiday stop. In this case, it was possible to free the TBM by hand-mining. In the back-up area (over a length of 100 m), longitudinal cracks in the segmental lining were observed. In the Tunnel 38 of the Yindaruqin Irrigation Project (China, double shielded TBM, D = 5.54 m), the TBM was trapped in a clayey sandstone during a maintenance stop.

Standstills are unfavourable also with respect to cutter head operation. Depending on the rheological behaviour of the ground, high ground pressures acting upon the cutter head (Figure 2.1a) or an extremely high extrusion rate of the core (Figure 2.1b) may develop. In this respect, the Gilgel Gibe II Tunnel (Ethiopia, double shielded TBM, D = 6.98 m) may be mentioned. In this project, in one case the core extruded with a rate of 4–6 cm/h and pushed the TBM back more than 60 cm (with a lateral displacement of more than 40 cm). As a consequence, the shield and the segmental lining were damaged. However, if the TBM is boring, the excavation speed is normally high enough to avoid problems (Gehring, 1996; Barla, 2001; Hoek, 2001). The development of the ground pressure upon the cutter head is, as a rule, not fast enough to lead to an immobilization of the TBM. However, this may occur during a standstill (depending on the duration of the standstill and the deformation rate of the ground). During continuous excavation, i.e., when the TBM is boring, other aspects have also to be considered. For example, cutter head operation may be obstructed in blocky or soft rock as a result of damage caused to the cutters by falling blocks, mucking problems or excessive torque demand (Figure 2.1c). The installed thrust force and torque have to be sufficiently high to advance the TBM. In the case of a gripper TBM, the ground plays an additional important role, as it must provide a sufficient reaction force to the grippers. This was a problem, e.g., for all three TBMs in the

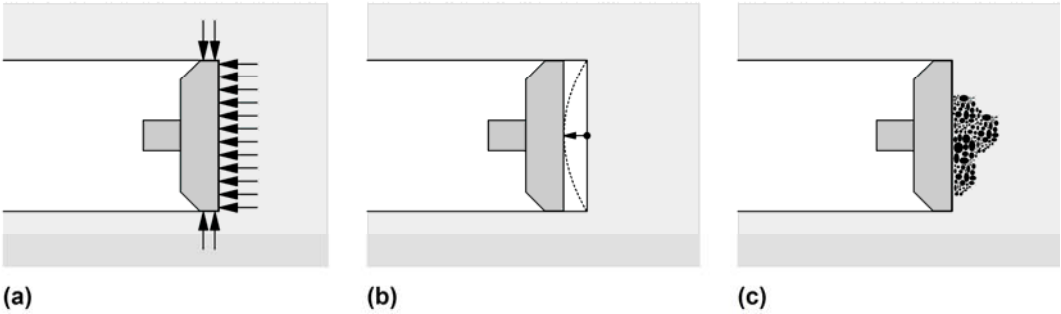

Figure 2.1. Sticking of the cutter head: (a) high ground pressure; (b) extremely high extrusion rate of the core; (c) excessive torque demand in blocky or soft rock.

Yacambú – Quibor Tunnel (the TBMs were also immobilized several times because of insufficient bracing of the grippers in very weak squeezing ground).

Maintaining a high advance rate is of course a major goal for any TBM drive. When tunnelling through squeezing ground it may also help to prevent the machine becoming trapped. Nevertheless, high gross advance rates should not be seen as a panacea for coping with squeezing. First of all, as can be seen from the last column of Appendix I, the ground deformations may develop very rapidly and very close to the working face. In such a situation, the achieved gross advance rate would play a secondary role (the TBM would become jammed even if operated at the highest feasible speed). Furthermore, standstills of TBM operation cannot be completely avoided (Lombardi, 1981; Gehring, 1996). Besides adverse ground conditions, unpredictable stops due to technical problems (e.g., electric power stoppages, mechanical breakdowns of the TBM, problems in the back-up system) have to be considered. For example, during the excavation of the Evinos – Mornos Tunnel (Greece) the cutter head of one of the gripper TBMs (D = 4.20 m) became jammed in highly fractured radiolarites at a depth of 950 m during an excavation standstill which was caused by an interruption of the electric power supply. The need to carry out regular maintenance work is also an important factor. This causes halts in excavation but it is at the same time important for reducing the risk of mechanical breakdown. Finally, it has also to be considered that a certain time is needed for support installation (a practically continuous excavation is possible only with double shielded TBMs advancing in the so-called "gripper mode").

In the case of time-dependent ground behaviour (which is characteristic for squeezing formations), the need for interruptions to allow support installation introduces important feedback effects and conflicting requirements. The maintenance of a sufficiently high gross advance rate is advantageous but difficult to achieve, especially in the case of poor quality ground. For example, if the tunnel is excavated with a gripper TBM, it becomes necessary to install a higher quantity of support and this lengthens standstill times. In extreme cases, the TBM becomes trapped and has to be freed with special measures that mostly require hand-mining. On the other hand, installing a lighter support for the sake of a higher advance rate may lead to inadmissible convergences in the back-up area. These aspects will be discussed in more detail in Section 2.3.2.

2.2.4 Thrusting system

When tunnelling by a single shielded TBM (or a double shielded TBM in the so-called "auxiliary mode"), the tunnel support (lining by precast segments) forms part of the thrusting system. There have been negative experiences in cases where a proper backfilling of the segmental lining was not achieved. The double shielded TBM (D = 2.91 m) that excavated a part of the Stillwater Tunnel (USA) may be mentioned in this context. This TBM was abandoned in September 1979 after becoming jammed in a fault zone consisting of clayey schist at a depth of cover of 650 m. The TBM probably became trapped in squeezing ground because of the impossibility of fully utilising its installed thrust force. Firstly, it was not possible to drive the double shielded TBM in the gripper mode and secondly, the segmental lining was not able to withstand the thrust force generated in the auxiliary mode. Due to blocky, poor ground conditions with frequent instabilities of the tunnel wall and related over-excavation it was not possible to backfill the segmental lining properly with pea gravel, as planned. Complementary injections of cement grout were carried out only after the passage of the back-up trailers. On the one hand, the insufficiently embedded segmental lining was not uniformly loaded from the start and was partially damaged by the ground pressure. On the other hand, attempts to use the full installed thrust force caused additional damage to the segments. In this case, there was a further difficulty in relation to the telescopic part of the shield, which had a smaller diameter than the front and the rear shield, favouring the accumulation of loose material in this area and thus leading to an increase in the friction that had to be overcome when moving the double shield. Similar problems also arose with gripper bracing, the backfilling of the segmental lining and the telescopic part of the shield during the excavation of the Los Rosales Tunnel (Colombia, double shielded TBM, D = 3.54 m).

2.2.5 Back-up area

Possible problems in the back-up area include inadmissible convergences of the bored profile or damage to the tunnel support. Such problems are basically the same as in conventional tunnelling, the main differences being that in conventional tunnelling, (i), there is the option of excavating a considerably larger profile in the critical stretches (in order to accommodate the deformations) and, (ii), there is also more flexibility concerning the location of support installation (stabilization measures can be taken practically wherever and whenever required). In TBM tunnelling, the space available for ground deformations and tunnel support is largely pre-determined by the fixed geometry of the excavated cross-section. The possibility of enlarging the boring diameter locally is very limited (up to 30 cm, if at all possible, cf. Section 2.4.3), while the design of the back-up equipment fixes the locations of the support installation and limits the scope for intervention in the back-up area.

Besides the typical problems mentioned above, jamming of the back-up equipment is an additional hazard scenario to be considered, particularly for gripper TBMs. For example, during the excavation of the Strada Section of the Tavanasa – Ilanz Tunnel (Switzerland, gripper TBM, D = 5.20 m) the convergences that occurred in the machine area were large enough to violate the clearance profile needed for the passage of the back-up trailers. Re-profiling works also became necessary along 20 m of the Northern Section of the Vereina Tunnel (Switzerland). In a heavily fractured zone in crystalline rock at a depth of 1250 m, the gripper TBM (D = 7.64 m) became blocked due to a cave-in above the cutter head. During the standstill, radial deformations of 20 cm developed behind the machine, making the passage of the back-up trailers impossible. Jamming of the back-up equipment has also been observed in the Faido Section of the Gotthard Base Tunnel (Switzerland). During excavation by a gripper TBM (D = 9.43 m) in micaceous gneiss at a depth of 1600 m, significant convergences occurred over a 250 m long stretch. The tunnel support was damaged although it was designed to be deformable and, in some cases, touched the main structure of the back-up equipment and it became necessary to remove or to dislocate part of the equipment in order to keep the back-up trailers moving.

2.3 Ground-equipment-support interactions

2.3.1 Introduction

Identifying the relevant interfaces between the main system components and understanding their interactions is essential to an assessment of the critical situations which might affect the performance or even the feasibility of a TBM drive. The following sections shall discuss the interactions between ground, tunnelling equipment and support, taking into account the peculiarities of existing TBM types with respect to thrusting system, tunnel support, the presence or absence of a shield (gripper TBMs are often also equipped with a canopy or a short cutter head shield with a length of about a half boring diameter) and the achievable gross advance rate, which is an influencing factor as well.

The discussion starts with the case of gripper TBMs (Section 2.3.2) because their greater flexibility concerning tunnel support increases system complexity. The case of single or double shielded TBMs thrusting against a segmental lining will be discussed later in Section 2.3.3.

2.3.2 Gripper TBM

Overview of interactions

The large number of interfaces between ground, tunnelling equipment and support in combination with the possibility of conflicting requirements and feedback effects introduces a high level of complexity, which necessitates an efficient mapping of the system and of its interfaces in order to identify and analyze the relevant interactions. The so-called "N^2 chart" offers the possibility of a systematic approach and a neat analysis. This

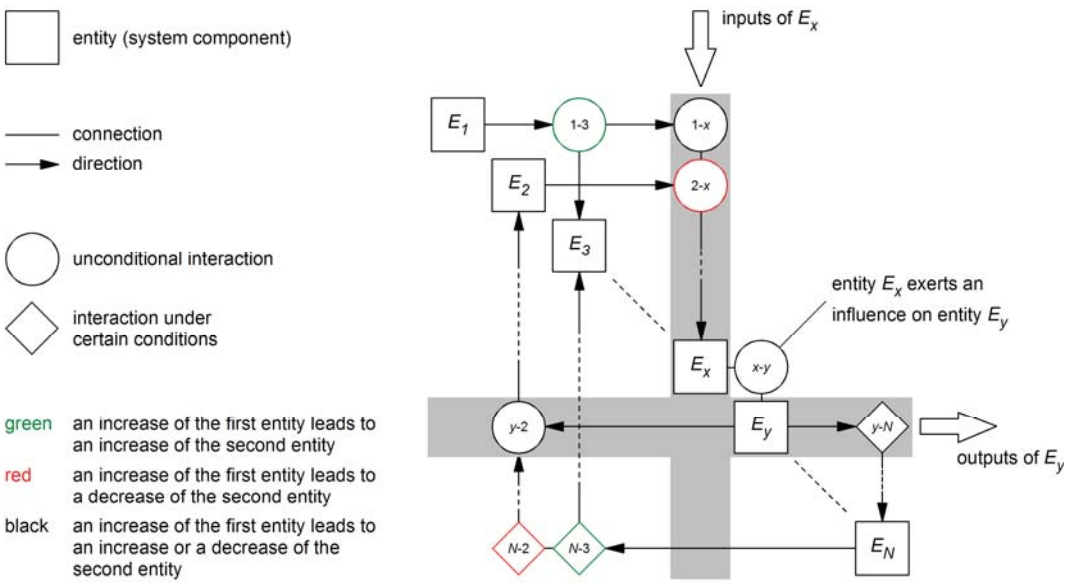

Figure 2.2. Principle and mapping rules of N^2 diagramming technique.

method was introduced by Lano (1990) and is a well-known diagramming technique in system engineering practice.

Following the description given by NASA (2007), an N^2 chart is an *N*-by-*N* square matrix (also-called an "interaction matrix") containing the *N* physical or functional entities of a system (also-called "system elements", "system components" or "functions") on the main diagonal and the interfaces between them in the remaining off-diagonal cells, while a blank off-diagonal cell means that there is no interaction between the respective system elements. As illustrated by the schematic example of Figure 2.2, the interactions have to be read directionally between the elements, i.e., first horizontally in the row and then clockwise in the column. For example, the fact that the cell at the intersection of Row *x* with Column *y* is non-empty indicates that entity E_x has an effect on entity E_y (the numbers *x*-*y* within the cell represent the parameters involved as well as the "direction" of the interaction). The non-empty cells in Row *y* show all of the entities that are influenced by entity E_y (i.e., the "outputs" of E_y), while the non-empty cells in Column *x* show which entities influence entity E_x (i.e., the "inputs" to E_x). The usefulness of this representation technique is illustrated by the interaction loop 2-*x*-*y*-2 which indicates a feedback effect.

In order to condense more information into one N^2 chart, the diagrammatic language has been enhanced adding two mapping rules that exploit the shape and color of the cells: rhombuses (e.g., cell *y*-*N* in Figure 2.2) indicate that an interaction exists only under certain conditions (for example, ground deformations may lead to TBM jamming only if a threshold value is exceeded), while circles (e.g., cell *x*-*y* in Figure 2.2) denote unconditional interactions (for example, standstills always reduce the gross advance rate). As for the colours, green is used for interactions of the type "an increase of E_x leads to an increase of E_y", red for interactions of the type "an increase of E_x leads to a decrease of E_y" and black for interactions where the effect of E_x on E_y may be either positive or negative.

Figure 2.3 shows the N^2 chart elaborated for the subject under investigation. The number of physical and functional entities represents the result of a trade-off, which has had to be made between the desired resolution of the partial processes and the space available on paper. As can be seen in Figure 2.3, the chosen entities include the physical components of the system (such as the ground or the TBM) as well as operational parameters (such as the cutter head rotational speed), the results of the boring process (such as the net advance rate) or events (such as problems in the back-up area or standstills due to TBM jamming). The interactions depicted have been classified as "relevant" based upon practical experience (cf. Section 2.2 and Appendix I) and theoretical factors. In spite of their limitations, the latter are indispensable as there are hardly any systematic field investigations available.

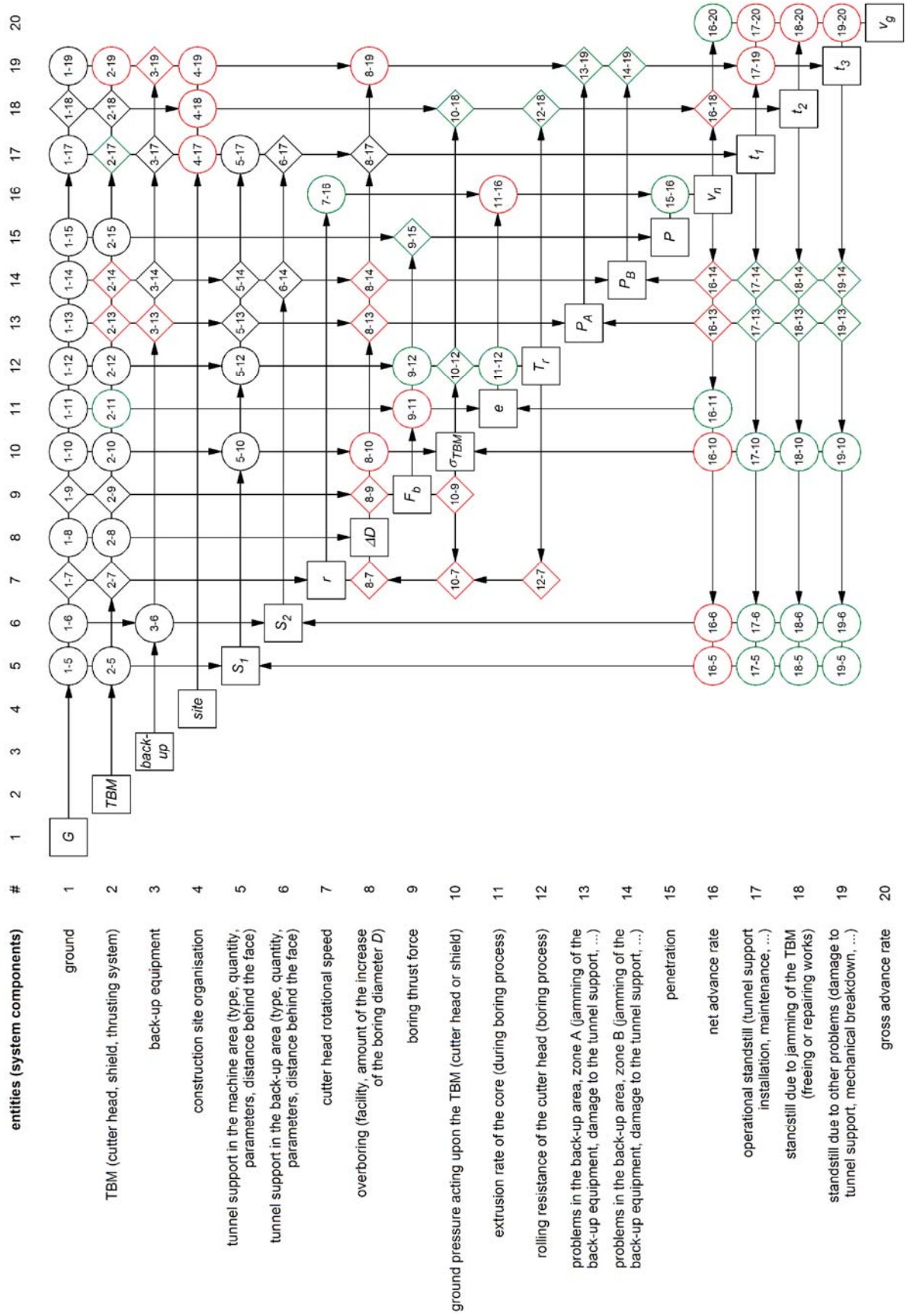

Figure 2.3. N^2 chart for a gripper TBM drive through squeezing ground.

Table 2.1. Comments on the interactions shown in Figure 2.3.

Entities	Remarks
1-5 1-6	The tunnel support to be installed in the machine area {1-5} or in the back-up area {1-6} is chosen on the basis of the ground conditions (although work safety must always be ensured).
2-5	The location of the first tunnel support installation depends on the length of the cutter head and of the shield. Furthermore, the design of the equipment installed on the TBM is relevant with respect to the type of tunnel support that can be installed and to the place available for the installation work.
16-5 17-5 18-5 19-5 16-6 17-6 18-6 19-6	The stiffness and the bearing capacity of the tunnel support may be time-dependent (e.g., shotcrete, grouted bolts). During a standstill, they increase with the elapsed time {17-5, 18-5, 19-5, 17-6, 18-6, 19-6}. During ongoing excavation, the more rapid the TBM advance, the lower will be the stiffness and the bearing capacity of the tunnel support at a given distance from the tunnel face {16-5, 16-6}.
3-6	The location of the second tunnel support installation, the type of tunnel support and the space available for support installation all depend on the design of the back-up equipment.
1-7 2-7 10-7 12-7	See Section 2.3.2 and Equation 2.5.
8-7	During overboring, the cutter head rotational speed may have to be reduced (cf. Section 2.4.3).
1-8	The choice of the overboring facility to be applied and the feasible increase in the boring diameter in particular will depend on the ground conditions (cf. Section 2.4.3).
2-8	Overboring is only possible if this option has been catered for in the design of the cutter head and of the shield (cf. Section 2.4.3).
1-9 2-9 10-9	See Section 2.3.2 and Equation 2.4.
8-9	During overboring, the boring thrust force may have to be reduced (cf. Section 2.4.3).
1-10 1-11	The ground pressure acting upon the TBM {1-10} and the extrusion rate of the core during the boring process {1-11} depend on the strength, stiffness and permeability of the ground as well as on the initial stress and the initial hydraulic head (cf. Section 3.4.3). Depending on the strength and stiffness of the ground, the reaction forces provided by the grippers may be insufficient for pulling back the cutter head during a standstill in order to reduce the ground pressure acting on it axially {1-10}.
2-10	Firstly, the dimensions (diameter, length) of the cutter head and the shield represent a "span" and therefore influence the amount of ground pressure acting upon the TBM. The ground pressure also depends on the stiffness of the different TBM components. The ground pressure acting upon the shield may be reduced, if the shield is shrinkable (cf. Section 2.4.4). Furthermore, the conicity of the cutter head and of the shield as well as the overcut (i.e., the difference between the cutter head diameter and the shield diameter) play an important role as regards steering the TBM and allowing ground deformations without loading the TBM. During a standstill, the ground pressure acting axially upon the cutter head can be reduced, if the TBM design allows it to be pulled back. In order to overcome the friction caused by the ground pressure acting upon the cutter head and the shield, a sufficient pull force must have been installed and the ground must offer sufficient resistance to the grippers.
5-10 5-12	The tunnel support immediately behind the shield facilitates arch action in the longitudinal direction, thus leading to lower loading of the shield {5-10} (cf. Section 2.4.7 and Figure 2.11). During a standstill, the ground pressure acting axially upon the cutter head as well as its rolling resistance when its rotation has to be restarted can be reduced by pulling it back. This presupposes that the tunnel support in the machine area does not impede the movement of the TBM backwards {5-10, 5-12}.
8-10	A larger overboring allows more ground deformation to take place and thus leads to a lower loading of the TBM.
16-10 17-10 18-10 19-10 16-11	In the case of pronounced time-dependent ground behaviour, an increase in the net advance rate leads to a reduction of the ground pressure acting upon the TBM {16-10} and to an increase of the extrusion rate of the core {16-11}. During a standstill, ground pressure increases with time {17-10, 19-10}. If the TBM is already jammed, the ground pressure acting upon it increases further {18-10}. Furthermore, as shown by numerical investigations (cf. Section 3.4.4), the conditions prevailing at the beginning of a standstill depend on the "history" of the TBM advance up to the time of the standstill (i.e., on the achieved gross advance rate).
2-11	The size of the tunnel face (boring diameter) represents a "span" and influences therefore core extrusion.
9-11	During the boring process, the boring thrust force acting upon the face reduces core extrusion.
1-12 2-12 10-12	See Section 2.3.2.
9-12	The rolling force of each cutter increases with increasing normal cutter force (the boring thrust force acting upon a single cutter), because of the deeper cuts and of the higher rolling friction.
11-12	A faster core extrusion leads to a greater depth of cut. This leads to an increase in the rolling force of each cutter and, therefore, in the rolling resistance of the cutter head.
1-13 1-14	The occurrence of problems in the back-up area depends on the ground characteristics.

Table 2.1 (continuation).

Entities	Remarks
2-13 2-14 3-13 3-14 8-13 8-14	Large deformations may impede passage of the back-up equipment. The magnitude of problematic deformations depends on the dimensions of the bored profile (and, therefore, on the cutter head diameter {2-13, 2-14} and on the amount of overboring {8-13, 8-14}) as well as on the design of the back-up equipment (the more compact, the better {3-13, 3-14}). The design of the back-up equipment (more specifically, its sensitivity to ground deformations) may also be decisive for other problems such as damage to pipes or heave of the tracks {3-14}.
5-13 5-14 6-14	Besides stiffness and bearing capacity of the tunnel support, its thickness is also relevant, as it reduces the space available to ground deformations.
16-13 17-13 18-13 19-13 16-14 17-14 18-14 19-14	In the case of a pronounced time-dependent ground behaviour, a reduction in the net advance rate or a standstill will lead to higher ground deformations or higher ground pressures at a given distance behind the tunnel face.
1-15 2-15	The relevant influencing factors are the cutter head design (e.g., its form as well as number, spacing, shape, diameter and wear of the cutters) and the characteristics of the rock mass (intact rock and discontinuities).
9-15	See Section 2.3.2.
7-16 11-16 15-16	See Equation 2.3.
1-17	The ground conditions are relevant with respect to cutter wear (e.g., abrasivity of the rock) and more generally to the required maintenance work (as, e.g., in the case of cutter head clogging). Difficult ground conditions (e.g., major water inflows) may also slow down the installation of the tunnel support.
2-17	The complexity of the TBM influences the frequency and duration of maintenance work.
3-17	See Section 2.4.6.
4-17 4-18 4-19	See Section 2.4.1.
5-17 6-17	The time needed for the installation of the tunnel support depends on the type and on the quantity of support measures to be installed {5-17, 6-17}. In the back-up area it is generally possible to install the tunnel support without slowing down the rate of TBM progress {6-17}.
8-17	Depending on the type of overboring equipment, the commencement of overboring operations may require a standstill (cf. Section 2.4.3).
1-18 2-18 10-18 12-18	See Section 2.3.2 and Equations 2.1 and 2.2.
16-18	If during ongoing excavation the net advance rate becomes equal to zero, the TBM is jammed and has to be freed.
1-19 2-19 3-19 8-19 17-19	The frequency of standstills associated with mechanical breakdowns depends on the ground conditions (e.g., damage to the cutters or to the conveyor belt in blocky ground), on the robustness of the TBM (including the overboring equipment) and the back-up equipment as well as on the maintenance work carried-out on a regular basis.
13-19 14-19	See Section 2.4.6.
16-20 17-20 18-20 19-20	By definition.

The main inputs of the N^2 chart of Figure 2.3 are the ground (denoted by *G*), the *TBM* itself, the *back-up* equipment and the tunnel support (denoted by the entities S_1 and S_2 that will be explained later), while the gross advance rate (v_g) can be seen as the main output since it best represents TBM performance (construction cost could also have been considered as an output entity, of course). The gross advance rate depends on the net advance rate (v_n) achieved during the boring process and on the duration of the standstills (denoted by t_1, t_2 and t_3 depending on their cause). In this respect a distinction is made here between the regular operational standstills needed for the installation of the tunnel support or for the execution of maintenance works, etc. (t_1); standstills due to TBM jamming, where the TBM has to be freed and possibly repaired (t_2); and standstills due to other problems such as damage to the tunnel support or mechanical breakdown (t_3).

The dense population of the first two rows of the N^2 chart (Figure 2.3) reflects the paramount importance and the manifold effect of the ground and of the TBM (cutter head, shield, thrusting system). These entities summarize a large number of properties and features, which become relevant only for one or two interactions. Resolving the entities *G* (ground) and *TBM* into their individual properties and features (strength, stiffness, permeability, ground heterogeneity, shield length, installed thrust force, etc.) is basically possible, but would increase the chart size beyond the limit that can be managed on paper.

The alternative possibility of including the lower-level entities, but grouping them into blocks – creating thus a hierarchy of N^2 charts that considers the major subsystems with appropriate resolution (cf. Lano, 1990) – was abandoned for reasons of complexity and because it would not add anything substantial. Instead, remarks concerning some of the relevant parameters under the headings *G* (ground) or *TBM* are given in Table 2.1 (which supplements the N^2 chart with comments) as well as in the remainder of this section, which addresses questions of boring, thrusting and support, including their interactions. For the sake of simplicity, pairs of numbers within curly brackets will be used for making reference to Figure 2.3 and denoting the interfaces of the respective entities (e.g., {9-15} denotes the effect of entity 9 on entity 15), while a series of number in curly brackets will denote a sequence of interactions (e.g., {16-18-20} abbreviates {16-18} and {18-20}).

Boring and thrusting

The jamming of the TBM represents a major hazard as it may lead to serious damage, necessitating lengthy standstills for freeing or repairing the machine (standstill t_2 in Figure 2.3). Besides being important from a practical point of view, this potential problem is also theoretically very interesting and has attracted several research efforts over recent years. A comprehensive review of the literature on analytical methods used for TBM tunnelling in squeezing ground can be found in Ramoni and Anagnostou (2011b). This section of the present report limits itself to a qualitative discussion of the basic interactions and mechanisms underlying, (i), the inability to resume TBM operation after a standstill (which may be necessary, e.g., for support installation, re-gripping, etc.) and, (ii), the immobilization of a TBM during ongoing excavation.

Restart after standstill

If the ground behaviour is time-dependent, which is very common for squeezing conditions, a radial ground pressure may develop upon the machine during a standstill. In order to resume TBM operation, i.e., to move the TBM forwards and to rotate the cutter head, the thrusting system must be able to cope with the frictional forces acting upon the cutter head and the shield (Figure 2.4).

In order to move the TBM forwards, both the installed thrust force F_i and the bearing capacity of the thrusting system F_g must be higher than the frictional resistance F_f (static friction):

$$\min(F_i,\ F_g) > F_f \ . \tag{2.1}$$

The frictional resistance F_f increases with the radial pressure acting upon the machine {10-18} (which may be high in the case of squeezing ground) and with the size of the loaded area (i.e., with the diameter and length of the cutter head and of the shield {2-18}). Furthermore, it depends on the type of the ground {1-18} and on the surface roughness of the cutter head and of the shield {2-18} as they are relevant with respect to the skin

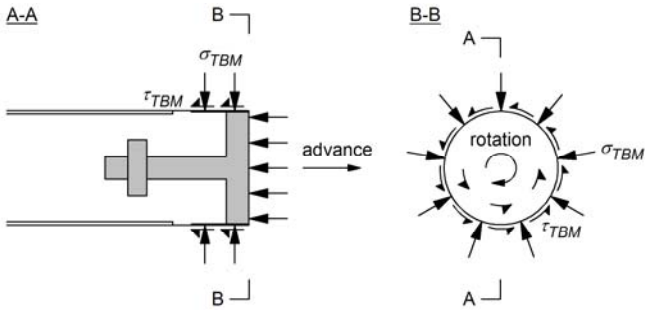

Figure 2.4. Loads acting on the TBM at restart (the shear and normal stresses at the face apply only in the case of a significant core extrusion).

friction coefficient. The installed thrust force F_i is a matter of TBM design {2-18}, while the bearing capacity F_g of the thrusting system depends both on the TBM design (the number, dimensions and surface roughness of the grippers and the installed gripper force) {2-18} and on the stiffness and the strength of the ground {1-18}. If the ground is weak and offers only insufficient resistance to the grippers, the effectively available thrust force will be lower than the installed one.

In order to restart the rotation of the cutter head, the effectively available torque must be high enough to overcome the frictional resistance T_f at the circumference of the cutter head (Figure 2.4) as well as its rolling resistance T_r:

$$\min(T_i,\ T_g) > T_f + T_r \ , \tag{2.2}$$

where T_i denotes the installed breakout torque (Figure 2.5) and T_g is the maximum torque that can be applied when taking into account the limited bearing capacity of the ground next to the grippers. Concerning the installed torque {2-18} and the bearing capacity of the thrusting system {1-18, 2-18} the factors are similar to those for the thrust force. The frictional resistance depends in this case on the geometry of the cutter head and on the ground pressure acting upon it {2-18, 10-18} as well as on the type of ground {1-18} and on the characteristics of the cutter head surface {2-18}, while the rolling resistance increases with the depth of cut at the moment when the cutter head rotation restarts.

Normally the rolling resistance of the cutter head should be lower than during the boring process, as no (or only a low) thrust force is applied to the cutter head when restarting its rotation {9-12}. Under squeezing conditions, however, the ground at the tunnel face may deform axially and around the cutters. The core extrusion thus leads to an increase of the depth of cut and, therefore, of the rolling resistance of the cutter head {1-12}. Furthermore, since the cutter head hinders ground deformations, an axial pressure develops upon it (Figure 2.4). It is obvious that in this case the demand both for thrust force and for torque increases. The increased thrust force demand is not so problematic, because a thrust force reserve is available at this stage since the TBM is not engaged in boring. The torque demand may, nevertheless, be critical to the resumption of operations.

If the ground pressure acting upon the TBM reaches its bearing capacity, damage will occur and repair work will be needed {2-18, 10-18}. This is particularly true if the TBM is already immobilized and the ground pressure increases further. During a standstill, the possibility of the TBM being pushed back by the axial ground pressure acting on the cutter head has also to be considered. Finally, when restarting TBM operation (or during ongoing excavation) overstressing due to combined loading (thrust force, torque and ground pressure) is also possible.

Immobilization during ongoing excavation

TBM immobilization during the boring process can be seen as equivalent to the borderline case of a zero net advance rate {16-18}. Usually the net advance rate v_n is expressed as the product of the achieved penetration P {15-16} with the chosen cutter head rotational speed r {7-16}. In the case of intensively squeezing ground, however, one should

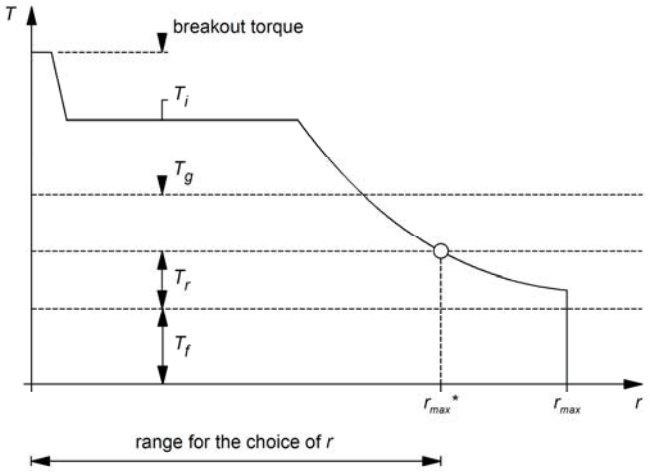

Figure 2.5. Relationship between cutter head rotational speed r and torque T.

bear in mind that before the machine moves forwards the extrusion of the core has first to be compensated and, consequently, the net advance rate

$$v_n = \max(0,\ Pr - e)\ , \tag{2.3}$$

where e denotes the extrusion rate of the core {11-16}. Under normal conditions (characterized by the usual values for penetration and rotational speed), the effect of the core extrusion rate is small, but it may become relevant in the case of a low penetration or a low rotational speed. In extreme cases, the cutter head penetrates and rotates without moving forward (the penetration is used-up just for removing the axially deforming ground at the working face). The circumstances leading to reduced values of penetration or rotational speed are outlined below.

The penetration rate depends on the rock mass characteristics (strength, discontinuities, etc.) {1-15}, on the cutter head design (form and stiffness, cutter spacing, size, etc.) {2-15} and on the boring thrust force {9-15}, i.e., on the force with which the cutter head is pushed against the working face. The boring thrust force F_b represents an operational parameter which can be chosen within certain limits that are imposed by the installed thrust force F_i {2-9}, by the bearing capacity of the thrusting system F_g {1-9, 2-9} and by the frictional resistance of the cutter head and the shield F_f (in this case sliding instead of static friction has to be considered) {2-9, 10-9}. The maximum possible boring thrust force

$$F_{b,\max} = \max(0,\ \min(F_i,\ F_g) - F_f)\ . \tag{2.4}$$

The analysis of TBM operational data and of field measurements, as done, e.g., from Farrokh and Rostami (2009) for the Ghomroud Tunnel (Iran, double shielded TBM, D = 4.50 m), confirmed that an increase of the frictional resistance F_f can lead to a limitation of the net cutter load and, consequently, of the penetration P {9-15}. Of course, a further reduction of the boring thrust force may also be necessary for reasons not related to squeezing (for example, in order to limit vibrations that could damage the equipment or in the case of blocky ground or mixed face conditions).

Squeezing behaviour – particularly if encountered in combination with gripper bracing problems – may limit the boring thrust force to such an extent that penetration is no longer possible {9-15}. Special problems may arise if squeezing weak ground alternates with hard rock. More specifically, when the TBM is exiting a weak zone and entering hard rock (Figure 2.6), a so-called "under-thrust situation" may occur (McCusker, 1996), which is characterized by the combination of several adverse factors: (i) low bearing capacity of the ground in the gripper area {1-9}; (ii) the need to overcome high frictional resistance {2-9, 10-9}; (iii) high resistance of the hard rock to the boring process {9-15}.

The cutter head rotational speed is another operational parameter directly affecting the net advance rate {7-16} (Equation 2.3) and is chosen on the basis of several limiting factors such as the diameter and the robustness of the cutter head {2-7}, the capacity of the

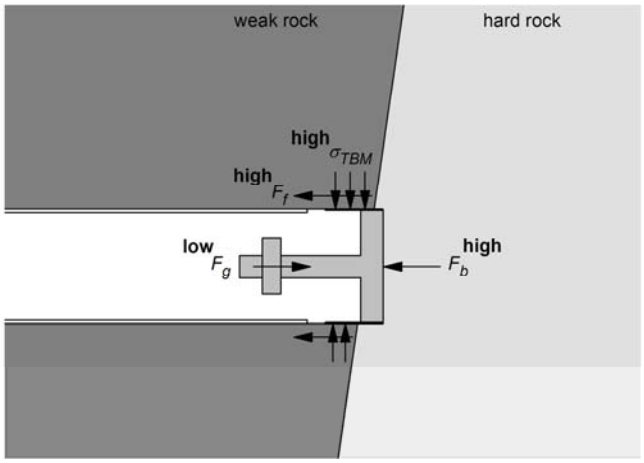

Figure 2.6. Gripper TBM leaving squeezing weak ground and entering hard rock.

mucking system and the torque demand $T_r + T_f$, where T_r denotes the rolling resistance of the cutter head {12-7} and T_f is the torque needed to overcome the frictional resistance (sliding friction) caused by the ground pressure acting axially and radially upon the cutter head {2-7, 10-7}. The rolling resistance of the cutter head depends on the ground {1-12} as well as on the characteristics of the cutters (e.g., number, spacing, arrangement, shape, diameter, wear) {2-12}. In weak ground, the torque demand may be very high and reduce the achievable rotational speed considerably, because rotational speed r and installed torque $T_i(r)$ are interrelated and determined by the TBM design {2-7} (Figure 2.5). Additionally, the effectively available torque may be smaller than the installed one as the torque T_g that can be reacted by the grippers may be low in poor quality ground {1-7, 2-7}. In general, the following condition must be satisfied in order to rotate the cutter head with a speed r:

$$\min(T_i(r),\ T_g) > T_f + T_r \ . \tag{2.5}$$

Under given operational conditions it may be necessary to reduce the cutter head rotational speed to a value $r < r_{max}$* (Figure 2.5) in order for sufficient torque to be available for overcoming the frictional and rolling resistances. Sticking of the cutter head will occur if the torque is insufficient in spite of the reduction of the rotational speed of the cutter head up to $r = 0$ ({1-7}, {2-7}, {10-7}, {12-7}, {7-16-18}.

Penetration P and rotational speed r determine the net advance rate v_n (Equation 2.3). It should be noted, however, that the latter is not only the main output of the boring process but may also be an important influencing factor. In the case of pronounced time-dependent ground behaviour, a slower advance leads to a higher loading of the machine {16-10} and this reduces both the achievable penetration {10-9-16} and the maximum possible rotational speed of the cutter head {10-7}, thereby causing a further reduction in the net advance rate {7-16, 15-16}, i.e., the system response to the given "perturbation" is amplified (so-called "positive feedback").

Tunnel support

The application of tunnel support usually takes place at two locations: in the machine area and later in the back-up area at a distance of 30–60 m behind the tunnel face (Maidl et al., 2001). The locations of the support installation are determined by the design of the tunnelling equipment. In the back-up area, it is generally possible to install the tunnel support without slowing down the rate of TBM progress. Support application in the machine area, however, interferes considerably with TBM operation because, as a rule, it necessitates a halt of the machine. Furthermore, the support in the machine area may influence the ground pressure acting upon the shield (cf. Section 2.4.7) or may limit the possibility of retracting the cutter head if necessary (cf. Section 2.4.3).

Interventions outside the two sectors mentioned above are, as a rule, not possible. According to Schneider et al. (2007), particularly critical in this respect is the zone between

the first and the second tunnel support installation points (zone A in Figure 2.7). In order to reduce the risk of problems in this area (e.g., jamming of the back-up equipment, inadmissible convergences of the bored profile, damage to the tunnel support) the installation of a higher quantity of tunnel support may be needed in the machine area and this, as said before, will affect general TBM performance.

For these reasons, the N^2 chart (Figure 2.3) was refined in order to take into account the specifics of the two locations for support installation. The two entities S_1 and S_2 denote the tunnel support applied in the TBM area and in the back-up area, respectively (Figure 2.7), and summarize all the relevant features of the support: the type (steel meshes, rock bolts, steel sets or shotcrete), the quantity (e.g., number of rock bolts per linear metre), the parameters (thickness, strength and stiffness) as well as the distance of the support installation point from the working face. With respect to the resolution of these two entities, the same remarks apply as the ones made above for the entities *G* (ground) and *TBM*.

Due to the impossibility of stabilizing interventions in given sectors of the back-up area, the two entities P_A and P_B have been introduced in order to summarize the problems that may occur in these zones (zones A and B, respectively, Figure 2.7). Similar problems to those depicted in Figure 2.7 may also occur of course behind the back-up area, i.e., after the passage of the tunnelling equipment. For example, in one of the drives of the Yacambú – Quibor Tunnel (Venezuela, gripper TBM, D = 4.80 m) major heave of the tunnel floor was observed starting 50–100 m behind the TBM. Such cases have not been included in Figure 2.3 although such a situation may also have an impact on TBM operation (for example, major heave or twisting of the tracks as well as the execution of repair works may impair rail operations and, thus, the supply of construction materials or the mucking).

The selection of the type, quantity and location of support application represents an important operational decision for a gripper TBM drive. As long as tunnel stability and working safety are not endangered, a trade-off between excavation progress and the quantity of support in the machine area is thoroughly conceivable. Deciding to apply as little as possible tunnel support in the machine area (in order to proceed more rapidly {5-17-20}) results, as a rule, in a lower support stiffness and bearing capacity and this may lead to problems in zone A (Figure 2.7), which may also reduce the gross advance rate {5-13-19-20}. Decision-making has to take into account the potential consequences of problems in the back-up area. A jamming of the equipment leads anyway to a standstill in TBM operation, while repair works after the passage of the equipment may often be carried out without slowing down the TBM drive very much.

A standstill may lead to an additional and longer standstill. During support installation, for example, the ground pressure acting upon the machine will increase {17-10} and, if the duration of the standstill t_1 is long or the development of the ground pressure fast, the required thrust force or torque (Equations 2.1 and 2.2) may become so high that an excavation restart is no longer possible {1-18, 2-18, 10-18} with the consequence that costly, time-consuming and sometimes also dangerous work is needed in order to free the TBM (t_2). Problems in the above-mentioned zones A and B may also cause a TBM standstill, during which the TBM may become trapped {e.g., 14-19-10-18}.

2.3.3 Single and double shielded TBMs

A similar N^2 chart to the one shown in Figure 2.3 could also be drawn for the case of single shielded TBMs. For the sake of economy, however, only the main differences between the two machine types will be discussed here. These differences include the TBM length, the thrusting system, the tunnel support and the advance rate.

Single shielded TBMs are longer than gripper machines. As the area exposed to the squeezing pressure is larger, a higher frictional resistance has to be overcome and, consequently, all other parameters being equal, the risk of shield jamming is higher (cf. Section 2.3.2). The disadvantage of a longer shield is, nevertheless, not of absolute significance because single shielded TBMs usually have a higher installed thrust force than gripper TBMs.

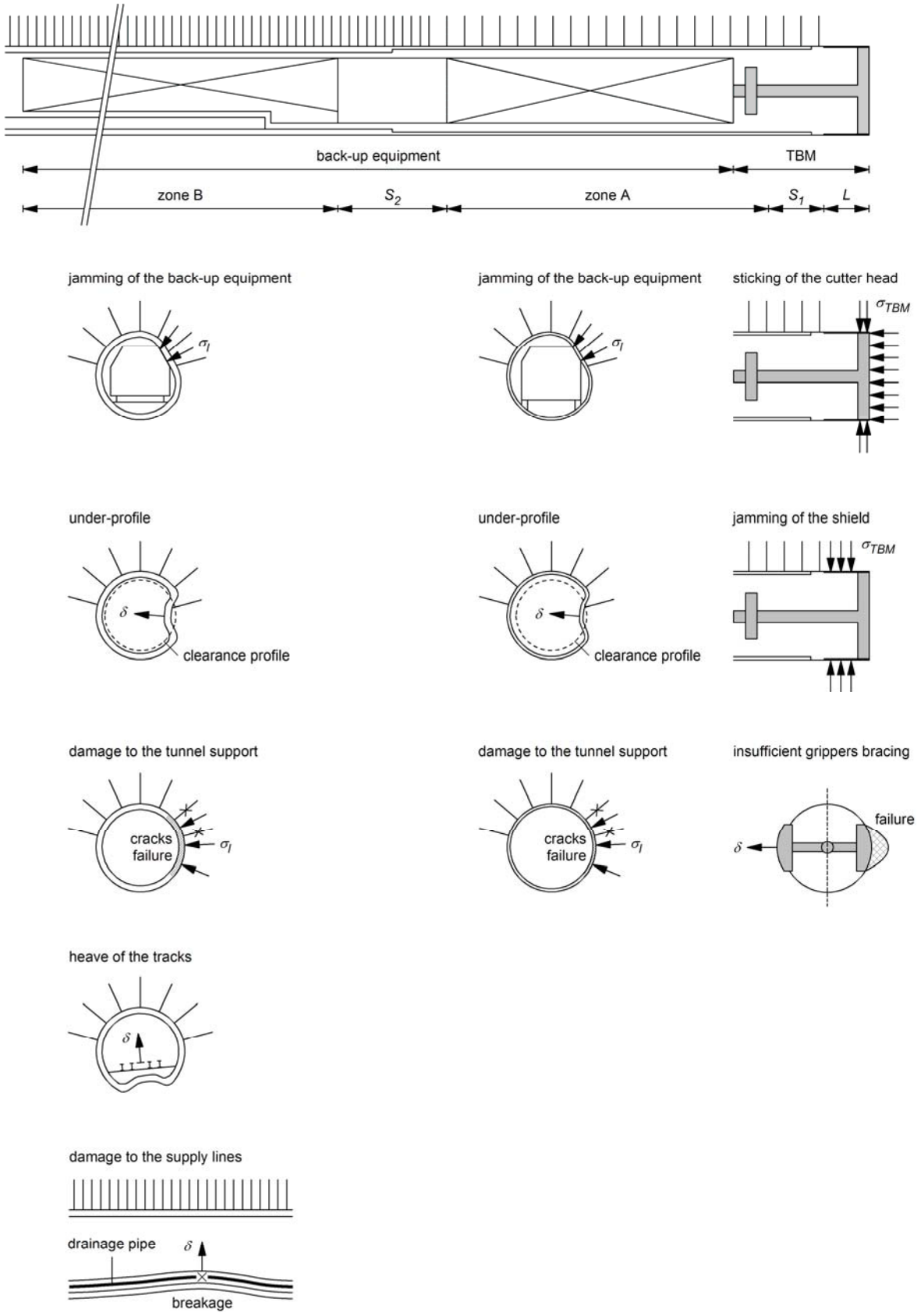

Figure 2.7. Layout of a gripper TBM and hazard scenarios in squeezing ground.

Instead of being thrusted via grippers, single shielded TBMs are jacked against segmental linings. The shield as well as the segmental lining have to be designed of course for the combined action of maximum jacking forces and ground pressure, in order to avoid overstressing or inadmissible ovalization. The structural design of the segmental lining plays an important role, as its bearing capacity limits the thrust force and torque that can be applied. This effect can be represented in the N^2 chart of Figure 2.3 by adding three interactions ({5-7, 5-9, 5-18}). Although the effect of the ground on the available thrust force and torque is not as important as in the case of gripper TBMs, in this regard the interactions {1-7, 1-9, 1-18} do not disappear completely because the quality of the annulus grouting depends also on the ground and an improper backfilling of the segments may reduce the capacity of the segmental lining to handle the jacking loads.

The type, location and thickness of the backfilling (which is not known a priori, as it depends, among other things, on the ground deformations occurring between the tunnel face and the point where the backfilling is completed) also play an important role with respect to the stiffness of the system composed of the backfilling and the segmental lining. The stiffness of the tunnel support not only has an effect on the ground pressure which the segmental lining has to accommodate, but also influences the loading of the shield (cf. Section 2.4.7). Therefore, the specifics of the backfilling have to be taken into account by analysing the interactions between shield, ground and tunnel support. A detailed discussion of this topic can be found in Section 6.

As described at the end of Section 2.3.2, the type, quantity and installation points of tunnel support represent important operational parameters for a gripper TBM drive. For shielded TBMs, however, these parameters are pre-determined (a segmental lining of given thickness is installed in the rear part of the shield). Therefore, the N^2 chart can be simplified by eliminating the differentiations made with respect to the tunnel support (S_1 and S_2) and to the locations of problems in the back-up area (P_A and P_B). Furthermore, due to pre-fabrication, the stiffness and the strength of the tunnel support do not change over time and, therefore, do not depend on the gross advance rate (i.e., the interactions {16-5, 17-5, 18-5, 19-5, 16-6, 17-6, 18-6, 19-6} do not exist).

Single shielded TBMs offer the advantage of a higher advance rate in poor quality ground (Peila and Pelizza, 2009), although feedback effects are possible for these machines as well. For example, high water inflows or unstable tunnel walls may make lining installation or annulus grouting difficult and, therefore, may slow down the advance rate.

Double shielded TBMs operating in gripper mode install the lining simultaneously with the boring process and, all other parameters being equal, therefore achieve a higher performance than single shielded machines. In the case of time-dependent ground behaviour, a higher advance rate is also advantageous with respect to the amount of shield skin friction to be overcome. Comparative studies should, nevertheless, take account of the fact that double shielded TBMs are in general longer than single shielded TBMs. Potential differences may exist, furthermore, concerning machine availability as double shields are more complex than single shields and necessitate a particularly careful and robust design in order to reduce maintenance times or breakdown times.

In weak ground, bracing by the grippers may become impossible. In this case, double shielded TBMs operate in so-called "auxiliary mode" jacking against the segmental lining with the consequence that it is no longer possible to install the segments simultaneously with the boring (unless a hexagonal segmental lining is applied). Depending on the machine design, unstable ground may also impair the extension and closure of the telescopic joint, thus necessitating machine operation in single shield mode. In both cases (auxiliary mode and single shield mode) the same remarks apply as for the single shielded TBM and the potential advantages of double shielded TBMs mentioned above are lost.

2.4 Countermeasures

2.4.1 Introduction

The basic interactions discussed in the last sections suggest not only how a given parameter is involved in the performance of the entire system, but also where it is possible to intervene, i.e., to apply measures in order to influence system behaviour. Section 2.4 will review possible countermeasures to deal with the problems associated with squeezing. As in the last sections, reference will be made to the interactions of Figure 2.3, reporting the corresponding numbers within curled brackets.

Over the years, technological improvements in various components of the TBMs have extended their range of applicability. The next sections aim to evaluate not only the well-established methods but also alternative lining and machine concepts, which have been proposed specifically for coping with squeezing ground. The order of this discussion reflects the location of the system components and, therefore, of the possible intervention points along the tunnel axis: the discussion starts with the ground ahead of the working face and in the machine area, continues with the TBM (cutter head, shield, thrusting system) and finishes with the back-up equipment and the tunnel support. Before doing so, however, some higher-level aspects, such as alignment, construction method and operational measures will be briefly addressed below.

The technical feasibility and the cost of a given measure (or package of measures) for dealing with the problems associated with squeezing depend on the number and the length of the tunnel stretches affected. If the geometry and the behaviour of critical geological zones are well-known, one would try first to reduce the length of the affected tunnel stretches by selecting another alignment in the planning phase. Such a route optimization presupposes knowledge of the geology with a degree of resolution that may be difficult to achieve particularly for long deep tunnels. Furthermore, it may lead to an unacceptably long tunnel or it may be impossible due to project constraints such as the location of the portals, access galleries or shafts, the minimum curve radiuses or the longitudinal gradients.

The conventional excavation of a critical section may lead to a reduction of the project schedule risks if it can be done in advance. However, this is only possible if the critical zone is well-known (position and length) and can be accessed via an auxiliary tunnel or a shaft. Switching to conventional excavation during a TBM drive is, as a rule, very difficult. Nevertheless, it represents an indispensable measure if the TBM is trapped and has to be freed. As a rule, this requires hand-mining over the shield or the construction of a bypass tunnel – demanding operations, particularly for small boring diameters due to the very limited space available. Special measures have to be planned in advance, in order to reduce standstill time as much as possible. The potential delays and additional costs also have to be analyzed before construction and taken into account in the construction schedule and in the contractual regulations. This is particularly true in the case of a long drive through predominately competent rock, where the possibility of the TBM jamming in individual short fault zones may even be regarded as an acceptable risk.

A larger boring diameter offers more space for ground deformations, thus reducing the risk of a violation of the minimum clearance profile and, when combined with a yielding support (cf. Section 2.4.7), will lead to lower ground pressures, thus reducing the risk of support overstressing as well {2-13, 2-14}. The choice of a larger boring diameter also reduces the risk of shield jamming – this will be the case, however, only if it is combined with a larger overcut, i.e., with a larger gap between the tunnel wall and the extrados of the shield {2-10}. Local enlargements of the boring diameter are often very problematic (cf. Section 2.4.3), but selecting a larger boring diameter for the entire tunnel may be a viable option particularly if squeezing conditions are expected to persist over a big percentage of the route. The financial viability of such a solution should be assessed case by case, since it will result in an unnecessarily large boring diameter in the tunnel stretches crossing competent rock (Amberg, 1992).

As mentioned in Sections 2.2 and 2.3, tunnelling practice as well as theoretical considerations indicate that maintaining a high overall advance rate may help with the problem of the TBM jamming due to squeezing ground. Operational measures and an appropriate

construction site organisation are important for keeping the frequency and the duration of standstills low and thus the overall advance rate high {4-17, 4-18, 4-19}. For example, if an identified critical zone has to be crossed, thorough maintenance work should be carried out in advance in order to reduce the risk of mechanical breakdowns {17-19} and the necessary logistical precautions should be taken to allow operations within the critical zone to be as continuous as possible {4-17}. Such operational measures have been applied systematically, e.g., during the construction of the Wienerwald Tunnel (Austria, single shielded TBM, D = 10.67 m) in order to reduce the risks in known fault zones (Matter et al., 2007). Holiday periods (and, depending on local conditions, even perhaps the possibility and frequency of strikes) have also to be taken into account. In the case of an unexpected critical zone, reducing the amount of maintenance work may speed-up the TBM advance and help temporarily to avoid TBM trapping, but it will increase the risk of mechanical breakdown and thus the risk of an even longer standstill {17-19}. Therefore, such a measure should not be applied as a matter of course.

Finally yet importantly, in addition to the technological and logistic aspects, the importance of the experience of the crew (the so-called "human factor") should not be overlooked. This general truth is particularly relevant for dealing with adverse geotechnical conditions such as squeezing ground.

2.4.2 Pre-treatment or pre-support of the ground

The ground is (together with the TBM design, of course) the most important parameter for achieving a given gross advance rate. It represents in practical terms a purely input parameter because the possibilities of influencing its properties and behaviour are very limited in relation to the particular problem investigated in this report.

The pre-treatment of the ground, e.g., by grouting or drainage, can be carried out basically either before or during the TBM drive. The first solution is of course preferable (as the improvement work will not interfere with the TBM operation) but necessitates in nearly all cases the construction of an intermediate access tunnel or a pilot tunnel, which may also be technically demanding, costly and time-consuming. The pre-treatment of the ground from the TBM itself does not require auxiliary structures, but slows down the TBM drive considerably, which (as discussed in Sections 2.2 and 2.3) may also lead to critical situations (isolated short stretches with squeezing ground are more favourable in this respect, because the pre-treatment can be done from the adjacent competent rock zone).

The applicability of grouting or drainage depends strongly on the ground characteristics. Squeezing grounds are unfavourable in this respect as they often have a high fraction of fines and, therefore, a low permeability. In addition, it has to be borne in mind that the cutter head and the shield, as well as the limited space available for the drilling equipment, impose geometric constraints on the layout of the boreholes. In the case of injection operations, the risk of cementing the cutter head has also to be investigated (Oreste and Peila, 2000). Chemical grout materials, if environmentally permitted, may be advantageous in this respect (Steiner, 2000; Peila and Pelizza, 2009). Another countermeasure would be to pull back the cutter head. This is, of course, only possible if the tunnel face is stable (Barla and Pelizza, 2000). Pore pressure relief by advance drainage is a highly effective measure for reducing deformations (Anagnostou, 2009a, 2009b) but investigations have to be performed in order to determine whether the technically feasible spacing and length of the boreholes are sufficient to achieve the necessary consolidation within an acceptable time period (Floria et al., 2008). In this respect, the heterogeneity of the ground permeability has also to be considered.

Concerning pre-support of the ground ahead of the working face, Einstein and Bobet (1997) suggested the application of jet grouting or of a steel pipe umbrella for TBM tunnelling through squeezing ground. Due to the limited space available for equipment, however, the execution of jet grouting is barely feasible and rarely used in mechanized tunnelling (Peila and Pelizza, 2009). The technical feasibility and effectiveness of pipe umbrellas are also questionable. Undoubtedly, forepoling would eliminate the risk of caveins, but would not reduce significantly the squeezing deformations or the load acting upon the shield (the stiffness of the steel pipes is very low).

Face bolts, which can be installed through openings in the cutter head (Lunardi and Focaracci, 2000), might limit core extrusion and represent a possible measure for overcoming short critical zones or for the case of long standstills (the time needed for the periodical installation of the bolts conflicts with the goal of maintaining a high advance rate and introduces a higher risk of TBM jamming). Furthermore, the effectiveness of such a measure is small because, as a rule, the openings in the cutter head do not allow for a close spacing of the bolts.

2.4.3 Cutter head

As discussed in Section 2.3.2, the design of the cutter head plays an important role with respect to the ground pressure acting upon it as well as the torque and thrust force required in order to keep the cutter head rotating and moving (during continuous excavation) or to get it restarted (after a standstill) {2-7, 2-9, 2-10, 2-12, 2-18}.

The sticking of the cutter head during a standstill may be avoided by rotating it at regular time intervals. This should be regarded as an operational measure, which must be applied during longer standstills such as, e.g., holiday stops, as experience shows that these are particularly critical periods (cf. Section 2.2). In order to facilitate unlocking, the cutter head should be rotatable in both directions {2-12} (Gütter, 2007).

Another measure for avoiding sticking of the cutter head where there is a major extrusion of ground at the working face is to pull back the cutter head or the TBM. For gripper TBMs this presupposes that the applied support does not impede a movement of the machine backwards {5-10, 5-12}. Single or double shielded TBMs have to be designed so that the cutter head can be moved independently from the shield. Of course, a movement of the cutter head backwards is possible only if the friction caused by the radial ground pressure can be overcome, if the machine possesses a sufficient pull force and if the ground is able to provide a sufficient reaction force to the grippers {1-10, 2-10, 1-12, 2-12, 10-12, 10-18}. Furthermore, during a standstill the cutter head may support the tunnel face. A careful evaluation of the face conditions is important, as moving back the cutter head may cause instability of the face (Barla and Pelizza, 2000).

The cutter head must also be stiff enough to guarantee an efficient boring process (Toolanen et al., 1993) and to allow for a full utilization of the installed torque {2-7, 2-9, 2-18}. Such aspects are usually the responsibility of the TBM manufacturer. As a rule, it should be possible to assume that the related requirements are met.

Geometry

To reduce the friction between ground and cutter head it is first of all important that the cutter head does not have greatly protruding parts (Barla and Pelizza, 2000; Schmid, 2006). This applies also for the cutters which should protrude as little as necessary for the boring process (McCusker, 1996). Korbin (1998) recommends 80 mm cutter protrusion beyond the cutter head on the face and 50 mm on the gauge.

Keeping the size of the cutter head small in the axial direction reduces the area exposed to the ground pressure and is, therefore, favourable (Grandori and Antonini, 1994; Foster, 1997; Maidl et al., 2001). Moreover, the cutter head can be slightly "conical". A reasonable conicity according to Lovat (1997) would be about 13 % of the boring diameter.

Theoretical considerations show that a spherical shape of the tunnel face (which off course necessitates a spherical form of the cutter head) may reduce core extrusion and deformations in the machine area considerably (Moulton et al., 1995). On the other hand, curvature of the tunnel face is very unfavourable for its stability (Beckmann, 1984; Steiner, 2000; Maidl et al., 2001). Nowadays almost all TBMs have flat cutter heads.

Overboring

A moderate amount of squeezing can be accommodated by boring a larger profile, using one to three extendable gauge cutters {8-10, 8-13, 8-14}. After Wolff and Goliasch (2003) and Toolanen et al. (1993), respectively, the first applications of an overboring system on full face hard rock TBMs were in the Shaft Project Lohberg (Germany, gripper TBM,

Table 2.2. Technologically feasible overboring in diameter ΔD.

(a) Overboring systems after Wolff and Goliasch (2003)			ΔD [cm]
Fixed mounted gauge cutters	The achievable ΔD depends on the number of additional mounted gauge cutters		≤ 30
Manual extendable gauge cutters	Moving the gauge cutters outwards by introducing a plate under their mounting; after Herrenknecht (2003)	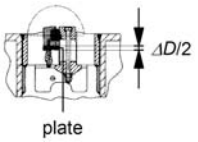	≤ 9
	Moving the gauge cutters outwards by sidewise offset of their mounting; the final ΔD is achieved by moving the various gauge cutters stepwise; after Wirth (2003)	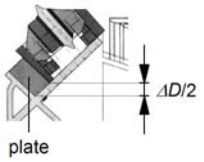	≤ 30
Hydraulic extendable gauge cutters	Rotatable, hydraulic movable gauge cutters (in their final position locked by pins); after Wirth (2003)	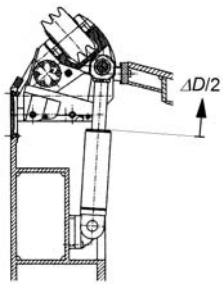	≤ 30
	Telescopic, hydraulic movable gauge cutters (in their final position locked by pins); after Herrenknecht (2003)	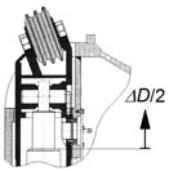	≤ 30

(b) Other sources	ΔD [cm]
Grandori (1993)	≤ 15–20
Barla (2001)	≤ 15–25
Downing et al. (2007), Gehring and Kogler (1997), Herrenknecht (2010), Mendaña (2007)	≤ 20
Voerckel (2001)	≤ 25
Vigl et al. (1999)	≤ 30
Hartwig (1995)	≤ 30–45

D = 6.50 m) and in the Piedimonte Tunnel (Italy, gripper TBM, D = 5.86 m). The adaptation of the boring diameter in order to create space for expected ground deformations was proposed on a conceptual basis by Lombardi (1981).

The increase of the boring diameter ΔD depends on the chosen system {2-8} and is, according to Wolff and Goliasch (2003), technologically limited to a maximum of 30 cm (Table 2.2a). Other authors suggest slightly different feasible values of ΔD (Table 2.2b). The amount of overboring does not depend on the boring diameter. Consequently, with increasing boring diameter, the ratio between overboring (allowed convergence) and boring diameter decreases and (since the ground pressure depends theoretically on this ratio) the efficiency of overboring also decreases.

Some authors suggest that allowing the occurrence of convergences may be counterproductive because the convergences cause softening or major loosening of the rock mass with a consequent increase in ground pressure or in the necessary support measures (Foster, 1997). As discussed by Kovári (1994), however, the load increase caused by loosening is of secondary importance for squeezing conditions. Consequently, a negative impact of the convergence on the ground characteristics {8-1} has not been introduced in the N^2 chart of Figure 2.3.

Wolff and Goliasch (2003) provided a detailed critical review of the different overboring systems and distinguished between the following types of additional gauge cutters (Table 2.2a): (a) fixed mounted; (b) manually extendable; (c) hydraulically extendable. The installation of the first type of gauge cutters requires a halt in excavation {8-17} and presupposes that appropriate, empty housings have been arranged in the cutter head {2-8}, which are covered by steel plates during normal operation. The manual extension of the second type of gauge cutters – in steps of 25 mm (Downing et al., 2007) – also necessitates a standstill. The hydraulic extension of the third type of gauge cutters, however, can be carried out during excavation.

When applying overboring with shielded TBMs the centreline of the cutter head has to be lifted with respect to the centreline of the shield, in order to avoid sinking of the TBM (Vigl and Jäger, 1997; Voerckel, 2001; Rehm, 2005). The overboring can easily be handled by gripper TBMs (Voerckel, 2001). If the TBM is equipped with a cutter head shield, a repositioning of its lower segment has to be carried out (Wolff and Goliasch, 2003). For all TBM types a re-positioning of the mucking buckets is also needed in order to ensure efficient muck removal during overboring (Schmid, 2008).

In order to avoid overstressing the gauge cutters (and, particularly, their supports), the rotational speed of the cutter head and the thrust force must be reduced during the overboring {8-7, 8-9} (Toolanen et al., 1993; Wolff and Goliasch, 2003) and this leads to a reduction of the net advance rate {7-16, 9-15-16}. So, the overboring, if successful, leads on the one hand to a reduction of the ground pressure acting upon the cutter head and the shield {8-10}. On the other hand, however, it causes a slow down of the TBM advance rate, which may lead to an increase of the TBM loading – either during the installation of the overboring facility {17-10} or during the boring process {16-10}. Furthermore, it is particularly critical to ensure timely decision-making during construction. Determining the right point in time for initiating complicated overboring procedures is not easy, since the system has to be activated before encountering a critical zone and before the convergences become too large.

Overboring technology is not yet well developed and its value is very uncertain, at least for long reaches with squeezing conditions (ITA, 2003), and their successful application has yet rarely been achieved (Wolff and Goliasch, 2003). The trouble-free application of overboring only seems possible in rather soft rocks. The reliability of today's overboring systems is in general critical {8-19}, the ones with continuous adjustment of the boring diameter being, as a rule, the most sensitive (McCusker, 1996; Gehring and Kogler, 1997). The concentrated loads acting upon the extended gauge cutters (Schneider and Kapeller, 1995) or their abrupt loading due to falling blocks (Toolanen et al., 1993) are particularly critical. This was observed, for example, in the Northern Section of the Vereina Tunnel (Switzerland, gripper TBM, D = 7.64 m), where the overcutters were very susceptible to failure in hard or blocky rock (Hentschel, 1997). Concerning the reliability of overboring systems, the experiences from the Raron Section of the Lötschberg Base Tunnel (Switzerland, gripper TBM, D = 9.43 m) are interesting (Wolff and Goliasch, 2003). The boring diameter was increased by 20 cm in the Lias-limestones with a considerable effort. The enlargement of the bored profile happened within a 20 m long tunnel stretch by using two hydraulic extendable and two fixed mounted gauge cutters. Particularly critical was the steering of the TBM during the enlargement phase as well as the very short lifetime of the four fixed mounted gauge cutters utilized to continue the excavation with overboring. Due to the considerable wear of the overboring system and the reduced penetration, one decided to reduce the overboring up to 10 cm in diameter and to realize it by shifting all gauge cutters and applying two fixed mounted extended gauge cutters. With this configuration, it was possible to drive about 860 m with a daily advance of 15.4 m.

Problems may also arise in heterogeneous rock masses where stretches with squeezing weak ground alternate with stretches of hard rock. The boring diameter should be enlarged before entering the critical squeezing zones, but this is only possible if the overboring system is able to bear the high load resulting from extending the gauge cutters within the hard rock stretch. Such a test has been carried out in the Bodio Section of the Gotthard Base Tunnel (Switzerland). In the initial phase of the TBM drive an enlargement of the boring diameter (gripper TBM, D = 8.80 m) of 30 cm has been attempted within a stretch of 200 m of crystalline rock. The test has not been successful (Rehm, 2005;

Vicenzi et al., 2007; Gollegger et al., 2009). The presence of mixed face conditions (hard and weak layers) was particularly unfavourable.

Another typical problem is represented by the blockage of the extendable gauge cutters in their start position due to their housings filling up with fine materials. In this case, it is still possible to extend them, but they do not rotate anymore and, therefore, wear faster and irregularly.

In the case of a large difference between the boring diameter and the diameter of the shield extrados, difficulties with the backfilling of the segmental lining may arise. On the one hand, the quantity of annulus grout is potentially larger. In this respect, questions arise concerning the costs and the supply. On the other hand, a grout flow towards the tunnel face is easier. After Gütter (2007), a solution might be to adapt the shield diameter to the overboring in such a way that the shield continuously supports the ground. In the same paper, however, this concept is rejected because of its technological complexity. Previous attempts to implement similar concepts have also been unsuccessful (cf. Section 2.4.4).

An alternative concept for a cutter head with a variable diameter was proposed by Baumann and Zischinsky (1993) of the company DMT (Deutsche Montan-Technologie). The first developed design was for applications in mining. The concept (Figure 3.8a) was later modified for a large cross-section (D = 9.20 m) and foresees a TBM with grippers placed near to the cutter head. The cutter head is composed of two radial adjustable arms (with four cutters each), is able to excavate non-circular profiles and allows for a continuous adjustment of the boring diameter depending on the thickness of the tunnel support. The boring process is carried out by applying the undercutting technique and requires, therefore, a pilot borehole to provide an additional free surface. The pilot borehole is bored, together with the enlargement of the main profile, by a small diameter "classical" cutter head (having seven cutters), which is located in the middle of the main cutter head. It is unknown whether such a machine has ever been applied. A first application was announced for a Canadian mine, but the applied machine was very different from the proposed one (Anonymus, 1993). Anyway, this concept seems to be very complex from the mechanical engineering point of view. The limited functionality and reliability of such a machine has to be expected.

2.4.4 Shield

The design of the shield, particularly its geometry, influences the thrust force that is required to overcome the skin friction {2-9, 2-10, 2-18}.

The shield should be as short as possible (Lombardi, 1981). In order to reduce the surface of the TBM exposed to ground pressure to a minimum, Robbins (1997) proposed the use of gripper TBMs without either a canopy or a cutter head shield. Such a so-called "Open Top TBM" (Figure 2.8b) allows support installation immediately behind the cutter head and was applied (in non-squeezing conditions) in the Melbourne Underground Rail Loop (Australia, D = 6.90 m) and in the Heitersberg Tunnel (Switzerland, D = 10.67 m). The DMT-concept (Figure 2.8a) mentioned in Section 2.4.3 also represents an attempt in this direction. Anyway, gripper TBMs are generally equipped with a short shield having a length of about half a boring diameter. Improvements in TBM technology actually allow for a significant reduction in the machine length (to about 1–2 boring diameters) for single and double shielded TBMs as well. Such reductions in length can be realized more easily with larger tunnel diameters (see also the TBM technical data collected in Section 5.2.3). For shielded TBMs, the shield length depends not only on the space needed for the equipment, but also on the size of the segments employed. After Foster (1997) an increase of the segment length necessitates an increase of double that value in the shield length. Bigger segments – nowadays with a width of up to 2.25 m (Stahn and Grimm, 2006) – allow for a higher gross advance rate because they reduce the operational standstill times (which is advantageous in squeezing ground {5-17-10}) but necessitate, at the same time, a longer shield (which is disadvantageous in squeezing ground {2-9, 2-10, 2-18}).

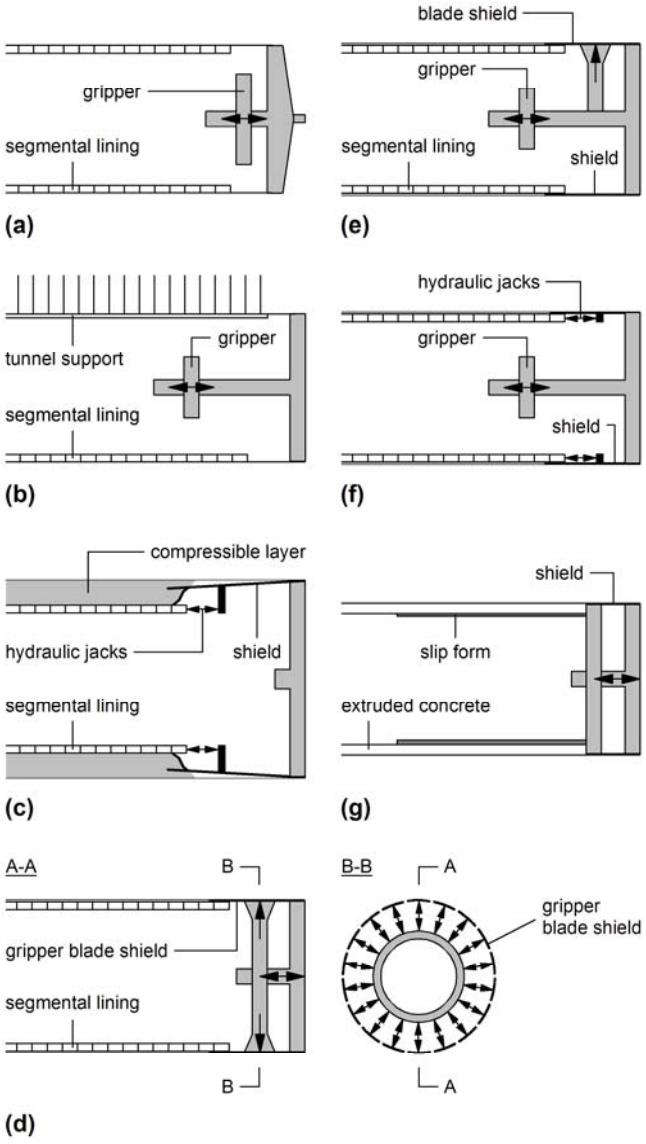

Figure 2.8. Principles of alternative TBM concepts developed for tunnelling in squeezing ground: (a) DMT-concept; (b) Open Top TBM (Robbins); (c) Wittke-concept; (d) Walking Gripper Blade Shield (Robbins); (e) Low Pressure Walking Blade Canopy (Robbins); (f) Hida Tunnel TBM (Robbins); (g) MIT Continuous TBM.

A slightly "conical" shield is also favourable (Lombardi, 1981). The conicity of today's single shielded TBMs amounts to 3–6 cm in diameter and is realised stepwise. Depending on their design, double shielded TBMs may have a slightly larger conicity of up to 10 cm in diameter. An increase in the conicity and, therefore, in the overcut as well, has a positive effect with respect to the risk of shield jamming as it provides more space for the deformations (Gehring and Kogler, 1997). The effectiveness of this measure increases with the ratio of overcut to boring diameter. This is a reliable measure, as it does not depend on the operability of mechanical parts. On the other hand, such a solution implies a larger boring diameter for the entire tunnel. In the stretches with non- or only slightly squeezing ground, a very wide annular gap may have to be filled (Dowden and Cass, 1991). Besides financial considerations, the potentially negative effect of the wide gap on the bearing capacity of the segmental lining has to be assessed from case to case. It should also be mentioned that the overcut and the conicity of the shield have first of all to permit the TBM to be steered (Amberg, 2008). If the gap between the shield and the ground becomes closed, steering the TBM may become difficult or even impossible. A change in the direction of the TBM will in this case cause a considerable constraint load on the shield, particularly if the latter is long.

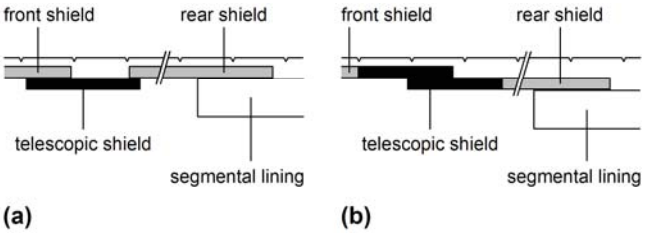

Figure 2.9. Construction schemes for the telescopic shield of double shielded TBMs: (a) "classic" design; (b) modified design after Concilia and Grandori (2004).

Wittke-Schmitt et al. (2005) examined the feasibility of a TBM concept with a strongly "conical" single shield (conicity 60 cm in diameter, Figure 2.8c) in the planning phase of the Kallidromo Tunnel (Greece) and came to the conclusion that the risks and the additional costs were unacceptably high. More specifically, two aspects have been assessed as critical to the planning of single shielded TBMs (D = 15.10 m): the structural detailing and reliability of the tail-shield seal (due to its enormous thickness of 2.10 m) and the risk of the TBM trapping and the shield overloading in the case of standstills longer than 1–2 days (in spite of the strong conicity of the shield).

The surface of the shield should be as smooth as possible. A favourable construction, which avoids the stepwise increase of the rear shield diameter, is nowadays possible also for the telescopic part of double shields (Figure 2.9). Such a design may, nevertheless, present problems with the backfilling of the segments as it leads to a wide gap between the tunnel wall and the extrados of the rear shield (Burger, 2009).

The bearing capacity of the shield has to be high enough for the ground pressure {10-18}, which acts in addition to the system loads (e.g., thrust force, torque, self weight). In this regard, structural reserves are recommended. The design load should be higher than the level of ground pressure that would lead to shield jamming. The probability of overloading with permanent damage to the shield can thus be reduced. Shield design should also take into account that the ground pressure may be markedly non-uniform both in the transversal and in the longitudinal direction.

An asymmetric loading may occur, for example, when approaching a weak zone, particularly if the latter crosses the alignment at a flat angle (Figure 2.10). This was observed, for example, in the Arrowhead Tunnels (USA, single shielded TBM, D = 5.82 m). The shields employed in this project had been equipped with strain gauges in order to monitor their deformations and to back-calculate the ground pressure. This instrumentation made it possible to obtain useful information about the shield loading, for example during a three-day maintenance period, where the ground pressure increased so much that hand-mining was necessary in order to free the TBM {17-10-18}. The standstill was due to maintenance work on the screw auger used for extracting the muck from the working chamber. On some occasions, the efficiency of the mucking system was unsatisfactory, with the consequence that fine-grained muck became packed beneath the shield and the TBM began to climb. A closure of the radial gap between shield and tunnel wall may therefore also be caused by the packing of muck around the shield, if the material mucked out is less than the material produced by the excavation, i.e., if the capacity of the mucking system is not attuned to the TBM advance rate. An understanding of the TBM's operational parameters is also important in this regard. Packing of fines around the shield reduces the space available for deformations and may therefore lead to an earlier development of ground pressure upon the shield.

A higher deformability of the shield leads, as a rule, to a decrease of the ground pressure acting upon it. Lombardi (1981) has remarked that having the possibility to reduce the diameter of the shield might be helpful in restarting the TBM after a standstill {2-10}. Grandori et al. (1995) proposed a flexible design of the rear part of the shield. The underlying idea was that, in the case of jamming, a small contraction of the shield should suffice in order to free it and continue the TBM drive. The shield should return back to its initial, undeformed condition as soon as possible in order to allow for any subsequent exploitation of its deformability as an unloading measure (Dowden and Cass, 1991). The application

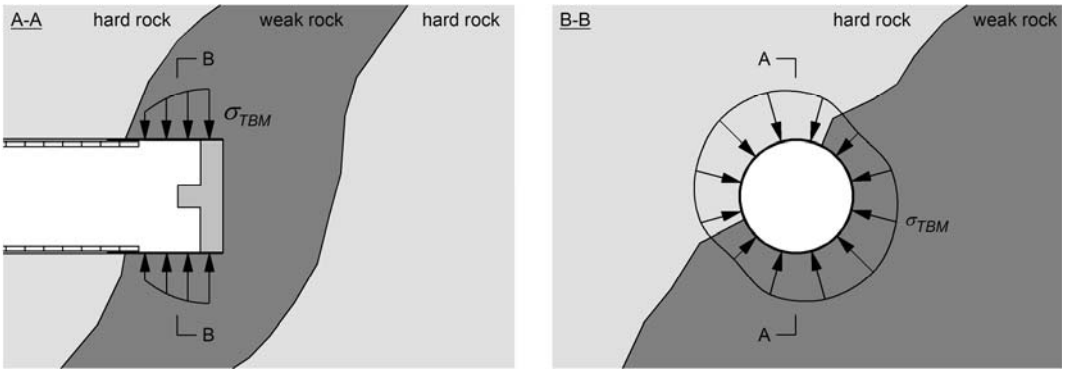

Figure 2.10. Non-uniformity of the ground pressure σ_{TBM} in the transversal and in the longitudinal direction when entering a weak zone.

of this principle presupposes the choice of a bigger boring diameter or, at least locally, the acceptance of an under-profile with the associated re-profiling works. This may be problematic particularly for segmental linings, as they impose a lower limit to the inner diameter of the shield.

Another TBM concept proposed by Robbins (1997) is characterized by a shield that is divided in several, 1.0–1.5 m wide "blades" (Figure 2.8d). This so-called "Walking Gripper Blade Shield" should be able to exert a support pressure on the surrounding ground of up to 2 MPa while advancing in steps of 10–15 cm. The blades form a deformable system that is able to contract inwards 7–10 cm. It is generally recognised that the complexity of such a machine has a negative impact of its functionality and reliability. The presence of several moving parts also increases the difficulties encountered when driving stretches in flowing or ravelling ground. The risk of the cutter head sticking or the shield jamming is still there, particularly in the case of a standstill. Despite the large surface of the grippers (i.e., of the blades), it is uncertain if the bracing of the TBM will be sufficient in weak ground. SNC Lavalin applied this concept by modifying a double shielded TBM (D = 2.91 m) for driving 1183 m of the Stillwater Tunnel in the USA in lightly squeezing ground. Problems have been reported with respect to blocky ground, steering of the machine and sealing of the main beam. Westfalia Lünen drove 1650 m of the exploratory tunnel (D = 5.20) of the Freudenstein Tunnel (Germany). In this case squeezing ground was neither expected nor encountered (Klonsdorf and Schaser, 1991), but the TBM drive was anyway unsatisfactory as the machine proved to be extremely sensitive to the presence of water (Maidl et al., 2001). Furthermore, the TBM drive was hindered by clogging of the cutter head (Babendererde, 1989) and suffered damage on several occasions (Klonsdorf and Schaser, 1991). A similar TBM concept was proposed, but not applied, by Moulton et al. (1995) for the drive of the Yacambú – Quibor Tunnel (Venezuela, D = 5.00 m).

Attempts to construct shrinkable shields for single shielded TBMs are still not satisfactory (Downing et al., 2007), although the implementation for gripper TBMs does seem to be possible. One example of a gripper TBM with a deformable shield is the gripper TBM (D = 7.64) that has driven the Zugwald Tunnel and the Northern Section of the Vereina Tunnel (Switzerland). This machine was equipped with a shrinkable cutter head shield, where hydraulic jacks allowed for a reduction of the shield diameter by up to 15 cm. Further examples include the gripper TBM (D = 9.53 m) of the Tscharner Tunnel (Switzerland) – which is described in Hentschel (2000) – as well as the two gripper TBMs (D = 8.80) of the Bodio Section of the Gotthard Base Tunnel (Switzerland). The design of the Gotthard machines permitted a reduction of up to 20 cm in the shield diameter. After a refurbishment, the TBMs were also used in the Faido Section (D = 9.43 m) of the same tunnel. Two further examples of such gripper TBMs – Tunnel Le Pougeot (France, D = 5.05 m) and Shaft Project Lohberg (Germany, D = 6.50 m) – can be found in Eistert (1982). Such a gripper TBM (D = 3.20) has also been used for one of the adits of the Stillwater Tunnel (USA).

Table 2.3. Skin friction coefficient for sliding and static friction (i.e., during TBM advance and for restart, respectively) with and without lubrication by bentonite after Gehring (1996), Herzog (1985) and Pohl (1979).

State	Sliding friction (continuous excavation)		Static friction (restart after a standstill)	
Lubrication	Not lubricated	Lubricated	Not lubricated	Lubricated
Rock	0.25–0.30	0.10–0.15	0.40–0.45	0.15–0.25
Gravel	0.25–0.30	0.15	0.40–0.55	0.20–0.30
Sand	0.35–0.40	0.15	0.45–0.55	0.20–0.30
Silt	0.35–0.40	0.10	0.30–0.50	0.15–0.20
Clay	0.30–0.35	0.10	0.20–0.55	0.15–0.20

Robbins (1997) proposed another gripper TBM concept (never used), which was the so-called "Low Pressure Walking Blade Canopy" (Figure 2.8e). In this concept the upper part of the cutter head shield of the gripper TBM would be deformable (a blade shield with the capability of exerting a support pressure) while the bottom part would be practically rigid.

For the friction between shield skin and ground, a coefficient according to Table 2.3 can be assumed. In the Arrowhead Tunnels (USA, single shielded TBM, D = 5.82 m), a field test along the first 15 m of the TBM drive has been carried out. The skin friction coefficients determined in situ amounted between 0.37 and 0.45 and agreed well with the values for rock-steel-contact reported in Table 2.3. As expected, the higher values have been registered when starting up the TBM (static instead sliding friction). The injection of lubricants such as bentonite can reduce considerably the friction between shield and ground (Table 2.3). The lubricant is injected through the shield {2-9, 2-18}. A thin lubricant film suffices to reduce skin friction. Therefore the bentonite should be sprayed and not be pumped, in order to reduce the amount needed and the risk of an uncontrolled flow of the suspension towards the cutter head (Schmid, 2008).

As a further measure for single and double shielded TBMs, Grandori (1996) as well as Vigl and Jäger (1997) remarked that it is advantageous to have the possibility of accessing the rock mass through the shield in order to be able to intervene (e.g., to free the TBM by hand-mining) whenever required. According to Grandori (2001) this is possible for double shielded TBMs through openings in the shield or through a complete opening of the telescopic shield. Before initiating such an operation, a careful evaluation should be made as to whether the stability of the rock mass is sufficient for ensuring working safety.

2.4.5 Thrust force and torque

Improvements in TBM technology allow the installation of higher thrust forces and torques (see also the TBM technical data collected in Section 5.2.3).

For gripper TBMs, the achievable reaction forces have to be borne in mind when selecting the installed thrust force and torque. For given ground parameters {1-7, 1-9, 1-18}, the achievable reaction forces depend primarily on the dimensions of the grippers and on the installed gripper force {2-7, 2-9, 2-18} (cf. Section 2.3.2). The total gripper force (perpendicularly to the tunnel axis) is, as a rule, higher by a factor 2.0 to 3.5 than the installed thrust force. An actual gripper TBM with a boring diameter of about 10 m can dispose of an installed thrust force of about 30–35 MN and a breakout torque of about 10–15 MNm.

For shielded TBMs with a similar boring diameter, a thrust force of up to 150–200 MN and a breakout torque of up to 30–40 MNm are nowadays feasible. As a temporary solution, the thrust force can be increased on the construction site by installing removable auxiliary hydraulic jacks. This has been done, for example, in the Uluabat Tunnel (Turkey, single shielded TBM, D = 5.05 m), in the Arrowhead Tunnels (USA, single shielded TBM, D = 5.82 m) and in the Section 4 of the Pajares Tunnel (Spain, single shielded TBM, D = 9.88 m). The TBM of the Uluabat Tunnel had an installed thrust force of 27 MN, which has been temporarily increased to 46 MN. The TBMs of the Arrowhead Project had an installed thrust force of 29 MN for normal operation and a maximum possible thrust

force of 37.5 MN. After a modification of the TBMs on site, the installed thrust force has been increased to 58.5 MN. Furthermore, a thrust force of up to 114 MN could be achieved temporarily by applying 11 removable auxiliary hydraulic jacks. In the Pajares Tunnel the TBM became trapped in squeezing ground in spite of the very high installed thrust force of 193 MN. The thrust force was temporarily increased to 225 MN in order to resume the excavation. In the first project, the segmental lining became damaged, while in the second and in the third project, it has already been able to bear the higher axial loads.

As reported by Iwasaki et al. (1999), Shimaya (2005) and Terada et al. (2008), a design combining the thrusting systems of gripper and single shielded TBM (Figure 2.8f) was developed and applied for the drive of the Hida Tunnel (Japan, D = 12.84 m). Along the entire TBM drive, a 45 cm thick segment was installed in the tunnel floor. The upper part of the bored profile was supported, depending on the ground conditions encountered, either with rock bolts and shotcrete or with seven, 25 cm thick segments. The thrusting mode (i.e., grippers or hydraulic jacks) was chosen according to the support applied. The possibility of installing a segmental lining was foreseen in order to achieve a higher thrust force (55 MN in single shielded TBM mode vs. 33 MN in gripper TBM mode) and to achieve a faster (and, therefore, favourable {16-10, 17-10}) TBM advance in difficult ground conditions, including but not limited to squeezing ground. The papers referred to do not describe any practical experience with squeezing ground that might or might not confirm the suitability of this concept.

2.4.6 Back-up equipment

The production rate of the TBM may also be affected by the performance and layout of the back-up equipment. From a logistical point of view, it is very important that supplies to the machine area and mucking out, as well as all activities in the back-up area (e.g., casting of an invert arch), do not affect TBM performance {3-17}. A robust design of the back-up equipment is important for reducing mechanical breakdowns, which might also affect TBM advance {3-19}.

Problems in the back-up area may also slow down or even halt the TBM drive {13-19, 14-19}. Jamming of the back-up equipment is particularly critical, as it always leads to the machine being stopped and, possibly, further problems as well {19-10, 19-13, 19-14}. Therefore, it is a good idea to make the back-up trailers small enough relatively to the boring diameter to gain some space in case of unexpectedly high ground deformations in the back-up area {3-13, 3-14}, i.e., if the support installed should not suffice to prevent ground deformations {5-13, 5-14, 6-14}.

It has also to be borne in mind that the options for intervention in the back-up area are limited to certain areas only, which are pre-determined by the design of the back-up equipment. As discussed in Section 2.3.2, this is particularly important for gripper TBMs. These constraints must be considered when planning a TBM drive for squeezing ground and, where necessary, requirements must be formulated in the TBM specifications.

2.4.7 Tunnel support

Concerning conceptual design of tunnel support in squeezing ground, a distinction is usually made between two principles: the "resistance principle" and the "yielding principle" (Kovári, 1998). In the first case, one applies a practically rigid lining, which must be strong enough to bear the ground pressure developing when preventing ground deformations. In the second case, one avoids the development of excessive ground pressures by accepting a certain amount of ground deformation. In reality, the interaction between lining and ground leads as a rule to a situation that is somewhere between the two extremes. For the sake of simplicity, however, the following discussion will retain the distinction between a practically rigid and a yielding support.

It should be noted that the tunnel support – besides ensuring stability and limiting deformations of the tunnel – may also reduce shield loading. The installation of a stiff support immediately behind the shield improves load transfer by arching in the longitudinal

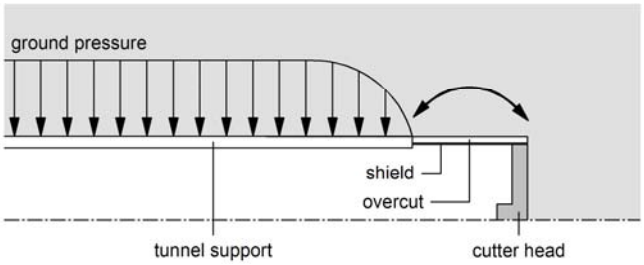

Figure 2.11. Arch action in longitudinal direction around the shield in the presence of a rigid lining.

direction (Figure 2.11), thus leading to a reduction of the ground pressure acting upon the shield {5-10} (cf. Sections 3.3.4 and 3.4.4). This effect is more pronounced for short shields and stiff linings according to the "resistance principle". On the other hand, the load developing upon a stiff lining installed immediately behind the shield is bound to be higher than the load upon a more deformable support installed at a greater distance behind the face.

Practically rigid supports

Segmental linings (the standard support with shielded TBMs) can be classified – on the basis of their high stiffness and strength – as tunnel supports which follow the "resistance principle". Prefabrication makes it possible to achieve high uniaxial compressive strengths in the concrete (up to 50 MPa or even more) with sufficient levels of reliability and thus the ability to cope with high ground pressures. In order to be able to utilize fully the installed thrust force and torque, the lining design has to take into account of course the combined action of ground pressure and TBM forces. A proper and fast-acting embedment of the segmental lining is very important for its bearing capacity. Rapidly setting, two-component grouts (applied through the shield tail as in soft ground TBMs) may be advantageous in this respect.

For shielded TBMs, it has also been proposed to use the segmental lining to support the tail shield in the case of major squeezing. For the Wienerwald Tunnel (Austria, single shielded TBM, D = 10.67 m) this has been planned as a counter measure for unexpected stops of the TBM drive in squeezing ground (Matter et al., 2007). As a similar special measure, Gütter (2007) suggested inserting air cushions between the tail shield and the segmental lining in order to provide a temporary support to the tail shield, which, as a rule, is thinner and less stiff than the rest of the shield.

As an alternative for implementing the "resistance principle", Babendererde (1986) proposed the use of extruded concrete: fluid concrete is extruded at a constant pressure directly behind the TBM, thus filling the gap between the bored profile and a slipform continuously during TBM advance. The advance rate is regulated with the quantity of pumped concrete. An advantage of this solution is the lower cost of ordinary concrete compared to precast segments. Furthermore, the continuity of the concrete extrusion allows for a continuous and, therefore, fast advance of the TBM drive. Additionally, no backfilling material is required and a proper bedding of the lining is assured. Nelson et al. (1992) and Einstein and Bobet (1997) also emphasized the advantages of a machine employing extruded concrete, particularly in combination with a shorter shield than the one of Babendererde (1986), and proposed the so-called "MIT Continuous TBM" (Figure 2.8g). The papers referred to do not describe any case histories where these TBM concepts have been applied in squeezing ground. In spite of the practical applications reported in Babendererde and Babendererde (2001), extruded concrete has not been established in tunnelling practice. One reason for this seems to be the high mechanical complexity of these machines. Furthermore, it is questionable whether the thrust force requirements for squeezing ground can be satisfied. A high thrust force would not be possible, as it would increase the fluid concrete pressure and this would be problematic for the bearing capacity and the sealing of the slipform.

In the case of gripper TBMs, the applicability of the "resistance principle" is more limited than in shielded TBMs because it is difficult to achieve the same high quality and resistance for the shotcrete applied in the machine area as in the case of a prefabricated segmental lining. In order to achieve a comparably high support resistance, a large quantity of shotcrete must be applied and this slows down the advance rate considerably. Furthermore, the load on the tunnel support in the machine area increases with the advance of the tunnel face and this happens simultaneously with the hardening of the shotcrete. The higher the gross advance rate, the lower will be the strength and stiffness of the shotcrete in the machine area {16-5, 17-5} and, therefore, the less the shotcrete will contribute to the load bearing action in the longitudinal direction around the shield (Figure 2.11). This is unfavourable for the shield {5-10}. During long standstills, however, the longitudinal arch action between core and tunnel support can be enhanced by building a thicker shotcrete ring (30 cm or more) immediately behind the shield. This leads to lower shield loads, as discussed above. Such a precautionary measure was applied, e.g., in the Faido Section of the Gotthard Base Tunnel (Switzerland, gripper TBM, D = 9.43 m) during the holiday break of Easter 2008.

Yielding supports

In tunnelling with gripper TBMs, the same yielding supports can be applied as for conventional tunnelling. The Northern Section of the Vereina Tunnel (Switzerland, D = 7.64 m) and the Sections Amsteg (D = 9.58 m) and Faido (D = 9.43 m) of the Gotthard Base Tunnel (Switzerland, cf. Section 4.3) may be mentioned as practical examples.

The applicability range of the "yielding principle" is, nevertheless, strongly limited by the fixed geometry of the tunnelling equipment and the required clearance profile. The design of the yielding support must be considered when selecting the boring diameter and the dimensions of the back-up equipment in order to avoid costly (and sometimes dangerous) re-profiling works or jamming of the back-up equipment {3-13, 5-13, 3-14, 5-14, 6-14}. The continuous adjustment of the boring diameter using overboring techniques is still not sufficiently reliable today (cf. Section 2.4.3) and, if at all feasible, the increase that can be achieved in the boring diameter is also limited (Table 2.2). On the other hand, the choice of a fixed, but larger boring diameter for the entire tunnel is often not economical.

It should be also noted, that the deformability of the lining leads to a reduction of its loading, but weakens the longitudinal arch action and thus leads to an increase in the ground pressure acting upon the shield {5-10}. Furthermore, allowing larger deformations may lead to major loosening phenomena or to a softening of the ground. This has to be taking into account in the design of the deformable tunnel support. In addition to an appropriate structural detailing, a sufficiently high yield pressure is very important for safety (Anagnostou and Cantieni, 2007; Cantieni and Anagnostou, 2009b), but may be difficult to be achieved in combination with shotcrete because (in contrast to conventional tunnelling) the advance rates are high relative to the time needed for shotcrete hardening. Steel sets with sliding connections are advantageous in this respect. Furthermore, long bolts (> 5–6 m for common cross-sections of traffic tunnels) are indispensable, particularly for coping with non-uniform rock convergences and in order to ensure the stability of deformable tunnel supports during the yielding phase (cf. Section 4.3.3). It should be noted that systematic bolting (in contrast to shotcrete or steel sets) does not consume bored space, thus leaving more space free for the ground deformations to occur. The support pressure achievable by bolts is, nevertheless, rather low (0.1–0.3 MPa).

In tunnelling with shielded TBMs, coping with squeezing pressure may necessitate very thick segments, which, besides increasing the required boring diameter, are difficult to handle. Deformable segmental lining systems specifically for shielded TBMs have therefore been the subject of intensive past and current research and development (e.g., Vigl, 2003; Schneider et al., 2005; Billig et al., 2007a). Such deformable linings could be applied either with a "conventional" TBM or, as proposed by Baumann and Zischinsky (1993), Robbins (1997) and Wittke-Schmitt et al. (2005), in combination with the alternative TBM concepts illustrated in Figure 2.8a–e.

A deformable segmental lining can be realized basically in two ways: either, (i), by arranging a compressible layer between the ground and the lining (the ground experiences convergences, while the deformations of the lining remain small, Figure 2.12a); or, (ii), by

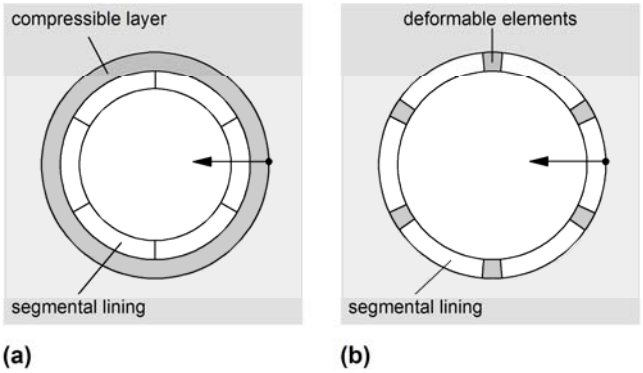

Figure 2.12. Concepts for deformable segmental linings: (a) compressible layer between rock and lining; (b) deformable elements in the longitudinal joints between the segments.

arranging special deformable elements in the longitudinal joints of the lining that allow for a reduction of its circumference (Figure 2.12b).

Yielding layers between segmental lining and ground

The basic idea has been proposed and was patented in England in 1979 – J. Mowlem, UK Patent application GB 2013 757 A, cf. Schneider et al. (2005). For a TBM drive through swelling ground, Lombardi (1981) proposed the application of a compressible layer consisting of polyurethane foam. Wittke-Schmitt et al. (2005) investigated the possibility of using expanded clay as a backfilling material in combination with the alternative TBM concept of Figure 2.8c. (Note that in order to allow radial ground deformations of 1.20 m and considering the deformability of the expanded clay, the concept requires a radial annular gap of 2.40 m, thus leading to a boring diameter of 15.10 m.) Vigl (2003) presented a "convergence-compatible" segmental lining. The segments in this so-called "CO-CO-system" incorporate at their extrados supporting ribs which are in contact with the rock. The ground is allowed to squeeze into the space between the ribs, which can be either empty or filled by a compressible material. Another possibility is given by the addition of a compressible layer fixed at the extrados of the segments in combination with a traditional annular grouting or a compressible grout (Schneider et al., 2005; Billig et al., 2007a).

A compressible annulus grouting material must have, with the exception of a high deformability of course, all of the other usual properties of gap grouting materials: easy processing, pumpability and high stability of the material. For these and for economic reasons light weight concrete is usually proposed (Strohhäusl, 1996). Schneider et al. (2005) developed the so-called "Compex", a compressible mortar with expanded polystyrene that can be compressed up to 50 %. Billig et al. (2007a) reported about the development of the so-called "DeCo Grout", a cement-based pumpable mortar with expanded polystyrene pearls and foam, which is also characterized by a maximum compression of about 50 %.

Deformable longitudinal joint elements

Wood was often used in the past as a compressible element in mining (Figure 2.13a) and it is interesting to note that it was also applied in combination with prefabricated concrete elements many years ago (Lenk, 1931). Recent, mainly experimental, attempts to increase the flexibility of precast segmental linings utilized neoprene elements or hydraulic devices, which are arranged in the longitudinal joints (Figure 2.13b–c).

Brunar and Powondra (1985) reported on the development of the so-called "Meypo deformable elements", which should be placed in the longitudinal joints of a segmental lining and allow for a reduction of its circumference by 1.80 m (6 joints, each experiencing a compression by 30 cm). According to the authors, these elements have been designed with such a high yield load (3 MN) that the lining already offers a considerable support pressure at small ground deformations and this is important in order to avoid loosening or

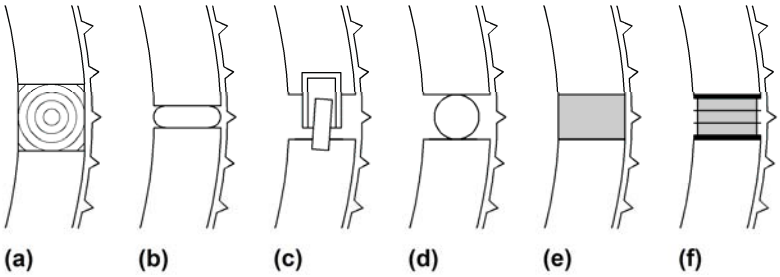

Figure 2.13. Prefabricated segmental lining with compressible longitudinal joints: (a) wood (Lenk, 1931); (b) neoprene layers and flatjacks (Croci, 1986); (c) hydraulic jacks (Baumann and Zischinsky, 1993); (d) steel tubes (Tusch and Thompson, 1996); (e) highly deformable concrete elements (Kovári, 2005); (f) Wabe-elements (Podjadtke and Weidig, 2010).

ravelling of the ground. The Meypo deformable elements have been applied in a tunnel in the Ibbenbüren Coalmine in Germany at a depth of about 1500 m (inner diameter of the segmental lining 9.47 m). In this case, however, the tunnel was driven conventionally, support during excavation consisted of shotcrete and rock bolts and the segmental lining was applied as a final tunnel support. The deformable elements fulfilled expectations, but it was also realized that the costs of such a solution would be too high for it to be systematically applied in tunnelling (Maidl et al., 2001). The suggestion was therefore made of deploying reusable deformable elements, which must be removed after the ground has deformed and before setting the system rigid by applying shotcrete into the longitudinal slots. Baumann and Zischinski (1993) proposed the use of hydraulic jacks for this purpose. These are also expensive, slowing down installation considerably and necessitating heavy reinforcement in order to overcome burst and shear forces.

As reported by Croci (1986), hydraulic jacks have also been applied earlier in the Tunnel Santomarco (Italy). In a section with squeezing crystalline and phyllitic rock, excavation was carried out mechanically under the protection of a shield (Caldarella, 1986). In order to reduce the load acting upon the segmental lining (45 cm thick, inner diameter 7 m) hydraulic jacks were introduced into the longitudinal joints in combination with deformable neoprene elements, which were glued onto the segments and allowed a convergence of 1 %. This application had mainly an experimental character. After 2.5 months, it became necessary to strengthen the tunnel support by applying steel sets and shotcrete.

The technical literature also includes other types of deformable elements. So, for example, Strohhäusl (1996) proposed plastic bodies, which are made from the same material as sealing gaskets and have cavities which can be filled with more or less stiff materials like polyurethane or lightweight concrete. The mechanical properties of these deformable elements can be regulated by determining the volume and the infillings of the cavities. Another possibility is the application of steel or plastic pipes, which become ovalized at a certain hoop force (Maidl et al., 2001). According to a method patented by Tusch and Thompson (1996), the steel tubes (Figure 2.13d) should be filled by a fluid and, in order to control the hoop force, be equipped with pressure valves.

Other technical options include the highly deformable concrete elements (Figure 2.13e) proposed by Kovári (2005) and the so called "Wabe-Elements" (Figure 2.13f) of the Bochumer Eisenhütte Heintzmann Company. Kovári's (2005) elements are composed of a mixture of cement, steel fibres and hollow glass particles and collapse at a pre-defined compressive stress depending on the composition of the concrete. Their main characteristic is that they exhibit a fairly high yield pressure, which is favourable with respect to the final load (Cantieni and Anagnostou 2009b). The recently developed Wabe-Elements (Podjadtke and Weidig, 2010) are designed as honeycomb-type steel tubes or grids positioned between two contact plates. The yielding load of these deformable elements depends on the size of the steel tubes or grids used.

On the appropriate support concept

Apart from a 20 m long successful test drive in no squeezing ground (Gamper et al., 2009; Schneider and Spiegl, 2009) accomplished with the "Compex" compressible mortar in the framework of the Jenbach Tunnel (Austria, mixshield, D = 13.00 m), up until today, in spite of considerable research and development efforts, no successful implementation of the "yielding principle" has been achieved for a shielded TBM with a segmental lining (Schneider and Spiegl, 2008). The reasons for this can be traced back to some critical aspects, which are common to all proposed concepts.

There is, first of all, a fundamental difference between implementing the yielding principle in a gripper TBM (or in conventional tunnelling) and implementing the yielding principle in a shielded TBM. In the first case, the tunnel support (which consists usually of shotcrete, steel sets and bolts) has as a rule only a temporary function: it has only to ensure stability and to preserve the shape of the opening during construction. After construction of the final lining by cast-in-situ concrete, the condition of the temporary support (whether heavily cracked or deformed) is absolutely irrelevant. This is not true for a tunnel support by precast segments as this support represents in most cases (with the exception of a few Swiss tunnels having a second inner lining of cast-in-situ concrete) the final lining as well and has, in general, to fulfil two requirements in addition to safety: the geometry of the clearance profile must not deviate too much from the theoretical one and, as a rule, the lining must be practically waterproof. The uncertainties are large with respect to these objectives, because a flexible lining adjusts its shape to the ground deformations and the distribution of the latter along the circumference of the opening cannot be predicted with sufficient reliability. This is true not only for segmental linings that stay in contact with the ground and consequently follow the ground deformations (i.e., linings incorporating yielding elements in the longitudinal joints), but also for the other type of yielding supports, i.e., for segmental linings that are embedded within the compressible material used for the annulus grouting. Such a system is very vulnerable to non-uniformly distributed pressures. An asymmetrically squeezing ground can displace the lining entirely.

In order to ensure that the clearance profile will not be violated, sufficient tolerances and thus a larger boring diameter are necessary. (According to Schneider and Spiegl (2008), the machine should allow for adjustments in the size of the annular gap.) Concerning continuous adjustments in the gap size, the same critical remarks apply as for the gripper TBMs. Furthermore, a reliable forecast of ground deformations is often difficult. An underestimation of the gap size will cause overstressing of the support. This applies of course to gripper TBMs as well. The difference is, again, that it may be acceptable to exploit a large percentage of the bearing capacity for a temporary structure (shotcrete shell, steel sets, bolts), but for a final structure it is not. A segmental lining has to fulfil the normal standards for permanent civil engineering works.

In addition to the fundamental issues addressed above, there is a series of specific disadvantages. So, for example, systems comprising deformable joints are very costly (in terms of materials and time), particularly if the tunnel lining must be waterproof and, consequently, the deformable elements need to provide a sealing function (another difficult problem, which is, nevertheless, irrelevant to the temporary support applied when employing a gripper TBM).

Questions also arise with respect to the other type of deformable segmental linings (employing a compressible layer between lining and rock). The characteristics of the backfilling material must be such that it is able to deform but at the same time it should be stiff enough to assure a proper bedding of the segmental lining. In general, the application of a compressible layer at the extrados of the segmental lining weakens its bedding (McCusker, 1996) and decreases, therefore, its bearing capacity with respect to non-uniformly distributed loads. A highly compressible backfill decreases the hoop forces but markedly increases the bending moments in the segments (cf., e.g., Graziani et al., 2007). This problem is probably less important for the system proposed by Vigl (2003) which, as mentioned above, foresees ribs at the lining extrados (on the other hand, the concentrated loads arising from the ribs in this system need a high quantity of shear reinforcement). Billig et al. (2007b) acknowledged the "bedding problem" and proposed adjusting the time-dependent development of the stiffness and strength of the compressible

mortar by using an appropriate mixture – a demanding task under construction site conditions.

Finally, a low stiffness of the annulus material may also present problems with respect to the jacking forces. Small, practically unavoidable deviations from the axial direction may push the lining aside. This is particularly true in the case of a rapidly squeezing ground that exerts a considerable load on the shield, thus necessitating a high thrust force in order to keep the machine advancing. In this respect, it is worth remembering that the ground pressure which develops upon the shield when applying a yielding support is in general higher than in the case of a practically rigid lining {5-10}, as the latter facilitates arch action in the longitudinal direction around the shield. A compressible layer around the segmental lining may therefore affect system behaviour in that, (i), it reduces the squeezing pressure acting upon the lining but, (ii), increases the ground loading of the shield and, (iii), this means that it may be necessary to increase the jacking forces, while, (iv), at the same time, the bearing capacity and the stiffness of the lining will in general be lower due to the weaker embedment.

In conclusion, the traditional, practically rigid segmental lining seems to be the appropriate solution for shielded TBMs crossing squeezing ground: precast segments can bear high ground pressures and, if properly bedded, high thrust forces as well. Indeed, it seems to be a contradiction to incorporate expensive, high-quality precast segments (which are constructed with tolerances of 1–2 mm) into a support system that may experience uncontrollable deformations of several cm – 10–20 cm radial convergence after Schneider et al. (2005) and Billig et al. (2007a). The large flexibility of deformable segmental linings is favourable with respect to their structural safety but (almost by definition) unfavourable as regards serviceability requirements, which as said above are particularly important given the permanent character of the structure.

For gripper TBMs, however, yielding supports appear to be more attractive: the serviceability requirements are of secondary importance for temporary supports; the implementation of the "yielding principle" in a gripper TBM bears less risks than in a shielded TBM because the thrusting system does not depend on the behaviour of the support and one can apply the same yielding elements as in conventional tunnelling. It should be noted, however, that the consequent application of the "yielding principle" is rarely possible as the boring diameter and the clearance profile determine the amount of permissible convergence. On the other hand, the implementation of the "resistance principle" may necessitate, depending on the ground pressure, such a thick shotcrete shell that the available space does not suffice. So, both design principles may require the choice of a bigger diameter in order to accommodate either a thicker lining or ground deformations. The scope of action is in fact fairly limited (cf. Section 4.3).

3 The interaction between shield, ground and tunnel support

3.1 Introduction

When evaluating the feasibility of a TBM drive in squeezing ground, it is of paramount importance to understand the mechanisms governing the interaction between shield, ground and tunnel support. For the design of the TBM and the tunnel support, a series of issues must be investigated in relation to the ground pressure p (acting upon the cutter head, the shield and the lining), the convergence of the tunnel wall u, the extrusion rate of the core e, the required thrust force F and the torque T as well as the resulting reaction forces $R_{F,T}$ (Figure 3.1). All of these parameters may also depend on the advance rate v or on the duration of any excavation standstill that may take place.

A number of different analytical, empirical and numerical approaches have been proposed in the literature for the quantitative assessment of these parameters. For a comprehensive review of the literature, the reader is referred to Ramoni and Anagnostou (2011b). The present report follows a numerical approach. Section 3.2 outlines the computational model and numerical solution method used. Sections 3.3 investigates the structural interplay between the ground, shield and tunnel support by means of computational results, using the simplifying assumption of time-independent ground behaviour, while Section 3.4 sketches out and quantifies the most important interrelations between the operational parameters (advance rate, standstill duration) and the time-dependent deformations of squeezing ground. The time-dependency of ground behaviour can be traced back to creep and consolidation processes taking place around the tunnel (Anagnostou and Kovári, 2005). The present report will focus on the consolidation-induced time-dependency of ground response. In order to reduce complexity, the effect of creep is not taken into account here.

3.2 Computational model

3.2.1 Introduction

The interaction between advancing shield, ground and tunnel support will be investigated on the basis of an axially symmetric model (Figure 3.2). The underlying simplifying assumptions are: deep, cylindrical tunnel; hydrostatic and uniform initial stress field; uniform initial hydraulic head field; homogeneous and isotropic ground; constant overcut around

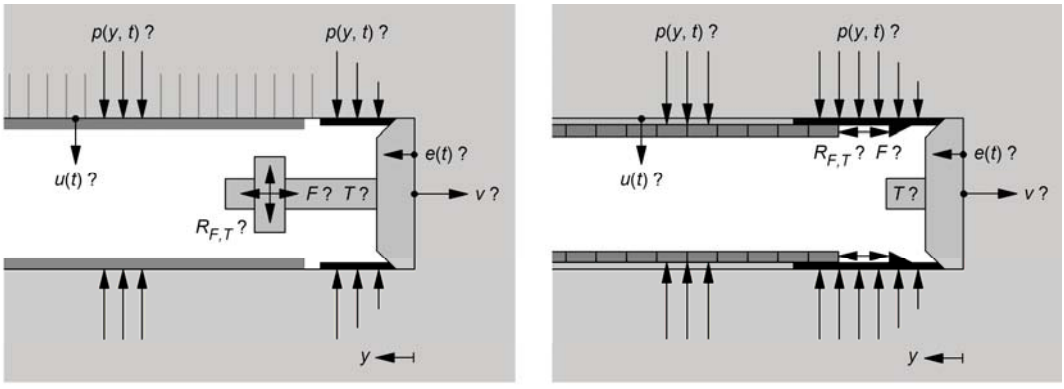

Figure 3.1. Critical parameters for a gripper TBM (a) and a single shielded TBM (b) in squeezing ground.

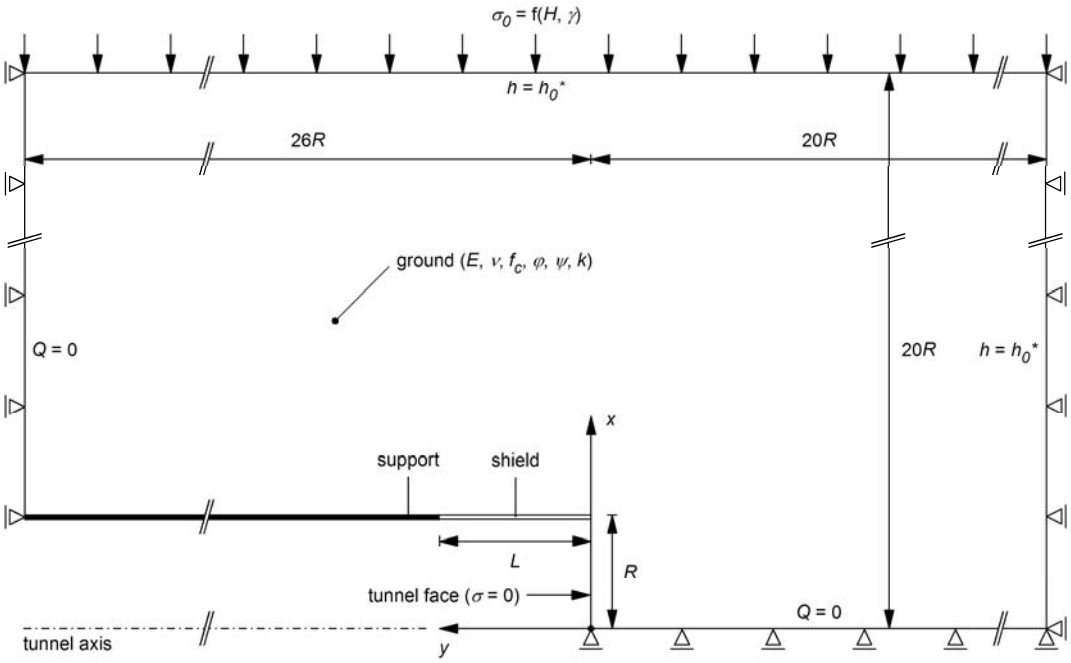

Figure 3.2. Problem layout and boundary conditions.

the circumference of the shield; negligible TBM weight; uniform tunnel support (and uniform annulus grouting along the tunnel periphery in the case of a segmental lining).

The mechanical behaviour of the ground is taken to be linearly elastic and perfectly plastic with the Mohr-Coulomb yield criterion and a non-associated flow rule. As stated in Section 3.1, creep has been disregarded. Pore pressures were taken into account by modelling the ground as a saturated porous medium according to the principle of effective stresses. Seepage flow was modelled by Darcy's law. Cavitation effects have been disregarded. Incompressible ground constituents have been assumed as the effect of the compressibility of the solid grains or of the pore water is negligible in the case of highly deformable weak rocks.

The mechanical and hydraulic boundary conditions at the tunnel face and at the far field boundary can be seen from Figure 3.2. The tunnel face is considered as being unsupported (the effect of a face support is discussed briefly in Section 3.4.4). At the far field boundary parallel to the tunnel axis the radial stress is kept constant to its initial value σ_0. The respective hydraulic head h is fixed to h_0*, where h_0* takes into account the initial hydraulic head h_0, the finite size of the computational domain and the deviation of the simplified axially symmetric head field from the actual one. The boundary value h_0* was estimated by means of preliminary two-dimensional seepage flow analyses according to Ramoni and Anagnostou (2011a).

A discussion of the major assumptions can be found in Section 5.2.1. The following section will briefly address the mixed non-uniform boundary conditions used for the simulation of the shield and the lining as well as the hydraulic boundary condition applied at the tunnel face and wall.

3.2.2 Boundary conditions at the tunnel wall

Ground-support interface

An accurate simulation of the two elements "shield" and "tunnel support" must take into account, (i), their different installation points (y = 0 and y = L in Figure 3.3, respectively) and, (ii), that the shield and the tunnel support experience smaller displacements than the ground at any given point y in the tunnel wall. This is due to the pre-deformation of the ground ahead of the tunnel face $u(0)$ and to the overcut ΔR, which is usually present

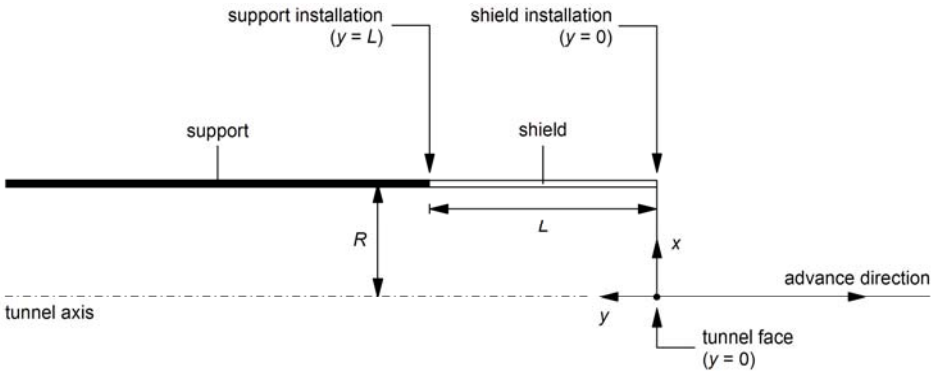

Figure 3.3. Problem layout indicating the different installation points of the shield and of the support.

between the shield and the excavation boundary. In order to take these aspects into account, a mixed and non-uniform boundary condition is introduced, which deals with the characteristics of the shield and of the support.

Shield

More specifically, the boundary condition takes account of the fact that the ground starts to exert a load upon the shield only after closing the radial gap around the shield, i.e., after experiencing an additional deformation of ΔR behind the face, where ΔR denotes the size of the radial gap (Figure 3.4a). After the closure of the gap, assuming that the shield is able to bear the load without being overstressed, there is a linear dependency between the developing ground pressure p and the radial displacement u (i.e., the shield stiffness K_s is constant).

Shields may have a "conical" shape. This so-called "conicity" of the shield is realised with a stepwise reduction of the shield diameter (Herrenknecht 2010, see also Figure 3.5). In the computational model, this can be taken into account defining a variable radial gap size $\Delta R(y)$. A numerical example illustrating the effect of the conicity of the shield will be discussed later in Section 3.3.3.

Tunnel support

With a mixed boundary condition, each kind of tunnel support can be simulated. Figure 3.4b shows the boundary condition applied for practically rigid supports (for example, a shotcrete layer or a segmental lining being immediately backfilled). Note that the assumption of a constant lining stiffness K_l presupposes that the lining is not overstressed. On the other hand, Figure 3.4c shows, in general terms, a definition of the boundary condition that would simulate the non-linear behaviour of a yielding support (for details see the application example described in Section 4.3).

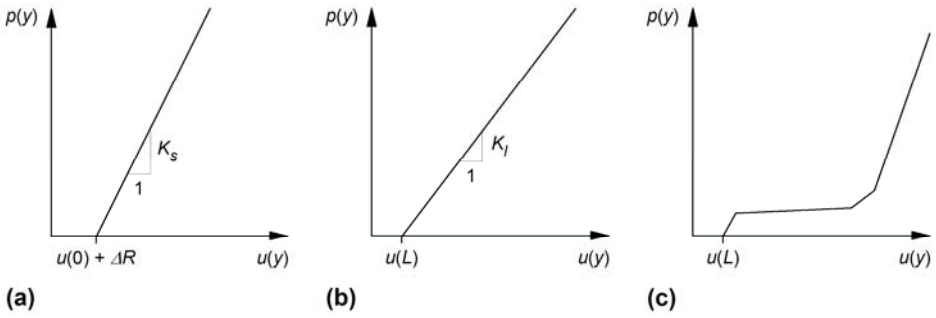

Figure 3.4. Boundary condition at the tunnel boundary for the simulation of: (a) shield; (b) rigid supports; (c) yielding supports.

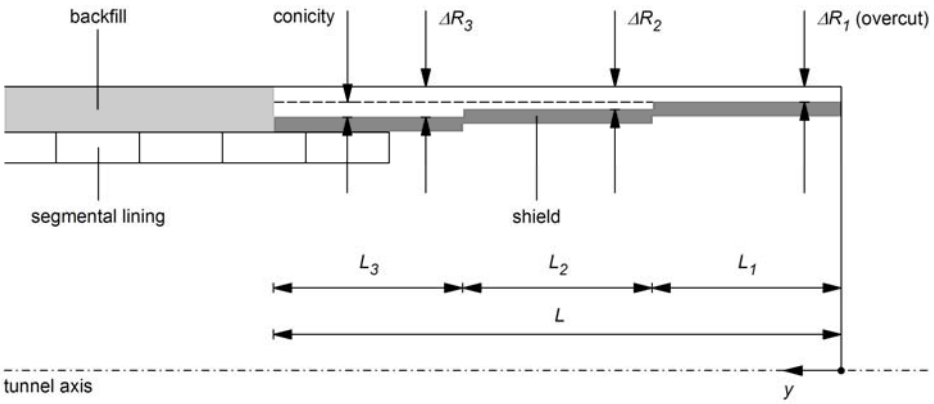

Figure 3.5. Stepwise reduction of the shield diameter (conicity).

As shown later (cf. Section 4.3.3), a detailed simulation of the behaviour of the tunnel support is also important for analyzing its interaction with the shield. More specifically, a rigid support that is installed close to the shield tail facilitates load transfer in the longitudinal direction, thus reducing the ground pressure acting upon the shield. On the other hand, the tunnel support has to bear a higher load in this case.

Hydraulic boundary conditions

Pore pressure at the excavation boundary (tunnel wall and face) can be considered as atmospheric. As a consequence of this boundary condition, a flow towards the ground through the excavation boundary would occur if the pore pressure within the ground were negative (suction). This means that the ground would be watered from the tunnel and presupposes the existence of free water along the tunnel boundary. As this assumption is in most cases unrealistic (Anagnostou, 1995), a mixed hydraulic boundary condition was adopted in order to avoid ground watering via the tunnel: no flow condition in the case of negative pore pressures, atmospheric boundary pressure in the case of positive pore pressures.

3.2.3 Numerical solution method

The numerical computations carried out in the framework of this research project have been performed applying the finite element code HYDMEC of ETH Zurich (Anagnostou, 1992) and using the so-called "steady state method".

The stedy state method was proposed by Nguyen Minh and Corbetta (1991) for solving elastoplastic and elasto-viscoplastic tunnelling problems and extended by Anagnostou (1993, 1995, 2007a, 2007b) for seepage flow or poro-elastoplastic tunnel analyses. This method solves the advancing tunnel heading problem in just one computational step, thus avoiding the extremely high computational cost and the numerical accuracy and stability problems of step-by-step tunnel advance and support installation simulations. Numerical comparisons with the step-by-step simulation of an advancing tunnel can be found in Cantieni and Anagnostou (2009a).

As shown by Cantieni and Anagnostou (2009a), the steady state method corresponds to the limit case of an excavation with zero round length. Therefore, it simulates TBM advance better than the commonly employed step-by-step method does, as the latter requires the arbitrary selection of a finite excavation round length, while TBM advance is actually a continuous process. For the commonly chosen, computationally manageable round length values of s = 1–2 m, the step-by-step method leads to a considerable underestimation of the shield and lining loading (Cantieni and Anagnostou, 2009a). The choice of a smaller round length (s = 0.5 m, cf. Section 4.2.3) improves accuracy but increases computer time (Ramoni and Anagnostou, 2011b).

The steady state method is particularly suitable for the purposes of the present report, not only because it produces an accurate simulation of the TBM advance, which occurs con-

tinuously rather than stepwise, but also because of its computational efficiency. Latter made it possible to carry out comprehensive parametric studies. In this respect, it is interesting to note that the large-scale parametric study underlying the design nomograms presented in Sections 5 and 6, would be practically unfeasible with the step-by-step method.

3.3 Basic aspects of the interaction between shield, ground and tunnel support

3.3.1 Introduction

Section 3.3 discusses some basic aspects of the interaction between shield, ground and tunnel support under the simplifying assumption of time-independent ground behaviour (i.e., disregarding creep and consolidation processes). In this case, the gradual increase in ground pressure and ground deformations in the longitudinal direction is due only to the spatial stress redistribution that is associated with the progressive advance of the working face (Lombardi, 1973).

The interaction between the shield, the ground and the tunnel support will be analyzed by means of numerical examples for the hypothetical case of a 400 m deep tunnel with a boring diameter of 10 m. The tunnel is excavated by a TBM with a 10 m long single shield. The support consists of a 30 cm thick segmental lining being immediately backfilled. The material constants are according to Table 3.1 (Set 1). The effect of a delayed backfilling will be discussed briefly in Sections 3.3.4 and 3.4.4 and more in detail in Section 6.

The ground pressure developing upon the shield is of paramount importance both for the structural design of the machine and for the frictional resistance to be overcome when advancing the TBM. As the ground starts to exert pressure upon the shield only after a certain amount of deformation has occurred, Section 3.3 starts with a discussion of the convergences and pressures developing along the tunnel (Section 3.3.2) and shows how much the geometrical parameters of the shield influence the thrust force required in order to overcome friction (Section 3.3.3). Furthermore, Section 3.3.4 shows that the stiffness of the tunnel support is essential not only for its loading but also for the pressure developing upon the shield.

Table 3.1. Assumed parameters values.

		Set	1	2
		Figures	3.6–3.8	3.9
Tunnel radius	R	[m]	5.00	5.00
Radial gap size	ΔR	[cm]	0–20	5
Length of the shield	L	[m]	6–12/∞	0–12
Stiffness of the shield	K_s	[MPa/m]	1008	1008
Stiffness of the lining	K_l	[MPa/m]	360	0/∞
Initial stress	σ_0	[MPa]	10	10
Young's modulus of the ground	E	[MPa]	1000	2000
Poisson's ratio of the ground	ν	[-]	0.25	0.25
Uniaxial compressive strength of the ground	f_c	[MPa]	3.0	4.5
Angle of internal friction of the ground	φ	[°]	25	25
Dilatancy angle of the ground	ψ	[°]	5	5
Skin friction coefficient	μ	[-]	0.15/0.25/0.30/0.45	0.45
Installed thrust force	F_i	[MN]	150	--
Boring thrust force	F_b	[MN]	0/18	0

3.3.2 Shield-ground interaction

Figure 3.6a shows the radial displacement u of the ground at the tunnel boundary for three values of the size ΔR of the radial gap between shield and ground. The latter determines the amount of convergence that can occur freely.

Figure 3.6b shows the convergence $u - u(0)$ of the bored profile, i.e., the total radial displacement u less the so-called "pre-deformation" $u(0)$ that occurs ahead of the tunnel face. In the case of a normal overcutting (ΔR = 5 cm) the ground closes the gap near to the face (at point A, Figure 3.6b). A larger gap (ΔR = 10 cm) remains open for a longer interval (up to point B).

After closing the gap, the ground starts to load the shield. Figure 3.6c shows the distribution of the ground pressure p acting upon the shield and the lining. The ground pressure increases with the distance from the tunnel face as the stabilizing effect of the core ahead of the face becomes less pronounced. The load concentration at the end of the shield can be traced back to the complete unloading of the tunnel boundary at the installation point of the lining.

As expected, the ground pressure p decreases (both for the shield and the lining) when a larger overboring is provided. In the case of a very large overboring of ΔR = 15 cm the gap between ground and shield would not close at all in this numerical example and the shield would remain unloaded. It should be noted, however, that the feasibility and the reliability of a large overboring has to be checked carefully, particularly for hard rocks (cf. Section 2.4.3).

Figure 3.6 also good illustrates the main advantage of axially symmetric models (such as the one applied for the numerical investigations of the present report, cf. Section 3.2) or three-dimensional numerical models, compared to the characteristic lines method. The latter does not provide the longitudinal distribution of the ground pressure acting upon the shield and the lining, and does not allow for a detailed modeling of the different system components (i.e., ground, shield, tunnel support) and their interfaces.

3.3.3 Thrust force

The thrust force F_f needed to overcome shield skin friction can be calculated by integrating the ground pressure p over the shield surface:

$$F_f = \mu \, 2\pi R \int_0^L p(y)dy = \mu \, 2\pi RL \, p_s \ , \tag{3.1}$$

where μ denotes the skin friction coefficient, R is the tunnel radius, L is the shield length and p_s is the average ground pressure acting upon the shield.

Two operational stages have to be considered with respect to the thrust force requirements: (i) ongoing excavation; (ii) restart after a regular short standstill (e.g., for the installation of the tunnel support or for the execution of routine maintenance work). For stage (i) the thrust force F_b needed for boring must also be taken into account (cf. Section 2.3.2). Therefore, the required thrust force

$$F_r = F_f + F_b \ , \tag{3.2}$$

where

$$F_b = \begin{cases} F_c n_c & \text{for ongoing excavation} \\ 0 & \text{for restart after a standstill} \end{cases} , \tag{3.3}$$

F_c is the maximum cutter force and n_c is the number of cutters. For cutters with a diameter of 17 inches F_c can be taken as equal to 267 kN (Sänger, 2006), while for n_c the following empirical expression applies (Vigl et al., 1999):

$$n_c = 6.7D \ , \tag{3.4}$$

where D is the boring diameter. The two operational stages mentioned above are also

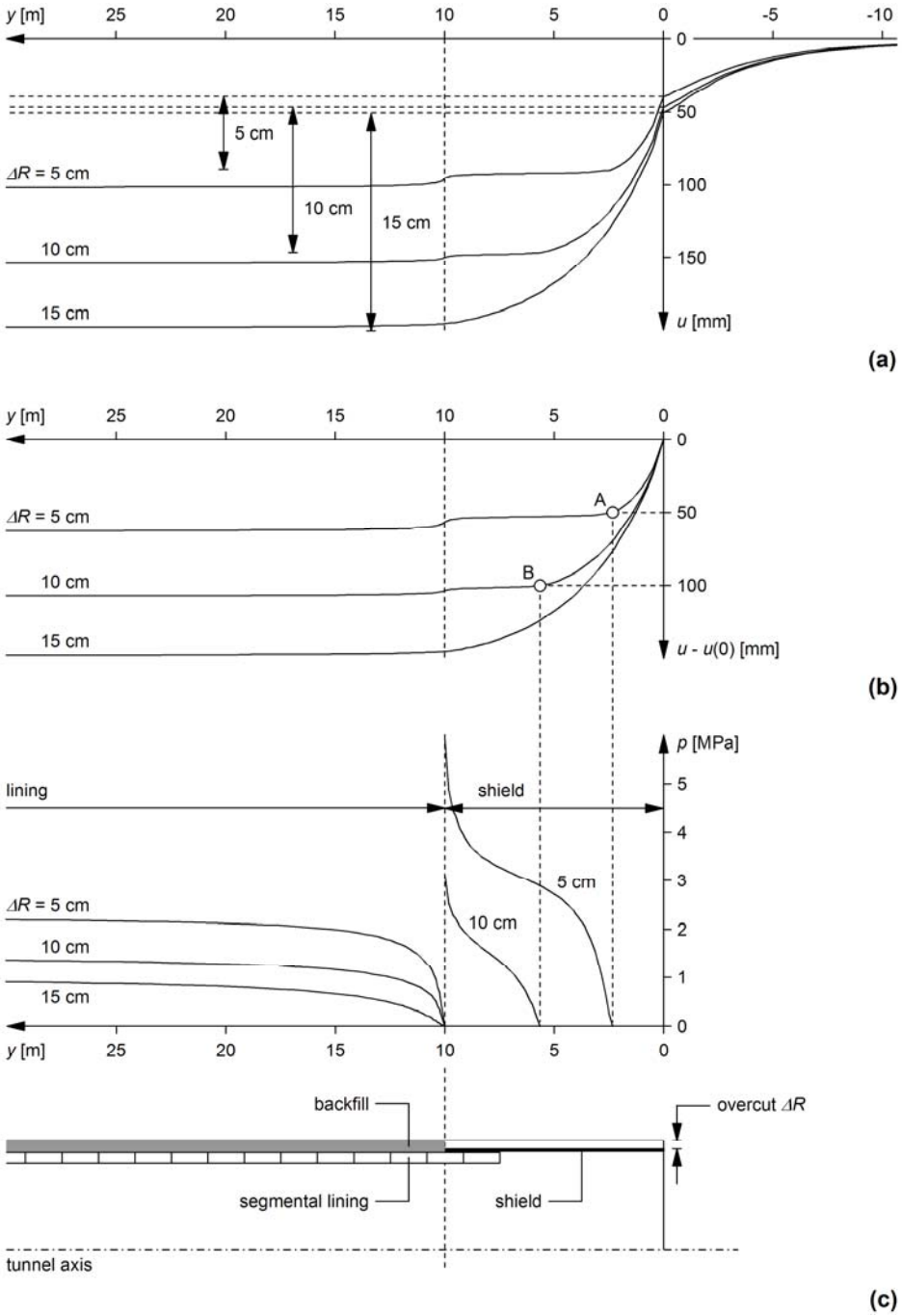

Figure 3.6. Results of numerical computations for a 10 m long shield and for an overboring ΔR of 5, 10 or 15 cm: (a) radial displacement u of the ground at the tunnel boundary; (b) convergence u – u(0) of the bored profile; (c) ground pressure p acting upon the shield and the lining; other parameters according to Table 3.1, Set 1.

different with respect to the skin friction coefficient μ. During ongoing excavation, the TBM has to overcome sliding friction, while static friction has to be taken into account when restarting the TBM.

Figure 3.7a shows the effect of the radial gap size ΔR on the required thrust force F_r for the two operational stages "ongoing excavation" and "restart after a standstill". In this example, the thrust force needed for the boring process has been taken to be F_b = 18 MN. According to Table 2.3, the skin friction coefficient was taken to be μ = 0.15 or 0.30 for sliding friction and μ = 0.25 or 0.45 for static friction, where the lower friction coefficient

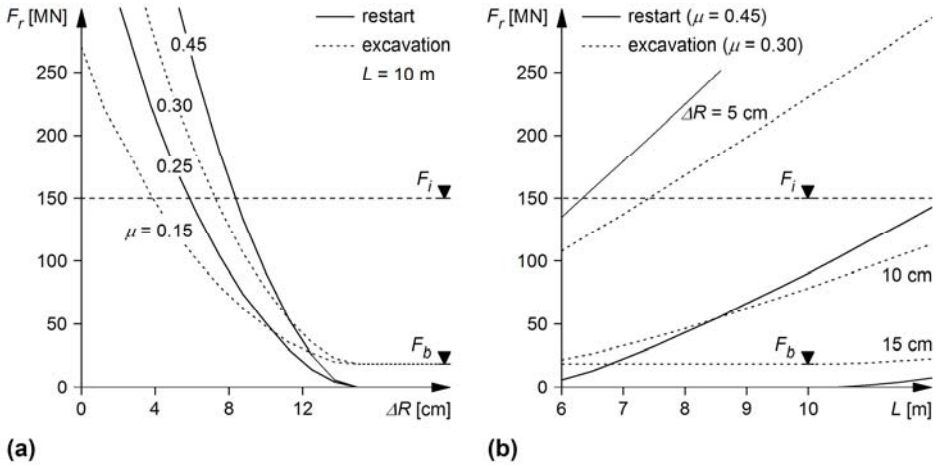

Figure 3.7. Required thrust force F_r during ongoing excavation (thrust force for the boring process F_b = 18 MN) and for the restart after a standstill with (skin friction coefficient μ = 0.15 or 0.25, respectively) or without (skin friction coefficient μ = 0.30 or 0.45, respectively) lubrication of the shield extrados: (a) as a function of the overboring ΔR for a 10 m long shield; (b) as a function of the shield length L for an overboring ΔR of 5, 10 or 15 cm; other parameters according to Table 3.1, Set 1.

values aim to illustrate the positive effects of lubrication of the shield extrados, e.g., by bentonite. The line marked by F_i denotes a high, but still feasible thrust force of 150 MN (see also the TBM technical data collected in Section 5.2.3).

Figure 3.7b shows the required thrust force F_r as a function of the shield length L for the two operational stages and an overcut of ΔR = 5–15 cm. The diagram illustrates the positive effect of a shorter shield. It has to be noted that the dependency of thrust force on the shield length is in general non-linear.

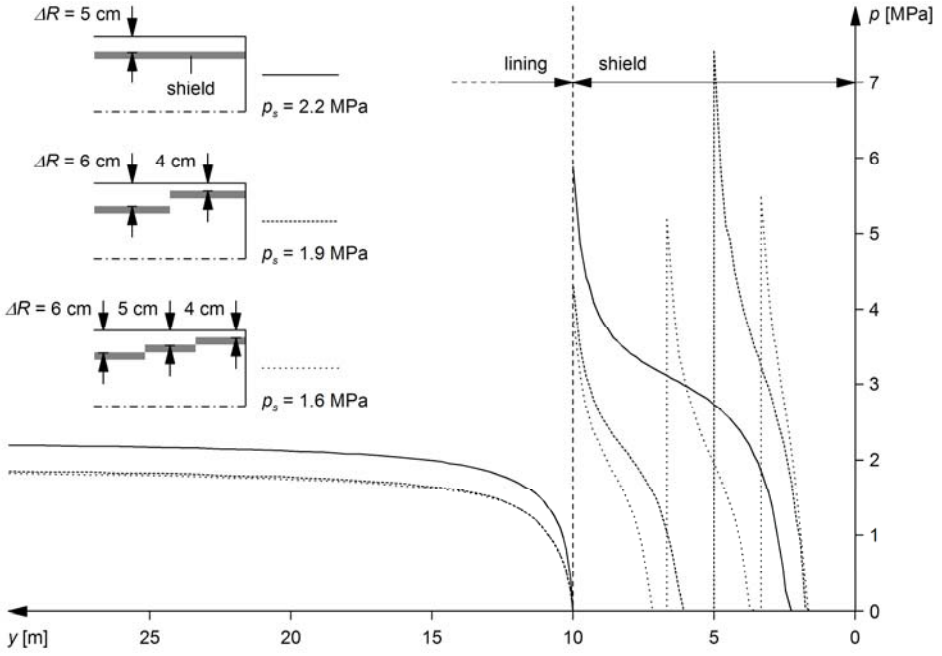

Figure 3.8. Ground pressure p acting upon the shield and the lining for three different shield geometries having the same average radial gap size (shield length L = 10 m, radial gap size ΔR = 4–6 cm; other parameters according to Table 3.1, Set 1).

As shown in a condensed form by Figure 3.7, the required thrust force F_r depends strongly on the shield length L, on the skin friction coefficient μ and on the overcut ΔR. Another important TBM design parameter is the so-called "conicity" of the shield, i.e., the variation $\Delta R(y)$ of the radial gap size along the shield (Figure 3.5). Figure 3.8 shows the ground pressure p acting upon the shield and the lining for three different shield geometries having the same average radial gap size of ΔR = 5 cm. The positive effect of a "stepwise" construction of the shield becomes evident when comparing the average ground pressure p_s (which governs the required thrust force) acting upon the shield. It decreases by 16 or 28 %, respectively, where there are two or three steps in the construction of the shield. A wide gap is more important for the rear part of the shield because the convergence of the ground increases with the distance behind the face.

3.3.4 Shield-support interaction

The installation of a stiff support close to the shield reduces the shield loading and the thrust force requirement because it improves load transfer in the longitudinal direction (cf. Section 2.4.7). (The case of yielding supports will be discussed later in Section 4.3.) The stiffer the lining and the shorter its distance from the face, the more pronounced will be the longitudinal arching effect and the bigger will be the reduction of the shield load.

The upper part of Figure 3.9a illustrates this effect by presenting the thrust force F_r (required for restarting TBM advance after a standstill) as a function of the shield length L for two borderline cases with respect to support stiffness: a rigid support (K_l = ∞) and an

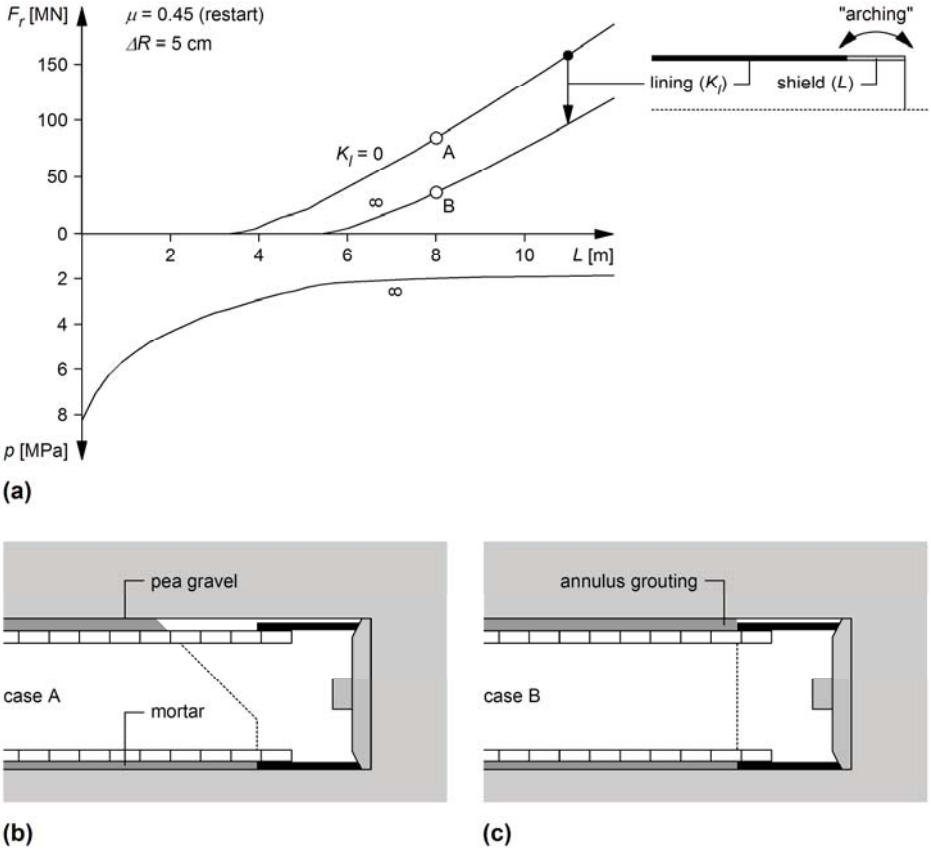

Figure 3.9. (a) Required thrust force F_r and final ground pressure p acting upon the lining as a function of the shield length L for a rigid support (K_l = ∞) as well as for an unsupported tunnel (K_l = 0); radial gap size ΔR = 5 cm, skin friction coefficient μ = 0.45; other parameters according to Table 3.1, Set 2; (b) single shielded TBM in rock with delayed backfilling of the segmental lining (case A of Figure 3.9a); (c) single shielded TBM with annulus grouting via the shield tail (case B of Figure 3.9a).

unsupported tunnel (K_l = 0). As expected, the unloading effect is more pronounced for short shields. A stiff support that is installed close to the face is favourable with respect to the shield but, nevertheless, attracts a higher ground load. In fact, for short shields (where the longitudinal arching effect is particularly pronounced) the final ground pressure p developing upon the rigid support (K_l = ∞) reaches values that cannot be sustained by the usual linings (Figure 3.9a, lower part). As expected, the load of the tunnel support p decreases with increasing shield length L, i.e., with decreasing arching effect.

It should be noted that the case of an unsupported tunnel is not only theoretically possible. As a matter of fact, in shield tunnelling through rock, backfilling of the segmental lining by pea gravel is carried out at a certain distance behind the shield with the consequence that the rock behind the shield actually remains unsupported (Figure 3.9b). There is no unloading effect in this case, of course (point A in Figure 3.9a). Shield load reduction (point B) via longitudinal arching between the face and the segmental lining presupposes annulus grouting simultaneously with TBM advance via the shield tail (Figure 3.9c). The peculiarities of segmental lining installation will be analyzed in Section 6.

3.4 Time-dependency of ground behaviour

3.4.1 Introduction

Although cases of rapidly converging ground are known in the literature (cf. Section 2.2), squeezing ground usually exhibits a markedly time-dependent behaviour. Depending on its characteristics, the ground may respond to the excavation with some delay and may continue to deform over a period of days, weeks or even months (Kovári and Staus, 1996; Barla, 2001). The delay in the ground response is favourable for a TBM because a TBM can accommodate only relatively small convergences in the machine area and the back-up area without running into problems. However, such favourable time effects can be considered in the planning phase only if there is sufficient advance knowledge of how the ground will behave over time. Failing this, it would be unwise to rely upon the assumption that deformations will develop only slowly and far behind the machine.

As a consequence of the time-dependency of ground behaviour, the overall advance rate not only represents the main outcome of the complex interaction between the ground, the TBM and the tunnel support, but also exercises a decisive influence over this interaction (cf. Section 2.3). More specifically, as emphasized repeatedly in the literature, a rapid excavation rate (involving high net advance rates and short standstills) reduces the risk of the shield or back-up jamming (e.g., Lombardi, 1981; Robbins, 1982; Kovári, 1986a, 1986b; McCusker, 1996; Herrenknecht and Rehm, 2007). The frequency and duration of standstills can be reduced through appropriate operational measures and construction site organisation. For example, necessary logistical precautions should be taken in order to allow operations within critical zones to proceed as continuously as possible. However, in spite of every effort, it is not always possible to avoid long interruptions (Lombardi, 1981; Gehring, 1996). Sudden changes in ground conditions, technical problems (e.g., electric power stoppages, mechanical breakdowns of the TBM with consequent repair work, problems in the back-up system), holiday periods, strikes and, of course, a TBM jamming during regular operation can cause unpredictable stoppages. Major maintenance operations are also an important factor as they may lead to an unfavourably long standstill. At the same time, however, they are important for reducing the risk of mechanical breakdown. The conflict in priorities here can be resolved by carrying out any lengthy maintenance operations before entering a critical zone, provided of course that the location of the critical zone is known and its length is sufficiently short that it can be crossed practically non-stop. In this respect, the timely identification of critical zones by means of reliable advance ground probing is very important (Peila and Pelizza, 2009; Anagnostou et al., 2010b).

The time-dependency of ground deformations is due to the creep and consolidation processes taking place around the tunnel (Anagnostou and Kovári, 2005). In the vicinity of the tunnel face, these processes develop simultaneously with the spatial stress redistribution caused by the face advance. Creep is associated with the rheological behaviour of the ground, becoming evident particularly when the ground is highly stressed. It is therefore

very important where squeezing conditions prevail. Section 3.4 will focus on the consolidation-induced time-dependency of ground response. This mechanism comes into play when tunnelling through water-bearing ground. From tunnelling experience, it is well-known that pore water under high pressure encourages the development of squeezing (Kovári and Staus, 1996). Consolidation represents a source of time-dependency in the case of a low-permeability ground. It is associated with the transient seepage flow process that is triggered by the tunnel excavation. Understanding the role of consolidation is important for deep alpine tunnels (Vogelhuber, 2007) as well as current or planned subsea tunnel projects crossing weak rocks, such as the Lake Mead Intake No 3 Tunnel in the USA (Anagnostou et al., 2010b) or the planned Gibraltar Strait Tunnel between Spain and Morocco (Pliego, 2005).

The present section of the report investigates the interaction between shield and ground by means of hydraulic-mechanical coupled numerical analyses, which account for the highly complex transient process of consolidation around the advancing tunnel heading. Section 3.4 starts with a qualitative discussion of the mechanisms underlying the ground response to tunnelling operations (Section 3.4.2) and continues with a quantification of the identified effects. More specifically, Section 3.4.3 deals with conditions during continuous excavation and analyzes the effect of the advance rate on shield loading, while Section 3.4.4 investigates ground pressure development during a standstill.

3.4.2 The consolidation mechanism

Squeezing is associated with overstressing and plastic yielding of the ground. Squeezing ground generally experiences an increase in volume (plastic dilatancy). If the ground is saturated, its water content also increases during squeezing. This occurs more or less rapidly depending on the permeability of the ground. In a low-permeability ground, the water content remains constant in the short term. Since the pore water hinders dilatancy, negative excess pore pressures are generated by to the excavation work. As these are higher in the vicinity of the tunnel than further away, a transient seepage flow process starts to develop towards the tunnel. The negative excess pore pressures dissipate over time, thus changing the effective stresses and leading to additional, time-dependent deformations (Anagnostou and Kovári, 2005). When a shield or a lining hinders ground deformations, the load acting on it will increase over time.

With respect to the transient process, two important states can be distinguished: the state immediately after excavation (i.e., at time $t = 0^+$) and the long-term state ($t = \infty$). The first state is characterized by the condition of constant water content (so-called "undrained conditions"). The second state is governed by the steady state pore pressure distribution (so-called "drained conditions"). As in other geotechnical problems involving "unloading" of the ground (e.g., deep excavations), the short-term behaviour is more favourable than the long-term behaviour. In fact, according to theoretical and experimental investigations (Anagnostou, 2007c; Vogelhuber, 2007), the negative excess pore pressures developing under undrained conditions strengthen the ground temporarily, as they increase the effective stress and thus the resistance to shearing. This so-called "dilatancy hardening" is temporary because the excess pore pressures dissipate with time.

The time-dependent development of ground deformations is governed by the ratio of advance rate v to ground permeability k (Anagnostou, 2007a). If this ratio is high (as in the case of rapid excavation through a low-permeability ground), undrained conditions, which are more favourable, will prevail in the machine area. On the other hand, if the excavation proceeds slowly or the ground permeability is high (low v/k-ratio), unfavourable drained conditions will set in almost immediately after excavation. The advance rate v means the gross advance rate resulting from the boring process and including regular short standstills for the installation of the tunnel support or for the execution of inspections and minor maintenance work. The effects of advance rate and permeability will be investigated quantitatively in Section 3.4.3.

Major maintenance or repair work (planned or not) or other problems may cause longer standstills, which cannot be classified among regular TBM operations and have to be investigated separately. The ground behaviour during such a standstill is governed by the mechanisms described above. If drained conditions have not already been reached dur-

ing the preceding regular excavation (i.e., if the ratio v/k was high enough), consolidation will continue during the standstill period until the steady state pore pressure distribution is reached. Again, due to the change in the effective stresses, the ground will deform and the ground pressure will increase over time. For a given ground permeability, the higher the advance rate during the preceding excavation, the more the conditions prevailing at the beginning of the standstill will deviate from the drained conditions and, consequently, the more time must elapse before the steady state is reached. Rapid excavation is therefore also advantageous with respect to subsequent standstills. The conditions prevailing during standstills will be investigated quantitatively in Section 3.4.4.

The risk of the TBM jamming depends on the ratio v/k as this governs the intensity of the deformations in the machine area. In general, the less permeable the ground, the more rapid the excavation and the shorter the standstills, the closer conditions will be to a favourable undrained state. The range of feasible advance rates is relatively narrow (i.e., v = 30 m/d – in difficult ground conditions v = 5–10 m/d), but the ground permeability k may vary over several magnitudes, thus playing a more important role with respect to the risk of the TBM jamming. As reliable estimations are particularly difficult for heterogenous ground, permeability introduces a prediction uncertainty, which has to be borne in mind in the design phase (Anagnostou and Kovári, 2005).

Similar considerations also apply to the creep-induced time-dependency of the ground response. As shown by Sterpi and Gioda (2007), a high advance rate is favourable as it leads to lower deformations in the machine area. In the borderline case of a very high advance rate, only small, elastic deformations develop in the vicinity of the tunnel face. However, as was the case with ground permeability, a reliable estimation of the ground creep parameters before construction may be very difficult to achieve.

3.4.3 Conditions during regular TBM operation

The role of excess pore pressure dissipation and the effect of the ratio of advance rate v to ground permeability k (cf. Section 3.4.2) will be analyzed by means of numerical computations concerning the hypothetical case of a 400 m deep tunnel crossing weak ground at a depth of 100 m beneath the water table. As in Section 3.3, the tunnel has a diameter of 10 m and is excavated by a 10 m long single shielded TBM. The applied segmental lining is 30 cm thick and supposed to be rigid. Table 3.2 summarizes the material constants and the other model parameters.

Distribution of the pore water pressures

As discussed qualitatively in Section 3.4.2, the distribution of the pore pressures is of paramount importance for the deformations of the ground and, therefore, for its interaction with the shield and for the thrust force that is required for overcoming friction. During regular TBM advance, the ground behaviour will be undrained, drained or somewhere in-between depending on the ratio of advance rate v to ground permeability k.

Figure 3.10 shows the contour lines of the pore pressure p_w for different ratios v/k, thus illustrating the transition from undrained conditions to less favourable drained conditions occurring when the advance rate decreases (or the ground permeability increases). Under practically undrained conditions (i.e., when the v/k-ratio is high), negative excess pore pressures develop within an extended region around the tunnel and dissipate far behind the working face. With a decreasing advance rate (or with increasing ground permeability), the dissipation of the excess pore pressures takes place faster, i.e., closer to the tunnel heading. Of course, the predicted high suctions can occur only in the absence of cavitation (i.e., in extremely fine-grained, clayey ground).

Interaction between shield, ground and support

The higher the ground permeability k (or the slower the TBM advance rate v), the quicker will be the development of the consolidation process and the larger will be the deformations in the machine area.

Figure 3.11a shows the radial displacement u of the ground at the tunnel boundary for different ratios v/k and a radial gap size ΔR of 5 cm (left side) or 10 cm (right side). The

Table 3.2. Assumed parameters values.

			Traffic tunnel	Service tunnel
Ground				
Young's modulus	E	[MPa]	1000	
Poisson's ratio	ν	[-]	0.25	
Uniaxial compressive strength	f_c	[MPa]	1.5 or 3.0	
Angle of internal friction	φ	[°]	25	
Dilatancy angle	ψ	[°]	5	
Permeability	k	[m/s]	variable	
Compressibility of the grains	c_g	[1/MPa]	0	
Compressibility of water	c_w	[1/MPa]	0	
Unit weight of water	γ_w	[kN/m^3]	10	
TBM				
Tunnel radius	R	[m]	5	2
Radial gap size	ΔR	[cm]	5 or 10	
Length of the shield	L	[m]	10	
Stiffness of the shield	K_s	[MPa/m]	1008	3150
Installed thrust force	F_i	[MN]	150	50
Boring thrust force	F_b	[MN]	18	7
Advance rate	v	[m/d]	variable	25
Lining				
Stiffness of the lining	K_l	[MPa/m]	360	1500
Radial gap size	ΔR_l	[cm]	0 [a]	0
Initial conditions				
Initial stress	σ_0	[MPa]	10	
Initial hydraulic head	h_0	[m]	100	
Reduced initial hydraulic head	h_0*	[m]	78	83

Notes

[a] With the exceptions of Figures 3.18 and 3.20, where $\Delta R_l = \Delta R + 7.5$ cm

radial gap size is equal to the difference between the radius of the bored profile and the outer radius of the shield and represents the space which is available for accommodating ground deformations without development of a ground load upon the shield. The radial displacement u according to Figure 3.11a includes the pre-deformation of the ground, i.e., the deformation $u(0)$ that occurs ahead of the face.

The risk of shield jamming depends on the convergence $u - u(0)$ of the bored profile (Figure 3.11b). Figure 3.11b shows that the higher the ground permeability k and the lower the advance rate v, the faster will the convergence develop and the nearer to the tunnel face will be the closure in the radial gap (compare, e.g., point B with point A in Figure 3.11b, left side).

After closing the gap, the ground starts to develop a load upon the shield (Figure 3.11c). The ground pressure p increases with the distance y behind the face and drops to zero at the installation point of the lining. Assuming that the annulus grouting is carried out via the shield tail with a very fast hardening mortar (cf., e.g., Pelizza et al., 2010) and simultaneously with the shield advance, a ground pressure starts to develop upon the lining immediately after its installation at the shield tail.

According to Figure 3.11c, the ratio of advance rate v to ground permeability k is decisive for the shield loading. Consider, for example, the case of a normal overcutting (ΔR = 5 cm, left side). If $v/k \geq 3 \times 10^5$, the ground does not close the gap and the shield remains unloaded, while for $v/k \leq 3 \times 10^3$ a considerable load develops, which may immobilize the shield (due to skin friction) or even endanger its structural safety. It should be noted that the v/k-ratio has the opposite effect on the final pressure developing upon the lining far behind the face. The higher this ratio, the smaller will be the deformations developing prior to lining installation and, consequently, the higher will be the final load (see Figure 3.12 for a numerical example). So, high ratios of v/k are favourable with respect to the risk of shield jamming but not with respect to a possible overstressing of the lining.

A larger radial gap ΔR has, as one might expect, a positive effect with respect to the shield loading, as it remains open for a longer interval behind the face (compare, e.g.,

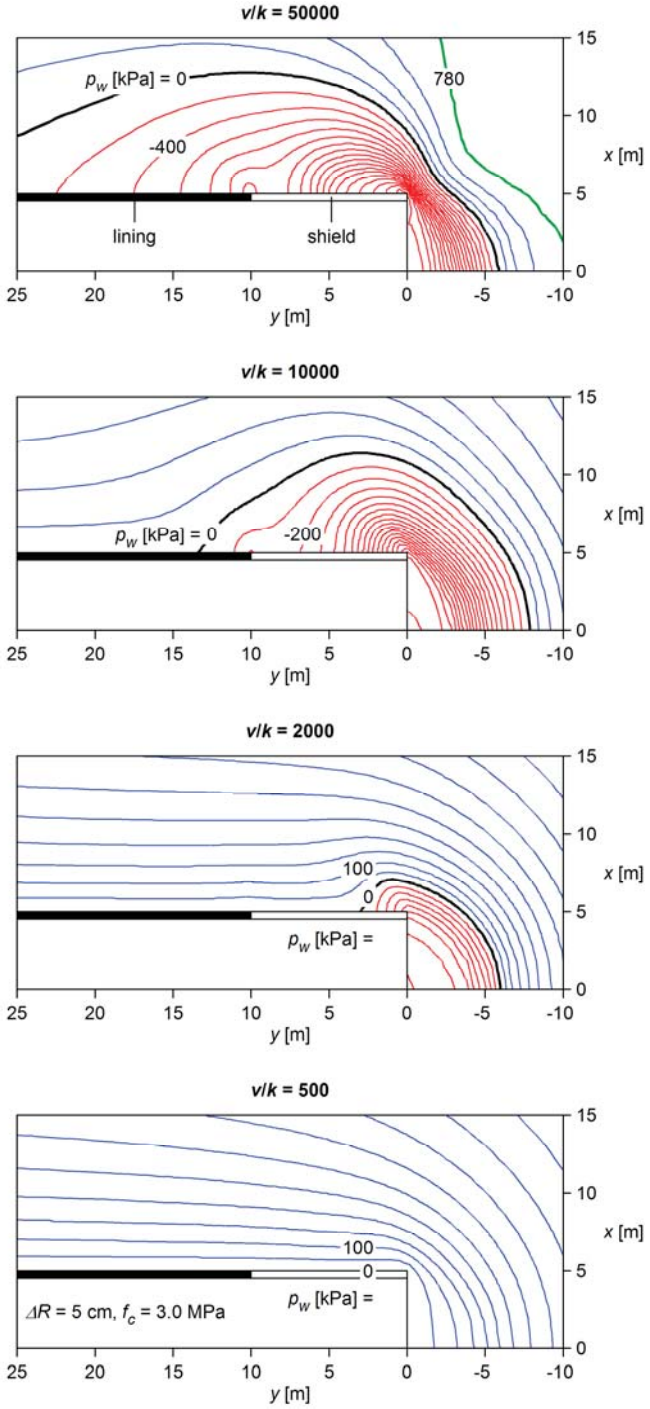

Figure 3.10. Contour lines of the pore pressure p_w for different values of the ratio of advance rate v to ground permeability k (radial gap size ΔR = 5 cm, uniaxial compressive strength of the ground f_c = 3.0 MPa; other parameters according to Table 3.2).

point C with point B in Figure 3.11b, right and left side, respectively) and widens the subcritical range. In order that the shield remains unloaded in this example, the v/k-ratio should be higher than about 3 x 10^5 if ΔR = 5 cm, while a v/k of 2 x 10^4 would be sufficient if ΔR = 10 cm. For a radial gap of ΔR = 15 cm, the shield would remain unloaded even for $v/k \rightarrow 0$ (i.e., standstill or a very rapid, practically time-independent ground response). The feasibility and the reliability of such a large overboring is nevertheless questionable and has to be checked carefully for given project conditions (cf. Section 2.4.3).

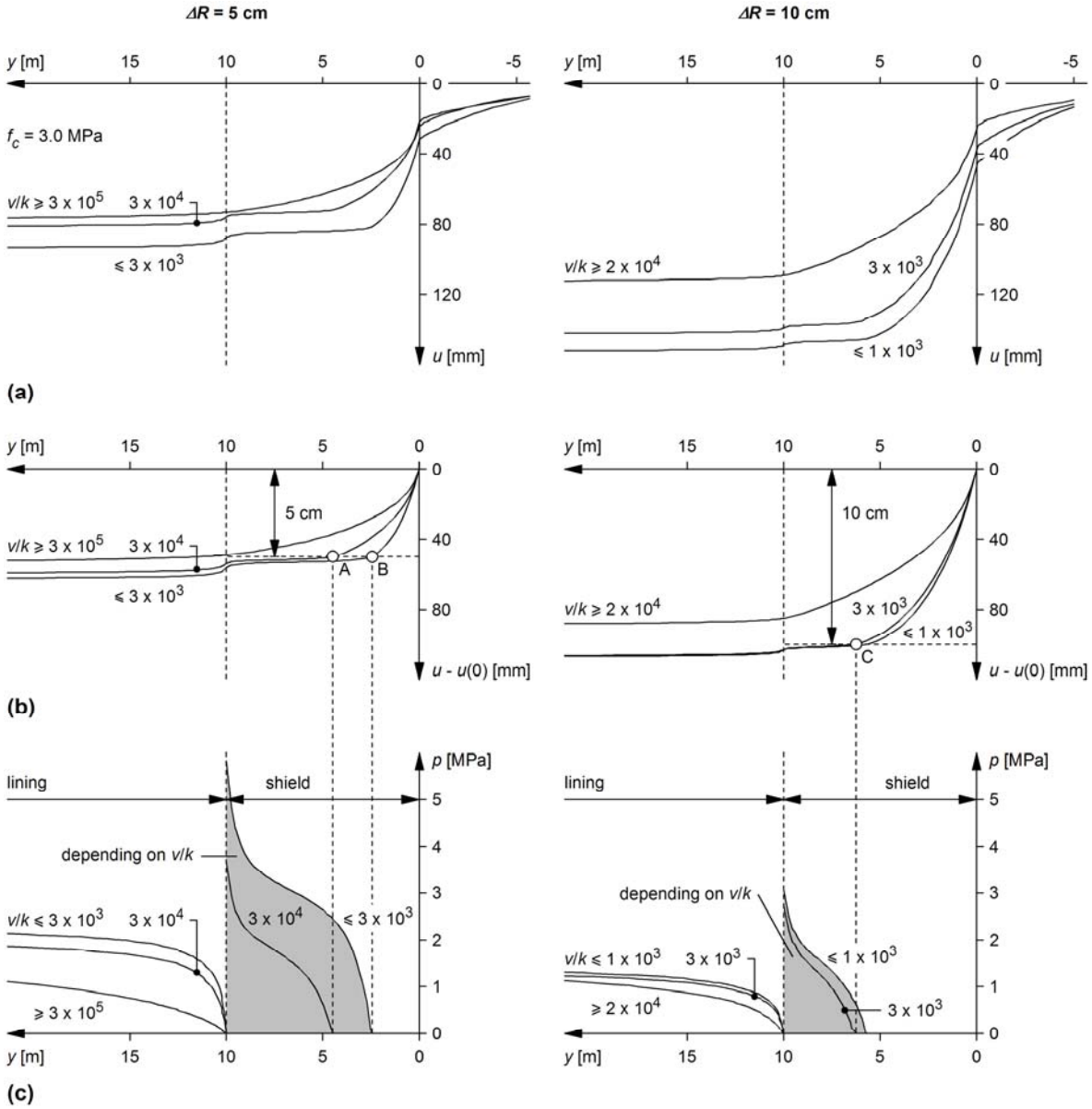

Figure 3.11. Results of numerical computations for a radial gap size of ΔR = 5 or 10 cm (left and right side, respectively) and for different ratios of advance rate v to ground permeability k: (a) radial displacement u of the ground at the tunnel boundary; (b) convergence u – u(0) of the bored profile; (c) ground pressure p acting upon the shield and the lining; uniaxial compressive strength of the ground f_c = 3.0 MPa; other parameters according to Table 3.2.

Thrust force

Figure 3.13 shows the required thrust force F_r as a function of the v/k-ratio for a radial gap size of ΔR = 5 cm (normal overcutting) or 10 cm (overboring). The dashed lines apply to ongoing excavation (the thrust force needed for the boring process has been taken to be F_b = 18 MN in this example), while the solid lines apply to a restart. The skin friction coefficient μ was taken to be 0.30 and 0.45 for sliding and static friction, respectively (according to Table 2.3).

Assuming that the installed thrust force F_i amounts to 150 MN – a high, but feasible value provided that the bearing capacity of the segmental lining is sufficient – and that the radial gap size ΔR is equal to 5 cm, the TBM would be trapped if $v/k \leq 2.5 \times 10^4$ (point A in Figure 3.13), i.e., if v = 1 m/d and $k \geq 4.6 \times 10^{-10}$ m/s or v = 10 m/d and $k \geq 4.6 \times 10^{-9}$ m/s (see axis at the bottom of Figure 3.13). Of course, the required thrust force can be

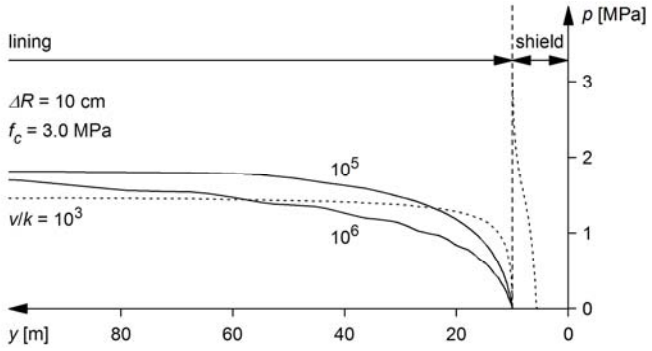

Figure 3.12. Ground pressure p acting upon the shield and the lining for different ratios of advance rate v to ground permeability k (radial gap size ΔR = 10 cm, uniaxial compressive strength of the ground f_c = 3.0 MPa; other parameters according to Table 3.2).

reduced considerably by overboring (to less than 100 MN in this example) – this comes, however, at the cost of possible steering difficulties and reduced production rates (cf. Section 2.4.3).

Besides overboring, another possible countermeasure for coping with squeezing is the lubrication of the shield extrados (e.g., by bentonite). Lubrication reduces the shield skin friction and thus the required thrust force (compare curves for μ = 0.15 or 0.25 with curves for μ = 0.30 or 0.45 in Figure 3.13). The effect of lubrication is smaller than that of overboring in this example. However, as overboring may be not sufficiently reliable, a combination of these two measures would be required in order to mitigate the risk of shield jamming.

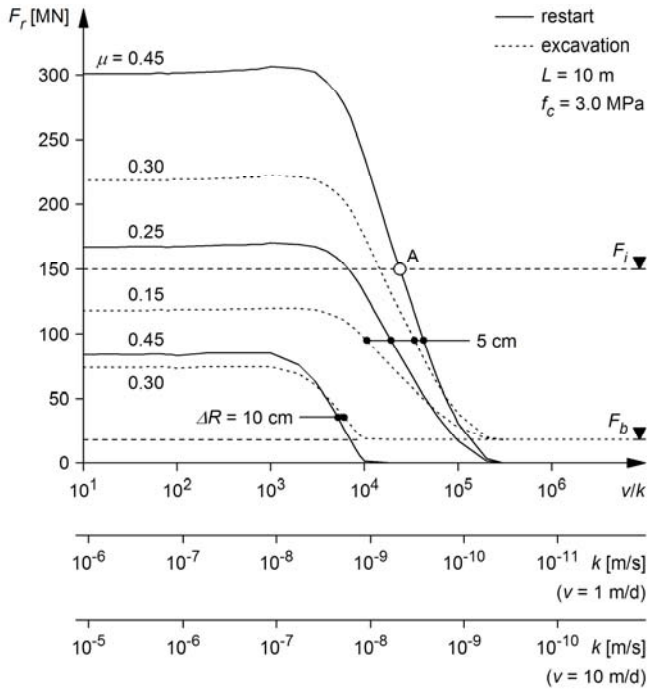

Figure 3.13. Required thrust force F_r during ongoing excavation (including the thrust force needed for boring F_b = 18 MN) and for restart with lubrication of the shield extrados (skin friction coefficient μ = 0.15 or 0.25) or without lubrication of the shield extrados (skin friction coefficient μ = 0.30 or 0.45) as a function of the ratio of advance rate v to ground permeability k (radial gap size ΔR = 5 or 10 cm, uniaxial compressive strength of the ground f_c = 3.0 MPa; other parameters according to Table 3.2).

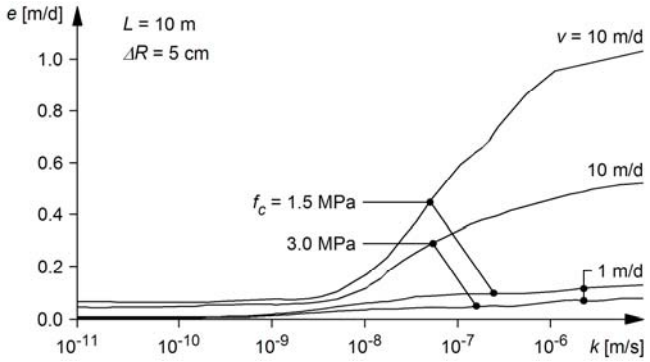

Figure 3.14. Extrusion rate of the core e as a function of ground permeability k (advance rate v = 1 or 10 m/d, radial gap size ΔR = 5 cm, uniaxial compressive strength of the ground f_c = 1.5 or 3.0 MPa; other parameters according to Table 3.2).

Figure 3.13 also shows that the consolidation process is practically irrelevant if $v/k \leq 10^3$ or, taking into account an assumed maximum feasible advance rate of v = 10 m/d, if the permeability k is higher than about 10^{-7}–10^{-8} m/s. There is no observable time-dependency in the ground response in such a case. Unfavourable steady state conditions apply continuously during excavation right from the start and may, depending on the countermeasures applied, affect the feasibility of the TBM drive. On the other hand, if $v/k \geq 10^6$ favourable undrained conditions would prevail and the required thrust force would be considerably lower. In a low-permeability ground ($k < 10^{-10}$–10^{-11} m/s) the shield would remain unloaded even at moderate advance rates of v = 1–10 m/d.

A large sensitivity in the results can be observed for permeabilities k between 10^{-8} and 10^{-10} m/s (cf. Figure 3.13). This permeability range is thoroughly relevant in practice. For example, the extensive laboratory testing program carried out for investigating the kakiritic rocks of the Gotthard Base Tunnel (Lot Sedrun) in Switzerland revealed permeabilities between 1.5 x 10^{-9} and 1.1 x 10^{-10} m/s (Vogelhuber, 2007). This large sensitivity in the numerical results indicates a major source of prediction uncertainty.

Extrusion rate of the core

"Extrusion of the core" means the axial displacement of the working face towards the tunnel. During the boring process, some of the TBM penetration is used up simply to compensate the extrusion, i.e., to excavate the ground that squeezed into the opening from the face. If the extrusion rate of the core e is very high, the penetration effort will be entirely used up in excavating the axially deforming ground at the tunnel face, i.e., the cutter head will penetrate and rotate without moving forward (cf. Section 2.3.2).

In general, the advance rate v actually achieved is the advance rate that would occur in the absence of relevant face deformations minus the extrusion rate of the core e:

$$v = \max(0,\ \alpha P r - e)\ , \tag{3.5}$$

where α is the utilisation degree of the TBM (i.e., the fraction of the total time used for boring), P is the penetration rate (i.e., the TBM advance relative to the ground at the working face per revolution of the cutter head) and r the cutter head rotational speed.

Figure 3.14 shows the extrusion rate e as a function of the ground permeability k for the numerical example considered throughout Section 3.4. The extrusion rate is small relative to commonly achievable advance rates. Since this numerical example concerns rather adverse conditions (in terms of ground strength and depth of cover), the results support the hypothesis that the excavation speed is normally high enough to avoid problems with deformations of the working face (Gehring, 1996; Barla, 2001; Hoek, 2001).

Role of tunnel diameter

An issue sometimes arising in the design phase concerns the option of constructing a smaller diameter tunnel (which may be part of the final structure – e.g., the service tunnel

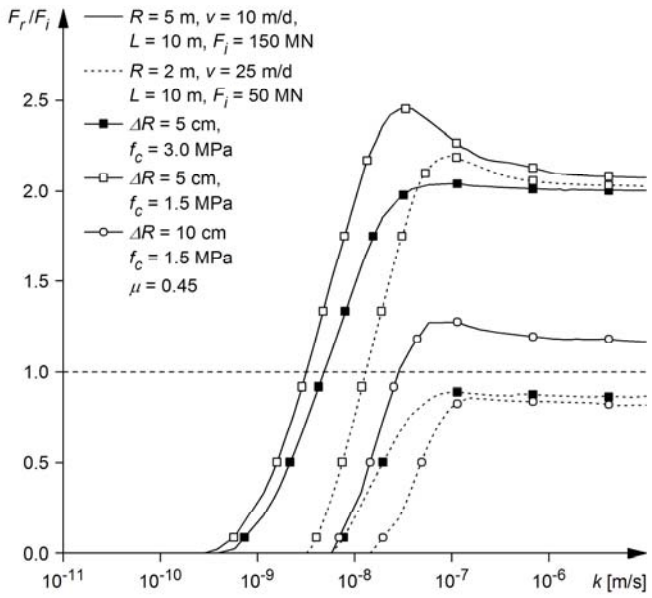

Figure 3.15. Thrust force utilization F_r/F_i for restarting operation of a "traffic tunnel" TBM and a "service tunnel" TBM (tunnel radius R = 5 and 2 m, respectively) as a function of ground permeability k (advance rate v = 10 or 25 m/d, radial gap size ΔR = 5 or 10 cm, skin friction coefficient μ = 0.45, uniaxial compressive strength of the ground f_c = 1.5 or 3.0 MPa, installed thrust force F_i = 150 or 50 MN; other parameters according to Table 3.2).

of a twin railway tunnel) for exploration or ground improvement in advance of the main, larger diameter tunnel. The underlying idea is that the potential geomechanical problems are less serious in the case of a smaller cross-section. It is a fact that there are many statical problems where the size of the opening represents a relevant parameter (e.g., the height and the width of the tunnel face may be decisive for its stability or the stability of the tunnel crown may depend on the round length).

Within the context of the present report, a question arises as to whether a smaller diameter tunnel offers advantages with respect to the risk of shield jamming. This question cannot be answered on the basis of qualitative considerations because some of the differences between small and large diameter tunnels are in favour of small cross-sections and others in favour of large diameter TBMs. More specifically, a smaller diameter TBM will be able, under normal operational conditions, to proceed faster (but the limited space available may present greater difficulties in the case of adverse conditions). Furthermore, a given amount of overboring ΔR (say 5–10 cm) will be more effective in reducing the ground pressure in the case of a small diameter machine (because the load reduction is governed by the ratio of radial gap size ΔR to tunnel radius R). On the other hand, as can be seen from the TBM technical data collected in Section 5.2.3, smaller diameter TBMs are relatively longer (the ratio of shield length L to tunnel radius R is higher than for traffic tunnel TBMs – typical values are L/R = 5.0 and 2.0, respectively) and have a lower installed thrust force (reported values – at the upper limit of the proven range – are F_i = 50 and 150 MN, respectively). This results in a slightly lower ratio of installed thrust force F_i to shield mantle surface $2\pi RL$ (i.e., the surface exposed to the ground pressure) for the smaller diameter TBMs than for the larger ones ($F_i/2\pi RL$ = 0.40 and 0.48 MPa, respectively).

Figure 3.15 compares a "traffic tunnel" TBM (assumed to advance at a rate of v = 10 m/d, solid curves) with a faster advancing "service tunnel" TBM (v = 25 m/d, dashed curves). The diagram shows the utilization degree of the thrust force as a function of the ground permeability k. The utilization degree of the thrust force is defined as the ratio of the thrust force F_r, required in order to overcome the frictional resistance of the ground, to the installed thrust force F_i. An utilization degree of more than 100 % means that the machine will be jammed. A low utilization degree indicates that the machine has a large reserve

against jamming. The diagram deals with the thrust force requirements for TBM restart, i.e., for overcoming static friction (cf. Section 3.3.3). It contains three curves for each TBM in order to show the effect of the overcut (radial gap size ΔR = 5 or 10 cm) and the ground quality (uniaxial compressive strength f_c = 1.5 or 3.0 MPa).

In a low strength and high permeability ground (f_c = 1.5 MPa, $k > 10^{-8}$ m/s) the thrust force requirements would be critical for both machines in the case of a normal overcut (ΔR = 5 cm). For the reasons mentioned above, the benefit of increasing the overcut (from ΔR = 5 to 10 cm in this example) is greater in the case of the smaller diameter tunnel. Furthermore, it is interesting that in the case of a better quality ground (f_c = 3.0 instead of 1.5 MPa) the situation would improve significantly for the smaller diameter TBM but not for the large TBM. The results of Figure 3.15 indicate that a smaller diameter TBM would cope slightly better with squeezing than the larger diameter machine under the conditions of this specific example.

3.4.4 Conditions during standstills

Dissipation of the excess pore water pressures

The conditions during a standstill will be discussed by means of numerical results relating to the example introduced in Section 3.4.3. The pore pressure distribution at the beginning of a standstill depends on the ratio of the advance rate v of the preceding excavation to the ground permeability k. As can be seen from Figure 3.10, the higher this ratio, the more the pore pressure field prevailing at the start of the standstill will deviate from the steady state. During the standstill, excess pressure dissipation and consolidation of the ground will continue until the steady state is reached.

The transition from favourable undrained conditions to unfavourable drained conditions can be observed in Figure 3.16, which shows the contour lines of the pore pressure p_w at different times t (since the start of the standstill) assuming that the ground has a permeability of $k = 10^{-9}$ m/s and that the preceding excavation proceeded at a rate of v = 10 m/d. In this example, the steady state is reached after about 10 days.

Longitudinal arching in the shield area

The dissipation of excess pore pressures leads to a time-dependent increase in ground deformations and, as the shield and lining allow only a limited amount of deformation, an increase in the ground pressure as well.

Figure 3.17a shows the increase of the convergence $u - u(0)_{t=0}$ over the time t (that has elapsed since the start of the standstill) for two values of radial gap size (ΔR = 5 or 10 cm, on the left and right side, respectively), where u denotes the total radial displacement of the ground at the excavation boundary, while $u(0)_{t=0}$ is the pre-deformation of the ground (i.e., the deformation which occurred ahead of the face during excavation). Figure 3.17b shows the time-development and spatial distribution of the ground pressure p acting upon the shield and lining. As in Section 3.4.3, the simplifying assumption is made that the backfilling of the segmental lining is carried out immediately after installation of the segments (Figure 3.9c) and this is why a load starts to develop upon the lining immediately behind the shield. The effect of a delayed annulus backfilling (Figure 3.9b) will be discussed later in this section.

In the case of normal overcut (ΔR = 5 cm), the ground already closes the gap around the rear part of the shield during TBM advance and, consequently, a load p already acts upon the shield at the start of the standstill (see curve for t = 0, left side of Figure 3.17b). During the standstill, the load acting upon the shield and the lining increases and reaches its final value after about 10 days (when the pore pressure distribution reaches the steady state, cf. Figure 3.16).

The convergence and pressure distribution are completely different in the case of the bigger overcut (right side of Figure 3.17). The 10 cm wide radial gap under consideration remains open during TBM advance. During standstill, the ground takes about 9 days to establish contact with the shield (and to start developing a load upon it) and another 10 days to reach the steady state. (The longer duration of the consolidation process is

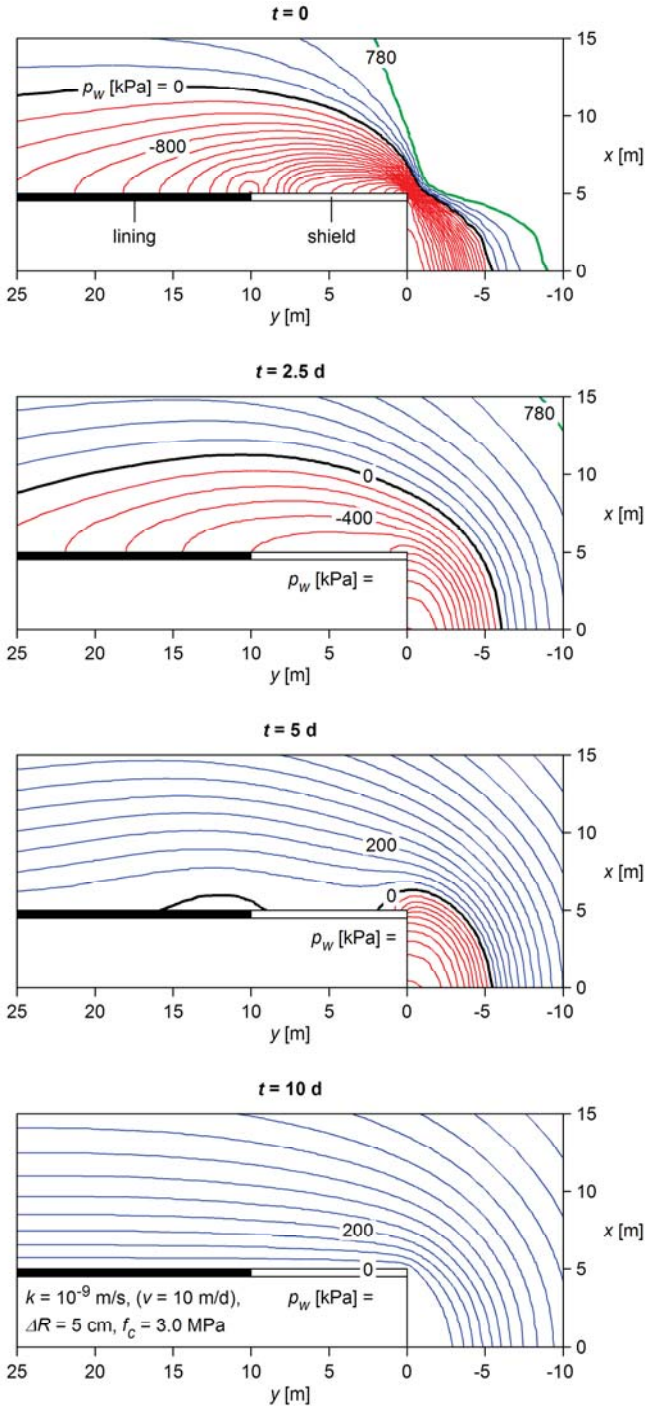

Figure 3.16. Contour lines of the pore pressure p_w at different times t during standstill (permeability of the ground k = 10^{-9} m/s, advance rate of the preceding excavation v = 10 m/d, radial gap size ΔR = 5 cm, uniaxial compressive strength of the ground f_c = 3.0 MPa; other parameters according to Table 3.2).

due to the lower system stiffness associated with the bigger overcut.) During the first phase of the standstill, where the ground remains unsupported over the shield area, a considerable load develops upon the front part of the lining. It is also interesting that the ground first makes contact with the shield in its middle part. The front and the rear parts of the shield remain unloaded due to the support action of the lining and the core, respectively. The observed pressure distribution illustrates a pronounced load transfer via arching in longitudinal direction between the lining and the ground ahead of the face. This

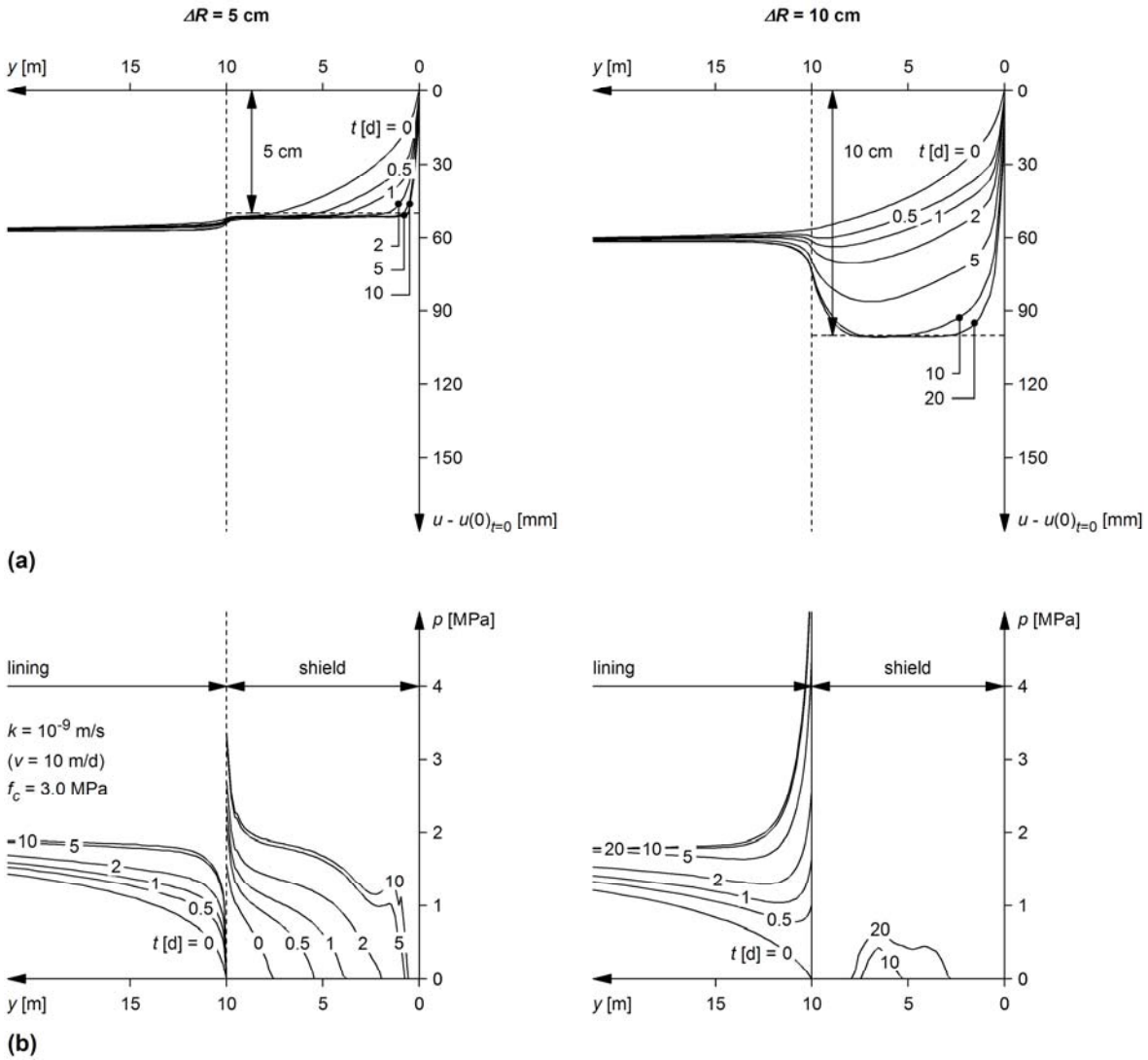

Figure 3.17. Numerical results for a radial gap size of ΔR = 5 or 10 cm (left and right side, respectively): (a) convergence $u - u(0)_{t=0}$ of the bored profile as a function of the standstill time t; (b) ground pressure p acting upon the shield and the lining as a function of the standstill time t; ground permeability $k = 10^{-9}$ m/s, advance rate of the preceding excavation v = 10 m/d, uniaxial compressive strength of the ground f_c = 3.0 MPa; other parameters according to Table 3.2.

effect becomes less pronounced with time due to the plastic yielding of the ground surrounding the middle part of the shield.

On the one hand, the arching effect is favourable with respect to shield loading and to the thrust force that is required in order to overcome the frictional resistance of the ground during TBM restart. On the other hand, arching increases ground pressure behind the shield and may endanger the structural safety of the lining. The practical conclusion is that a reinforcement of the tunnel support close to the shield may be necessary in the case of longer standstills and, as mentioned above, of complete backfilling of the segmental lining immediately behind the shield.

The arching effect discussed above depends on the resistance offered by the lining behind the shield and the stiffness of the core ahead of the shield. The influence of these two factors will be discussed next in this section.

Effect of backfilling of the segments close to the shield

A significant load transfer in the longitudinal direction (which is favourable for the shield, but unfavourable for the lining) is possible only if the segments are "perfectly" backfilled

directly behind the shield, i.e., if annulus grouting is carried out simultaneously with TBM advance via the shield tail (Figure 3.9c). This is normally the case with closed shields, where the counter-pressure offered by the supporting medium prevents the flow of grout around the shield towards the cutter head. In rock TBMs, however, where pea gravel is used for backfilling, it is not possible to achieve a contact between ground and segmental lining right from the start and, as sketched in Figure 3.9b, a certain "span" behind the shield remains unsupported. Shield load reduction via longitudinal arching is practically impossible in this case.

For the sake of comparison, consider the borderline case of a segmental lining without backfilling. In this case, the ground starts to develop a pressure p upon the lining only after experiencing sufficient deformation and closing the lining annulus gap ΔR_l. The latter denotes the difference between the boring radius and the outer radius of the segmental lining and is taken to be ΔR + 7.5 cm, where ΔR is the radial gap size of the shield. The lining annulus gap ΔR_l is taken into account by prescribing a corresponding boundary condition (cf. Section 6.3.2).

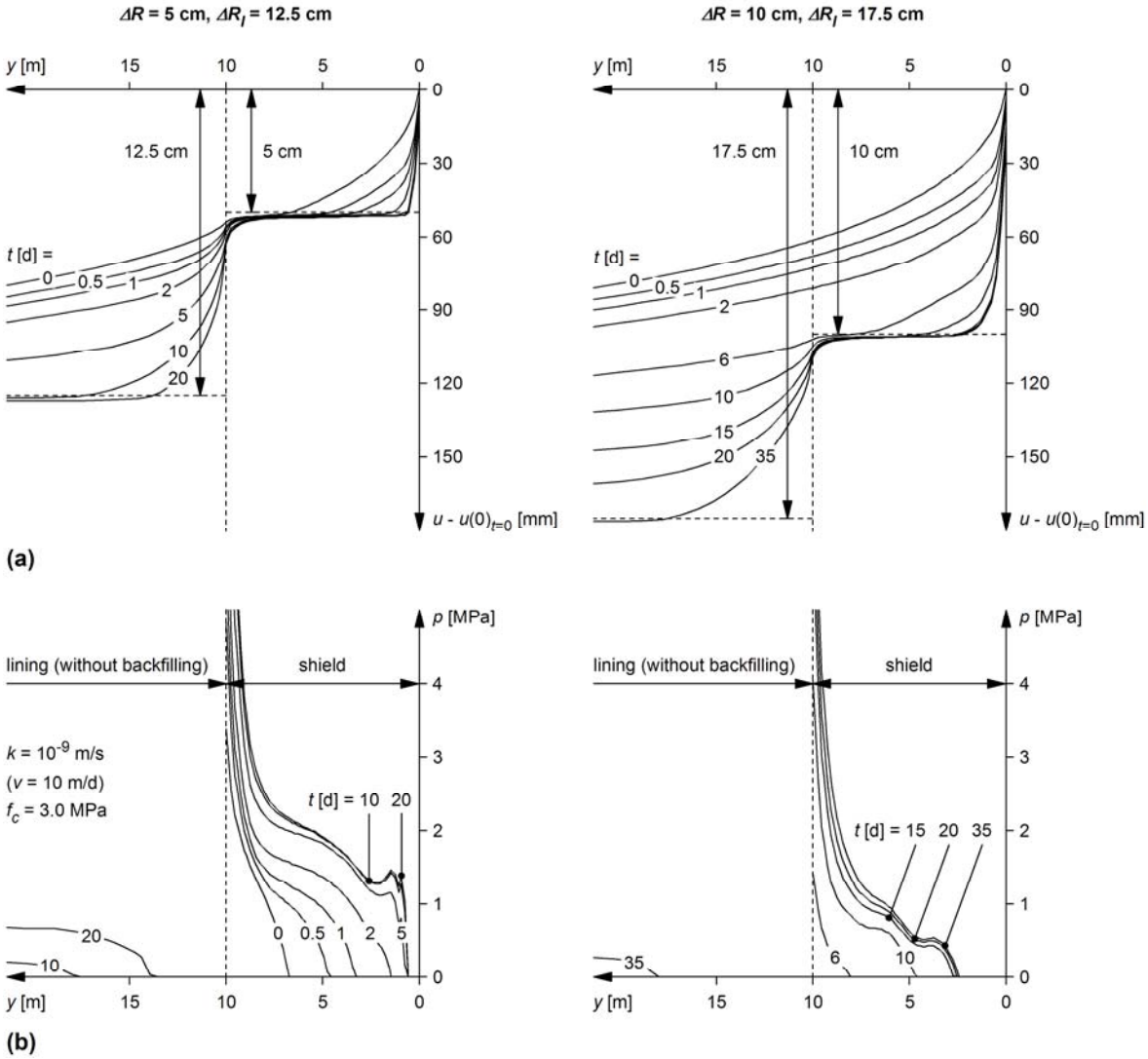

Figure 3.18. Numerical results for the borderline case of a segmental lining without backfilling for a radial annulus of ΔR_l = 12.5 or 17.5 cm (left and right side, respectively): (a) convergence $u - u(0)_{t=0}$ of the bored profile as a function of the standstill time t; (b) ground pressure p acting upon the shield and the lining as a function of the standstill time t; ground permeability $k = 10^{-9}$ m/s, advance rate of the preceding excavation v = 10 m/d, radial gap size ΔR = 5 or 10 cm, uniaxial compressive strength of the ground f_c = 3.0 MPa; other parameters according to Table 3.2.

Figure 3.18 presents the numerical results in the same way as Figure 3.17 did previously, i.e., it shows the spatial distribution and time-development of ground convergence and pressure for two values of the radial gap size ΔR of 5 or 10 cm (on the left and right side, respectively). As expected, the ground starts to develop a pressure p upon the lining later (after closing the lining annulus gap) and the final load is significantly lower than for the case with perfect backfilling of the segments – this, however, at the cost of a much higher shield load. (In this computational example, the load developing on the rear part of the shield would endanger its structural safety.)

The comparison of Figures 3.17 and 3.18 shows that conflicting requirements may have to be met. On the one hand, backfilling of the segments immediately behind the shield facilitates longitudinal arching and reduces shield load. On the other hand, ground deformation should be allowed in order to reduce lining load to a manageable level.

For fast excavation through a low-permeability ground (i.e., for a high v/k-ratio), where undrained conditions prevail in the shield area and the ground pressure p acting upon the shield at the beginning of the standstill is very low (see curves for $t = 0$ in Figure 3.18b), it seems advantageous to delay the backfilling of the segments. It should be noted, however, that improper backfilling of the segments may reduce the bearing capacity of the lining and may therefore limit the effectively available thrust force (it may be impossible to utilize the installed thrust force).

In the other borderline case of a slow excavation or a high permeability ground (i.e., low v/k-ratio), where almost drained conditions prevail in the shield area and the shield loading is significant even during continuous excavation, a careful backfilling of the segments close to the shield may help avoid TBM jamming. Nevertheless, it should also be noted that the backfilling work may slow down the TBM advance rate, thus leading, as a rule, to a less favourable situation.

Load transfer to the core ahead of the face

Longitudinal arching presupposes, in addition to the development of lining resistance close to the shield tail, a sufficiently stiff core ahead of the face. The radial resistance of the core depends in general on the face support pressure (as mentioned in Section 3.2.1, the computational model regards the tunnel face as being unsupported). The lower the face support pressure, the more the core yields and extrudes in the axial direction, the more the radial stress ahead of the face decreases and the more load is transferred to the shield. This is why the ground pressure in the front part of the shield increases with time during the standstill (see pressure peak at $y = 1.5$ m behind the face in Figure 3.17b, left side).

This effect becomes clearer from Figure 3.19a, which shows the ground pressure p at $y = 1.5$ m behind the face as a function of standstill time t (the inset in Figure 3.19a shows the final pressure distribution along the shield). The solid line applies to an unsupported face, while the marked line applies to the case of zero core extrusion (where axial displacement is constrained by the cutter head). In the first case the face experiences an additional axial displacement $u_e(t)$ during the standstill (Figure 3.19b), while in the second case an axial pressure develops upon the cutter head (Figure 3.19c). In this example, the horizontal load is very high (up to 2 MPa, cf. Figure 3.19 c) and may endanger the structural safety of the cutter head. However, the simplifying assumption of zero core extrusion disregards the deformability of the cutter head (which is, nevertheless, very low) as well as any possible gap between cutter head and tunnel face, thus overestimating the axial pressure developing upon the cutter head.

The ground pressure developing upon the shield is lower when the core cannot extrude. Face support therefore has a positive effect on the shield load during standstill. The cutter head provides a certain degree of face support – this however at the cost of higher thrust force and torque requirements (cf. Section 2.3.2). Of course, the extrusion of the core u_e also plays an important role with respect to face stability, as excessive deformations may lead to collapse. The linear increase in axial displacement over time (Figure 3.19b) indicates such a collapse scenario.

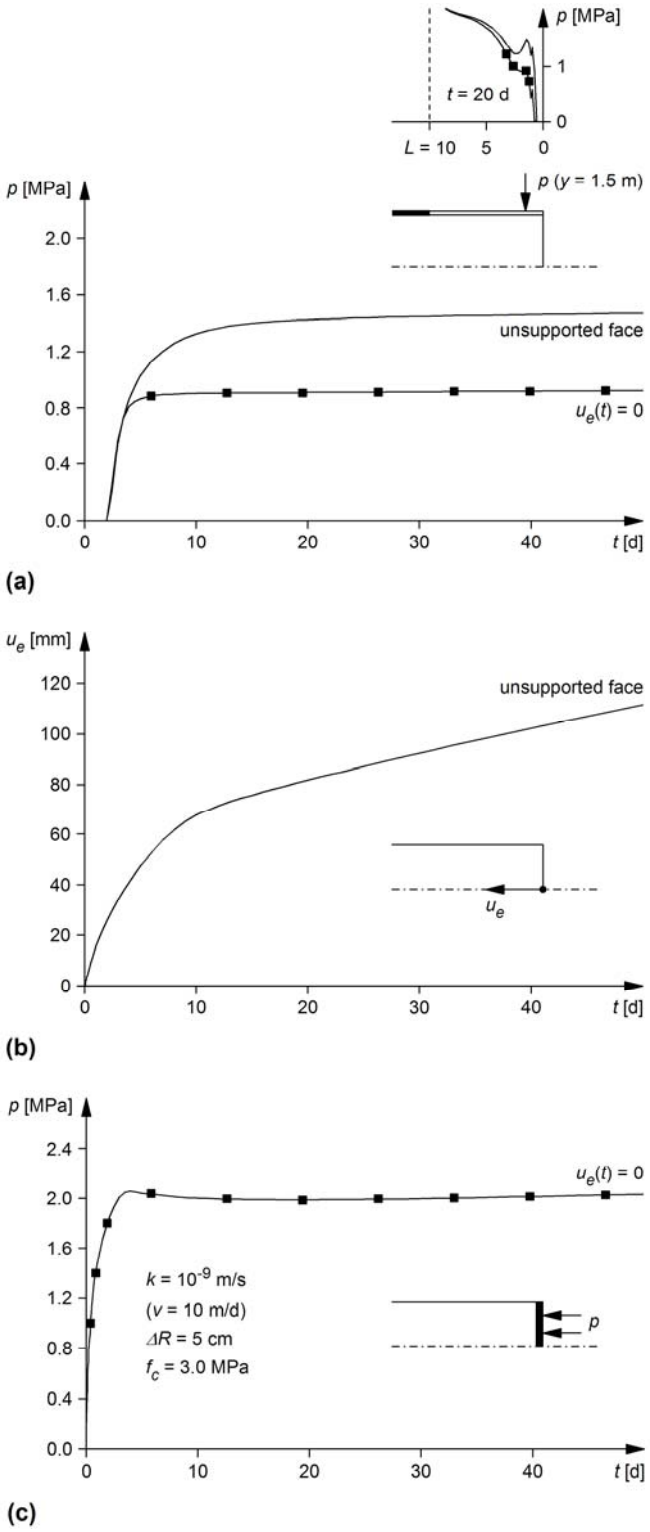

Figure 3.19. (a) Ground pressure p developing at y = 1.5 m during a standstill as a function of time t (unsupported or fixed face); (b) core extrusion u_e developing during a standstill as a function of time t (unsupported face); (c) axial loading p developing upon the cutter head as a function of time t (fixed face); ground permeability k = 10^{-9} m/s, advance rate of the preceding excavation v = 10 m/d, radial gap size ΔR = 5 cm, uniaxial compressive strength of the ground f_c = 3.0 MPa; other parameters according to Table 3.2.

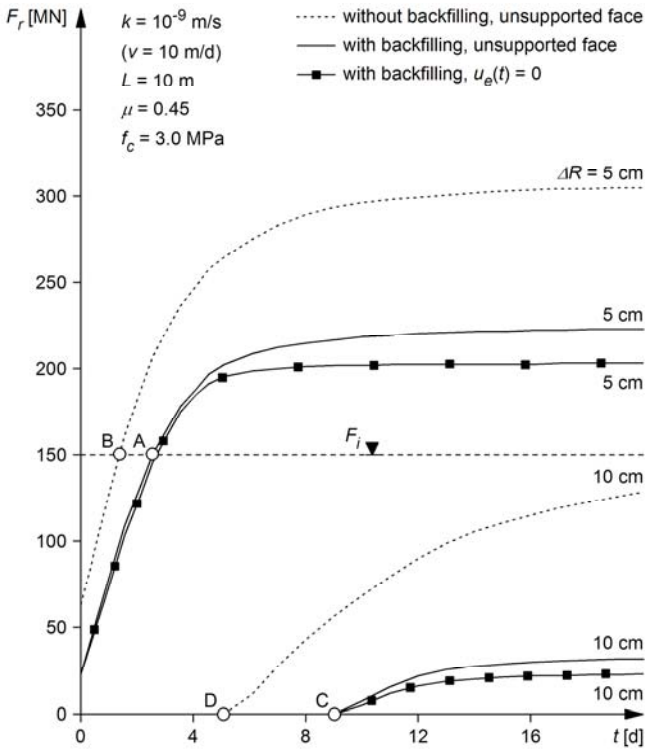

Figure 3.20. Required thrust force F_r for different model assumptions (unsupported or fixed face, with and without backfilling of the segmental lining close to the shield) as a function of the standstill time t (ground permeability k = 10^{-9} m/s, advance rate of the preceding excavation v = 10 m/d, radial gap size ΔR = 5 or 10 cm, shield skin friction coefficient μ = 0.45, uniaxial compressive strength of the ground f_c = 3.0 MPa; other parameters according to Table 3.2).

Thrust force needed for restarting TBM operation

Due to the increasing shield load (Figures 3.17 to 3.19), the thrust force F_r, which is required in order to overcome skin friction during a TBM restart, increases as well. Figure 3.20 shows the time-development of the required thrust force F_r (as mentioned in Section 3.3.3, the thrust force calculation takes into account static friction, but not the boring thrust force).

The solid lines presuppose a complete backfilling of the segments immediately behind the shield and an unsupported face. In the case of an installed thrust force of F_i = 150 MN and a normal overcutting of ΔR = 5 cm, the TBM can be restarted if the standstill is shorter than about 2.5 days (see point A in Figure 3.20). In the case of a larger radial gap size (ΔR = 10 cm), it would always be possible to restart the TBM in this example. This could be achieved also by lubricating the shield extrados (i.e., reducing the skin friction coefficient μ from 0.45 to 0.25).

The dashed lines in Figure 3.20 concern the borderline case without backfilling of the segments (Figure 3.9b). The positive effect of backfilling with respect to the risk of shield jamming can be seen clearly by comparing these dashed lines with the solid lines. Without backfilling, the critical standstill duration decreases from 2.5 days to about 1.5 day in the case of a normal overcut of ΔR = 5 cm (see points B and A in Figure 3.20). For an overboring of ΔR = 10 cm, the shield becomes loaded earlier (after 5 instead of 9 days, see points D and C) and the required thrust force increases considerably over time.

The marked lines in Figure 3.20 apply to the case of a fixed face, thus illustrating the positive effect of a face support. This effect is, however, of minor relevance in the numerical example under consideration.

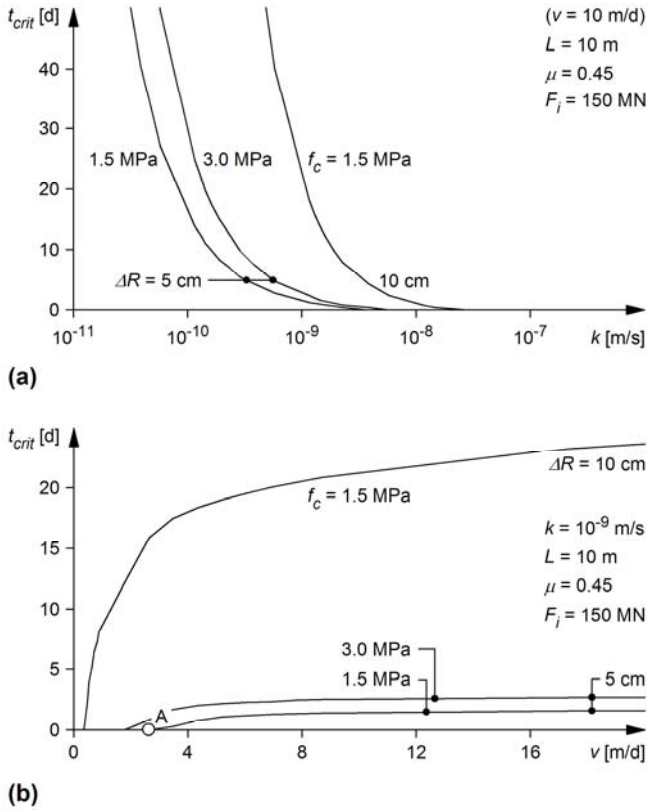

Figure 3.21. (a) Critical standstill duration t_{crit} as a function of ground permeability k (advance rate of the preceding excavation v = 10 m/d); (b) critical standstill duration t_{crit} as a function of the advance rate v (ground permeability k = 10^{-9} m/s); radial gap size ΔR = 5 or 10 cm, shield skin friction coefficient μ = 0.45, uniaxial compressive strength of the ground f_c = 1.5 or 3.0 MPa, installed thrust force F_i = 150 MN; other parameters according to Table 3.2.

As shown in Figure 3.20, the required thrust force F_r may increase to the level of the installed thrust force F_i after a certain period of time t (e.g., 2.5 days for ΔR = 5 cm and complete backfilling of the segmental lining). Figure 3.21a shows the influence of ground permeability k on the critical standstill duration t_{crit} under the assumption that the advance rate during the preceding excavation was v = 10 m/d and the installed thrust force amounts to F_i = 150 MN. The higher the ground permeability k, the faster will be the consolidation and the shorter the critical standstill duration t_{crit}. In this numerical example, for a normal overcutting of ΔR = 5 cm and a uniaxial compressive strength of the ground of f_c = 3.0 MPa, regular TBM operation as well as standstills of 2–2.5 day or more (depending on the ground permeability k) will be possible if the ground permeability is lower than 10^{-9} m/s. On the contrary, for a ground permeability higher than 10^{-8} m/s the shield would become jammed even during regular TBM operation (cf. Figure 3.13). During the standstill, the ground pressure acting upon the shield may increase further, thus making the job of freeing the TBM even more difficult. For ground permeabilities of k = 10^{-8}–10^{-9} m/s the critical standstill duration t_{crit} decreases down to zero. At this permeability range, the required thrust force F_r was close to the installed one F_i even during the previous regular TBM operation that proceeded with a rate of v = 10 m/d (cf. Figure 3.13). From the practical point of view, this means that all possible precautions should be taken in order to make TBM operation as continuous as possible, as each further unexpected standstill will significantly increase the risk of shield jamming.

As shown above (Sections 3.4.2 and 3.4.3), the ratio of advance rate v to ground permeability k governs the distribution of the pore pressure at the beginning of the standstill. Therefore, for a given ground permeability k, the advance rate v of the preceding regular TBM operation will influence the conditions prevailing at the beginning of the standstill to a considerable extent: the higher the advance rate v, the lower must have been the re-

quired thrust force F_r during excavation (cf. Figure 3.13) and, therefore, the more time will have to elapse during a standstill before the required thrust force reaches the installed one (Figure 3.21b). Figure 3.21b also suggests that a critical advance rate exists for which the critical standstill duration t_{crit} decreases up to zero (e.g., v = 2.6 m/d for ΔR = 5 cm and f_c = 1.5 MPa, see point A in Figure 3.21b). This advance rate corresponds to the borderline case where the required thrust force F_r is already equal to the installed one F_i during regular TBM operation. This confirms the practical experience that making the TBM advance as fast as possible may help to avoid shield jamming in squeezing ground.

4 Application examples

4.1 Introduction

Section 4 presents two examples of real world applications, which illustrate possible methodical approaches to the assessment of a TBM drive in squeezing ground. The first case history (Section 4.2) – the Uluabat Tunnel (Turkey) – mainly concerns the investigation of TBM design measures with the aim of reducing the risk of shield jamming. The second case history (Section 4.3) – the Faido Section of the Gotthard Base Tunnel (Switzerland) – deals with the different types of tunnel support installed behind a gripper TBM. A considerable degree of engineering judgement is required in cases such as this – in contrast to shielded TBMs where the support is, as a rule, pre-determined (precast segmental lining).

4.2 An example of a single shielded TBM

4.2.1 Introduction

The first application example concerns the 11.8 km long Uluabat Tunnel in Turkey (about 100 km south of Istanbul). A 12 m long single shielded TBM with a boring diameter of 5.05 m and an installed thrust force of about 30 MN started work in 2006. The overcut ΔR was 3 cm at the front part of the shield and increased to 4 cm at the shield tail. The ground is of Triassic origin and consists of a claystone matrix containing 1–50 cm big sandstone lenses. The claystone fraction amounts to about 80 %. The claystones are intensively sheared, have several slickensides and disintegrate quickly under the action of water. Laboratory results revealed a Young's modulus of E = 200–1000 MPa, an angle of internal friction of about φ = 20 º and strongly variable cohesion values (c = 50–400 kPa). During the first 3 km of TBM operation, squeezing caused jamming of the shield on several occasions although the depth of cover was rather moderate (about 120 m, i.e., an estimated initial stress of σ_0 = 3 MPa). The available monitoring results were sparse, but indicated a large variability in squeezing intensity with maximum deformation rates of up to 6 cm/h.

A comprehensive parametric study was carried out in order to gain a better understanding of the observed phenomena, analyze the factors influencing the jamming of the TBM and evaluate the effectiveness of possible TBM improvements (Kovári and Ramoni, 2008; Ramoni and Anagnostou, 2008). On account of the variability of the squeezing phenomena, attention was paid to the specific situation prevailing in certain critical zones. The following sections outline the most important results.

4.2.2 Investigations on TBM optimization

The numerical investigations were carried out on the basis of a simplified model which considers the shield and the lining as a single infinitely long cylindrical body of constant stiffness and constant radial gap size. This simplification allows a faster investigation to be made of the effect of the shield length on the thrust force that is required to overcome shield skin friction but leads to an overestimation of the lining loading and to an underestimation of the shield loading – see Ramoni and Anagnostou (2010a, 2011b) for a detailled discussion.

The calculations disregarded a possible time-dependency of the ground behaviour – a reasonable assumption considering the high convergence rates observed in situ. Furthermore, on account of the low strength of the ground, the thrust force calculations neglected the boring thrust force. The skin friction coefficient was taken to μ = 0.50 according to Table 2.3. This value is relevant for the static friction conditions prevailing when attempting to restart excavation after a stop for the installation of the segmental lining. The other problem parameters are shown in Table 4.1.

Table 4.1. Assumed parameters values.

		Set	1	2	3
		Figures	4.1	4.3–4.4	4.7
Tunnel radius	R	[m]	2.50	2.50	4.75
Radial gap size	ΔR	[cm]	3/6/9/12	3	12
Length of the shield	L	[m]	10/12	12	5
Stiffness of the shield	K_s	[MPa/m]	2688	2688	558
Stiffness of the lining	K_l	[MPa/m]	2688	2688	variable
Initial stress	σ_0	[MPa]	3	3	40
Young's modulus of the ground	E	[MPa]	200–1000	2000 [a] 400 [b]	3235
Poisson's ratio of the ground	ν	[-]	0.20	0.20	0.30
Uniaxial compressive strength of the ground	f_c	[MPa]	--	--	5.5
Cohesion of the ground	c	[kPa]	50–400	200 [b]	--
Angle of internal friction of the ground	φ	[°]	20	20 [b]	35
Dilatancy angle of the ground	ψ	[°]	1	1 [b]	5
Skin friction coefficient	μ	[-]	0.25/0.50	0.50	0.30
Installed thrust force	F_i	[MN]	30/60	30	27.5
Boring thrust force	F_b	[MN]	0	0	17
Step length	s	[m]	--	0.5/1.0	--

Notes

[a] Competent rock

[b] Weak zone

For a given depth of cover and for given TBM parameters, a critical range of rock mass parameters can be determined beyond which the required thrust force is higher than the installed one, thus indicating that shield jamming may occur. In the present case, the critical range was defined in terms of the Young's modulus E and of the cohesion c of the rock mass (all other ground parameters being kept constant). The reason for this choice was the large uncertainty concerning these two parameters in combination with the great sensitivity of the ground response with respect to their variations.

Figure 4.1a shows the critical ground conditions for a depth of cover of H = 120 m and an overcut ΔR of 3, 6 or 9 cm (the 6 to 9 cm applies to the case of an increased overcut). The points of each curve (hereafter referred to as "critical curve") fulfil the condition that the required thrust force (for the specific value of ΔR) is equal to the installed thrust force. The lower the Young's modulus E, the higher the cohesion c must be in order that the average ground pressure acting upon the shield remains equal to a given value. Value-pairs (c, E) above a certain curve characterize subcritical ground conditions (i.e., the installed thrust force is sufficient for overcoming the frictional resistance of the ground). On the other hand, the region below the critical curve indicates ground conditions that may trap the TBM. The grey box shows the actual range of the two ground parameters based upon the results of laboratory tests. By considering the position of the critical curve relative to this box, an optical assessment can be made of TBM operating conditions. The fact that the critical curves diagonally cross the box representing the laboratory values points to a prediction uncertainty and agrees with the variability experienced during the TBM drive: depending on the variation of the ground conditions the shield may or may not be jammed.

In order to reduce the risk of major delays in the completion of the project, the option of an additional TBM drive from the other portal of the tunnel was investigated (but finally rejected for contractual reasons). The second TBM would cross the same formation, where the first TBM experienced difficulties, but under an even higher overburden (up to 240 m in the deepest portion of the alignment). A main goal of the investigations was, therefore, the optimization of the second TBM in order to cope with squeezing ground. Figure 4.1b shows the critical curves for a depth of cover of 120 m (curves A and B) or 240 m (curves C and D). The critical curves for the first machine are denoted by A and C, while the curves B and D apply to a new machine implementing a series of technical

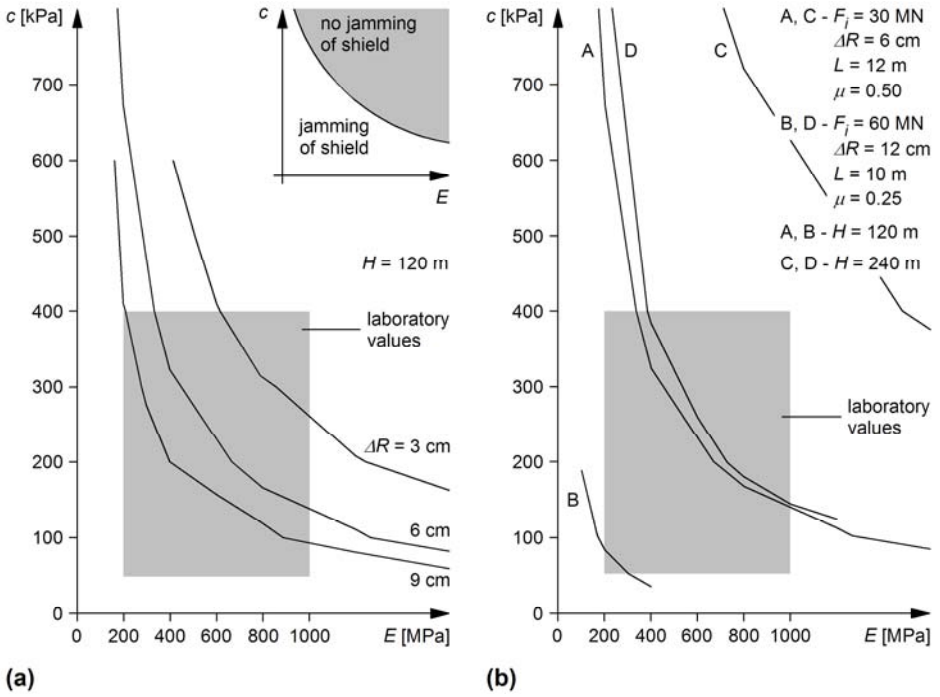

Figure 4.1. (a) Critical ground conditions for an installed thrust force of F_i = 30 MN (radial gap size ΔR = 3, 6 or 9 cm, shield length L = 12 m, skin friction coefficient μ = 0.50, depth of cover H = 120 m, safety factor for the required thrust force SF = 2.0); (b) effect of a combination of several technical improvements (installed thrust force F_i = 30 → 60 MN, radial gap size ΔR = 6 → 12 cm, shield length L = 12 → 10 m, skin friction coefficient μ = 0.50 → 0.25, depth of cover H = 120 or 240 m, safety factor for the required thrust force SF = 2.0); other parameters according to Table 4.1, Set 1.

improvements: a higher thrust force F_i (60 instead of 30 MN), a 2 m shorter shield length L, a bigger overboring ΔR and reduced skin friction μ (achieved by lubrication of the shield extrados). The combination of all these measures would shift the critical curve from curve A to curve B in the bottom-left corner of the diagram and this means that an improved TBM would be able to cope with adverse conditions such as those encountered by the first TBM at a depth of cover of H = 120 m. However, the possibility of shield jamming would persist in the deepest portion of the alignment (H = 240 m). According to curve D of Figure 4.1b, the improved TBM would perform at a depth of 240 m similarly to the current TBM at a depth of 120 m (curve A), while operation of the current TBM at the maximum depth would be possible only in the case of considerable improvements to ground strength and stiffness (curve C).

4.2.3 Effect of shorter weaker zones

The numerical computations presented in the last section were based on the assumption of homogeneous ground in the longitudinal direction. During the TBM drive in Uluabat, however, the ground behaviour, as reflected by the thrust force needed in order to keep the TBM advancing, changed within short intervals, thus indicating a succession of weak zones with stretches of more competent ground.

According to past research on the mechanics of deformation in short geological fault zones, the adjacent competent rock also has a stabilizing effect with respect to the fault zone (Kovári and Anagnostou, 1995; Cantieni and Anagnostou, 2007). When crossing a single weak zone, shear stresses are mobilized at its interface with the adjacent competent rock, because the latter experiences smaller deformations. The shear stresses reduce the convergences within the weaker zone, particularly when its length is small. As shown, e.g., by Matter et al. (2007) and in more detail by Graziani et al. (2007), this so-called "wall effect" is also favourable with respect to the risk of TBM jamming.

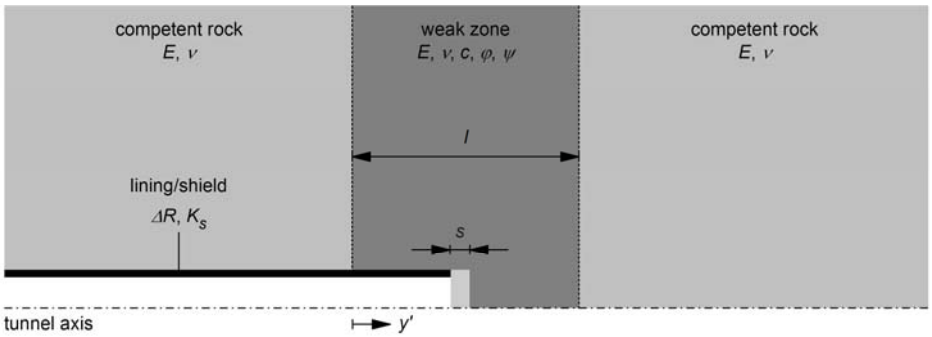

Figure 4.2. Layout of the short fault zone problem investigated with step-by-step calculations.

Due to these considerations, an examination was performed as to whether the variability of the ground behaviour observed in Uluabat could be explained by the existence of weak zones of variable extent and an analysis was conducted into the effect of the length of a weak zone on the required thrust force. Figure 4.2 and Table 4.1 (Set 2) show the layout of the problem and the assumed parameters, respectively. The main assumptions are the same as in the last section. In order to reduce the computational cost, the numerical investigations assumed that the behaviour of the competent rock before and after the weaker zone is linearly elastic. Due to the non-uniformity of the conditions in the longitudinal direction, it was not possible to apply the steady state numerical solution method (cf. Section 3.2.3) and, therefore, the tunnel excavation and support installation were modelled step-by-step on the basis of a step length *s* of 0.5 or 1.0 m.

Figure 4.3 shows the required thrust force F_r as a function of the tunnel face position *y'* (the latter refers to the onset of the critical zone, cf. Figure 4.2). The curves apply to weak zones of different lengths *l*. As expected, the required thrust force increases when the TBM enters into the weak zone and decreases when the TBM leaves it. Assuming that practically the entire installed thrust force of F_i = 30 MN is available for overcoming skin friction, the TBM would be able to cope with a 5–10 m thick weak zone. In the case of a weak zone longer than about 10 m, however, the TBM might become trapped. The observed variability might therefore be associated with a sequence of weaker and stronger rock zones.

Figure 4.4 shows the maximum required thrust force F_r as a function of the length *l* of the weak zone for step lengths *s* of 0.5 or 1 m. The shorter the weak zone, the more

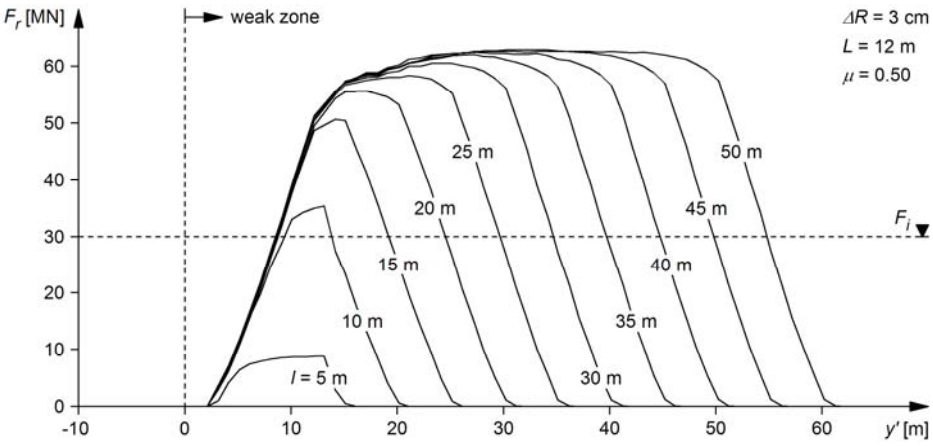

Figure 4.3. Required thrust force F_r as a function of the position y' of the tunnel face (cf. Figure 4.2) for different lengths l of the weak zone (step length s = 1 m, radial gap size ΔR = 3 cm, shield length L = 12 m, skin friction coefficient μ = 0.50, safety factor for the required thrust force SF = 1.0; other parameters according to Table 4.1, Set 2).

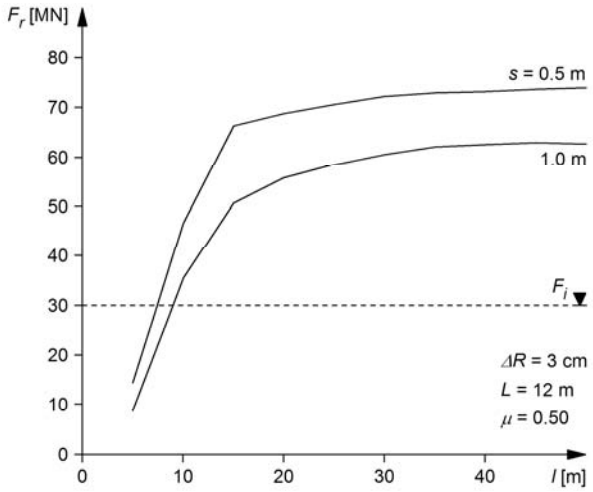

Figure 4.4. Maximum required thrust force F_r in the weak zone as a function of their length l (radial gap size ΔR = 3 cm, shield length L = 12 m, skin friction coefficient μ = 0.50, safety factor for the required thrust force SF = 1.0; other parameters according to Table 4.1, Set 2).

pronounced will be the wall-effect and the lower will be the risk of shield jamming. In the example of Figure 4.4, the wall-effect is remarkable for critical zones shorter than about 10–15 m, i.e., two or three tunnel diameters. Figure 4.4 also shows that the computations carried out with the commonly chosen round length of s = 1.0 m underestimates the required thrust force F_r (by 15 % in this example). For the reasons mentioned in Section 3.2.3, more accurate results can be obtained choosing a smaller round length (s = 0.5 m in Figure 4.4).

4.3 An example of a gripper TBM

4.3.1 Introduction

Other than in the case of shielded TBMs, where the support characteristics are largely pre-defined (precast segments, maybe of variable reinforcement content), a certain degree of flexibility exists in gripper TBMs with respect to the means and quantities of support. Due to the largely predefined boring diameter, decision-making is nevertheless constricted within a relatively narrow space as the geometrical constraints of the tunnelling equipment limit both the admissible convergence and the possible thickness of the tunnel support. Decision-making may also be particularly challenging because of the conflictive criteria often existing in squeezing ground (cf. Section 2.3). Stabilizing interventions behind the machine are generally possible only in some locations that are dictated by the TBM design. In order to avoid problems such as a violation of the clearance profile, a high quantity of support may have to be installed shortly after excavation, i.e., behind the cutter head. This, however, slows down TBM advance and, in the case of time-dependent ground behaviour, increases the risk of the machine becoming trapped.

The present section discusses the effect of different support types based upon the results of numerical investigations carried out by Anagnostou and Ramoni (2007) for the 14.2 km long Faido Section of the Gotthard Base Tunnel in Switzerland. The tunnel was excavated by means of two gripper TBMs (D = 9.43 m) having 5 m long cutter head shields and installed thrust forces of 27.5 MN.

The TBM drives in the Faido Section started in July and October 2007, respectively, with manually shifted gauge cutters (D = 9.50 m). Squeezing related phenomena were observed in the so-called "Lucomagno-Gneiss" – a metamorphic, micaceous, crystalline rock – at a depth of 1600 m (estimated initial stress σ_0 = 40 MPa). In a 250 m long stretch, convergences in the roof (of up to 5–10 cm in the eastern tube and of up to

25 cm in the western tube) and heave of the tunnel floor (of up to 30 cm in the eastern tube and of up to 75 cm in the western tube) caused damage to the tunnel support and jamming of the back-up trailers (Böckli, 2008; Boissonnas, 2008; Flury and Priller, 2008; Gollegger et al., 2009; Herrenknecht et al., 2009). Deformations of up to 10 cm occurred within the short interval between the working face and the shield tail, thus using up most of the convergence margin offered by the shield articulation, without however to immobilize the TBM.

4.3.2 Investigations

The aim of the investigations was to find out which support type would present the lowest risks (with respect to a series of squeezing-related hazard scenarios), thereby maximizing the range of manageable squeezing conditions. For this purpose, the hazard scenarios, (i), jamming of the shield, (ii), overstressing of the tunnel support and, (iii), violation of the clearance profile have been analyzed for a series of hypothetical rock mass constants covering a wide range of squeezing intensity.

The parameterization of the squeezing intensity was done on the basis of the free convergence u/R (i.e., the convergence that would occur in the theoretical case of an unsupported opening) and of the non-linearity of the ground response curve. Figure 4.5a shows the range of ground response curves for the rock types under consideration: the free convergence u/R amounts to 2–9 %, while, for a given free convergence, the ground response curve may be more or less curved depending on the uniaxial compressive strength f_c and on the Young's modulus E of the ground. The values of the friction angle, the dilatancy angle and the Poisson's ratio were fixed to φ = 35 °, ψ = 5 ° and ν = 0.30, respectively. Figure 4.5b shows the value pairs (f_c, E) considered in the numerical analyses (different markers are used in order to show the corresponding free convergence values u/R). In the present report, only the results for the material constants from Table 4.2 will be presented, as the curvature of the ground response curve does not significantly affect the main conclusions in the present case. The term "rock mass type" used hereafter refers to the parameters of Table 4.2.

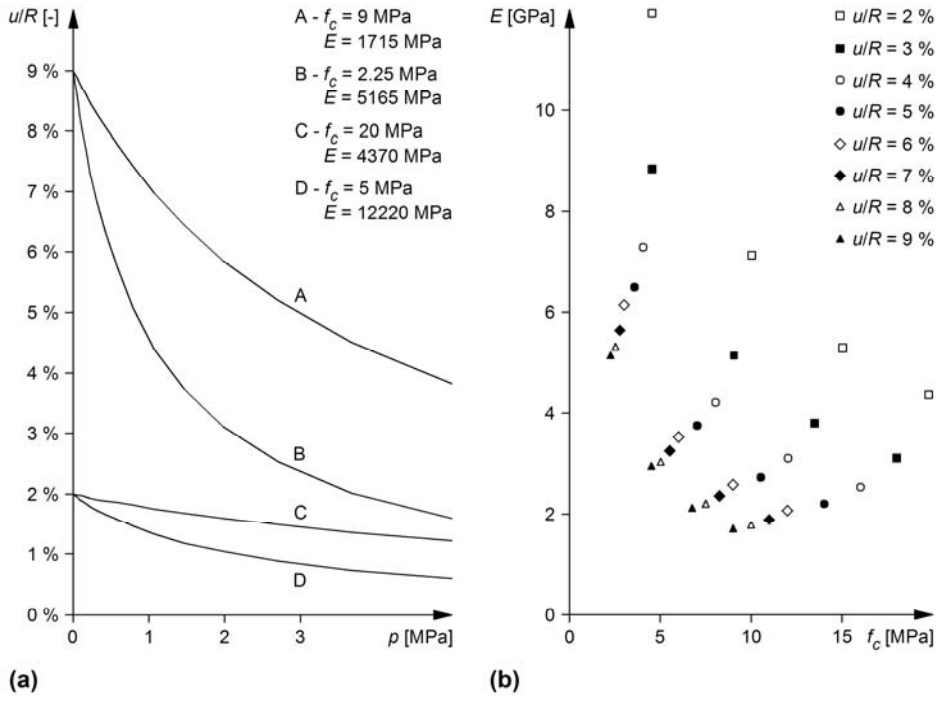

Figure 4.5. Range of the ground response curves (a) and uniaxial compressive strengths f_c and Young's moduli E (b) of the "rock mass types" considered in the numerical computations (initial stress σ_0 = 40 MPa; other parameters according to Table 4.2).

Table 4.2. Assumed parameters values for the "rock mass types".

	Rock mass type							
Parameter	1	2	3	4	5	6	7	8
u/R [-]	2 %	3 %	4 %	5 %	6 %	7 %	8 %	9 %
f_c [MPa]	10.0	9.0	8.0	7.0	6.0	5.5	5.0	4.5
E [MPa]	7140	5140	4225	3750	3525	3235	3055	2950
ν [-]	0.30							
φ [°]	35							
ψ [°]	5							

The numerical calculations were based upon the axially symmetric model with uniform support characteristics over the tunnel cross-section introduced in Section 3.2. The assumption of rotational symmetry represents a strong simplification in the present case in view of the observed asymmetric ground deformations. Table 4.3 shows the investigated tunnel support types. The systems *RS15* and *RS25* are practically rigid supports including a 15 or 25 cm thick shotcrete ring, respectively. The systems *YS15/S5*, *YS15/C5*, *YS15/C15* and *YS25/C15* are yielding supports with a 15 or 25 cm thick shotcrete ring incorporating either 5 cm thick Styrofoam plates (which can be compressed completely) or 15 cm thick high ductility concrete elements which can experience a yield strain of about 50 % (Solexperts, 2007). All of the support types include steel sets (TH 36) at 1 m spacing and with sliding connections in the case of the yielding support systems. Additionally to the support types of Table 4.3, the hypothetical case of an unsupported tunnel was also considered for comparison purposes and as a simplified model of very light tunnel support.

For all support cases the assumption was made that the tunnel support is installed immediately behind the shield, i.e., at a distance of 5 m from the working face. Concerning overcut, two radial gap sizes of ΔR = 6 or 12 cm have been considered, taking into account the shifting of the gauge cutters and the kinematics of the articulated shield.

The computational model simulates the support types described above by mixed, nonlinear boundary conditions (cf. Section 3.2.2 and Figure 3.4b-c) according to the different characteristic lines of Figure 4.6. The latter take due account of the characteristic lines of the different support components as well to the sizes and the number of the yielding elements, including the sliding connections of the steel sets. The time-dependency of the shotcrete stiffness was taken into account in a simplified way by adopting a reduced Young's modulus of E_{sc} = 10 GPa. An example concerning the computation of the characteristic line of a yielding support can be found in Ramoni and Anagnostou (2011b).

Table 4.3. Investigated support systems.

		Shotcrete	Steel set	Deformable elements		
		Thickness	Type	Number x yield deformation	Material	Height
Rigid support	*RS15*	d_1 = 15 cm	TH 36			
	RS25	d_1 = 25 cm	TH 36			
Yielding support	*YS15/S5*	d_1 = 15 cm	TH 36	4 x 5.0 cm	Styrofoam	d_2 = 5 cm
	YS15/C5	d_1 = 15 cm	TH 36	4 x 2.5 cm	Concrete	d_2 = 5 cm
	YS15/C15	d_1 = 15 cm	TH 36	4 x 7.5 cm	Concrete	d_2 = 15 cm
	YS25/C15	d_1 = 25 cm	TH 36	4 x 7.5 cm	Concrete	d_2 = 15 cm

Rigid support

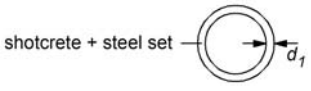

Yielding support

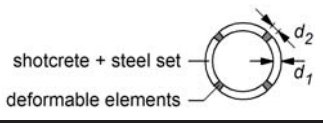

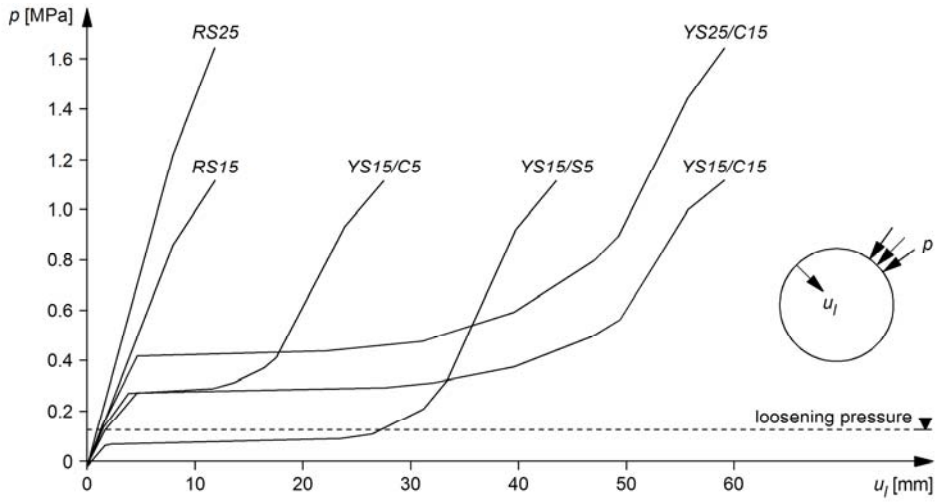

Figure 4.6. Characteristic lines (ground pressure p as a function of the radial displacement of the lining u_l) of the investigated support systems (cf. Table 4.3).

4.3.3 Discussion of the results

The numerical analyses have been carried out for all combinations of rock and support types (Figure 4.5b and Table 4.3, respectively). The main results of each numerical analysis are the ground pressure distribution along the shield and the tunnel and the deformations of the bored profile. These results were evaluated with respect to the following criteria: (i) Is the installed thrust force sufficient to overcome frictional resistance? (ii) Is the structural safety of the tunnel support sufficient? (iii) Do the rock mass convergences violate the clearance profile (under-profile)?

Concerning the thrust force requirements, the investigations considered the conditions both during ongoing excavation and for restart after a standstill (cf. Section 3.3.3). These are different with respect to the skin friction coefficient – μ = 0.30 or 0.45, respectively, cf. Table 2.3 – and to the thrust force needed for boring (F_b = 17 MN). Furthermore, the evaluation disregarded possible limitations of the available thrust force due to problems with the gripper bracing – a reasonable assumption considering the crystalline character of the rock. The operational stage "ongoing excavation" is the relevant one in the present case. This is due to the fact that the thrust force needed for boring (which in the present example amounts to 62 % of the installed thrust force) overweighs the positive effect of having a lower skin friction coefficient.

In order to evaluate structural safety, the lining hoop stress was compared to the shotcrete strength not only at the final state (assuming $f_{c,sc}$ = 25 MPa) far behind the TBM, but also at a section located at 2 m behind the shield in order to check overstressing of the green shotcrete. The early strength of the shotcrete at this section was taken to $f_{c,sc}$ = 10 MPa according to lab tests on 8–10 hours old specimens. This age is relevant for the shotcrete loading taking into account the actual gross advance rate of v = 5–6 m/d.

In order to check the clearance profile, the space used up by the actual thickness of each support system was taken into account. (A thicker shotcrete lining needs more space but leads to smaller deformations on account of its higher stiffness.)

Table 4.4 shows the combined evaluation of the criteria (i)–(iii) mentioned above. The yielding support systems in combination with the bigger overcut (ΔR = 12 cm) cover the widest spectrum of geological conditions (this conclusion is also true for the other parameter combinations of Figure 4.5b).

The rigid support systems (*RS15* and *RS25*) have a positive effect with respect to the thrust force requirements because they rapidly offer a high resistance to the ground deformations close to the shield (cf. Section 3.3.4). This becomes evident by comparing the distribution of the ground pressure p acting upon the shield and the lining for the support

Table 4.4. Combined evaluation of the hazard scenarios "shield jamming", "support overstressing" and "under-profile" for ongoing excavation (support systems according to Table 4.3, rock mass parameters according to Table 4.2).

		Rock mass type							
Overboring	Support system	1	2	3	4	5	6	7	8
	Unsupported	0	B	B	B	B	B	A	A
	RS15	0	C	A	A	A	A	A	A
	RS25	0	C	A	A	A	A	A	A
6 cm	*YS15/S5*	0	B	B	A	A	A	A	A
	YS15/C5	0	B	A	A	A	A	A	A
	YS15/C15	0	B	B	B	A	A	A	A
	YS25/C15	0	B	B	B	B	A	A	A
	Unsupported	0	0	0	0	B	B	A	A
	RS15	0	C	C	C	C	C	C	A
	RS25	0	C	C	C	C	C	C	A
12 cm	*YS15/S5*	0	0	0	0	C	A	A	A
	YS15/C5	0	0	0	C	C	C	A	A
	YS15/C15	0	0	0	0	0	A	A	A
	YS25/C15	0	0	0	C	C	A	A	A

Legend

0 Installed thrust force sufficient, structural safety of the tunnel support warranted, no under-profile

A Installed thrust force not sufficient, structural safety of the tunnel support not warranted and/or under-profile

B Installed thrust force not sufficient, structural safety of the tunnel support warranted, no under-profile

C Installed thrust force sufficient, structural safety of the tunnel support not warranted and/or under-profile

systems *RS15* (rigid) and *YS15/S5* (yielding). As shown in Figure 4.7, the shield remains practically unloaded in the first case, while a high load develops at the shield tail in the second case and may immobilize or even damage the shield. Nevertheless, in the most of the cases that were investigated, the load developing upon the rigid support systems is much higher than their bearing capacity. Even a simplified estimation of their bearing capacity – disregarding possible bending moments (axial symmetry) – shows an insufficient level of structural safety. Applying a thicker shotcrete layer (d_1 = 25 instead of 15 cm) does not improve matters substantially. At this point, it has also to be noted that the load developing upon the rigid support systems close to the shield depends strongly on the assumed stiffness of the shotcrete. If the assumed "average" value of E_{sc} = 10 GPa overestimates the actual Young's modulus of the green shotcrete, the computations overestimate the ground pressure acting upon the lining near to the shield and, consequently, the positive longitudinal arching effect.

Limitations also exist, however, for yielding supports. Taking into account the boring diameter, the clearance profile and the space needed for the final lining, 40 cm in the tunnel radius was available for the thickness of the tunnel support and for admitting some load-reducing convergences without violating the clearance profile.

A very light support (a practically unsupported tunnel) is theoretically satisfactory. Assuming that the tunnel support would use 10 cm of the tunnel radius, the calculated deformations would violate the clearance profile only for "rock mass types" 7 and 8. However, such a solution would not allow ground deformations to be controlled and would be unacceptable with regard to possible gravity-driven instabilities.

After Table 4.4, the support systems *YS15/S5* and *YS15/C15* employing 15 cm shotcrete in combination with Styrofoam or high ductility concrete elements are the most advantageous. (The first one has been successfully applied, while the second one has only been tested along 30 m of the TBM drive shortly before the end of the critical stretch.) However, when comparing these systems, it has to be borne in mind that the admission of ground deformations may cause more loosening of the rock. The thickness of the plastic

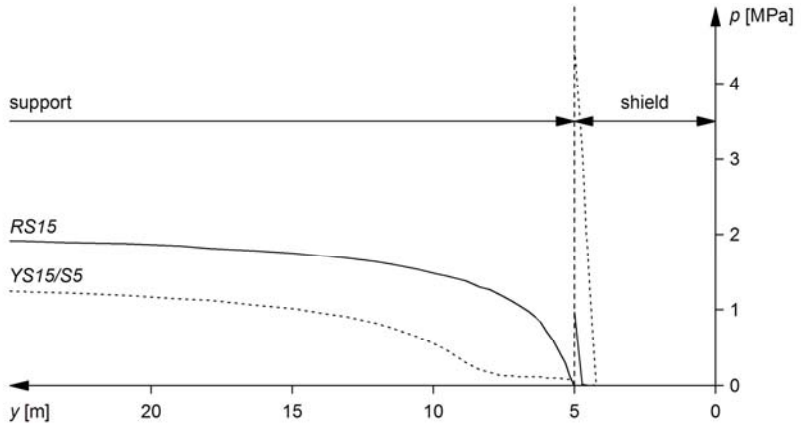

Figure 4.7. Ground pressure p acting upon the shield and the lining ("rock mass type" 6 according to Table 4.2, shield length L = 5 m, radial gap size ΔR = 12 cm, support system RS15 or YS15/S5 according to Table 4.3; other parameters according to Table 4.1, Set 3).

zone (3.7 m), which results from the calculations, provides a rough indication of the extent of the loosened zone and thus of the possible loosening pressure. Assuming a unit weight of the rock of 25 kN/m^2, the resulting loosening pressure amounts to about 90–100 kPa. This value is lower than the yield pressure of the support system with the high ductility concrete elements (*YS15/C15*), but exceeds the resistance of the support system with the Styrofoam elements (*YS15/S5*). Consequently, the latter might start to deform under the action of the loosened rock mass (Figure 4.6) and would use up its deformation capacity with the consequence that it would behave like the rigid support *RS15* during the squeezing phase. The support system *YS15/S5* would therefore be equivalent to *YS15/C15* only if combined with 5–6 m long rock bolts at the crown that would bear the loosening pressure of about 100 kPa. On the other hand, and as shown by tunnelling experience, the application of the support system *YS15/C15* presupposes – due to the relatively high stiffness of the high ductility concrete elements – that the shotcrete develops a sufficiently high early strength (i.e., at least the same compressive strength as the deformable concrete elements). This may be a problem if the time-dependent development of the resistance of the shotcrete is too slow relative to the TBM advance (this aspect is in general less relevant in conventional tunnelling because of the lower advance rates).

5 Thrust force requirements

5.1 Introduction

Section 5 of the present report focuses on the risk of shield jamming and particularly on the thrust force required in order to overcome the skin friction developing when attempting to advance a loaded shield. An insufficient thrust force may make it impossible to restart the TBM after a standstill. The TBM may also become trapped during the actual excavation. In both cases, the TBM will have to be freed by hand-mining around the machine or by the less commonly used method of installing auxiliary thrust cylinders.

It is essential to have information on the frictional force when designing a new TBM and when assessing the feasibility of a proposed TBM drive. Concerning the utilization of a second-hand TBM, checks have to be made as to whether the installed thrust force is sufficiently high or whether the TBM has to be refurbished.

For the majority of practical tunnelling issues, computational investigations are – together with experience gained from projects with comparable geological conditions – indispensable for evaluating potential hazards, as they provide indications as to the magnitude of the key parameters. This is particularly true for assessments of thrust force requirements, because such assessments rely on a detailed knowledge of the distribution of the ground pressure acting upon the shield. Plausibility considerations and engineering judgement, although indispensable, offer limited help in this respect. Empirical methods are based upon correlations of field data obtained in specific projects with potentially different conditions. The widely used simplified closed-form solutions are also of limited value for the problem under consideration as they provide only a rough assessment of the squeezing potential without providing any information concerning ground pressure distribution in the longitudinal direction. Furthermore, the assumption of plane strain conditions, which underlies the closed-form solutions, introduces large errors in the case of heavily squeezing ground (Cantieni and Anagnostou, 2009a). Three-dimensional numerical models take account of the spatial stress redistribution in the vicinity of the advancing face and thereby remedy, at least in principle, these difficulties.

Section 5 presents the assumptions, the method and the results of a comprehensive parametric study into the thrust force required for overcoming friction. The numerical investigations cover the relevant range of material constants, initial stress and TBM characteristics and have been carried out for many different combinations of these parameters. Based upon the results of the parametric study, dimensionless design nomograms have been developed that allow a quick preliminary assessment to be made of the thrust force required in order to overcome shield skin friction and avoid jamming of the shield. The nomograms also make it possible to evaluate rapidly the effect of potential design parameters and operational measures such as reductions in the shield length, the installation of a higher thrust force, increases in the overcut or the lubrication of the shield surface. Section 5 also includes a large amount TBM technical data that is helpful in assessing the technical feasibility of such measures, i.e., for checking whether a particular technical measure is within the normal range of present-day TBMs.

5.2 Decision aids

5.2.1 Computational model

The numerical investigations underlying the nomograms have been carried out applying the axially symmetric computational model of Section 3.2. In the present section, the report discusses the underlying simplifying assumptions, which must be borne in mind when using the nomograms.

Axial symmetry

The assumption of axial symmetry presupposes, in addition to the obvious condition of a cylindrical tunnel, that, (i), the initial stress field is hydrostatic, (ii), the material behaviour is isotropic, and, (iii), the tunnel support is uniform. The first two conditions are usual in the analysis of overstressed rock masses (cf., e.g., Kovári, 1998; Hoek and Marinos, 2000a, 2000b), while condition (iii) implies that the effect of the TBM weight can be neglected and, in the case of a segmental lining, that annulus grouting is uniform along the tunnel periphery.

The most significant consequence of the assumption of axial symmetry is that only normal forces are seen developing in the shield and in the lining, while in reality bending may also occur. Given the goal of the design nomograms (which is to assess thrust force requirements), however, it is sufficient to determine the overall ground pressure acting upon the shield. As a consequence of the assumption of axial symmetry, the pressure obtained is "homogenized" over the tunnel cross-section due to the fact that the model assumes an overcut that is constant around the circumference of the shield, while in reality the shield slides along the tunnel floor, which means that the overcut is bigger above the centre than in the lower portion of the tunnel cross-section.

Another consequence of the assumption of axial symmetry is that the response of the model shield and lining tends to be stiffer than it is in reality and this should lead to an overestimation of the ground pressure and of the necessary thrust force.

Variability of the ground

The nomograms have been worked out assuming a homogeneous ground. Although this assumption is standard, it should be borne in mind that the intensity of squeezing may vary considerably within short stretches along the tunnel alignment (Cantieni and Anagnostou, 2007) and, as pointed out by Kovári (1998), this variability is often responsible for the setbacks often experienced when tunnelling in squeezing ground.

The assumption of homogeneity presupposes that uniform ground conditions persist along the alignment and may be conservative if the TBM crosses a single short geological fault zone. Past research (Kovári and Anagnostou, 1995; Cantieni and Anagnostou, 2007) has shown that in this case the adjacent competent rock has a stabilizing effect as shear stresses are mobilized at its interface with the weaker zone. The shorter the fault zone, the more pronounced the favourable effect of the adjacent competent rock. As shown in Section 4.2.3, this so-called "wall effect" also has a positive influence in TBM tunnelling (see also, e.g., Graziani et al., 2007; Matter et al., 2007).

Time-dependency of ground behaviour

In order to reduce complexity, time-dependent ground response – due to creep or consolidation, cf. Anagnostou and Kovári (2005) – is not taken into account here. According to this simplifying assumption, all plastic deformations occur instantaneously. As the actual behaviour of squeezing ground is often time-dependent (i.e., the deformations develop with a delay with respect to excavation), the model tends to overestimate deformations in the vicinity of the advancing face and the pressure acting upon the shield during continuous excavation. Consequently, with respect to the shield loading, a safety margin exists in this case, which may be bigger or smaller depending on how quickly the ground responds to the excavation. This safety margin can be taken into account qualitatively in the evaluation of the results, but this presupposes that sufficient knowledge exists as to the behaviour of the ground over time. In most cases there is a large uncertainty about the time-development of squeezing and it may be unwise to rely upon the hypothesis that deformations will develop slowly far behind the face. It should be noted that rapidly developing convergences have been observed in a number of tunnels in the past (cf. Section 2.2).

Constitutive model

For the mechanical behaviour of the ground, the standard linearly elastic, perfectly plastic material model with the Mohr-Coulomb yield criterion and non-associated flow rule has been adopted (cf. Section 3.2.1). The implementation of a more complex material law

would be possible and might lead to a better representation of phenomena such as softening. However, such models contain a larger number of parameters which cannot be determined with sufficient reliability and therefore necessitate additional assumptions, which themselves introduce further uncertainties. Furthermore, there are in practice many relevant materials – e.g., intensively sheared or kakiritic rocks – which exhibit a material behaviour that can be mapped reasonably well by the assumed constitutive law (Vogelhuber, 2007).

The material model, which has been employed, is familiar in tunnel engineering practice and it offers the additional advantage of having a relatively small number of easily interpretable parameters (Kovári, 1977): the Young's modulus E, the Poisson's ratio ν, the uniaxial compressive strength f_c, the angle of internal friction φ and the dilatancy angle ψ. It is, therefore, a reasonable model at least for making an initial assessment of a TBM drive (which is the objective of the design nomograms).

Even with this relatively simple constitutive model, the number of problem parameters is still large and, therefore, a trade-off has had to be made between the completeness of the parametric study and the cost of computation and data processing. For this reason, the Poisson's ratio was kept constant to $\nu = 0.25$, while the dilatancy angle ψ was not treated as an independent parameter but was taken as a function of the angle of internal friction φ (Vermeer and de Borst, 1984):

$$\psi = \begin{cases} 1° & \text{for } \varphi \le 20° \\ \varphi - 20° & \text{for } \varphi > 20° \end{cases} . \tag{5.1}$$

The computations account, however, for a wide variation of the other three material constants (E, φ and f_c) and cover the relevant range of ground strength and deformability for tunnelling practice.

Equation 5.1 leads to dilatancy angles of up to 5 ° for friction angles of φ = 20–25 °. This prediction is reasonable according to laboratory results obtained by ETH Zurich with weak squeezing rocks (Vogelhuber, 2007). In the case of a more pronouncedly dilatant behaviour of the ground, however, the assumption made (Equation 5.1) would underestimate the squeezing pressures and deformations.

As for every geomechanical analysis, the estimation of representative ground parameters (based on experience, laboratory tests, field tests or back analysis of field measurements) is demanding. The inherent uncertainties associated with the material constants of the ground should be kept in mind when using the nomograms. In this respect, sensitivity analyses are indispensable.

5.2.2 Dimensionless parameters

With respect to the main goal of the present investigation, which is to determine the required thrust force, the main computational result is the spatial distribution of the radial pressure acting upon the shield. Typical load distributions $p(y)$ are shown, e.g., in Figure 3.6c. The load concentration in the rear part of the shield is a consequence of the complete unloading experienced by the tunnel boundary at $y = L$ (cf. Section 3.3.2). The load concentration is nevertheless of minor importance for the required thrust force, as it affects only a narrow area.

The thrust force F_f required to overcome shield skin friction can be calculated by integrating the ground pressure p over the shield surface according to Equation 3.1. The required thrust force F_f generally depends on all of the parameters of the problem under consideration, which are the material constants of the ground (Young's modulus E, Poisson's ratio ν, uniaxial compressive strength f_c, angle of internal friction φ and dilatancy angle ψ), the initial stress σ_0, the characteristics of the TBM (tunnel radius R, radial gap size ΔR, shield length L and shield stiffness K_s), the skin friction coefficient μ and the stiffness of the lining K_l:

$$F_f = f\left(E,\ \nu,\ f_c,\ \varphi,\ \psi,\ \sigma_0,\ R,\ \Delta R,\ L,\ K_s,\ \mu,\ K_l\right) , \tag{5.2}$$

where the radial gap size ΔR is assumed to be constant. According to Ramoni and

Anagnostou (2010a), the number of parameters can be reduced by performing a dimensional analysis and taking into account both Equation 3.1 and a general property of elasto-plastic materials according to Anagnostou and Kovári (1993):

$$F_f^* = \frac{F_f}{\mu\ 2\pi RL\ \sigma_0} = f\left(\frac{E}{\sigma_0}\frac{\Delta R}{R},\ \nu,\ \frac{f_c}{\sigma_0},\ \varphi,\ \psi,\ \frac{L}{R},\ \frac{K_s\ R}{E},\ \frac{K_l\ R}{E}\right) . \tag{5.3}$$

As Equation 5.3 assumes a constant radial gap size, a slightly different expression applies to the case of double shielded TBMs having a bigger gap in the rear shield than in the front shield:

$$F_f^* = \frac{F_f}{\mu\ 2\pi RL\ \sigma_0} = f\left(\frac{E}{\sigma_0}\frac{\Delta R}{R},\ \nu,\ \frac{f_c}{\sigma_0},\ \varphi,\ \psi,\ \frac{L}{R},\ \frac{K_s\ R}{E},\ \frac{K_l\ R}{E},\ \frac{\Delta R_r}{\Delta R},\ \frac{L_r}{L}\right) , \tag{5.4}$$

where $\Delta R = \Delta R_f$ denotes the overcut of the front shield, L is the total shield length and ΔR_r and L_r denote the radial gap size and the length of the rear shield, respectively.

The normalized thrust force F_f^* has a clear physical meaning: it is equal to the ratio of average ground pressure p_s acting upon the shield to the initial stress σ_0 (cf. Equation 3.1), i.e.,

$$p_s = F_f^* \sigma_0 \ . \tag{5.5}$$

The design nomograms presented in this report are also useful, therefore, with respect to the structural design of the shield. Although the distribution of the ground pressure $p(y)$ is non-linear (cf., e.g., Figure 3.6c), the average value p_s indicates the loading level of the shield and can be used for a first assessment of the structural safety of the shield (e.g., assuming, as a simplification, a linear distribution of $p(y)$ along the shield, where $p(L/2) = p_s$).

5.2.3 The parameter range covered

In order to reduce computational effort, the numerical analyses have been carried out only for selected machine and lining parameters.

Shield stiffness

The stiffer the shield, the higher will be the ground pressure upon it. All calculations have been carried out for a normalized shield stiffness of K_sR/E = 10. If the actual stiffness K_sR/E is lower than this value, the required thrust force will be overestimated by the nomograms. The value of K_sR/E = 10 corresponds to a rather stiff shield and has been chosen in order to be on the safe side for most cases. Figure 5.1 shows the influence of this dimensionless parameter on the normalized required thrust force F_f^* for the given ground conditions and typical geometrical data of single shielded TBMs. It can be observed that the overestimation of F_f^* can be quite relevant in the case of thin shields or a ground with a high Young's modulus E.

Lining stiffness

Figure 5.1 also shows the effect of the normalized stiffness of the lining K_lR/E. It is interesting to note that the stiffer the lining, the lower the required thrust force. As can be observed by comparing Figure 5.1a, which applies for a normalized shield length L/R = 2.0, with Figure 5.1b (L/R = 5.0) this effect is more pronounced for short than for long shields. The reason for this behaviour is that a stiff lining, which is installed close to the face, facilitates arch action in the longitudinal direction and thus reduces shield loading (cf. Section 2.4.7).

The calculations for the shielded TBMs have been carried out assuming a normalized lining stiffness of K_lR/E = 0.5. As this value corresponds to a rather soft lining, the nomograms are on the safe side for most cases. This conservative assumption is also justified by the fact that the annulus backfill has a lower stiffness than the segmental lining, thus reducing the overall stiffness of the system (the stiffness K_l introduced in the computation

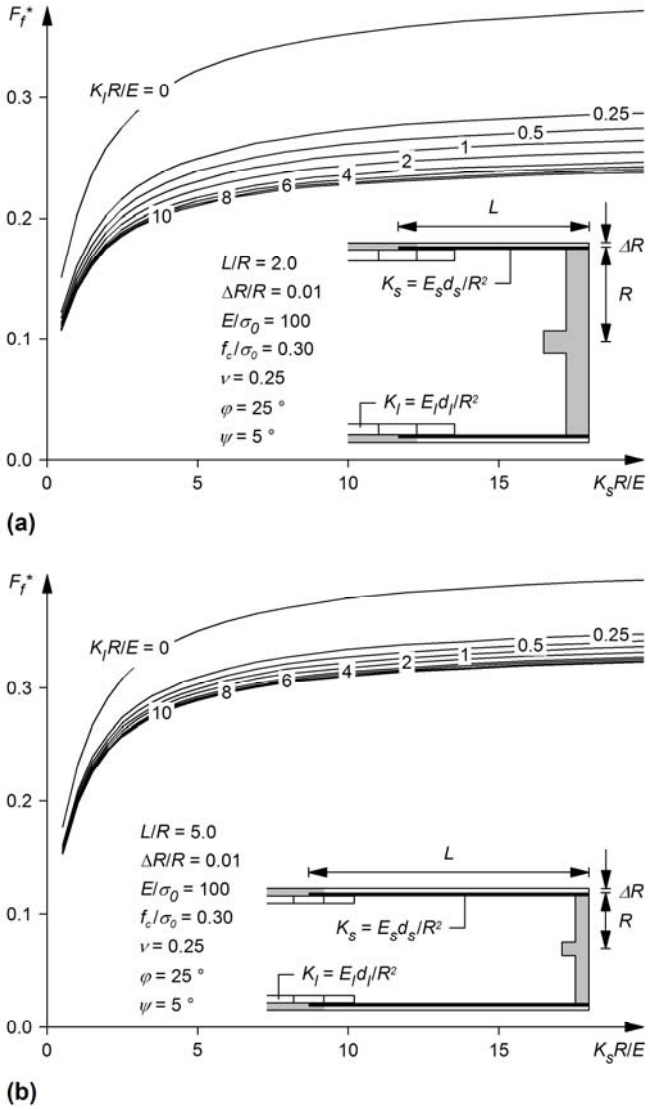

Figure 5.1. Effect of the normalized stiffness of the shield K_sR/E and of the normalized stiffness of the lining K_lR/E on the normalized required thrust force F_f^* for single shielded TBM with a normalized shield length of L/R = 2.0 (a) and L/R = 5.0 (b).

has to be seen as an "average" one). On the other hand, if the actual normalized lining stiffness K_lR/E is lower than 0.5, the required thrust force will be underestimated by the nomograms.

In the case of gripper TBMs, the installation of a stiff lining in the machine area is difficult. It has also to be considered that the development of stiffness in the shotcrete takes time and is, in general, slow relatively to the advance rate. On account of the uncertainties existing with respect to the support stiffness immediately behind the shield, the decisions has been taken to work out the gripper TBM nomograms without taking into account a tunnel support (i.e., K_lR/E = 0).

Machine layouts

The calculations have been carried out for a limited number of normalized shield length values L/R, which however are typical for the different TBM types and have been selected on the basis of the technical data of geometrical nature collected in Figure 5.2.

The normalized shield length is shorter for gripper TBMs (L/R = 1.0) than for single shielded TBMs (L/R = 2.0 to 5.0, depending on the tunnel diameter, the larger values applying to small diameters). This is also true for double shielded TBMs, which show,

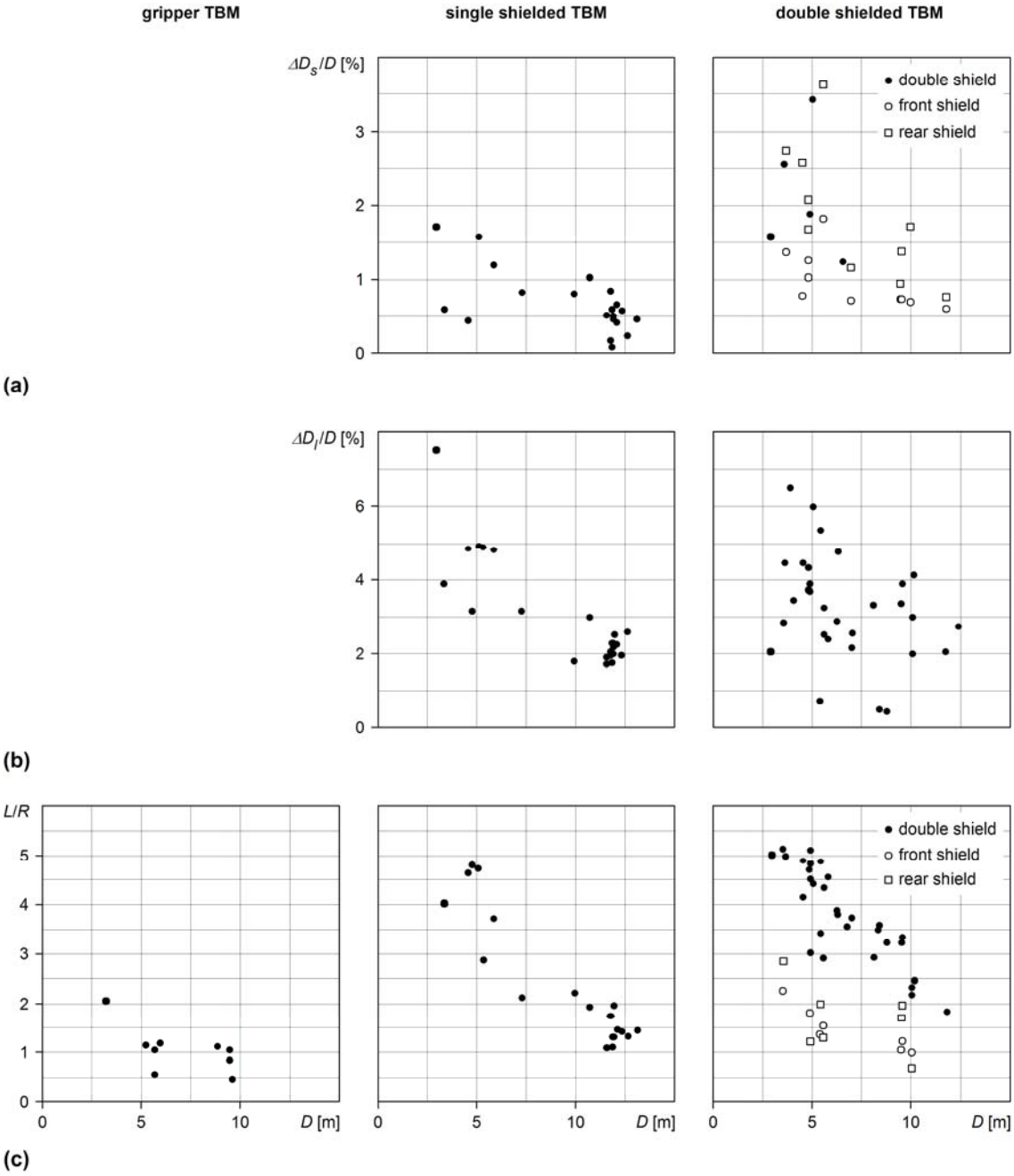

Figure 5.2. Technical data of various TBMs as a function of the boring diameter D: (a) ratio $\Delta D_s/D$ between overcut ΔD_s (in diameter) and boring diameter D; (b) ratio $\Delta D_l/D$ between annular gap ΔD_l (in diameter) and boring diameter D; (c) normalized shield length L/R.

however, a wider variation of the normalized shield length. In order to cover the relevant range better, the calculations have been carried out for three values (L/R = 2.0, 3.5 and 5.0). Furthermore, as different components of the thrusting system are employed for advancing the front and the rear shield, the ground pressure and the frictional resistance of the two shields have to be considered separately and this necessitates assumptions as to their lengths. On account of Figure 5.2c, the ratio between the length of the rear shield L_r and the length of the front shield L_f was taken as 1.5 in the numerical analyses (i.e., the length of the rear shield L_r amounts to 60 % of the total length L). The overcut ΔR is also bigger for the rear shield (ΔR_r) than it is for the front shield (ΔR_f). A typical ratio of $\Delta R_r/\Delta R_f$ = 1.5 was assumed (cf. Figure 5.2a) and separate nomograms have been worked out for the front and the rear shield. The thrust force required for

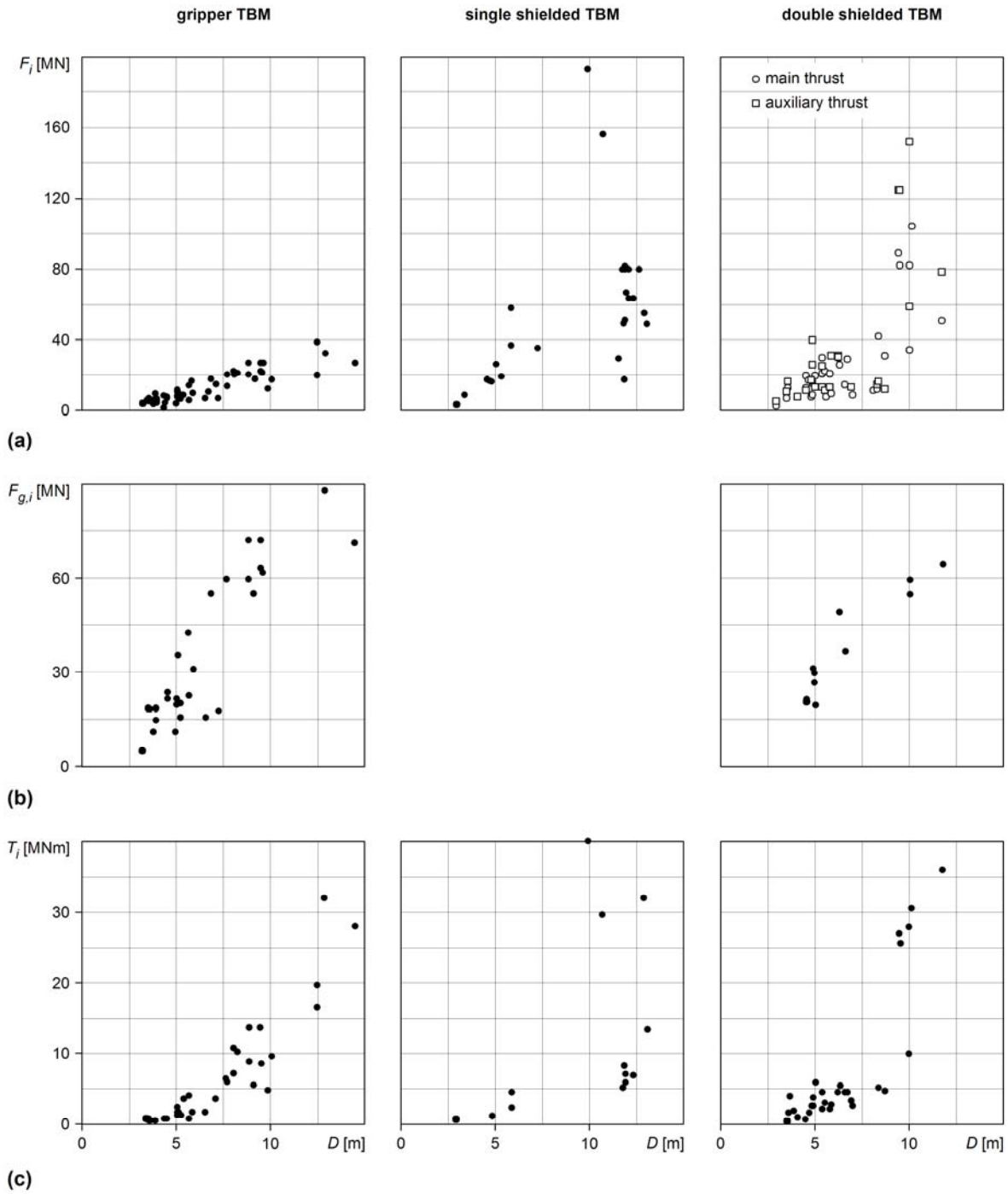

Figure 5.3. Technical data of various TBMs as a function of the boring diameter D: (a) installed thrust force F_i; (b) installed gripper force $F_{g,i}$; (c) installed torque T_i.

moving the entire double shield can be determined easily by adding the forces necessary for overcoming the skin friction of its two parts.

Figure 5.3 enhances the TBM data collection mentioned above by presenting data about thrust force and torque. Figure 5.3 allows, e.g., to evaluate quickly whether the required thrust force determined with the nomograms is feasible or not. The data has been collected based upon a comprehensive literature study concerning a number of projects. The detailed data underlying Figures 5.2 and 5.3 can be found in Ramoni (2010).

5.2.4 The nomograms

Bearing in mind that the values of some of the parameters have been fixed as discussed above, the normalized required thrust force depends on the four remaining parameters:

$$F_f^* = \frac{F_f}{\mu\ 2\pi RL\ \sigma_0} = f\left(\frac{E}{\sigma_0}\frac{\Delta R}{R},\ \frac{f_c}{\sigma_0},\ \varphi,\ \frac{L}{R}\right) . \tag{5.6}$$

Equation 5.6 is represented graphically in the diagrams of Appendix II (Figures II.1 to II.9). Each figure applies to a different TBM type and normalized shield length L/R, while each diagram applies to a different value of the angle of internal friction φ and includes a band of curves (each curve corresponding to another value of the normalized uniaxial compressive strength f_c/σ_0) showing the normalized thrust force F_f* required to overcome shield skin friction as a function of the dimensionless product of E/σ_0 by $\Delta R/R$.

5.2.5 Model behaviour

According to the numerical results of Figures II.1 to II.9, the shorter the shield and the larger the radial size of the gap, the lower will be the required thrust force. The effect of the uniaxial compressive strength of the ground is, however, not as straightforward as one might expect. At low values of $(E\Delta R)/(\sigma_0 R)$, an increase in the normalized uniaxial compressive strength f_c/σ_0 leads to an increase in the normalized required thrust force F_f*, i.e., for a given value of $(E\Delta R)/(\sigma_0 R)$, a better quality ground requires a higher thrust force. This counter-intuitive behaviour is well-known in the literature (Cantieni and Anagnostou, 2010).

5.3 Application examples

The use of the design nomograms will be demonstrated by returning to the example of Section 3.3.1 (a 400 m deep, 10 m diameter tunnel, which is driven by a 10 m long single shielded TBM). Table 5.1 contains the input parameters as well as detailed, step-by-step calculations. Columns 1 to 5 show how to compute the required thrust force for given ground conditions, TBM parameters and operating states, i.e., these columns deal with dimensioning, while Columns 6 to 9 address the inverse problem and show how to estimate the feasibility limits of a given TBM (in terms of the ground quality and the given thrust force, shield length, overcut, etc.).

5.3.1 Determining the required thrust force

Columns 1 to 3 calculate the force required during the boring process for normal, medium and major overcuts ΔR (of 5, 10 or 15 cm, respectively, see Row 10), while Columns 4 and 5 concern the thrust force requirements for restarting the machine after a standstill. As no time-dependency is considered in respect of the ground behaviour, the two operational states differ only with respect to the skin friction coefficient μ (static vs. sliding friction, Row 15) and to the force F_b required for the boring process (Row 19), on the assumption that the boring thrust force is equal to zero at the moment of restarting the TBM (i.e., with a retractable cutter head).

Considering the present normalized shield length of L/R = 2.0 (Row 26), Figure II.2 applies, while the appropriate curve has to be selected according to the actual values of the angle of internal friction (φ = 25 °, Row 4) and the normalized uniaxial compressive strength (f_c/σ_0 = 0.3, Row 24). The dimensionless gap size (Row 29) is calculated on the basis of the parameters of Rows 1, 8, 9 and 10 and is entered into the nomogram in order to depict the value of the normalized thrust force F_f* (Row 30) and to calculate the required thrust force F_r (Row 32). For a normal overboring of ΔR = 5 cm, the required thrust force amounts to F_r = 263 MN (Row 32, Column 1). This value exceeds the installed thrust force (F_i = 150 MN, Row 16), thus indicating that the shield may become jammed. As the value of 263 MN is far beyond the normal range (cf. Figure 5.3a), it is questionable

Table 5.1. Application examples.

	Application example			1	2	3	4	5	6	7	8	9
	State			Continuous excavation			Restart after a standstill					
	Thrust force requirements			F_r = ?					$F_r = F_i$		F_r = 0	
	Ground											
1	Young's modulus	E	[MPa]	1000	1000	1000	1000	1000	**900**	1000	**1425**	1000
2	Poisson's ratio	ν	[-]	0.25								
3	Uniaxial compressive strength	f_c	[MPa]	3.0	3.0	3.0	3.0	3.0	3.0	**2.4**	3.0	**4.6**
4	Angle of internal friction	φ	[°]	25								
5	Dilatancy angle	ψ	[°]	5								
6	Unit weight	γ	[kN/m^3]	25								
	Initial stress											
7	Depth of cover	H	[m]	400								
8	Initial stress	σ_0	[MPa]	10 [a]								
	TBM											
9	Boring diameter, boring radius	D, R	[m]	10, 5								
10	Radial gape size	ΔR	[cm]	5	10	15	5	10	10	10	10	10
11	Length (shield)	L	[m]	10								
12	Young's modulus (shield)	E_s	[MPa]	210000								
13	Thickness (shield)	d_s	[cm]	12								
14	Stiffness (shield)	K_s	[MPa/m]	1008 [b]								
15	Skin friction coefficient	μ	[-]	0.30 [c]	0.30 [c]	0.30 [c]	0.45 [c]	0.45 [c]	0.45 [c]	0.45 [c]	0.45 [c]	0.45 [c]
16	Installed thrust force	F_i	[MN]	150 [d]								
17	Maximum cutter force	F_c	[kN]	267 [e]								
18	Number of cutters	n_c	[-]	67 [f]								
19	Thrust force (boring process)	F_b	[MN]	18 [g]	18 [g]	18 [g]	0	0	0	0	0	0
	Lining											
20	Young's modulus	E_l	[MPa]	30000								
21	Thickness	d_l	[cm]	30								
22	Stiffness	K_l	[MPa/m]	360 [h]								
	Dimensionless products											
23		E/σ_0	[-]	100.00	100.00	100.00	100.00	100.00	90.00	100.00	142.50	100.00
24		f_c/σ_0	[-]	0.30	0.30	0.30	0.30	0.30	0.30	0.24 [i]	0.30	0.46 [i]
25		$\Delta R/R$	[-]	0.01	0.02	0.03	0.01	0.02	0.02	0.02	0.02	0.02
26		L/R	[-]	2.00								
27		K_sR/E	[-]	5.04								
28		K_lR/E	[-]	1.80								
29		$(E\Delta R)/(\sigma_0 R)$	[-]	1.00	2.00	3.00	1.00	2.00	1.80 [j]	2.00	2.85 [j]	2.00
	Thrust force requirements											
30	Normalized required thrust force	F_f*	[-]	0.26 [j]	0.08 [j]	0 [j]	0.26 [j]	0.08 [j]	0.11 [k]	0.11 [k]	0 [k]	0 [k]
31	Required thrust force (friction)	F_f	[MN]	245 [l]	75 [l]	0 [l]	367 [l]	113 [l]	150 [m]	150 [m]	0 [m]	0 [m]
32	Total required thrust force	F_r	[MN]	**263** [n]	**93** [n]	**18** [n]	**367** [n]	**113** [n]	150 [o]	150 [o]	0 [o]	0 [o]

Notes

[a] $\sigma_0 = H\gamma$
[b] $K_s = E_s d_s / R^2$
[c] According to Table 2.3
[d] Assumed
[e] After Sänger (2006)
[f] $n_c = 6.7D$, after Vigl et al. (1999)
[g] $F_b = F_c n_c$
[h] $K_l = E_l d_l / R^2$
[i] Figure II.2, design nomogram for $\varphi = 25°$, based upon linear interpolation
[j] Figure II.2, design nomogram for $\varphi = 25°$, curve for $f_c/\sigma_0 = 0.30$
[k] $F_f^* = F_f / \mu 2\pi RL\sigma_0$
[l] $F_f = F_f^* \mu 2\pi RL\sigma_0$
[m] $F_f = F_r - F_b$
[n] $F_r = F_f + F_b$
[o] "Given", in this column the calculation proceeds from down to top

whether a higher thrust force can be installed at all. However, a larger overboring (ΔR = 10 cm) leads to a considerable reduction in the required thrust force to a feasible value of F_r = 93 MN (Row 32, Column 2). In the case of a major overboring (ΔR = 15 cm), the shield would remain unloaded (F_f = 0, Row 31, Column 3) and a thrust force would be needed only for the boring process (F_r = 18 MN, Row 32, Column 3).

The thrust force required in order to restart the TBM can be calculated analogously (Columns 4 and 5) and amounts to 367 and 113 MN, respectively, i.e., it is higher than the thrust force required during the boring process. This is due to the change in the friction regime (static instead of sliding friction), which overweighs the advantage of not having to take into account a boring thrust force. The contrary is also possible, particularly for short shields, where the friction may become less relevant relative to the boring thrust force.

The results obtained by applying the nomograms agree well with the results of the numerical analyses that were carried out specifically for the example of Section 3.3.1 and

lead to the same basic conclusions. For this example, the design nomograms overestimate the required thrust force by about 15–25 %. According to Figure 5.1a this deviation can be traced back to the overestimation of the shield stiffness and to the underestimation of the stiffness of the segmental lining. A single shielded TBM typically has a 12 cm thick shield (Maidl et al., 1995). For the example under consideration, the actual normalized stiffness of the shield would be $K_s R/E \approx 5$ (Row 27) instead of the value of 10 which underlies the nomograms, while the actual normalized stiffness of a 30 cm thick segmental lining would be $K_l R/E \approx 1.8$ (Row 28, neglecting the compressibility of the backfill) instead of 0.5.

The results of the examples discussed above suggest that, for the ground conditions under consideration, both continuous excavation and a restart after a standstill are possible with a medium size overboring (ΔR = 10 cm). As discussed in Section 2.4.3, the reliability of overboring may nevertheless be limited (particularly for hard rocks). It should be noted, furthermore, that the overcut (together with the conicity of the shield) must first of all allow the TBM to be steered. If the ground deforms and closes the gap, any attempt to steer the TBM will lead to the development of constraint loads. In this respect, it is necessary to build in some reserves when applying the nomograms (i.e., a reduced radial gap size ΔR should be introduced into the calculations).

5.3.2 Vulnerability with respect to ground variations

The variability of squeezing along a tunnel alignment may be significant (Cantieni and Anagnostou, 2007). It is therefore important to investigate the influence of variations in the ground conditions on the required thrust force. For the sake of simplicity, one assumes that the ground can be described by combinations of its Young's modulus E and its uniaxial compressive strength f_c and that all other ground parameters can be kept constant. Combinations of these two parameters would thus describe the quality of the ground.

The reference ground for the investigations in this section of the report is that of Column 5 of Table 5.1, i.e., a Young's modulus of E = 1000 MPa and a uniaxial compressive strength of f_c = 3 MPa. Assuming a medium overboring (ΔR = 10 cm), a thrust force of 113 MN is required in order to restart TBM advance (Row 32, Column 5). This value is high but thoroughly feasible and lower than the installed thrust force of 150 MN.

How much worse would have to be the ground in order for the TBM to become trapped? In order to answer this question the required thrust force F_r is made equal to the installed thrust force of F_i = 150 MN, the uniaxial compressive strength f_c is kept equal to the reference value of 3 MPa and the Young's modulus E is calculate back (down to top). According to the calculation in Column 6, a decrease in the Young's modulus E of just 10 % may endanger the TBM drive. A similar result can be achieved keeping the Young's modulus E equal to its reference value of 1000 MPa and calculating the critical reduction of the uniaxial compressive strength f_c: according to Column 7, a reduction of 20 % would lead to the jamming of the shield.

In the interests of a stricter set of design criteria, this section will now address the other borderline case, where the required thrust force F_r is equal to zero. How much better should the ground be in order that no squeezing pressure develops upon the shield? This condition is true for the intersection points of the curves with the x-axes of the nomograms (i.e., for F_f^* = 0). According to Columns 8 and 9, the Young's modulus E should be higher by about 40 %, while the necessary uniaxial compressive strength f_c amounts about 1.5 time the reference value of Column 5.

The examples in this section of the report demonstrate that the design nomograms allow a quick sensitivity analysis to be made, while also identifying the critical geotechnical conditions with respect to a given set of design criteria. The nomograms also make it possible to assess planned TBM drives, at least on a preliminary basis, as well as the effects of other possible design measures such as lubrication of the extrados of the shield or reductions in shield length.

5.3.3 Analysis of case histories

In this section, the suitability of the proposed design nomograms will be shown by means of a simplified back-analysis of seven case histories. Table 5.2 summarizes the project data, the TBM data, the geology of the critical stretches and the ground parameters. The corresponding references can be found in Ramoni (2010). Furthermore, in its right part, Table 5.2 compares the installed thrust force F_i of the used TBMs with the required thrust force F_r calculated using the design nomograms. For the sake of simplicity, Table 5.2 reports only the results concerning thrust force requirements for restarting the machine after a standstill (cf. Section 5.3.1).

Bodio Section of the Gotthard Base Tunnel (Switzerland)

The Bodio Section of the Gotthard Base Tunnel (Switzerland) was excavated by two gripper TBMs (D = 8.80 m). Squeezing ground conditions were not anticipated in the planning phase. During construction, however, the shield of the western tube TBM was jammed in March 2006, the bored profile experienced a convergence of 7–10 cm in the machine area and of 14–22 cm in the back-up area and the tunnel support became damaged. At this time, the TBM drive was proceeding in strong anisotropic micaceous gneiss under a depth of cover of 1000 m approaching at a small angle a fault zone with a thickness of 3–5 m. The ground parameters reported in Table 5.2 are based upon laboratory tests carried out after the TBM became trapped. Depending on the ground parameters that are introduced, the required thrust force computed with the design nomograms varies from zero to very high values (Table 5.2), which, of course, are clearly not feasible with a gripper TBM. The large uncertainty – depending on the sort of ground encountered the TBM may or may not become trapped – was confirmed by what actually happened: the western TBM ground to a halt and its shield was damaged, while the following eastern TBM only slowed down without becoming trapped. The damage to the shield claimed by the contractor suggests that a high ground pressure did develop and, therefore, that the computed high values of the required thrust force are not unreasonable.

Faido Section of the Gotthard Base Tunnel (Switzerland)

This section of the Gotthard Base Tunnel was excavated by the refurbished gripper TBMs (D = 9.43 m) that excavated the Bodio Section. The TBM drives started in July and October 2007, respectively, in micaceous gneiss under a depth of cover of 1600 m. After what happened in the Bodio Section and in the Faido Multi-function Station, squeezing ground conditions were expected. The Bodio TBMs were refurbished with a bigger boring diameter (D = 9.43 m instead of 9.30 m) and the TBM drive started with shifted gauge cutters (so-called "overboring", D = 9.50 m). During excavation, convergences of up to 5–10 cm occurred in the shield area (observed at the shield tail about 5 m behind the face) but shield jamming was avoided. However, convergences in the machine and in the back-up area occurred over a length of 250 m (of up to 5–10 cm in the roof and of up to 30 cm in the floor of the eastern tube as well as of up to 25 cm in the roof and of up to 75 cm in the floor of the western tube). The yielding tunnel support thereby became damaged and the back-up locally jammed. The nomograms (applied with the design ground parameters) return a large range of values for the required thrust force depending on the variation of the Young's modulus E (Table 5.2). The fact that the TBM did not become jammed does not mean that the nomograms cannot be applied but only suggests that the quality of the ground was better than the expected "worst case" (see also Section 4.3).

Uluabat Tunnel (Turkey)

The TBM drive (single shielded TBM, D = 5.05 m) started in April 2006 in a ground consisting of a claystone matrix (80 %) containing 1–50 cm big sandstone lenses (20 %). The claystones are intensively sheared, have several slickensides and disintegrate quickly under the action of water. During the first 3 km of TBM operation, squeezing caused jamming of the shield on several occasions although the depth of cover was rather moderate (120 m). An increase in the installed thrust force by applying additional thrust cylinders was not successful as it caused damage to the segmental lining. The available monitoring results are very sparse, but some observations indicated a large variability of squeezing intensity and maximum deformation rates of up to 6 cm/h. The range of ground

Table 5.2. Analysis of case histories.

Project (country) TBM type, Manufacturer, Start year of TBM drive	TBM	Depth of cover Geology	Ground	Thrust force F_i [MN]	 F_r [MN]
Gotthard Base Tunnel, Bodio Section (Switzerland) Gripper TBM, Herrenknecht, 2003	D [m] = 8.80 L [m] = 5.00 ΔR [cm] = 6 [a]	H [m] = 1000 Micaceous gneiss	E [MPa] = 4400–18000 f_c [MPa] = 5.2–34.5 φ [°] = 32–49 γ [kN/m^3] = 26	27.5	0–117 [b,c]
Gotthard Base Tunnel, Faido Section (Switzerland) Gripper TBM, Herrenknecht, 2007	D [m] = 9.43 L [m] = 5.00 ΔR [cm] = 12 [d]	H [m] = 1600 Micaceous gneiss	E [MPa] = 7500–15000 f_c [MPa] = 2.5 φ [°] = 32 γ [kN/m^3] = 26	27.5	15–319 [b,c]
Uluabat Tunnel (Turkey) Single shielded TBM, Herrenknecht, 2006	D [m] = 5.05 L [m] = 11.95 ΔR [cm] = 4 [e]	H [m] = 120 Claystone	E [MPa] = 200–1000 f_c [MPa] = 0.2–1.2 φ [°] = 20 γ [kN/m^3] = 25	27.0 40.0 [f]	0–85 [b,g]
Pajares Tunnel, Section 4 (Spain) Single shielded TBM, Robbins, 2006	D [m] = 9.88 L [m] = 11.00 ΔR [cm] = 4	H [m] = 650 Shale	E [MPa] = 2500–4500 f_c [MPa] = 1.5–3.0 φ [°] = 23 γ [kN/m^3] = 26	139.5 193.0 [h] 225.0 [f]	201–381 [g,i]
Wienerwald Tunnel (Austria) Single shielded TBM, Herrenknecht, 2005	D [m] = 10.67 L [m] = 10.40 ΔR [cm] = 7 [e]	H [m] = 220 Fault zone	E [MPa] = 150–250 f_c [MPa] = 0.5–1.0 [a] φ [°] = 15–20 γ [kN/m^3] = 25 [a]	156.3	159–178 [g,i]
Guadiaro – Majaceite Tunnel (Spain) Double shielded TBM, NFM-Boretec-Mitsubishi, 1995	D [m] = 4.88 L [m] = 11.00 L_f [m] = 4.40 [a] L_r [m] = 6.60 [a] ΔR_f [cm] = 6 [a] ΔR_r [cm] = 9 [d]	H [m] = 400 Sandy and clayey flysch, claystone	E [MPa] = 1000 f_c [MPa] = 0.5–1.0 φ [°] = 23 γ [kN/m^3] = 21	15.2 [j] 23.3 [k] 40.0 [h,k]	21–29 [i,j,l] 26–38 [i,k,m]
Guadarrama Tunnel (Spain) Double shielded TBM, Wirth-NFM, 2002	D [m] = 9.46 L [m] = 15.24 L_f [m] = 5.04 L_r [m] = 8.10 ΔR_f [cm] = 4 ΔR_r [cm] = 5	H [m] = 300 Fault zone	E [MPa] = 300–700 f_c [MPa] = 0.5–7.5 φ [°] = 20 [a] γ [kN/m^3] = 25 [a]	89.0 [j] 108.0 [k] 125.0 [h,k]	35–73 [i,j,n] 57–135 [i,k,o]

Legend

- D Boring diameter
- E Young's modulus of the ground
- f_c Uniaxial compressive strength of the ground
- F_i Installed thrust force
- F_r Required thrust force
- H Depth of cover
- L Length of the shield
- L_f Length of the front shield
- L_r Length of the rear shield
- ΔR Radial gap size
- ΔR_f Radial gap size (front shield)
- ΔR_r Radial gap size (rear shield)
- φ Angle of internal friction of the ground
- ψ Dilatancy angle of the ground

Notes

- [a] Assumed
- [b] Skin friction coefficient μ = 0.45, according to Table 2.3
- [c] Figure II.1
- [d] With overboring
- [e] Tail shield
- [f] By installing removable auxiliary hydraulic jacks
- [g] Figures II.2 and II.3 (linear interpolation)
- [h] Maximal possible thrust force
- [i] Skin friction coefficient μ = 0.25 (with lubrication of the shield mantle), according to Table 2.3
- [j] Main system
- [k] Auxiliary system
- [l] Figures II.6 and II.8 (linear interpolation)
- [m] Figures II.7 and II.9 (linear interpolation)
- [n] Figures II.4 and II.6 (linear interpolation)
- [o] Figures II.5 and II.7 (linear interpolation)

parameters given in Table 5.2 is based upon laboratory tests. The latter are representative for the ground, given its very weak character up to the scale of the specimen. The computed thrust force requirements (Table 5.2) agree very well with what happened during the TBM drive: depending on the variation of the ground conditions, the shield may or may not become jammed (see also Section 4.2).

Section 4 of the Pajares Tunnel (Spain)

The tunnel excavation started with a single shielded TBM (D = 9.88 m) in August 2006 and finished in July 2009. Heavily squeezing ground was expected in the so-called "Formigoso Formation", particularly in sections exhibiting a high degree of tectonization. In fact, the TBM became trapped in November 2007 in spite of the very high installed thrust force (F_i = 193 MN). The excavation was resumed with an increase of the thrust force (F_i = 225 MN) by installing removable auxiliary hydraulic jacks (this operation also required a reinforcement of the shield) and lubricating the shield mantle with bentonite in order to reduce shield skin friction. The thrust force resulting from the application of the

design nomograms and computed with the design parameters (the "worst" ones in Table 5.2) is higher than the installed one (F_r = 381 MN vs. F_i = 225 MN), which was sufficient for resuming excavation. This can be explained by a number of factors, which concern the uncertainties related to the structure and the parameters of the ground. Firstly, as only the tail shield was blocked, it seems that the squeezing ground was localized in a short fault zone. In such a case, the design nomograms overestimate the required thrust force as they disregard the "wall effect" (cf. Section 5.2.1). Secondly, detailed field investigations showed that the rock mass was better than expected. In fact, the assumption of a "better" combination of ground parameters (E = 4500 MPa and f_c = 3 MPa, Table 5.2) leads to a lower required thrust force, which is near to the installed one (F_r = 201 MN vs. F_i = 225 MN).

Wienerwald Tunnel (Austria)

This tunnel was excavated by two single shielded TBMs (D = 10.67 m) between October 2005 and August 2007. Squeezing ground conditions did not occur. In the planning phase, however, attention was paid to the potential hazard of shield jamming with respect to the crossing of several long fault zones with poor ground conditions. For this case history, the required thrust force has been computed with a reduced skin friction coefficient (Table 5.2) in order to take account of the lubrication of the shield mantle carried out on the construction site as a preventive counter measure before entering the fault zones. The thrust force resulting from the application of the design nomograms is only slighty higher than the installed one (Table 5.2). This result can be traced back to the fact that the nomograms are on the safe side in most cases (cf. Section 5.2.3).

Guadiaro – Majaceite Tunnel (Spain)

The TBM drive (double shielded TBM, D = 4.88 m) started in November 1995 and finished in February 1997. Squeezing ground conditions were expected in the planning phase and occurred during construction. The TBM was trapped when excavating flysch consisting almost entirely of claystone under a depth of cover of 400 m. The TBM drive was restarted after freeing of only 10 % of the shield surface. This suggests that a slightly higher thrust force would be sufficient in order to avoid shield jamming. The required thrust force computed with the design nomograms (Table 5.2) agrees very well with what happened during construction.

Guadarrama Tunnel (Spain)

This tunnel was driven between October 2002 and June 2005 by four double shielded TBMs (D = 9.46 m and D = 9.51 m). Squeezing ground conditions were expected in the 600 m long fault zone "La Umbria" under a depth of cover of 300 m but did not occur under construction. This confirms the suitability of the result returned by the design nomograms (also in this case the computations of Table 5.2 take into account the lubrication of the shield mantle carried out during construction).

6 Squeezing pressure on segmental linings

6.1 Introduction

The main hazard scenarios for shielded TBM tunnelling in squeezing ground are sticking of the cutter head, jamming of the shield or damage to the tunnel support. Furthermore, the occurrence of significant deformations (ovalization) or even horizontal or vertical shifting of the segmental lining may lead to jamming of the back-up equipment or to violation of the clearance profile. The present section of the reports deals with the specific problem of lining overstressing addressing the key question of the ground pressure acting upon a segmental lining installed behind a single shielded TBM

A realistic estimation of the loading of a segmental lining is only possible if due account is taken of the backfilling features. Section 6.2 shows – with a structured discussion of the influencing factors and their interactions – that the type, location and thickness of the backfilling play an important role with respect to the ground pressure acting upon a segmental lining. Section 6.3 explains how to take due account of these features in a numerical simulation and, more specifically, how to deal with the non-linearity of the problem. The problem is demanding because the actual thickness of the backfilling is not known a priori, as it depends on the ground deformations that occur between the tunnel face and the point at which the backfilling is completed. Section 6.4 presents, in the form of dimensionless design nomograms, the results of a comprehensive parametric study into the ground pressure acting upon a segmental lining. The nomograms cover the relevant range of ground parameters and initial stress, as well as different characteristics of the TBM, the segmental lining and the backfilling (type and location), and allow a quick preliminary assessment to be made of the loading of a segmental lining.

6.2 Backfilling

6.2.1 Introduction

The factors influencing the ground pressure acting upon a segmental lining (particularly the properties of the backfilling) and their interactions can be mapped easily and efficiently using the N^2 chart (cf. Section 2.3.2). Figure 6.1 shows the N^2 chart drawn up for the topic of the present section.

Section 6.2.2 discusses – by making reference to the N^2 chart of Figure 6.1 – the usual case for rock TBM tunnelling, where backfilling of the segmental lining is carried out with pea gravel in the upper part and with mortar in the bottom third of the cross-section at a given distance behind the shield (Figure 6.2a). Section 6.2.3 deals with the rather rare case of grouting immediately behind the shield via the shield tail (Figure 6.2b).

As the shield slides along the tunnel floor, the gap around the shield and the segmental lining is wider above the centre than in the lower portion of the tunnel cross-section (cf. Figure 6.2). However, for the sake of simplicity, Sections 6.2.2 and 6.2.3 consider the theoretical case of axial symmetry, as this simplification can be made without loss of generality in the conclusions drawn.

6.2.2 Backfilling with pea gravel and mortar

Composite stiffness

The ground pressure p acting upon a backfilled segmental lining depends on the ground characteristics {1-13} and on the stiffness K_c of the tunnel support, which consists of the segments and the backfilling {12-13}. The composite stiffness K_c results from the stiffness of the segmental lining K_l {4-12} and the stiffness of the backfilling K_b {11-12}. In contrast to the lining stiffness K_l, the backfilling stiffness K_b is not known a priori. On the one hand, the properties of the backfilling material are known {5-11} but, on the other hand, the

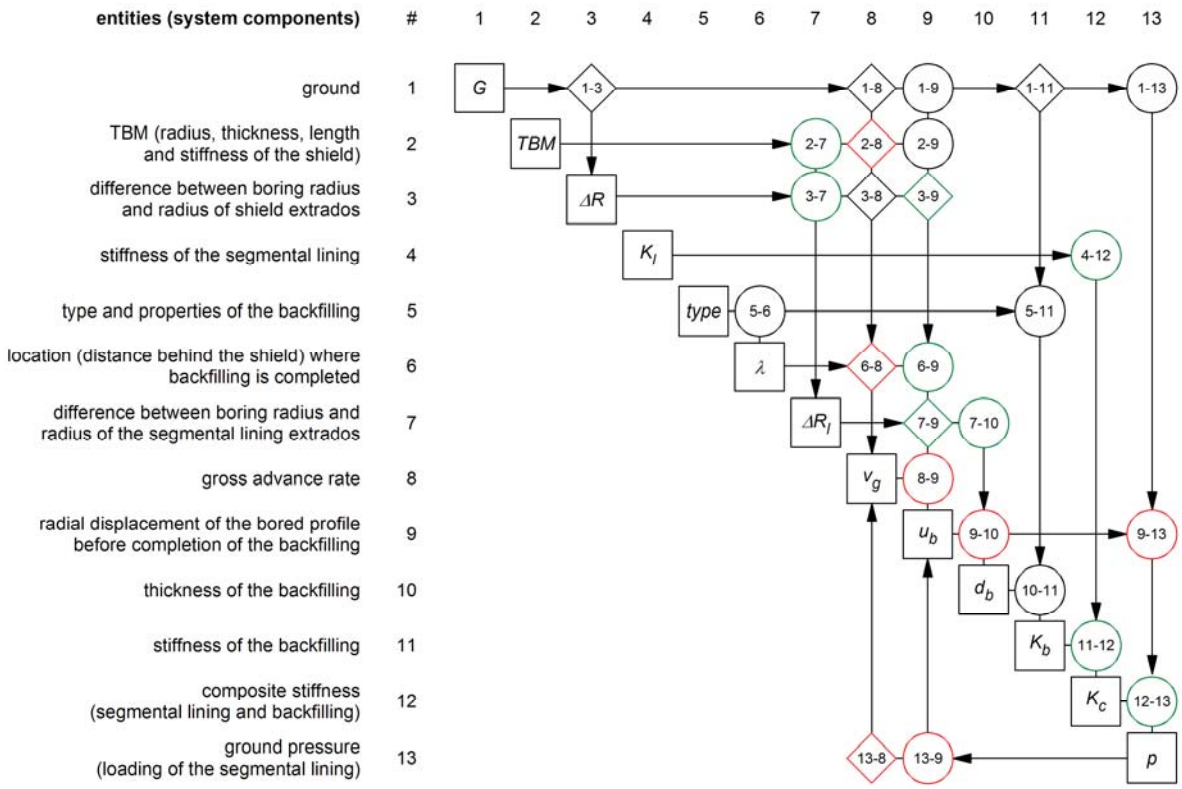

Figure 6.1. N^2 chart concerning the ground pressure p acting upon a segmental lining (for the mapping rules, see Figure 2.2).

characteristics of the ground encountered will influence the quality of the backfilling (e.g., blocky ground may lead to difficulties) {1-11}. Furthermore, the stiffness K_b depends on the thickness of the backfilling d_b (the thinner the backfilling layer, the higher its stiffness {10-11}) and, therefore, on the deformations of the ground.

Thickness of the backfilling

The actual thickness of the backfilling d_b depends on the radial displacement of the bored profile u_b {9-10} occurring behind the tunnel face up to the point at which the backfilling is completed (Figure 6.3a):

$$\begin{cases} d_b = \Delta R_l - u_b \\ 0 \le u_b \le \Delta R_l \end{cases}, \tag{6.1}$$

where ΔR_l is the planned size of the radial gap of the segmental lining {7-10}. ΔR_l is equal to the difference between the boring radius R and the radius of the segmental lining extrados $R_{l,o}$ (cf. Figure 6.3a) and represents an upper limit for the radial displacement of the bored profile u_b {7-9}. Equation 6.1 disregards possible deformations of the segmental lining. This simplification is reasonable, as the deformations of the segmental lining are small (due to its high stiffness) compared to those of the ground.

With respect to the thickness of the backfilling d_b, two borderline cases can be distinguished. If the ground does not deform (i.e., $u_b = 0$, Figure 6.3b), the backfilling is as thick as the planned size ΔR_l of the radial gap between segments and ground. On the other hand, if the ground closes the radial gap before backfilling occurs (i.e., $u_b = \Delta R_l$, Figure 6.3c), the thickness of the annular gap becomes equal to zero and backfilling is no longer possible.

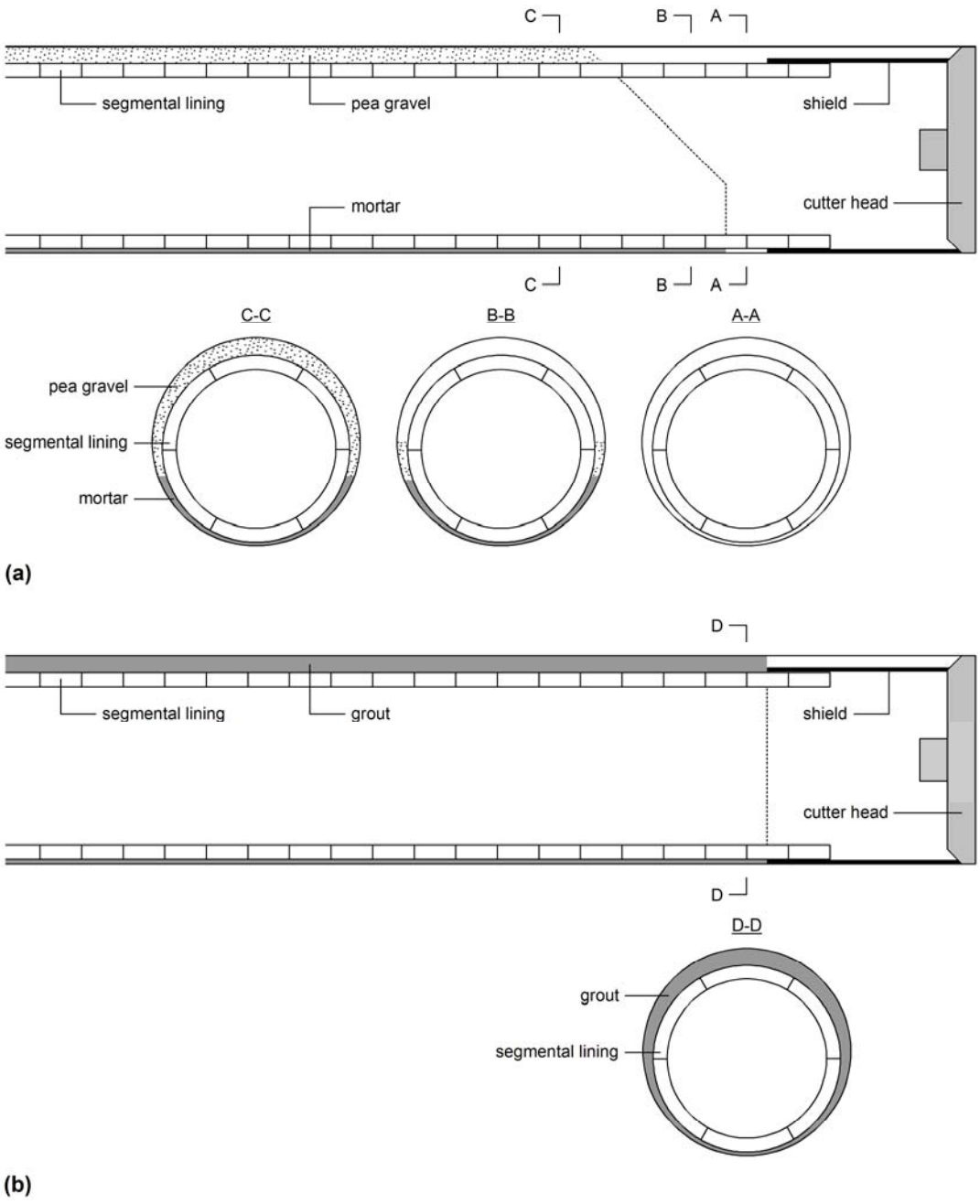

Figure 6.2. (a) Backfilling with pea gravel and mortar; (b) annulus grouting via the shield tail.

Radial gap size

The radial gap size of the segmental lining ΔR_l and the radial gap size of the shield ΔR – i.e., the difference between boring radius R and radius of the shield extrados $R_{s,o}$ (cf. Figure 6.3a) – are geometrically coupled with each other. An increase of the radial gap ΔR leads automatically to an increase of the radial gap ΔR_l {3-7}:

$$\Delta R_l = \Delta R + d_s + t_s \ , \tag{6.2}$$

where d_s is the thickness of the shield and t_s the difference between the radius of the shield intrados $R_{s,i}$ {2-7} and the radius of the segmental lining extrados $R_{s,o}$ (cf. Figure 6.3a). With respect to the radial gap ΔR, it has also to be mentioned that if the shield has a "conical" shape the radial gap size increases with increasing distance from the tunnel face, i.e., $\Delta R = \Delta R(y)$.

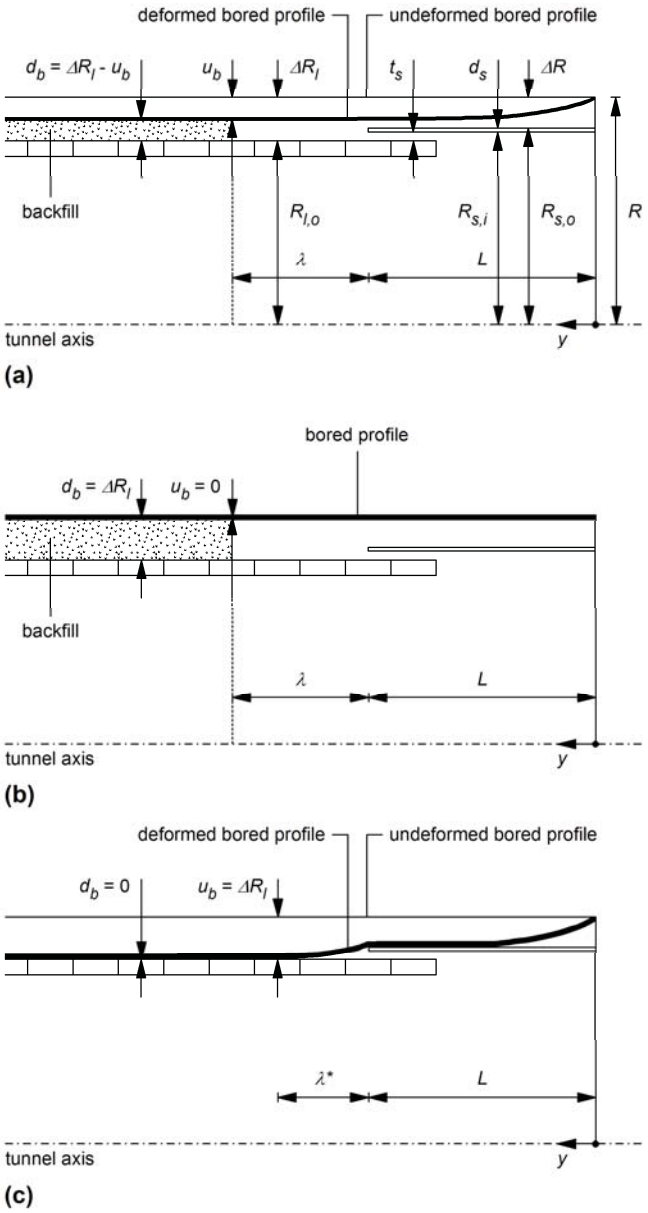

Figure 6.3. Thickness of the backfilling d_b when applying pea gravel and mortar: (a) general case; (b) borderline case of practically zero ground deformations between face and location of backfilling; (c) rapidly converging ground closing the gap around the lining before completion of backfilling.

Radial displacement of the bored profile

The radial displacement of the bored profile u_b not only affects the thickness of the backfilling d_b {9-10} but also has a direct effect on the ground pressure p {9-13}, as it is a part of the "pre-deformation" that the ground experiences before the segmental lining becomes loaded. It should be noted, that the convergence u_b may increase (path {9-10-11-12-13}) or decrease (path {9-13}) the final load p.

The radial displacement of the bored profile u_b depends, of course, on the ground characteristics {1-9}. Two further influencing factors are of a geometrical nature: the shield length L {2-9} and the distance behind the shield λ {6-9}, where backfilling should occur. The shield length L is a matter of TBM design, while the length λ depends on the type of the backfilling material {5-6} and on operational decisions taken on the construction site. The longer the distance from the tunnel face $L + \lambda$ (cf. Figure 6.3a), the bigger will be the radial displacement of the bored profile u_b {2-9, 6-9} and therefore the smaller the thick-

ness of the backfilling d_b {9-10}. In the extreme case of Figure 6.3c, where the convergence u_b uses up the available space ΔR_l at a certain distance $\lambda^* \leq \lambda$ behind the shield, backfilling is no longer possible. It should be noted that a delayed backfilling might also be problematic with respect to the thrust force that the segmental lining can accommodate. In fact, an improper bedding of the segmental lining reduces its bearing capacity in case of eccentric loading and this may limit the effectively available thrust force and slow down the TBM advance {6-8}.

Advance rate

First of all, the gross advance rate v_g plays a role with respect to the radial displacement of the bored profile u_b {8-9}. A slower TBM advance results, as a rule, in bigger ground deformations in the machine area (cf. Section 3.4).

In adverse ground conditions it is generally more difficult to maintain a fast TBM advance {1-8}. For example, a high ground pressure p may lead to an overstressing of the segmental lining, thus necessitating repair works that may cause standstills and, consequently, reduce the gross advance rate v_g {13-8}. Furthermore, if the segmental lining near the TBM is subjected to a loading in the proximity of its bearing capacity, it may be impossible to utilise the full installed thrust force of the TBM, if required, and the TBM may become jammed {13-8}. In this respect, a shorter shield may be advantageous {2-8}, as the required thrust force for overcoming shield skin friction decreases with the shield length L (cf. Section 3.3.3).

Another countermeasure that can be applied for reducing the required thrust force and avoiding TBM jamming is an increase in the overcut ΔR {3-8}. This can be either a fixed countermeasure realised a priori (by changing the layout of the TBM already in the planning phase) or a temporary countermeasure realised during construction through so-called "overboring" (cf. Section 2.4.3). However, the application of overboring may lead to a reduction in the gross advance rate {3-8} and the feasibility of the increase in the boring radius will depend on the ground conditions encountered {1-3}.

Load transfer in longitudinal direction

The overcut ΔR may also have a direct effect on the radial displacement of the bored profile u_b {3-9}. A smaller gap between shield and ground is more likely to close than a larger gap. After closing the gap, the ground starts to exert a load upon the shield and, vice versa, the shield supports the ground (the stiffer the shield, the more pronounced will be its support action and the lower will be the ground deformations {2-9}). This longitudinal arch action between the shield and the backfilled segmental lining (Figure 6.4a) leads to a reduction of the ground deformations in this area {13-9}.

Such an effect is also possible between the core ahead of the face and the backfilled segmental lining (Figure 6.4b). This effect is more evident for short shields (cf. Section 3.3.4) and if the backfilling is carried out near to the shield (i.e., if the distance $L + \lambda$ is short). Such a load transfer has a positive effect on the shield loading, but leads at the same time to a higher loading of the segmental lining. It should be noted that the feedback effects {13-9-10-11-12-13} and {13-9-13} are conflictive with respect to lining loading.

6.2.3 Backfilling with grouting via the shield tail

Immediate backfilling with grouting via the shield tail is rather rare in rock tunnelling. Basically, the same factors apply as in the last section.

One major difference concerns the parameter λ, which becomes equal to zero (Figure 6.5) {5-6}. Consequently, the thickness of the backfilling d_b is governed by the radial displacement u_b of the bored profile at the shield tail {9-10}. As this displacement is limited by the overcut ΔR (rather than by the radial gap size ΔR_l of the segmental lining), in this respect interaction {3-9} substitutes interaction {7-9}. In contrast to the case of "backfilling with pea gravel and mortar", where rapidly converging ground may make

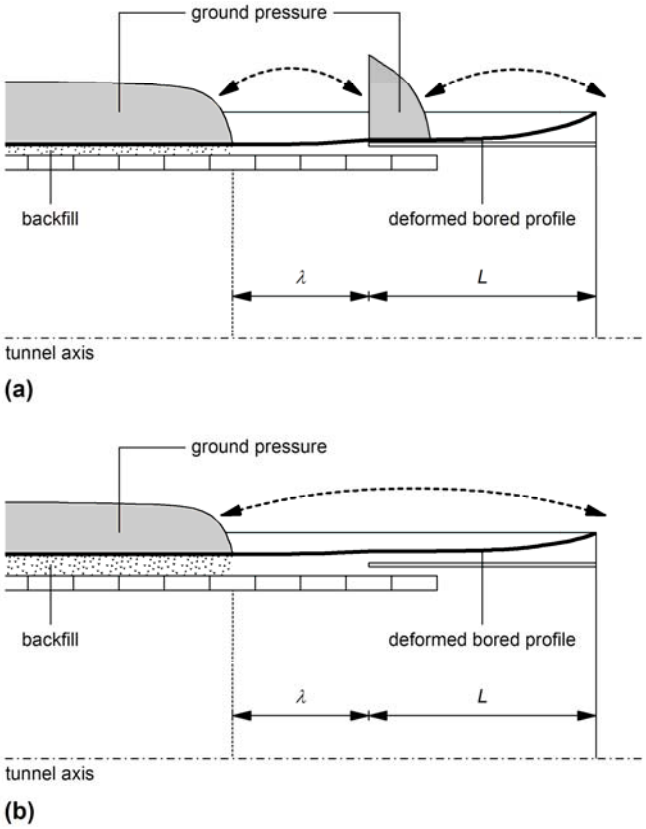

Figure 6.4. Longitudinal arching action: (a) between shield and backfilled segmental lining (and between the shield and the core ahead of the tunnel face); (b) between the core ahead of the tunnel face and the backfilled segmental lining.

annulus backfilling impossible, the thickness of the backfilling layer is here at least equal to the radius difference between the lining extrados and the shield extrados:

$$\begin{cases} d_b = \Delta R_l - u_b \geq d_s + t_s \\ 0 \leq u_b \leq \Delta R \end{cases}, \tag{6.3}$$

where, as before, the deformations of the segmental lining and the shield were disregarded.

Another difference to the case of backfilling with pea gravel and mortar concerns the longitudinal arching mentioned in Section 6.2.2. This effect is more pronounced in the case of grouting via the shield tail (cf. Sections 3.3.4 and 3.4.4), as the segmental lining begins to support the ground at a shorter distance behind the tunnel face. This is particularly true if a rapidly hardening mortar is used, because the backfilling and the segmental lining then constitute a stiff system right from the start.

The considerations of Section 6.2.2 assumed that the backfilling layer represents a compressible buffer and that its stiffness K_b (and therefore the loading of the segmental lining p) increases if the thickness of the layer d_b decreases. However, this assumption does not apply if the segmental lining is perfectly backfilled with grout – a rather rare case considering the unavoidable imperfections in construction. In this case, the backfilling layer forms a perfect ring and, as shown later in Section 6.3.2, a reduction of its thickness d_b leads to a decrease and not to an increase in the stiffness K_b. If a perfect ring is assumed, the effect of u_b (paths {9-10-11-12-13} and {9-13}) will no longer be ambiguous and the feedback effects {13-9-10-11-12-13} and {13-9-13} (cf. Section 6.2.2) will no longer be conflictive.

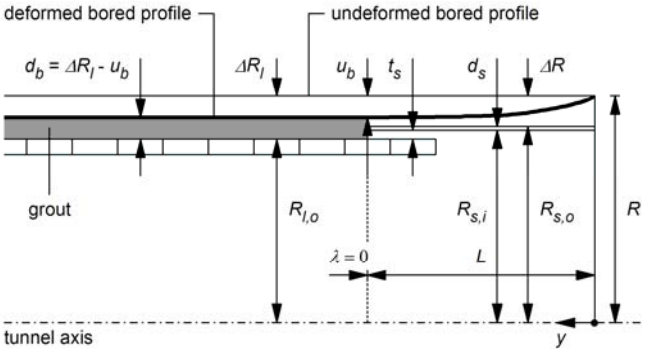

Figure 6.5. Thickness of the backfilling d_b in the case of grouting via the shield tail.

The N^2 chart of Figure 6.1 also assumes that backfilling with pea gravel and mortar slow-downs the TBM advance to the same degree as grouting via the shield tail. Otherwise, an interaction {5-8} should be added in the N^2 chart.

6.3 Computational model

6.3.1 Introduction

The numerical investigations are based upon the axially symmetric model of Section 3.2. Figure 6.6 shows the problem layout. For a detailed discussion of the assumptions underlying axial symmetry, see Section 5.2.1.

An important consequence of the axial symmetry is that only normal forces are shown to develop in the segmental lining, while in reality bending may also occur. The axially symmetric model is in general stiffer than in reality and should lead to an overestimation of the ground pressure. However, the stress peaks associated with bending moments may exceed the compressive stresses developed in the axially symmetric model. The occurrence of bending moments can be taken into account in the structural assessment of the segmental lining in a simplified manner by choosing a higher safety factor.

As in Section 5, the ground is assumed to be homogeneous and isotropic and is modelled as a linearly elastic, perfectly plastic material obeying the Mohr-Coulomb yield criterion and a non-associated flow rule. Again, in order to reduce complexity, the time-dependency of the ground behaviour (due to creep or consolidation) is disregarded.

The shield is modelled by a mixed boundary condition according to Section 3.2.2:

$$p(y) = \begin{cases} 0 & \text{if } u(y) - u(0) \le \Delta R \\ K_s \left(u(y) - u(0) - \Delta R \right) & \text{if } u(y) - u(0) > \Delta R \end{cases} \quad (\text{for } 0 \le y \le L) \ , \tag{6.4}$$

where p is the ground pressure developing upon the shield, u the radial displacement of the ground at the excavation boundary (and, consequently, $u(0)$ denotes the pre-deformation of the ground ahead of the tunnel face), L the shield length and ΔR the overcut. K_s denotes the stiffness of the shield and reads as follows:

$$K_s = \frac{E_s d_s}{R^2} \ , \tag{6.5}$$

where E_s and d_s denote the Young's modulus and the thickness of the shield, respectively, and R is the tunnel radius. The assumption of a constant shield stiffness K_s presupposes that the shield is not overstressed.

A mixed boundary condition also applies to the segmental lining, whereby, as explained in the next two sections, the features of the two backfilling types (pea gravel and mortar or grouting via the shield tail) should be taken into account.

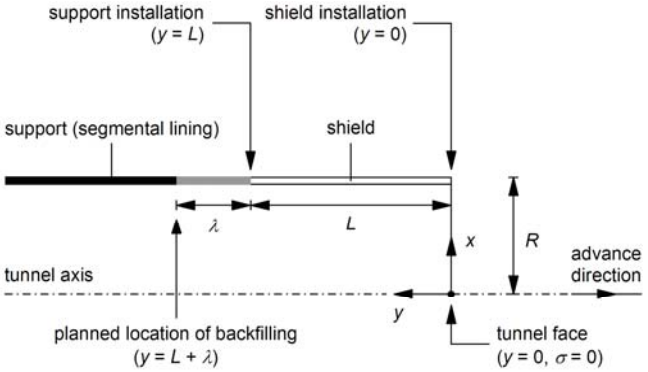

Figure 6.6. Problem layout.

6.3.2 Backfilling with pea gravel and mortar

Boundary condition

In this case, complete backfilling is achieved only after a certain interval behind the shield (Figure 6.2a, cross-section C-C). The segmental lining is initially either not backfilled (cross-section A-A) or partially backfilled (cross-section B-B). The length of the tunnel section with incomplete backfilling depends on the steepness of the pea gravel "slope". Of course, with an axially symmetric computational model it is not possible to model the case of partial backfilling. Disregarding the "intermediate" stage is, however, a reasonable simplification with respect to the ground pressure acting upon the segmental lining because the stiffness of a partially backfilled segmental lining is negligible (Lavdas, 2010).

It is, nevertheless, important to distinguish between the backfilled and the non-backfilled sections of the lining (Figure 6.6) and also to take into account the deformations that occur before backfilling (i.e., up to $y = L + \lambda$, where λ is the distance behind the shield where completion of backfilling is planned), because they influence the thickness of the backfilling layer and thus the stiffness of the system composed of the backfilling and the segmental lining. In this respect, a distinction must be made in the boundary condition of the lined tunnel section depending on whether the ground closes the annular gap before backfilling or not. In the first case, i.e.,

$$\text{for } u_b \geq \Delta R_l \text{ and } y > L,\ p(y) = \begin{cases} 0 & \text{if } u(y) - u(0) \leq \Delta R_l \\ K_l \left(u(y) - u(0) - \Delta R_l \right) & \text{if } u(y) - u(0) > \Delta R_l \end{cases}, \quad (6.6)$$

while in the second case, i.e.,

$$\text{for } u_b < \Delta R_l,\ p(y) = \begin{cases} 0 & \text{if } L < y \leq L + \lambda \\ K_c \left(u(y) - u(L + \lambda) \right) & \text{if } y > L + \lambda \end{cases}, \quad (6.7)$$

where u_b and ΔR_l denote the radial displacement of the bored profile before completion of the backfilling ($u_b = u(L+\lambda) - u(0)$) and the theoretical size of the radial gap of the segmental lining, respectively.

In the first case, there is no backfilling layer at all and the ground pressure p depends only on the stiffness of the segmental lining (cf. Equation 6.6):

$$K_l = \frac{E_l d_l}{R^2}, \quad (6.8)$$

where E_l is the Young's modulus of the concrete, d_l the thickness of the segments and R the tunnel radius. The assumption of a constant stiffness K_l presupposes that the segmental lining is not overstressed.

In general, the convergence u_b, which occurs between the tunnel face ($y = 0$, cf. Figure 6.6) and the location of completion of backfilling ($y = L + \lambda$), uses up only a part of the radial gap of the segmental lining ΔR_l (Figure 6.3a). In this case, the stiffness K_c of the

system composed of the backfilling and the segmental lining shall be introduced in the mixed boundary condition of Equation 6.7. The composite stiffness K_c depends essentially on whether the backfilling layer forms a perfect ring or represents rather a compressible buffer between the segmental lining and the ground. In the first case, the support consists of two concentric rings and the composite stiffness

$$K_c = K_l + K_b \ . \tag{6.9}$$

K_b is the stiffness of the outer ring:

$$K_b = \frac{E_b d_b}{R^2} \ , \tag{6.10}$$

where E_b and d_b denote the Young's modulus and the thickness of the backfilling, respectively. According to Equation 6.9, the backfilling would in this case increase the stiffness of the support. In view of the common construction imperfections, the correctness of this conclusion is rather questionable. It is much more plausible to assume that the backfilling rather represents a compressible layer – a layer that actually reduces the overall stiffness. In this case, the composite stiffness

$$K_c = \frac{1}{\frac{1}{K_l} + \frac{1}{K_b}} \ , \tag{6.11}$$

where K_b is the stiffness of the backfilling layer under one-dimensional loading:

$$K_b = \frac{E_b}{d_b} \ . \tag{6.12}$$

If the backfill is highly compressible and highly deformed, a non-linear deformation behaviour (i.e., a non-constant stiffness K_b) should be considered.

As mentioned in Section 6.2.2, the thickness of the backfilling d_b (which is important for the composite stiffness according to Equations 6.10 and 6.12) depends on the radial displacement of the bored profile u_b:

$$d_b = \Delta R_l - u_b = \Delta R_l - u(L+\lambda) + u(0) \ . \tag{6.13}$$

As the deformation u_b of the bored profile is not known a priori and itself depends on the composite stiffness K_c, Equations 6.7 introduces a strong non-linearity that cannot be dealt with by a standard finite element code. In account of this, an iterative procedure will be employed in order to find the numerical solution satisfying the highly non-linear boundary condition of Equations 6.6 and 6.7.

Iterative treatment of the boundary condition

Figure 6.7 shows the iterative procedure used for dealing with the boundary condition according to Equations 6.6 and 6.7. The procedure starts with the assumption that the ground closes the annular gap around the lining before backfilling. The computation for this first iteration is carried out on the basis of Model A (upper part of Figure 6.7). As there is no backfilling layer, the segmental lining is modelled by means of the following mixed boundary condition:

$$p(y)_1 = \begin{cases} 0 & \text{if } \ u(y) - u(0) \le \Delta R_l \\ K_l \left(u(y)_1 - u(0)_1 - \Delta R_l \right) & \text{if } \ u(y) - u(0) > \Delta R_l \end{cases} \quad (\text{for } y > L) \ . \tag{6.14}$$

The first iteration provides the actual location of gap closure λ^*_1. If the gap is already closed at the planned location of backfilling (i.e., if $\lambda^*_1 \le \lambda$), the assumption made (no backfilling) is correct and the calculation is already finished after the first iteration. This happens in the numerical example of Figure 6.8, which concerns the hypothetical case of a 400 m deep tunnel crossing weak ground. The boring diameter is equal to 10 m and the shield 10 m long. The segmental lining is 40 cm thick and has a radial gap size of 15 cm. Backfilling is planned 5 m behind the shield. Figure 6.8a–b show the convergence $u - u(0)$ of the tunnel boundary and the distribution of the ground pressure p,

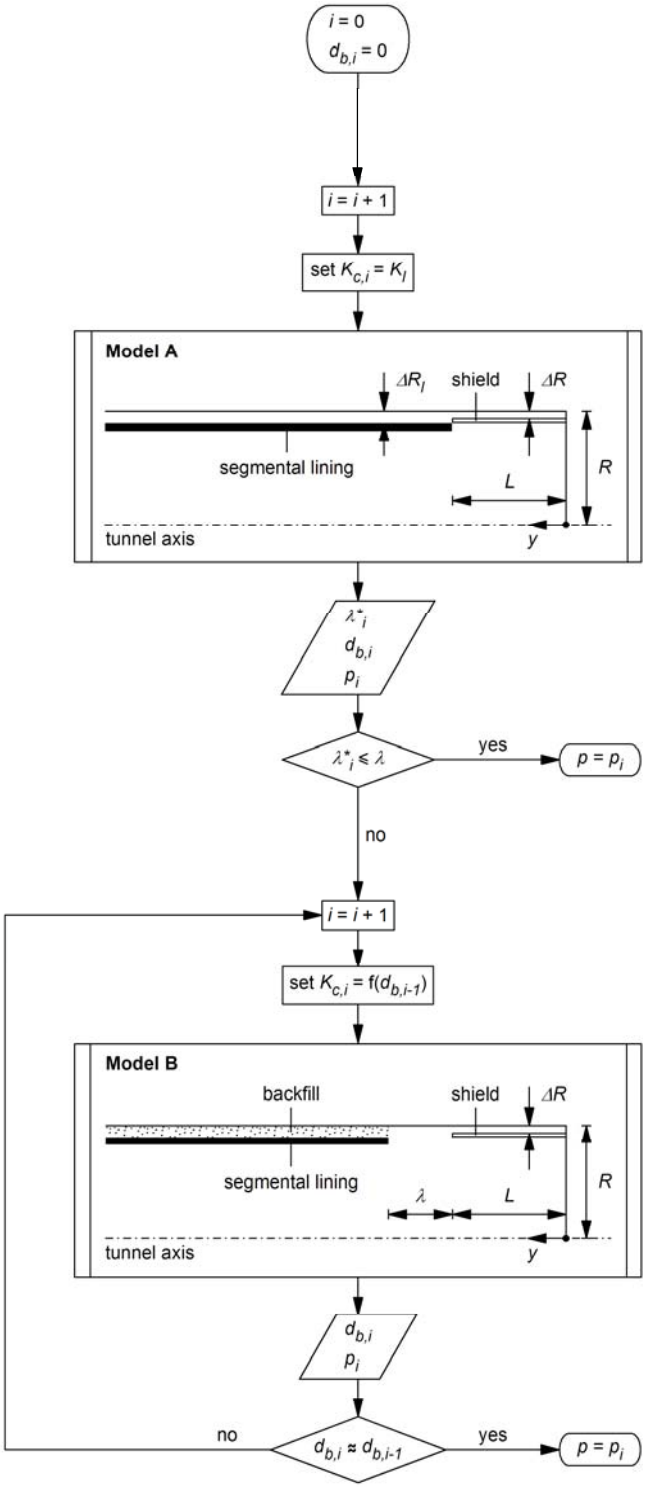

Figure 6.7. Iterative procedure for the case of backfilling with pea gravel and mortar.

respectively, resulting from the first iteration with Model A. The numerical results show that the ground establishes contact with the segmental lining at a distance of λ^*_1 = 4.4 m behind the shield, i.e., before the planned backfilling, and confirm, therefore, the assumption underlying Model A, i.e., that there is no backfilling layer. The ground pressure developing upon the lining far behind the shield amounts to p_1 = 2.4 MPa.

Consider now the example of Figure 6.9. The parameters of this example are the same as in Figure 6.8, with the exception of the Young's modulus E and the uniaxial compressive strength f_c of the ground. (The ground is stiffer and stronger than in the previous

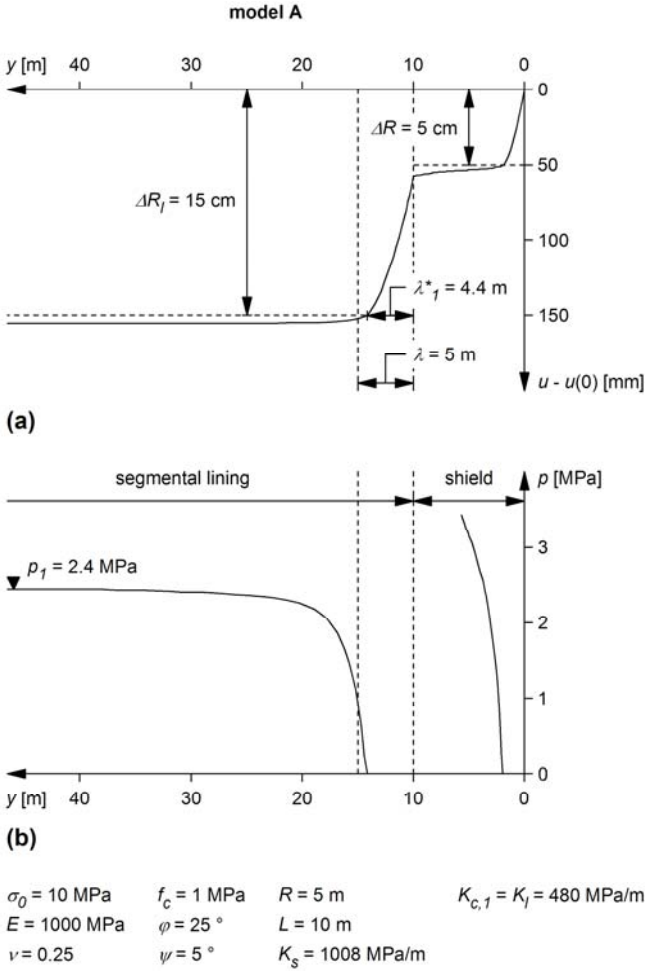

Figure 6.8. First numerical example concerning the iterative procedure of Figure 6.7: (a) convergence u – u(0) of the bored profile computed with Model A; (b) ground pressure p acting upon the shield and the segmental lining computed with Model A.

example.) Figure 6.9a shows the convergence along the tunnel based upon Model A, i.e., assuming that there is no backfilling. In this example, the ground does not close the gap at all. The numerical results are wrong because the model assumes that the support pressure is zero for $y > L + \lambda = 15$ m, while in reality a pressure will develop there due to the backfilling. The same remark applies should the ground close the gap at a distance $\lambda^*_1 > \lambda$, as occurs in the numerical example of Figure 6.10 ($\lambda^*_1 = 19$ m, point A), which concerns a ground with a slightly higher Young's modulus E. In this case, Model A assumes that the ground is unsupported in the interval $L + \lambda < y < L + \lambda^*_1$, while backfilling of the segmental lining already occurs at $y = L + \lambda$. Additionally, Model A is erroneous with respect to the support stiffness in the tunnel section $y > L + \lambda^*_1$, because it does not consider the effect of backfilling on the stiffness of the support.

The results obtained from the first iteration are improved iteratively by applying Model B, which takes into account the backfilling at $y = L + \lambda$. In this case, the mixed boundary condition for the simulation of the segmental lining in the second iteration reads as follows:

$$p(y)_2 = \begin{cases} 0 & \text{if } L < y \le L + \lambda \\ K_{c,2}\left(u(y)_2 - u(L+\lambda)_2\right) & \text{if } y > L + \lambda \end{cases} . \qquad (6.15)$$

The composite stiffness $K_{c,2}$ is calculated after Equations 6.8, 6.11, 6.12 and 6.13, where the thickness of the backfilling $d_{b,1}$ is taken from the first iteration (in the example of Figure 6.9 $d_{b,1} = 68$ mm and $K_{c,2} = 362$ MPa/m). The second iteration provides a new

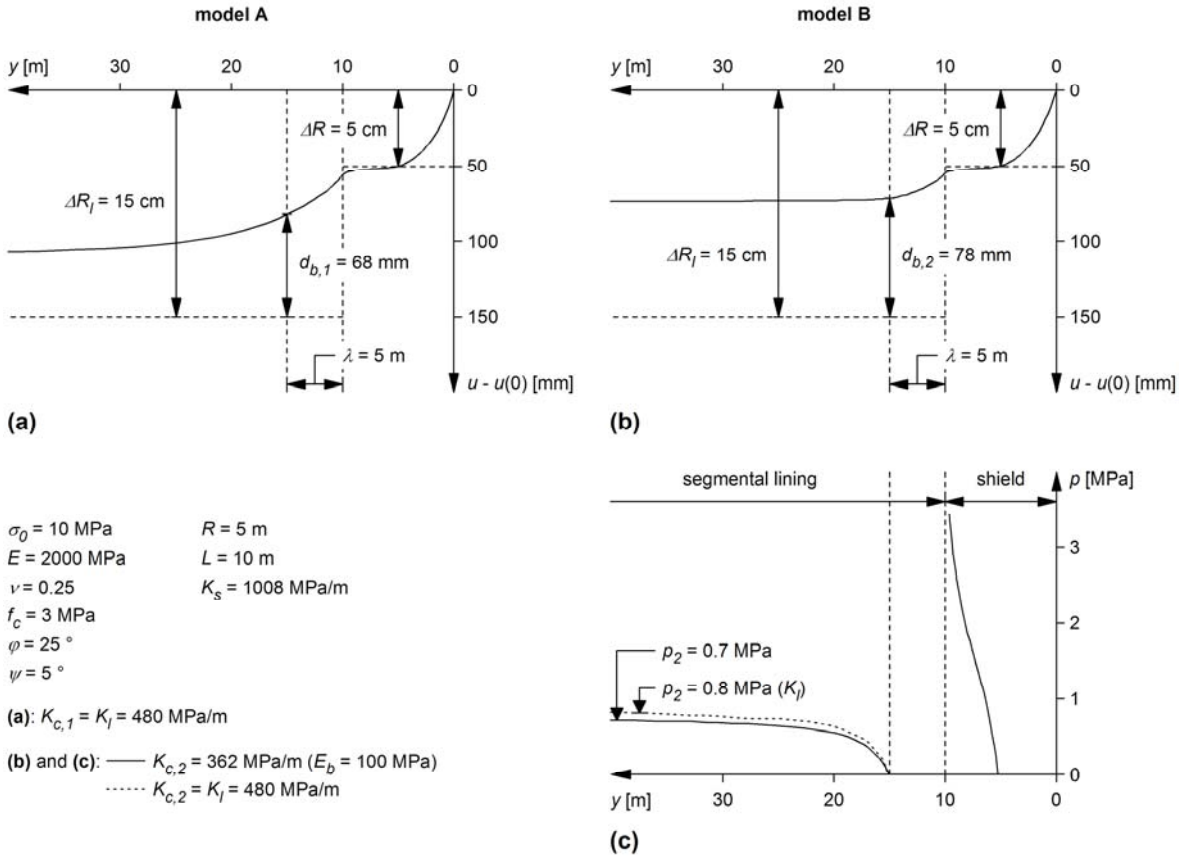

Figure 6.9. Second numerical example concerning the iterative procedure of Figure 6.7: (a) and (b) convergence u – u(0) of the bored profile computed with Models A and B, respectively; (c) ground pressure p acting upon the shield and the segmental lining computed with Model B.

distribution of the convergence of the tunnel boundary $u - u(0)$ and allows a new value to be determined in respect of the thickness of the backfilling $d_{b,2}$ (see, for example, Figure 6.9b, where $d_{b,2}$ = 78 mm), which is used for the calculation of the composite stiffness in the next iteration step. The procedure is repeated as long as the value of d_b changes significantly, i.e., until $d_{b,i} \approx d_{b,i-1}$.

This iterative procedure converges very quickly and, in most cases, three to four iterations suffice. This is true for both examples of Figures 6.9 and 6.10. In the example of Figure 6.9, the third iteration, which is carried out on the basis of a composite stiffness of $K_{c,3}$ = 349 MPa/m (calculated according to the thickness of the backfilling after the second iteration, i.e., $d_{b,2}$ = 78 mm), leads to following results: $d_{b,3}$ = 78.20 mm ≈ $d_{b,2}$ = 78.25 mm and p_3 = 0.71 MPa ≈ p_2 =0.72 MPa. The example of Figure 6.10 (where the backfilling is weaker than in the example of Figure 6.9) converges after four iterations, according to the following results (the results of the third iteration are not plotted in Figure 6.10 for the sake of clarity): $d_{b,4}$ = 54.71 mm ≈ $d_{b,3}$ = 54.61 mm ($d_{b,2}$ = 55.49 mm) and p_4 = 0.71 MPa ≈ p_3 =0.70 MPa (p_2 =0.78 MPa) calculated with $K_{c,4}$ = 133 MPa/m and $K_{c,3}$ = 131 MPa/m ($K_{c,2}$ = 170 MPa/m), respectively.

Simplifying assumption

The computational effort can be reduced by assuming that the backfilling is very stiff (i.e., $K_b \rightarrow \infty$). With this simplification, which is on the safe side with respect to the ground pressure p acting upon the segmental lining, the displacement-dependency of the composed stiffness K_c disappears, as $K_c = K_l$ applies (cf. Equation 6.11). In this case, the procedure in Figure 6.7 consists only of the first two iterations (i.e., one calculation with Model A and one with Model B), and since these iterations are no longer coupled to each other, it has only to be evaluated whether Model A or Model B delivers the correct results for the given situation.

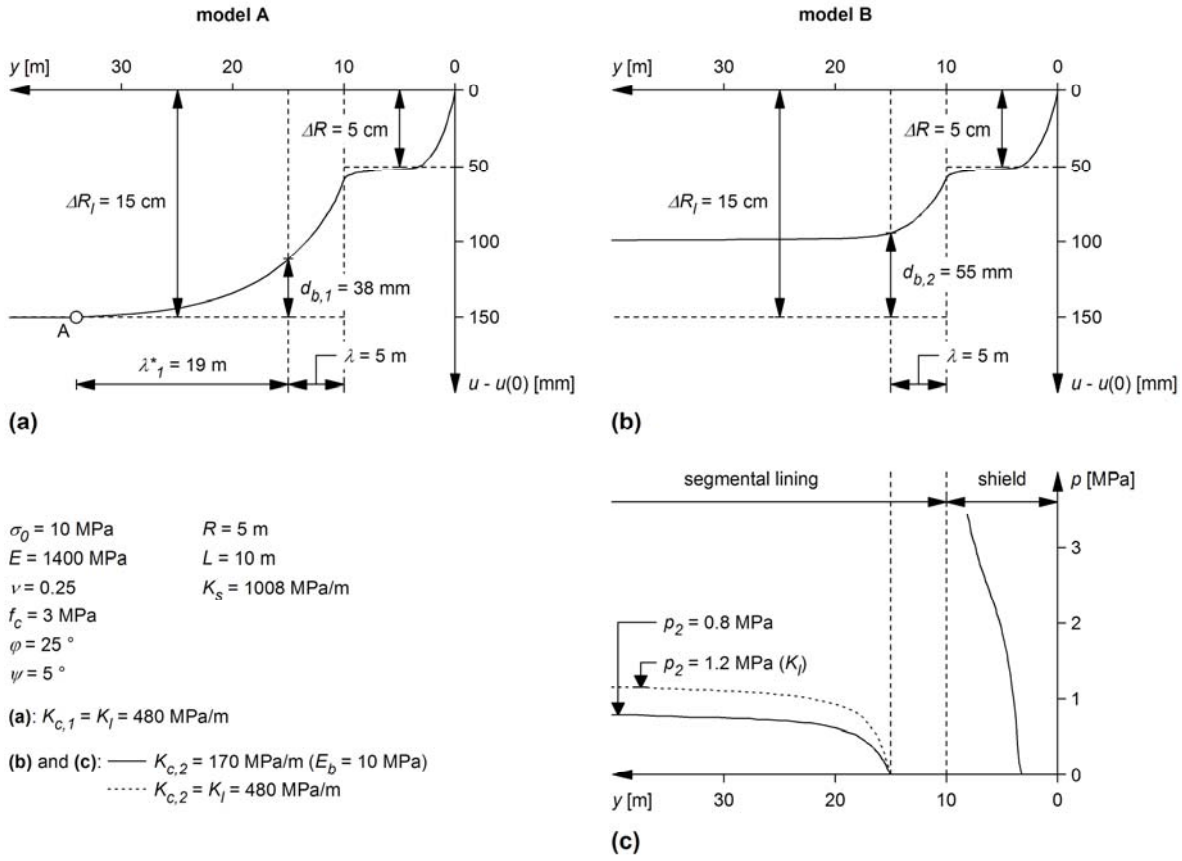

Figure 6.10. Third numerical example concerning the iterative procedure of Figure 6.7: (a) and (b) convergence u – u(0) of the bored profile computed with Models A and B, respectively; (c) ground pressure p acting upon the shield and the segmental lining computed with Model B.

The assumption of $K_c = K_l$ is correct in the particularly adverse conditions where the ground closes the annular gap before backfilling is possible. Otherwise, it represents a simplification on the safe side because it overestimates the stiffness of the tunnel support. Figure 6.11a, which applies for the example introduced above (and assumes that the backfilling layer is a compressible buffer), shows this overestimation by means of the ratio of stiffness of the segmental lining K_l to composite stiffness K_c. As can be seen from Figure 6.11a, the overestimation of the stiffness of the tunnel support decreases with decreasing thickness of the backfilling d_b – i.e., for increasing ground deformations – and for increasing value of the Young's modulus of the backfilling E_b. In account of this, the conclusion can be drawn that the overestimation decreases with increasing squeezing potential of the ground and increasing stiffness of the backfilling material. However, as shown later (cf. Section 6.4.2), the ground pressure p acting upon the segmental lining does not depend linearly from the stiffness of the tunnel support used for the computations. Therefore, the overestimation of the support stiffness does not necessarily lead to a significant overestimation of the lining loading. This can be observed, e.g., in Figure 6.9c, where, for the sake of comparison, the dashed line plots the ground pressure p acting upon the segmental lining computed assuming $K_{c,2} = K_l = 480$ MPa/m instead of $K_{c,2} = 362$ MPa/m. In this example, the overestimation of about 11 % in the loading of the segmental lining is not relevant from a practical point of view. On the contrary, there is a far more important overestimation (of 64 %) in the example of Figure 6.10c, which involves a much weaker backfilling material.

6.3.3 Backfilling with grouting via the shield tail

An iterative procedure is also necessary for the case of grouting via the shield tail. As can be seen in Figure 6.12, however, the procedure is simpler than in Figure 6.7 and requires

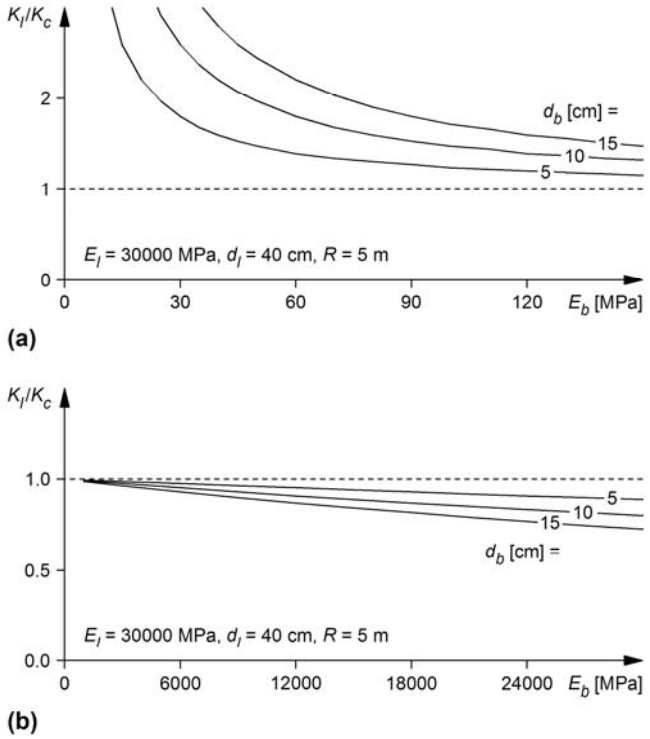

Figure 6.11. Ratio of stiffness of the segmental lining K_l to composed stiffness K_c (segmental lining and backfilling) for different values of the thickness of the backfilling d_b as a function of the Young's modulus of the backfilling E_b: (a) the backfilling layer represents a compressible buffer; (b) the backfilling layer forms a perfect ring.

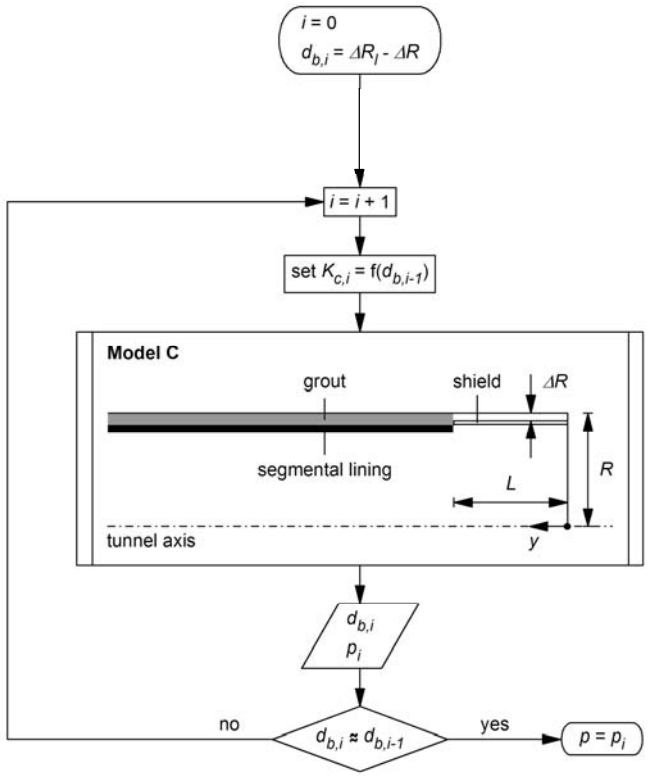

Figure 6.12. Iterative procedure for the case of grouting via the shield tail.

only one computational model, which is practically identical to Model B of Figure 6.7, the only difference being that here $\lambda = 0$. The boundary condition therefore becomes simpler than in Equation 6.15:

$$p(y)_i = K_{c,i}\left(u(y)_i - u(L)_i\right) \text{ (for } y > L) \ , \tag{6.16}$$

where $K_{c,i}$ is the composite stiffness (segmental lining and annulus grout), which has to be determined iteratively, because it depends on the thickness of the backfilling layer and thus on the ground convergence at the shield tail. The procedure begins (Figure 6.12) with $K_{c,1}$ calculated according to an assumed initial value of backfilling thickness $d_{b,0} = \Delta R_l - \Delta R$. For the further iterations, the stiffness $K_{c,i}$ is calculated with Equations 6.8, 6.11, 6.12 and 6.13 (or Equations 6.8, 6.9, 6.10 and 6.13 if one assumes that the backfilling layer represents a perfect ring) using the improved value of $d_{b,i-1}$ resulting from the previous iteration. Analogously to Section 6.3.2, the procedure ends when the convergence criterion $d_{b,i} \approx d_{b,i-1}$ is fulfilled. The main result of the procedure is the loading of the segmental lining $p = p_i$.

The assumption of a very stiff backfilling (i.e., $K_b \rightarrow \infty$, analogously to Section 6.3.2) also leads in the present case (grouting via the shield tail) to a considerable reduction in the computational effort. With this simplification, which is particularly appropriate if a rapidly hardening mortar is used, the computation of the ground pressure acting upon the segmental lining requires only one iteration (i.e., $p = p_1$). Depending on the static action of the backfilling layer (compressible buffer or perfect ring) the simplification leads to an overestimation (Figure 6.11a) or to an underestimation (Figure 6.11b) of the stiffness of the tunnel support. For the first case, the considerations done at the end of the last section apply analogously, while for the rather rare case of a "perfect ring", according to Figure 6.11b the conclusion can be drawn that the underestimation of the stiffness of the tunnel support becomes relevant only for very stiff backfilling materials.

6.4 Decision aids

6.4.1 Dimensionless parameters

With respect to the main goal of the present investigation, the main result of the numerical computations is the final value of the ground pressure far behind the tunnel face. Figures 6.8b, 6.9c and 6.10c show typical load distributions $p(y)$ along the tunnel.

The ground pressure p acting upon the segmental lining depends on the material constants of the ground (Young's modulus E, Poisson's ratio ν, uniaxial compressive strength f_c, angle of internal friction φ and dilatancy angle ψ), on the initial stress σ_0, on the characteristics of the TBM (tunnel radius R, shield stiffness K_s, radial gap size ΔR and shield length L) and on the characteristics of the backfilled segmental lining (composite stiffness K_c, radial gap size ΔR_l and location of backfilling λ):

$$p = f\left(E,\ \nu,\ f_c,\ \varphi,\ \psi,\ \sigma_0,\ R,\ K_s,\ \Delta R,\ L,\ K_c,\ \Delta R_l,\ \lambda\right) \ . \tag{6.17}$$

In order to reduce the computational effort, the calculations were carried out on the basis of the simplifying assumption $K_c = K_l$ (cf. Sections 6.3.2 and 6.3.3). A dimensional analysis (cf. Lavdas, 2010) in combination with a general property of elasto-plastic materials (cf. Anagnostou and Kovári, 1993) leads to the following expression:

$$p^* = \frac{p}{\sigma_0} = f\left(\frac{E}{\sigma_0}\frac{\Delta R}{R},\ \nu,\ \frac{f_c}{\sigma_0},\ \varphi,\ \psi,\ \frac{K_s R}{E},\ \frac{L}{R},\ \frac{K_l R}{E},\ \frac{\Delta R_l}{\Delta R},\ \frac{\lambda}{R}\right) \ , \tag{6.18}$$

where p^* denotes the normalized ground pressure.

It is important to note that Equation 6.18 is true only for a constant ratio $\Delta R_l/\Delta R$ and not for a constant ratio $\Delta R_l/R$ (Lavdas, 2010). Therefore, and with regard to the fact that the radial gap size of the segmental lining ΔR_l depends geometrically on the radial gap size of the shield ΔR (Equation 6.2), it was more reasonable to include in Equation 6.18 the dimensionless parameter $\Delta R_l/\Delta R$ rather than the ratio $\Delta R_l/R$.

6.4.2 The parameter range covered

Although the applied computational method is very efficient, a trade-off has had to be made between the completeness of the parametric study and the cost of computation and data processing. The numerical analyses have therefore been carried out only for selected parameters of the ground, TBM and segmental lining, as well as selected layouts of the backfilling.

Poisson's ratio and dilatancy angle of the ground

With respect to the ground parameters, the first compromise concerns the Poisson's ratio, which has been kept constant to $\nu = 0.25$.

As a further simplification, analogously to Section 5.2, the dilatancy angle of the ground ψ was taken as a function of the angle of internal friction φ (Equation 5.1) and not as an independent parameter.

However, the nomograms account for a wide variation in the other three material constants (E, φ and f_c) and cover the relevant range of ground strength and deformability.

Length and stiffness of the shield

According to the TBM technical data collected in Section 5.2.3, the normalized shield length L/R of single shielded TBMs is between 1 and 5 (the larger values applying to small diameter TBMs). The nomograms were worked out for $L/R = 1$. This assumption is safe with respect to the loading of the segmental lining, as a shorter shield length facilitates load transfer in the longitudinal direction (cf. Section 6.2.2 and Figure 6.4b) and this results in a higher ground pressure acting upon the segmental lining. Figure 6.13a shows some of the results of a large series of numerical investigations carried out by Lavdas (2010) for testing this assumption. The solid lines apply to an overcut ΔR of $0.006R$ and different ground "qualities" (in terms of the normalized Young's modulus E/σ_0 and the normalized uniaxial compressive strength f_c/σ_0), while the dashed lines concern the case of a larger overcut ($\Delta R = 0.010R$). As can be seen from Figure 6.13a, the effect of the normalized shield length L/R on the normalized ground pressure p^* is negligible for $L/R > 2$ but may be important in the range $1 \le L/R \le 2$, particularly in the case of a higher quality ground and of a larger radial gap (compare, for example, points A and B). The load is higher if the shield is short (point A) because of the longitudinal arching (Figure 6.4b). This effect disappears if the gap is small, the ground quality low or the shield long, because the ground closes the gap around the rear part of the shield and the arching occurs according to Figure 6.4a.

The normalized shield stiffness K_sR/E has been kept constant assuming the same value of $K_sR/E = 10$ as in Section 5.2. As can be seen from Figure 6.13b, which shows the effect of the normalized shield stiffness K_sR/E on the normalized ground pressure p^*, the assumed value of K_sR/E is on the safe side with respect to the problem under consideration. Of course, the normalized shield stiffness K_sR/E does not play a role if the shield is not loaded at all by the ground (this happens in the case of the lowest curve in Figure 6.13b), because a longitudinal arching action between shield and backfilled segmental lining (Figure 6.4a) does not exist in this case.

Stiffness and radial gap size of the segmental lining

Figure 6.13c shows the effect of the normalized support stiffness K_lR/E on the normalized ground pressure p^*. As expected, the stiffer the segmental lining, the higher will be the ground pressure acting upon it. In order to cover the relevant stiffness range, the nomograms were worked out for $K_lR/E = 1$, 3 and 10.

In the most cases, the ratio of the radial gap size ΔR_l of the segmental lining to the radial gap size ΔR of the shield is between 3 and 10 (see also the TBM technical data collected in Section 5.2.3). The nomograms apply for a constant ratio of $\Delta R_l/\Delta R = 3$ and are on the safe side for most cases. The radial gap ΔR_l affects the normalized ground pressure p^* only in the cases where the radial gap ΔR_l is closed before backfilling can occur (i.e., the cases where Model A applies, cf. Section 6.3.2). Otherwise, if the ground does not close

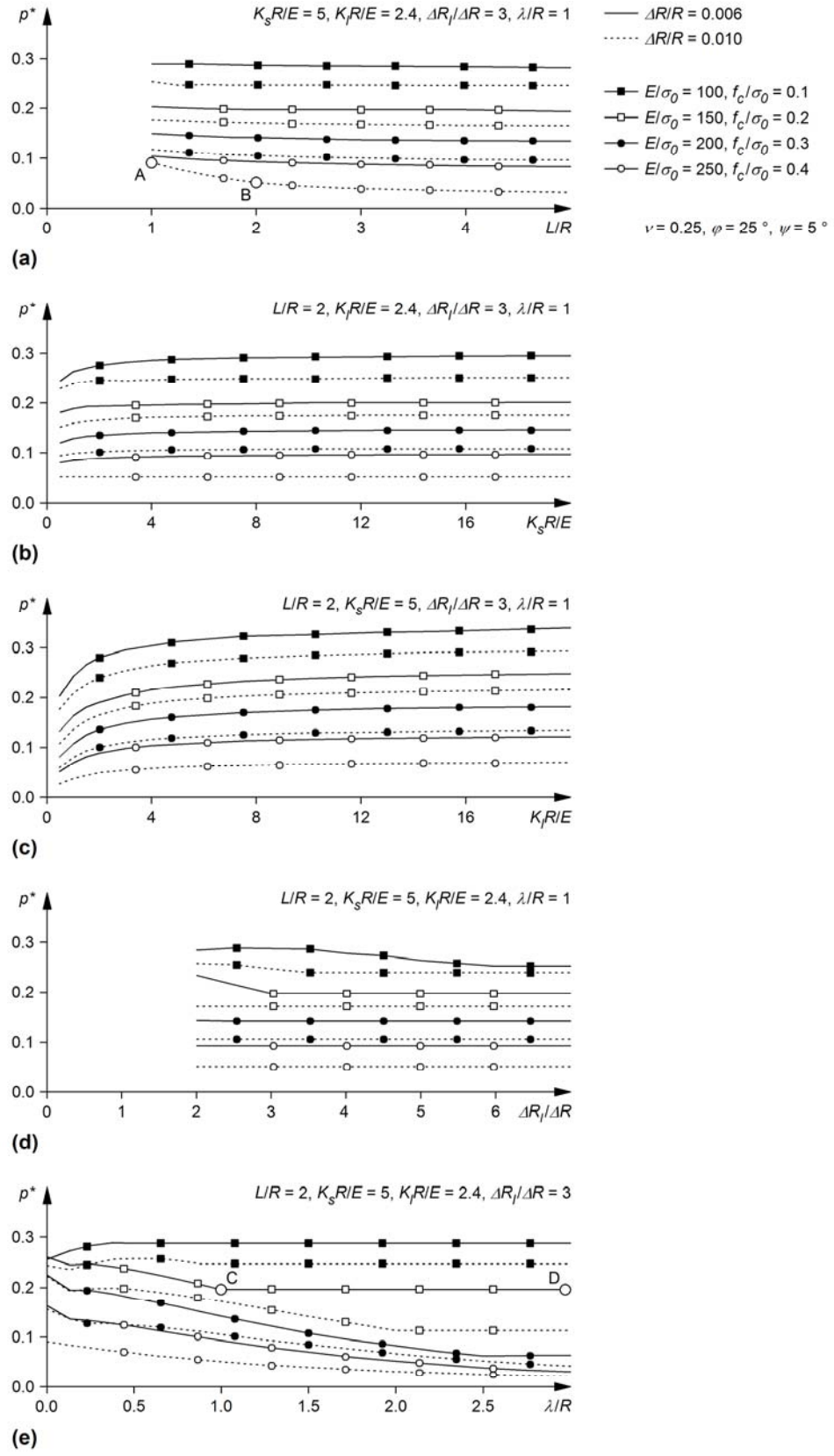

Figure 6.13. Numerical results concerning the dependency of the normalized ground pressure p on: (a) the normalized shield length L/R; (b) the normalized shield stiffness K_sR/E; (c) the normalized lining stiffness K_lR/E; (d) the ratio of radial gap size ΔR_l of the lining to the radial gap size ΔR of the shield; (e) normalized location of backfilling λ/R.*

the radial gap ΔR_l (i.e., if Model B applies), the ratio $\Delta R_l/\Delta R$ does not play any role. This is because of the simplifying assumption of a very stiff backfilling done for working out the nomograms (cf. Sections 6.3.2 and 6.3.3), which leads to the introduction of a constant stiffness $K_c = K_l$ in the Model B (cf. Section 6.4.1). As the stiffness of the simplified model does not depend on the actual thickness of the backfilling, the normalized ground pressure p^* does not depend on the radial gap ΔR_l. This applies for the majority of the results shown in Figure 6.13d, particularly in the practically relevant range $\Delta R_l/\Delta R$ = 3–10.

Location of backfilling

The nomograms were developed for the backfilling locations of λ = 0, R and 2R behind the shield (λ = 0 applies to grouting via the shield tail). Figure 6.13e shows the effect of the normalized backfilling location λ/R on the normalized ground pressure p^*. In general, the loading of the segmental lining decreases if backfilling is carried out later. This happens, however, only up to a certain value of the distance λ behind the shield (point C). If the planned location of the backfilling is far behind the shield, the ground closes the gap earlier and the parameter λ does not play a role anymore (points C and D show the same ground pressure).

6.4.3 The nomograms

Taking account of the dimensional analysis of Section 6.4.1 and bearing in mind that some of the model parameters are kept constant (cf. Section 6.4.2), the following expression applies for the normalized ground pressure:

$$\frac{p}{\sigma_0} = f\left(\frac{E}{\sigma_0}\frac{\Delta R}{R},\ \frac{f_c}{\sigma_0},\ \varphi,\ \frac{K_l R}{E},\ \frac{\lambda}{R}\right) . \tag{6.19}$$

Appendix III contains the graphical representation of this relationship (Figures III.1 to III.9). Each figure applies to a different pair of values (λ/R, K_lR/E). The diagrams of each figure apply to different values of the angle of internal friction φ and show the normalized ground pressure p/σ_0 as a function of the dimensionless parameter $(E/\sigma_0)(\Delta R/R)$ and of the normalized uniaxial compressive strength f_c/σ_0.

Effect of the radial gap size of the shield

As can be seen from the nomograms (Figures III.1 to III.9), for given values of Young's modulus E, uniaxial compressive strength of the ground f_c, initial stress σ_0 and tunnel radius R an increase of the radial gap size of the shield ΔR leads to a reduction of the ground pressure p only up to a certain value of ΔR. For higher values of ΔR, the loading of the segmental lining p remains constant. This is because a bigger radial gap size ΔR of the shield means a higher radial gap size ΔR_l of the segmental lining (Equation 6.2) and the latter, with the assumptions underlying the nomograms (cf. Section 6.4.2), affects the ground pressure p only if the ground closes the gap before backfilling occurs.

Effect of the location of backfilling

A closer examination of Figures III.1 to III.9 reveals that the curves in the left part of the nomograms, i.e., at small values of the dimensionless parameter $(E/\sigma_0)(\Delta R/R)$, are the same for all λ/R values (all other parameters being constant). This is because the backfilling location λ/R does not affect the ground pressure if the ground closes the radial gap of the segmental lining before backfilling (cf. Section 6.4.2) and this happens when the Young's modulus E of the ground is low or the radial gap size of the shield ΔR small.

Counter-intuitive model behaviour

According to the numerical results of Figures III.1 to III.9, the effect of the uniaxial compressive strength is not as straightforward as one might expect. At low values of $(E\Delta R)/(\sigma_0 R)$, an increase in the normalized uniaxial compressive strength f_c/σ_0 leads to an increase in the normalized ground pressure p/σ_0, i.e., a better ground leads to a higher

loading of the segmental lining. As already mentioned in Section 5.2.5, this counter-intuitive model behaviour is well-known in the literature – for a detailled discussion, see Cantieni and Anagnostou (2010) – and is associated with the pre-deformations of the ground ahead of the tunnel face (the bigger the pre-deformation, the more pronounced the stress relief).

6.4.4 Application examples

The nomograms enable an easy and quick computation to be made of the ground pressure acting upon the segmental lining. The use of the nomograms will be illustrated by means of the application example introduced in Section 6.3.2. Table 6.1 shows the input parameters as well as the calculations steps.

Assessment of the segmental lining for given conditions

Column 1 of Table 6.1 shows how to calculate the ground pressure acting upon the segmental lining for given ground conditions and parameters of the TBM and of the segmental lining (i.e., this column deals with dimensioning).

Table 6.1. Application examples.

	Application example			1	2	3
	Ground					
1	Young's modulus	E	[MPa]	1000	**570** [h]	**1000**
2	Poisson's ratio	ν	[-]	0.25		
3	Uniaxial compressive strength	f_c	[MPa]	3.0	3.0	1.0 [j]
4	Angle of internal friction	φ	[°]	25		
5	Dilatancy angle	ψ	[°]	5		
6	Unit weight	γ	[kN/m^3]	25		
	Initial stress					
7	Depth of cover	H	[m]	400		
8	Initial stress	σ_0	[MPa]	10 [a]		
	TBM					
9	Boring diameter, boring radius	D, R	[m]	10, 5		
10	Radial gap size	ΔR	[cm]	5		
	Backfilled segmental lining					
11	Young's modulus	E_l	[MPa]	30000		
12	Thickness	d_l	[cm]	40		
13	Stiffness	K_l	[MPa/m]	480 [b]		
14	Uniaxial compressive strength	$f_{c,l}$	[MPa]	30		
15	Radial gap size	ΔR_l	[cm]	15		
16	Location of backfilling	λ	[m]	5		
	Dimensionless products					
17		E/σ_0	[-]	100.00	57.00	100.00
18		$\Delta R/R$	[-]	0.01		
19		$(E\Delta R)/(\sigma_0 R)$	[-]	1.00	0.57	1.00
20		f_c/σ_0	[-]	0.30	0.30	0.10
21		$K_l R/E$	[-]	2.40	4.21	2.40
22		λ/R	[-]	1.00		
	Structural safety					
23	Normalized ground pressure	p^*	[-]	0.15 [c]	0.24	0.24
24	Ground pressure	p	[MPa]	**1.5** [d,e]	2.4 [i]	2.4 [i]
25	Bearing capacity	p_{max}	[MPa]	2.4 [f]		
26	Safety factor	SF	[-]	1.6 [g]	1.0	1.0

Notes

[a] $\sigma_0 = H\gamma$
[b] $K_l = E_l d_l / R^2$
[c] Linear interpolation between Figures III.4 and III.5, design nomograms for $\varphi = 25$ °, curve for $f_c/\sigma_0 = 0.30$
[d] $p = p^*\sigma_0$
[e] Bold value: main result of the calculation
[f] $p_{max} = d_l f_{c,l} / R$
[g] $SF = p_{max}/p$
[h] Linear interpolation between Figures III.5 and III.6, design nomograms for $\varphi = 25$ °, curve for $f_c/\sigma_0 = 0.30$
[i] "Given", in this column the calculation proceeds from down to top
[j] Linear interpolation between Figures III.4 and III.5, design nomograms for $\varphi = 25$ °, curve for $f_c/\sigma_0 = 0.10$

With regard to the present normalized stiffness of the segmental lining $K_l R/E$ = 2.4 (Row 21) and the normalized location of backfilling λ/R = 1 (Row 22), the normalized ground pressure p^* (Row 23) is calculated by interpolating linearly between Figures III.4 and III.5. The appropriate curves have to be selected according to the actual values of the angle of internal friction (φ = 25 °, Row 4) and normalized uniaxial compressive strength (f_c/σ_0 = 0.3, Row 20). The dimensionless parameter $E\Delta R/\sigma_0 R$ (Row 19), which is entered in the nomograms in order to depict the value of the normalized ground pressure, is calculated on the basis of the parameters of Rows 1, 8, 9 and 10. In this example, p^* = 0.15 (Row 23), thus results in a loading of the segmental lining of p = 1.5 MPa (Row 24). Taking into account the thickness and the uniaxial compressive strength of the segmental lining (d_l = 40 cm and $f_{c,l}$ = 30 MPa according to Rows 12 and 14, respectively), a safety factor of SF = 1.6 (Row 26) results.

Estimation of critical ground conditions for a given segmental lining

Columns 2 and 3 of Table 6.1 show how to estimate the applicability range (in terms of ground quality) of a given segmental lining. For this purpose (and for the sake of simplicity), the present example assumes that the quality of the ground can be described by combinations of its Young's modulus E and its uniaxial compressive strength f_c (all other ground parameters considered as being constant).

The reference ground for the present investigation is that of Column 1 of Table 6.1 (i.e., a Young's modulus of E = 1000 MPa and a uniaxial compressive strength of f_c = 3 MPa). The question addressed here is: how much worse would the ground have to be in order to endanger the structural safety of the segmental lining? In order to answer this question, the bearing capacity of the segmental lining p_{max} = 2.4 MPa (Row 25) is made equal to the ground pressure p (Row 24) acting upon it. Keeping the uniaxial compressive strength equal to the reference value of f_c = 3 MPa (Row 3), it is possible to calculate back (Column 2, down to top) the critical Young's modulus E (Row 1) for which the structural safety of the segmental lining becomes critical. In this example, this occurs if the Young's modulus is E = 570 MPa. A similar calculation (Column 3) shows that (keeping the Young's modulus equal to its reference value of E = 1000 MPa) the critical uniaxial compressive strength amounts to f_c = 1 MPa.

Sensitivity analyses are important in order to identify the critical geotechnical conditions with respect to a given set of design criteria and problem parameters, as the intensity of squeezing may vary significantly along the tunnel alignment (Cantieni and Anagnostou, 2007). The examples of this section of the report demonstrate that such investigations can be carried out easily and quickly applying the proposed nomograms.

6.4.5 Applicability range of the nomograms

Comparison with numerical investigations

As mentioned above (cf. Section 6.4.2), the nomograms were worked out only for specific values of the normalized support stiffness $K_l R/E$ and normalized backfilling locations λ/R. If the actual values of $K_l R/E$ and λ/R deviate from the values assumed for the nomograms, the ground pressure can be obtained by interpolating linearly between the nomograms (as done in the examples of the last section).

The suitability of this procedure and, more general, the applicability range of the nomograms has been tested extensively by comparing the ground pressures p obtained from the nomograms with the pressures resulting from numerical analyses which take account of the actual values of the model parameters (only the simplifying assumption of Sections 6.3.2 and 6.3.3 was retained). Table 6.2 shows such a comparison for three sets of ground parameters and initial conditions (Columns 1–6, 7–12 and 13–18, respectively). For each set, three TBM and backfilling layouts (e.g., Columns 1–2, 3–4, 5–6) and two different segmental linings (odd end even columns) have been considered. Figure 6.14 shows that the results obtained by applying the nomograms agree well with the results of the numerical investigations. As expected, the nomograms overestimate the loading of the segmental lining in the most cases. The overestimation is large only in the case of small diameter TBMs and of relatively good quality ground (Columns 13 to 16).

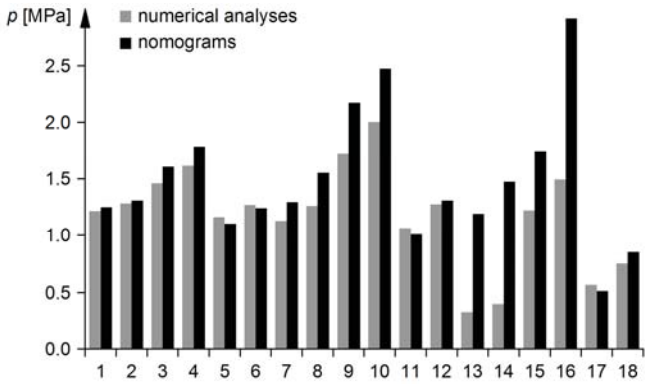

Figure 6.14. Histogram of the comparative calculations of Table 6.2.

This is because the assumption of a normalized shield length L/R = 1, which has been made for working out the nomograms (cf. Section 6.4.2), is particularly safe in these cases (cf. Figure 6.13a).

Double shielded TBMs

Although the present section focused on single shielded TBMs, the basic approach also applies to double shielded TBMs. In fact, there is no difference between the two machine types with respect to the normalized location of the backfilling λ/R. Furthermore, the normalized shield length L/R ($L = L_f + L_r$) and the ratio $\Delta R_l/\Delta R_r$ (where ΔR_r denotes the radial gap of the rear shield) are in the same range as L/R and $\Delta R_l/\Delta R$ for single shielded TBMs (see also the TBM technical data collected in Section 5.2.3). Consequently, the nomograms which were developed for single shielded TBMs can also be applied to double shielded TBMs provided that the radial gap size of the rear shield ΔR_r is taken into account in the computations (instead of the radial gap size of the single shield ΔR). This approach was confirmed by a series of comparative computations (such as the ones in Table 6.2 and Figure 6.14), which, for the sake of economy, are not reported here.

Composite stiffness of the tunnel support

In order to reduce the computational effort, the nomograms disregard the fact that the stiffness K_c of the tunnel support depends on the deformations of the bored profile, i.e., they assume a constant stiffness $K_c = K_l$ (cf. Sections 6.3.2 and 6.3.3), where K_l is the stiffness of the segmental lining. This assumption is easy and reasonable (cf., e.g., Figure 6.9), but not mandatory. The introduction into the computation of another tunnel support stiffness value is possible, but requires, of course, sufficient and reliable knowledge as to the actual value of the stiffness K_c of the system composed of the backfilling and the segmental lining.

Ground behaviour

With respect to the ground behaviour, on the one hand it has to be said that disregarding its possible time-dependency is a major simplification which is, nevertheless, usually made due to a lack of knowledge concerning the behaviour of the ground over time. Neglecting time-dependency may be unsafe with respect to the lining loading. In fact, as shown in Section 3.4.3, in some cases a slower development of the ground deformations (or a faster TBM advance) may lead to a higher lining load.

On the other hand, it must also be said that the proposed nomograms assume homogeneous ground. This is another standard assumption in tunnel analysis, but it is conservative for the frequently encountered case of short weak zones alternating with stabilizing, competent rock (cf. Section 4.2.3).

Table 6.2. Comparison between the ground pressure p obtained from numerical analyses carried out specifically for each example and by applying the nomograms.

	Application example			1	2	3	4	5	6	7	8	9	10	11	12	13	14	15	16	17	18
	Ground																				
1	Young's modulus	E	[MPa]	1000	1000	1000	1000	1000	1000	2000	2000	2000	2000	2000	2000	4000	4000	4000	4000	4000	4000
2	Poisson's ratio	ν	[-]	0.25																	
3	Uniaxial compressive strength	f_c	[MPa]	1	1	1	1	1	1	3	3	3	3	3	3	10	10	10	10	10	10
4	Angle of internal friction	φ	[°]	20	20	20	20	20	20	25	25	25	25	25	25	30	30	30	30	30	30
5	Dilatancy angle	ψ	[°]	1	1	1	1	1	1	5	5	5	5	5	5	10	10	10	10	10	10
6	Unit weight	γ	[kN/m^3]	25																	
	Initial stress																				
7	Depth of cover	H	[m]	250	250	250	250	250	250	500	500	500	500	500	500	1000	1000	1000	1000	1000	1000
8	Initial stress [a]	σ_0	[MPa]	6.25	6.25	6.25	6.25	6.25	6.25	12.50	12.50	12.50	12.50	25.00	25.00	25.00	25.00	25.00	25.00	25.00	25.00
	TBM																				
9	Boring radius	R	[m]	2.5	2.5	4	4	5.5	5.5	2.5	2.5	4	4	5.5	5.5	2.5	2.5	4	4	5.5	5.5
10	Radial gap size	ΔR	[cm]	4	4	5	5	6	6	4	4	5	5	6	6	4	4	5	5	6	6
11	Length (shield)	L	[m]	10.0	10.0	11.5	11.5	13.0	13.0	10.0	10.0	11.5	11.5	13.0	13.0	10.0	10.0	11.5	11.5	13.0	13.0
12	Young's modulus (shield)	E_s	[MPa]	210000																	
13	Thickness (shield)	d_s	[cm]	7.5	7.5	10.0	10.0	12.5	12.5	8.0	8.0	10.0	10.0	12.5	12.5	8.0	8.0	10.0	10.0	12.5	12.5
14	Stiffness (shield) [b]	K_s	[MPa/m]	2520	2520	1313	1313	868	868	2520	2520	1313	1313	868	868	2520	2520	1313	1313	868	868
	Backfilled segmental lining																				
15	Young's modulus	E_l	[MPa]	30000																	
16	Thickness	d_l	[cm]	30	50	30	50	30	50	30	50	30	50	30	50	30	50	30	50	30	50
17	Stiffness [c]	K_l	[MPa/m]	1440	2400	563	938	298	496	1440	2400	563	938	298	496	1440	2400	563	938	298	496
18	Uniaxial compressive strength	$f_{c,l}$	[MPa]	30																	
19	Radial gap size	ΔR_l	[cm]	14	14	17	17	20	20	14	14	17	17	20	20	14	14	17	17	20	20
20	Location of backfilling	λ	[m]	3	3	0	0	8	8	3	3	0	0	8	8	3	3	0	0	8	8
	Numerical analyses																				
21	Ground pressure	p	[-]	1.2	1.3	1.5	1.6	1.2	1.3	1.1	1.3	1.7	2.0	1.1	1.3	0.3	0.4	1.2	1.5	0.6	0.8
	Nomograms																				
22	Ground pressure	p	[-]	1.2	1.3	1.6	1.8	1.1	1.2	1.3	1.6	2.2	2.5	1.0	1.3	1.2	1.5	1.7	2.9	0.5	0.9

Notes

[a] $\sigma_0 = H\gamma$ [b] $K_s = E_s d_s / R^2$ [c] $K_l = E_l d_l / R^2$

Time-dependent stiffness of the backfilling material

Besides the possible time-dependency of the ground behaviour, the nomograms also disregards a time-dependency in the stiffness of the backfilling material. This is a reasonable assumption for pea gravel (the stiffness of which does not vary over the time) or rapidly hardening mortars (the stiffness of which achieves its final value very quickly). This does not apply, however, to backfilling materials with a pronounced time-dependent behaviour. For these cases (and assuming that the backfilling layer represents a compressible buffer between the segmental lining and the ground), the approach proposed in this report leads to an overestimation of the final value of the loading of the segmental lining. This overestimation decreases with decreasing thickness of the backfilling layer (cf. Figure 6.11a), i.e., with increasing squeezing potential of the ground.

7 Conclusions and outlook

The main goal of each TBM drive is to achieve the highest possible gross advance rate. The latter represents the main outcome of the interaction between the ground, the tunnelling equipment (TBM and back-up) and the support and, at the same time, a factor influencing this interaction. As a series of factors resulting from the three main components of the system and "external" factors (such as the organization of the construction site) affect the TBM drive simultaneously and are usually coupled with each other, planning a mechanized excavation in squeezing ground is a complex task, where conflicting requirements and several feedback effects may be present.

In the tunnel engineering community there is a certain degree of controversy concerning the most appropriate machine type for coping with squeezing ground. The application of gripper TBMs is proposed on the grounds of their shorter length as well as their greater flexibility with respect to tunnel support. On the other hand, it is emphasized that single or double shielded TBMs allow for highly industrialized tunnel construction and this – in combination with the higher thrust force and torque that can be applied by these machines – results in a higher advance rate. The differing opinions can possibly be traced back to the different project-specific geological conditions and tunnelling experience of the authors. Consider, for example, a small diameter tunnel and compare a gripper TBM (equipped with only a short cutter head shield) with a double shielded TBM. The length of the double shield is potentially disadvantageous with respect to the risk of jamming. It cannot, however, be said that this disadvantage is really relevant in a particular geotechnical situation (it depends on how rapidly the ground converges). On the other hand, a gripper TBM also has potential disadvantages such as lower thrust (particularly in the case of gripper bracing problems) or lower advance rate (particularly if the support requirements are big). Again, these disadvantages may be relevant or not depending on the geology: on how high the bearing capacity of the ground is in the gripper area; on how rapidly the convergences or ground pressures develop; and on how much support has to be installed in the TBM area in order to stabilize the opening and control the deformations. Without a thorough analysis – which will take into account all the specifics of the given geotechnical situation, the TBM and the back-up to be used as well as the tunnel support to be installed – it is not easy to judge which factor will have the greater impact. Depending on the geological conditions, the advantages of one TBM type may or may not counteract the disadvantages of the other types. It is therefore impossible to provide universally valid recommendations. A systematic approach such as the one outlined in Section 2.3 is indispensable for the identification and assessment of the interactions between ground, tunnelling equipment and support.

Due to the complexity of the problem, the assessment of a TBM drive in squeezing ground cannot be based solely on plausibility considerations or on experience from projects with comparable geological conditions. Besides engineering judgement, numerical investigations are helpful for evaluating potential hazards, as they provide indications of the magnitude of the key parameters. In this respect, the computational model presented and applied in this report (cf. Section 3.2) undoubtedly represents a powerful tool for the simulation of a TBM drive in squeezing ground. On the one hand, it provides an accurate simulation of the interface between the ground and the shield as well as the ground and any kind of tunnel support. On the other hand, it incorporates the longitudinal distribution of the ground pressure acting upon the shield and the lining and takes due account of the stress history, thus avoiding the errors introduced by plane strain analyses (Cantieni and Anagnostou, 2009a).

In the case of time-dependent ground behaviour, interruptions in the TBM operation may be unfavourable in squeezing ground. Tunnelling experience (cf. Section 2.2) as well as theoretical considerations (cf. Section 3.4) suggest that maintaining a high advance rate and reducing the standstill times may have a positive effect. This is, of course, a major goal for any TBM drive. Nevertheless, a fast TBM advance should not be seen as a panacea for coping with squeezing conditions. Firstly, it may be difficult to achieve it in the case of poor quality ground. Secondly, ground deformations may develop very rapidly

and very close to the tunnel face (cf. Section 2.2). And finally, the possibility of unpredicted long standstills cannot be excluded a priori with sufficient certainty.

The design nomograms (together with the extensive collection of TBM technical data) presented in Section 5, represent a valuable contribution to decision-making in the design process. The nomograms show in a condensed form the statical conditions that have to be fulfilled in the design of a TBM (with respect to the thrust force requirements) in order to avoid jamming of the shield when crossing squeezing ground, while the collected data reviews the state of present-day TBMs. Their application enables quantitative statements to be made concerning the feasibility of a TBM drive as well as the effectiveness of potential design or operational measures. The dimensionless design charts of Section 6 enhance the set of decision aids presented in this report. These nomograms cover the practically relevant range of material constants, initial stress, TBM, segmental lining and backfilling characteristics and allow an easy and quick assessment to be made in respect of the ground pressure acting upon a segmental lining. Of course, the design nomograms of Sections 5 and 6 cannot eliminate the uncertainties associated with ground parameters and ground behaviour. Such uncertainties are intrinsic to every geomechanical calculation. In the planning phase, the tunnelling engineer deals with this uncertainty and utilises the computational results as a decision aid for his risk analysis. In this respect, the design nomograms represent a powerful tool.

The suitability of the methodical approaches, the computational model and the decision aids developed within the framework of this research project has already been verified by applying them successfully in a series of real world projects involving TBM drives in squeezing ground: during construction of the Uluabat Tunnel in Turkey (cf. Section 4.2) and the Faido Section of the Gotthard Base Tunnel in Switzerland (cf. Section 4.3), in the planning phase of the Lake Mead No 3 Intake Tunnel (Anagnostou et al., 2010b) and the Bosslertunnel in Germany (Anagnostou and Ramoni, 2009) as well as for the tender design of the El Teniente New Access Tunnels in Chile (Anagnostou et al., 2010c).

Of course, as is the case with all research work, some questions remain "open".

A series of practically relevant questions concerns the tunnel face. Firstly, the torque requirements in squeezing ground should be investigated more in detail. This issue is particularly challenging, since – as described qualitatively in Section 2 – several effects may affect both the friction to be overcome and the boring process. Additionally, questions arise concerning the stability of the face in weak ground. This is particularly important in water-bearing ground, where seepage forces develop towards the face. In this respect, pore pressure relief by advance drainage is a highly effective measure for reducing deformations (Anagnostou, 2009a, 2009b) and improving face stability (Anagnostou et al., 2010b, 2010a). This topic is currently under investigation at the ETH Zurich within the framework of the research project FGU 2010/004 "Static effects, feasibility and execution of drainages in tunneling". Considering the possibility of having a superposition of squeezing and unstable ground, another interesting research project might be to extend the investigations of this report to cover slurry or EPB shields, i.e., to analyse the effects of an active face and tunnel boundary support on the development of ground deformations and pressure in the machine area.

Another future research topic concerns the time-dependency of ground behaviour. The present report discusses only the effect of consolidation (cf. Section 3.4). In a further research step, the effects of creep should be investigated in order to understand the mechanism governing the interaction between the ground, the tunnelling equipment (TBM and back-up) and the support in creeping ground. A second step might then be to analyze the superimposed effect of creep and consolidation and to identify distinguishing features of these two mechanisms.

There is a further group of open questions regarding the choice of an appropriate support concept. As discussed qualitatively in Section 2.4.7, a question arises in the planning phase as to whether a rigid or a yielding support should be applied. The choice of the right solution, which should cover the greatest possible range of squeezing conditions, is particularly demanding for shielded TBM tunnelling, as deformable segmental linings have not yet proven themselves in tunnelling practice. However, it is questionable if a high deformability of the segmental lining is at all necessary. As indicated by numerical simulations, jamming of the shield (rather than overstressing of the lining) is the relevant

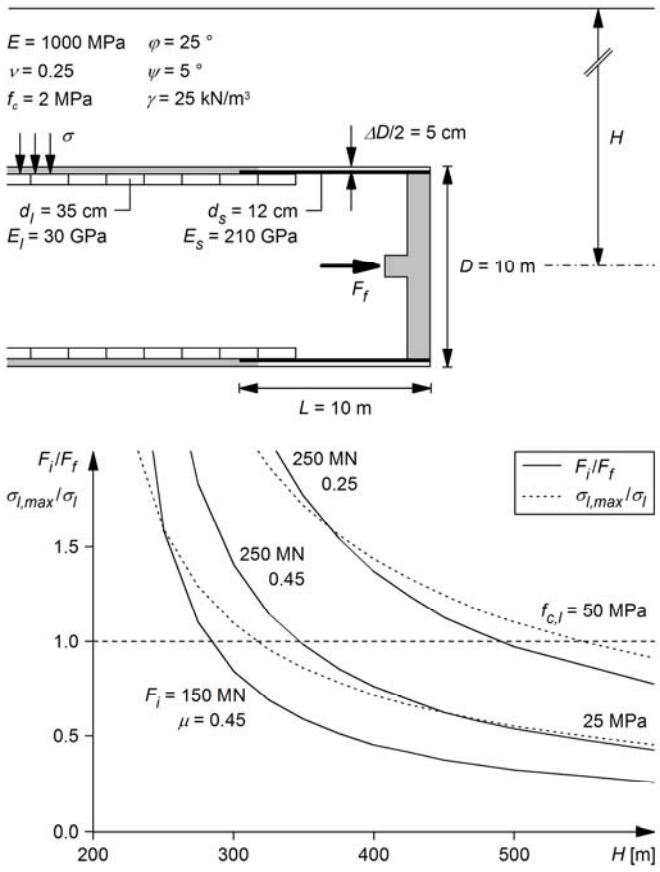

Figure 7.1. Effect of an increase of the depth of cover H on the risk of shield jamming (safety factor F_i/F_f) or of overstressing of the lining (safety factor $\sigma_{l,max}/\sigma_l$) for a 10 m long single shielded TBM with a boring diameter of 10 m.

hazard scenario in many cases: under adverse conditions, squeezing will halt the TBM advance before endangering the structural safety of the segmental lining.

Figure 7.1 shows computational results obtained for a 10 m long, single shielded TBM boring a 10 m diameter tunnel in weak sedimentary rock. The computational method is described in Section 3.2 of the present report and assumes axial symmetry and linearly elastic, perfectly plastic ground behaviour with the Mohr-Coulomb yield criterion as well as a backfilling of the segments by grouting via the shield tail. The diagram shows the effect of the depth of cover H on the risk of shield jamming or lining overstressing (solid and dashed lines, respectively). The risk of shield jamming is expressed by the ratio of the installed thrust force F_i to the force F_f needed for overcoming friction. The risk of overstressing is expressed by the ratio of the allowable loading of the lining $\sigma_{l,max}$ to the ground pressure σ_l developing far behind the face. For an installed thrust force F_i = 150 MN (a high but nevertheless achievable value) and a uniaxial compressive strength for the lining of $f_{c,l}$ = 25 MPa (a design value already incorporating a safety factor), the diagram shows that the ground would immobilize the TBM at a depth of about 300 m, which is slightly lower than the depth at which overstressing of the 35 cm thick lining would occur. By installing a higher thrust force of 250 MN – which, according to Burger (2009), is technologically possible for common boring diameters of traffic tunnels applying high-pressure hydraulic systems – and by taking additional measures to reduce skin friction (lubrication), jamming would not occur until the depth of cover reached about 500 m, while the bearing capacity of the lining would become relevant at a depth of 300–350 m. Lining design for greater depths should also take into account the higher axial load caused by the thrust force. A solution based on the resistance principle would be, nevertheless, still possible in the present example: one could increase the thickness of the segments (which is feasible up to 70 cm) or apply segments made of high

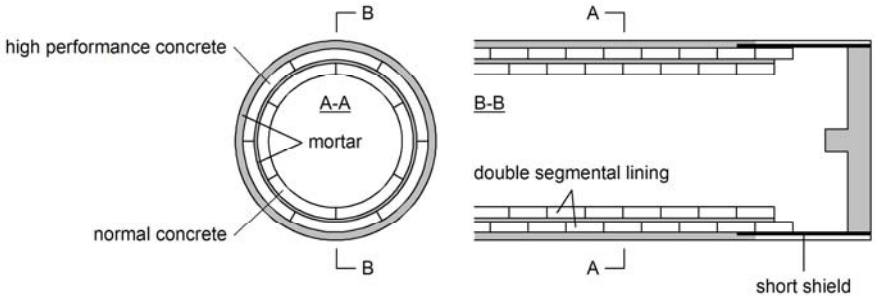

Figure 7.2. Double segmental lining.

performance concrete (HPC) having a very high uniaxial compressive strength (a design value of up to 50–60 MPa).

Should it be necessary to further increase the resistance of the segmental lining (beyond the resistance offered by segments of manageable thickness and weight), it is possible to design a lining system consisting of two concentric segment rings (Figure 7.2). The inner segmental lining would be applied (by the same erector) only when required. The outer ring could be made of HPC, while normal concrete would be advantageous for the inner ring (on account of its higher fire resistance). Depending on the water pressures in the project area, it might be also possible for the inner ring alone to be waterproof. A solution with a double segmental lining makes sense only in heavily squeezing ground and should, therefore, be combined with a minimum possible shield length in order to reduce the surface exposed to ground pressure and to utilize the favourable longitudinal arching (cf. Section 2.4.7).

The above discussion suggests that shield jamming limits feasibility to a larger extent than lining overstressing. It could be argued, however, (i), that shield jamming, in contrast to segmental lining damage, may be regarded as an acceptable risk and, (ii), that if the deformations develop slowly, the shield may advance without any problems even if a high rock load develops far behind the face (in this case too, lining overstressing rather shield jamming would be the relevant factor). Concerning the first point, it is impossible to make a generally valid statement as the acceptance of jamming depends of course on the potential damage to the TBM as well as on the frequency of the events necessitating hand-mining for freeing the TBM. With regard to the second objection, it should be noted that estimating the intensity of squeezing is an extremely uncertain task in the planning phase and, consequently, decision-making should make some contingency for rapidly developing deformations (such as are occasionally observed, cf. Section 2.2). This is also why the computational methods employed in engineering practice (during design for the assessment of squeezing) usually do not take into account the time-dependency of ground behaviour.

The investigations described above also suggest that an assessment of the suitability of a given support system requires a systematic approach and a thorough analysis, taking due account of the interactions between ground, shield and support. In fact, it is reasonable to expect that a yielding support will be advantageous with respect to the lining loading, but not with respect to the shield loading. On the contrary, the question arises as to whether a rigid segmental lining, which is favourable with respect to the thrust force requirements, will be able to accommodate the high ground pressure resulting from the longitudinal load transfer (cf. Section 3.3.4). Further research work – involving aspects related to concrete technology, TBM technology, tunnelling logistics and statics – is needed in order to investigate in more detail the applicability ranges of the different support systems and to evaluate their effect on the risk of shield jamming.

Appendixes

I Case histories

This Appendix provides an overview of case histories, where TBM drives encountered problems due to squeezing ground. For the sake of economy, the references are not listed in the present report, but can be found in Ramoni (2010).

Project (country), Tunnel length TBM type, Manufacturer, Boring diameter, TBM operation time	*Overburden*, Geology	Sticking of the cutter head	Jamming of the shield	Inadmissible convergences	Damage to the tunnel support	Jamming of the back-up equipment	Observed deformations
Yacambú – Quibor Tunnel (Venezuela), 24.3 km							
Gripper TBM, Robbins, 4.80 m, 1975–1980	*350–400 m*, graphitic phyllite	x [a]	x [a]	x [a]	x [a]	x [a]	Along 250 m, bored profile practically closed within 30 days
Gripper TBM (2x) [b], Robbins, 4.80 m, 1975–1980	*150–600 m*, mudstone, sandstone		x				
Stillwater Tunnel (USA), 12.9 km							
Double shielded TBM, Robbins, 2.91 m, 1978–1979	*600–800 m*, sandstone, siltstone, blocky		x [b,c]		x [d]		
Walking Gripper Blade Shield, SNC Lavalin, 2.91 m, 1982–1983	clayey schist, fault zones						Only small convergences
Gripper TBM, Robbins, 3.20 m, 1982–1983				x	x		Convergences of 4 %; convergence rate of 0.4 %/d after 1 day and of 0.09 %/d after 10 days
Pueblo Viejo – Quixal Tunnel (Guatemala), 26.0 km							
Gripper TBM, Wirth, 5.64 m, 1978–1981	*500 m*, sandstone	x [e]	x [e]				
Gripper TBM, Wirth, 5.64 m, 1978–1981	≤ *1500 m*, marl		x	x	x		Radial displacements of ≤ 50 cm
Tavanasa – Ilanz Tunnel, Strada Section (Switzerland), 4.2 km							
Gripper TBM, Demag, 5.20 m, 1985–1988	*200 m*, phyllitic verrucano, 150–300 m long overthrust zone			x	x		Reduction of the bored profile by 25 cm within just a half day already in the machine area
Los Rosales Tunnel (Colombia), 9.1 km							
Double shielded TBM, Robbins, 3.54 m, 1987–1990	≤ *350 m*, lutite		x [f]				
Yindaruqin Irrigation Project, Tunnel 38 (China), 5.1 km							
Double shielded TBM, Robbins, 5.54 m, 1990–1992	*200–430 m*, clayey sandstone		x				
Evinos – Mornos Tunnel (Greece), 29.4 km							
Gripper TBM (2x), Robbins, 4.20 m, 1993–1994	≤ *1300 m*, flysch, thrust zones	x [g]		x	x		Radial displacements of 3–5 cm at the cutter head and 5–8 cm at the location of support installation
Double shielded TBM, Robbins, 4.04 m, 1993–1994	*700–950 m*, flysch, 650 m long overthrust zone		x				Convergences of 15 cm within less than 1 hour at a distance of 1–2 m from the working face
Amsteg Power Plant Tunnel (Switzerland), 7.3 km							
Gripper TBM, Atlas Copco, 5.08 m, 1995–1996	*500 m*, cataclastic seritical phyllite						Only small convergences

Project (country), Tunnel length TBM type, Manufacturer, Boring diameter, TBM operation time	*Overburden*, Geology	Sticking of the cutter head	Jamming of the shield	Inadmissible convergences	Damage to the tunnel support	Jamming of the back-up equipment	Observed deformations
Guadiaro – Majaceite Tunnel (Spain), 12.2 km Double shielded TBM, NFM-Boretec-Mitsubishi, 4.88 m, 1995–1997	*150–400 m*, sandy and clayey flysch, claystone	x [h]	x [h,i]	x	x [i]		Gap between shield and ground closed at a distance of 1 m from the working face; radial displacements of 5–6 cm of the damaged segmental lining
Vereina Tunnel, Nord Section (Switzerland), 11.6 km Gripper TBM, Wirth, 7.64 m, 1995–1997	*1250 m*, heavy fractured crystalline rock	x	x	x			Radial displacements of 20 cm at the cutter head during standstill due to ravelling or squeezing ground (the cause is unclear); execution of re-profiling works along 20 m
Umiray – Angat Tunnel (Philippines), 13.2 km Double shielded TBM, Robbins, 4.88 m, 1998–2000	*1000–1200 m*, basalt combined with other metamorphic volcanic rocks		x	x			Convergence rate of 20 cm/h; in two cases reduction of the bored profile of 12 cm at a distance of 1 m from the working face, in a third case convergences of 37 cm within less then 2 hours in the machine area
Misicuni Tunnel (Bolivia), 19.8 km Gripper TBM, Robbins, 3.50 m, 1998–2002	*800–1200 m*, cataclastic rocks within a 700 m long fault zone						Convergences of 10–12 cm in the machine area with a convergence rate of 3 mm/min together with instabilities in the tunnel crown; the cause of the ground deformations is not clear (squeezing or ravelling)
Fujikawa Transport and Pilot Tunnels (Japan), 4.5 and 3.7 km Double shielded TBM, (unknown), 3.50 m, 1999–1999	*250–300 m*, 100 m long fault zone with clayey material	x	x				Convergence rate of 15 cm/d
Double shielded TBM, (unknown), 5.00 m, 2000–2001							Reduction of the bored profile by 60 cm with a convergence rate of 29 cm/d; the gap between ground and tail shield became closed within 1 day
Nuovo Canale Val Viola Tunnel (Italy), 18.8 km Double shielded TBM, Wirth, 3.60 m, 1999–2004	*200–800 m*, pelitic and phyllitic rock		x [j]		x		The gap between shield and ground (8 cm in diameter) closed at a distance of 9 m from the working face (at the end of the shield) within 6 to 10 hours
Salazie Aval Tunnel (France), 9.4 km Double shielded TBM, Herrenknecht, 3.85 m, 1999–2005	*900–1000 m*, basalt		x				

Project (country), Tunnel length TBM type, Manufacturer, Boring diameter, TBM operation time	*Overburden*, Geology	Sticking of the cutter head	Jamming of the shield	Inadmissible convergences	Damage to the tunnel support	Jamming of the back-up equipment	Observed deformations
Shanxi Wanjiazhai Yellow River Diversion Project, Connection Works Tunnel Nr. 7 (China), 13.5 km							
Double shielded TBM, Robbins, 4.82 m, 2000–2001	*300 m*, marly rock		x				Convergence rate of 2–4 cm/h, gap between shield and ground (5–8 cm in diameter) closed within less than 2 hours
Shanggongshan Tunnel (China), 13.8 km							
Double shielded TBM [b], Robbins, 3.65 m, 2003–2005	*200–250 m*, alternating stratification of sandstones and clayey schists with cataclastic shear zones		x [k]		x		Gap between shield and ground (5–10 cm) closed practically instantaneously
Gotthard Base Tunnel, Amsteg Section (Switzerland), 11.4 km							
Gripper TBM (2x), Herrenknecht, 9.58 m, 2003–2006	*700 m*, cataclastic sericitical phyllite			x			Radial displacements of 15–30 cm in the back-up area
Gotthard Base Tunnel, Bodio Section (Switzerland), 15.9 km							
Gripper TBM (2x), Herrenknecht, 8.80 m, 2003–2006	*1000 m*, micaceous gneiss		x [l]	x	x		Radial displacements of 7 cm at a distance of 4 m (at the end of the shield), of 10 cm at a distance of 8 m (after support installation) and of 14–22 cm at a distance of 55 m (back-up area) from the working face, respectively
Arrowhead Tunnels East and West (USA), 9.3 and 6.1 km							
Single shielded TBM (2x), Herrenknecht, 5.82 m, 2003–2008	≤ *650 m*, hydrothermally altered granite, gneiss, fault zones with sandy and clayey material		x				
Ghomroud Tunnel, Sections 3 and 4 (Iran), 16.5 km							
Double shielded TBM, Wirth, 4.50 m, 2004–2008	≤ *650 m*, graphitic schists and sandstones		x				Radial displacements of 6 cm within 2 days after installation of the segmental lining; considering that the TBM was already blocked for eight weeks 300 m before in the same geology due to instability of the working face and of the tunnel walls, it is possible that the ground deformations were due to ravelling and not to squeezing ground

Project (country), Tunnel length TBM type, Manufacturer, Boring diameter, TBM operation time	*Overburden*, Geology	Sticking of the cutter head	Jamming of the shield	Inadmissible convergences	Damage to the tunnel support	Jamming of the back-up equipment	Observed deformations
Gilgel Gibe II Tunnel (Ethiopia), 25.8 km Double shielded TBM, Seli, 6.98 m, 2005–2009	*670 m*, weathered, brecciated and decomposed basalt	x	x		x		Extrusion rate of the core of 4–6 cm/h; TBM pushed back more than 60 cm and displaced laterally more than 40 cm
Pajares Tunnel, Section 4 (Spain), 10.3 km Single shielded TBM, Robbins, 9.88 m, 2006–2009	*650 m*, shale		x				
Uluabat Tunnel (Turkey), 11.8 km Single shielded TBM, Herrenknecht, 5.05 m, 2006–2010	*120 m*, claystone		x		x [m]		Convergence rate of 6 cm/h; gap between shield and ground (3–9 cm) rapidly closed
Gotthard Base Tunnel, Faido Section (Switzerland), 14.2 km Gripper TBM (2x), Herrenknecht, 9.43 m, 2007–2011	*1600 m*, micaceous gneiss			x	x	x	Convergences already in the machine and also in the back-up area along 250 m; in the east tunnel convergences of up to 5–10 cm in the roof and heave of the tunnel floor of up to 30 cm; in the west tunnel convergences of up to 25 cm in the roof and heave of the tunnel floor of up to 75 cm

Notes

[a] Loss of the TBM
[b] TBM drives abandoned
[c] TBM jammed in a fault zone consisting of clayey schist (overburden: 650 m)
[d] Due to insufficient backfilling of the segmental lining and to the combined action of ground pressure and thrust force
[e] TBM drive abandoned after loss of the TBM (ground collapse, major water inflow after sticking of the cutter head and jamming of the shield)
[f] Jamming of the shield three times avoided by applying the maximum possible thrust force
[g] One TBM jammed in highly fractured radiolarit (overburden: 950 m)
[h] Sticking of the cutter head and jamming of the shield in sandy and clayey flysch one time avoided by applying the maximum possible torque and thrust force (overburden: 150 m)
[i] Claystone (overburden: 400 m); damage to the segmental lining due to the application of a high thrust force (shield jamming could not be avoided)
[j] Jamming of the shield two times due to rapid convergences and one time during a one-week holiday stop
[k] In one case damage to the rear shield due to its lateral displacement
[l] Damage to the shield claimed by the contractor
[m] Due to the application of a high thrust force (shield jamming could not be avoided)

II Nomograms for the assessment of the required thrust force

Overview of the nomograms

TBM type	Normalized shield length	Shield type	Nomogram
Gripper TBM	L/R = 1.0	Cutter head shield	Figure II.1
Single shielded TBM	L/R = 2.0		Figure II.2
	L/R = 5.0		Figure II.3
Double shielded TBM	L/R = 2.0	Front shield	Figure II.4
		Rear shield	Figure II.5
	L/R = 3.5	Front shield	Figure II.6
		Rear shield	Figure II.7
	L/R = 5.0	Front shield	Figure II.8
		Rear shield	Figure II.9

Considered parameter ranges

Ground		
Poisson's ratio	ν [-]	0.25
Angle of internal friction	φ [°]	15–35
Dilatancy angle	ψ [°]	max(1, φ – 20)
Normalized compressive strength	f_c/σ_0 [-]	0.05–0.50
TBM		
Normalized shield stiffness	$K_s R/E$ [-]	10
Normalized shield length	L/R [-]	See above
Additionally for double shielded TBMs:		
Normalized rear shield length	L_r/L [-]	0.60
Normalized rear shield radial gap size	$\Delta R_r/\Delta R$ [-]	1.50
Lining		
Normalized lining stiffness	$K_l R/E$ [-]	0.0 (gripper TBMs) 0.5 (shielded TBMs)

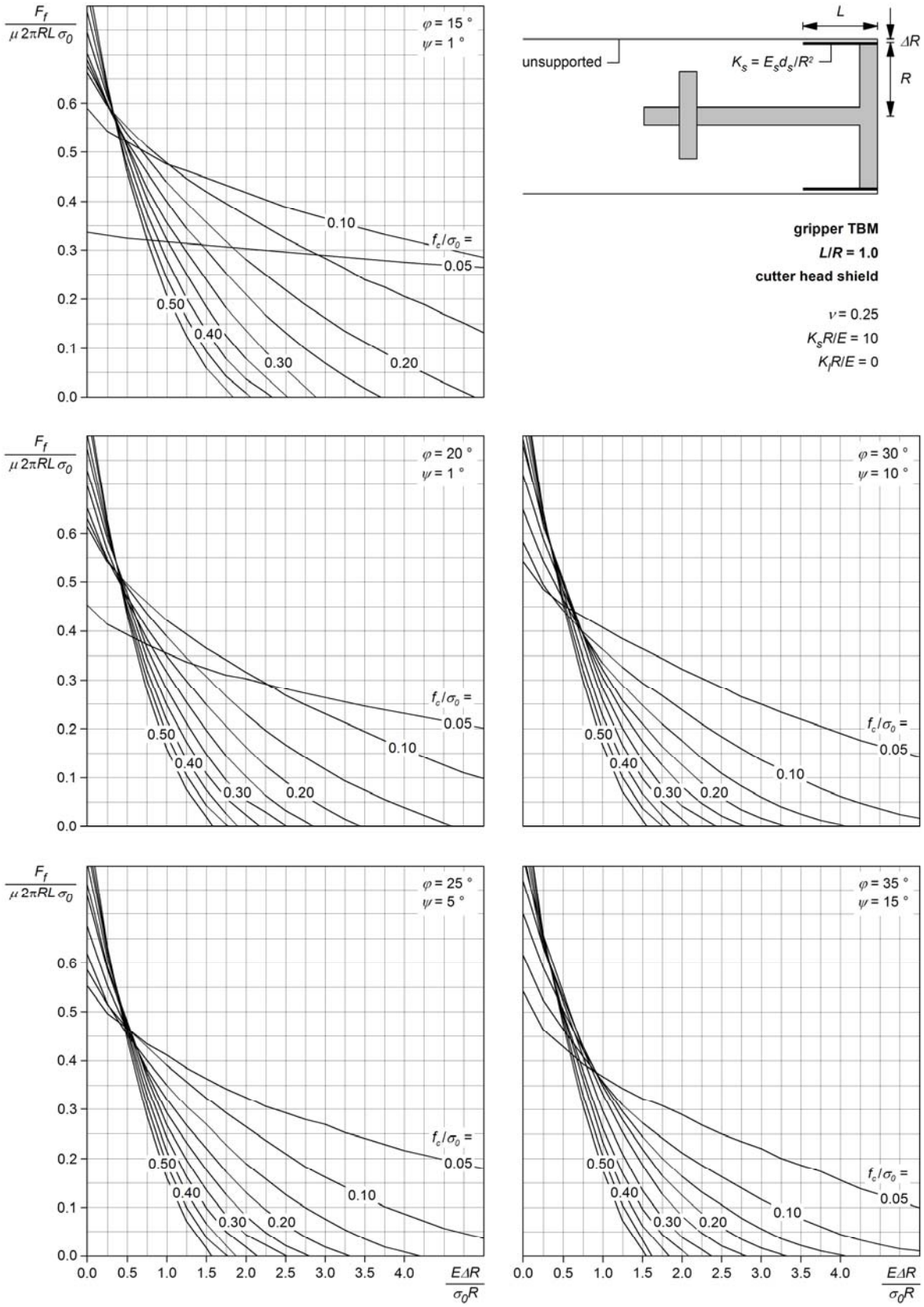

Figure II.1. Gripper TBM: nomograms for L/R = 1.0.

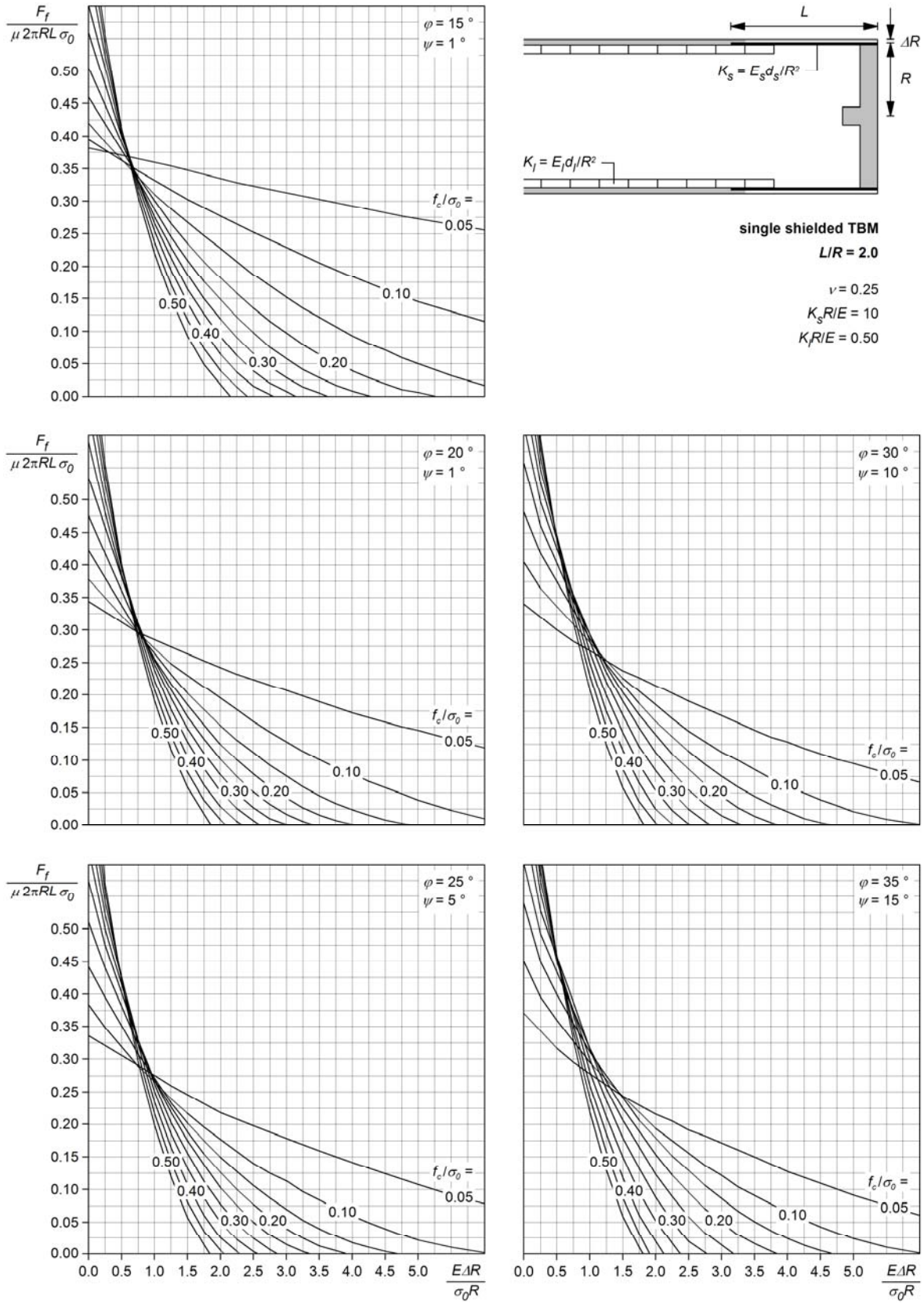

Figure II.2. Single shielded TBM: nomograms for L/R = 2.0.

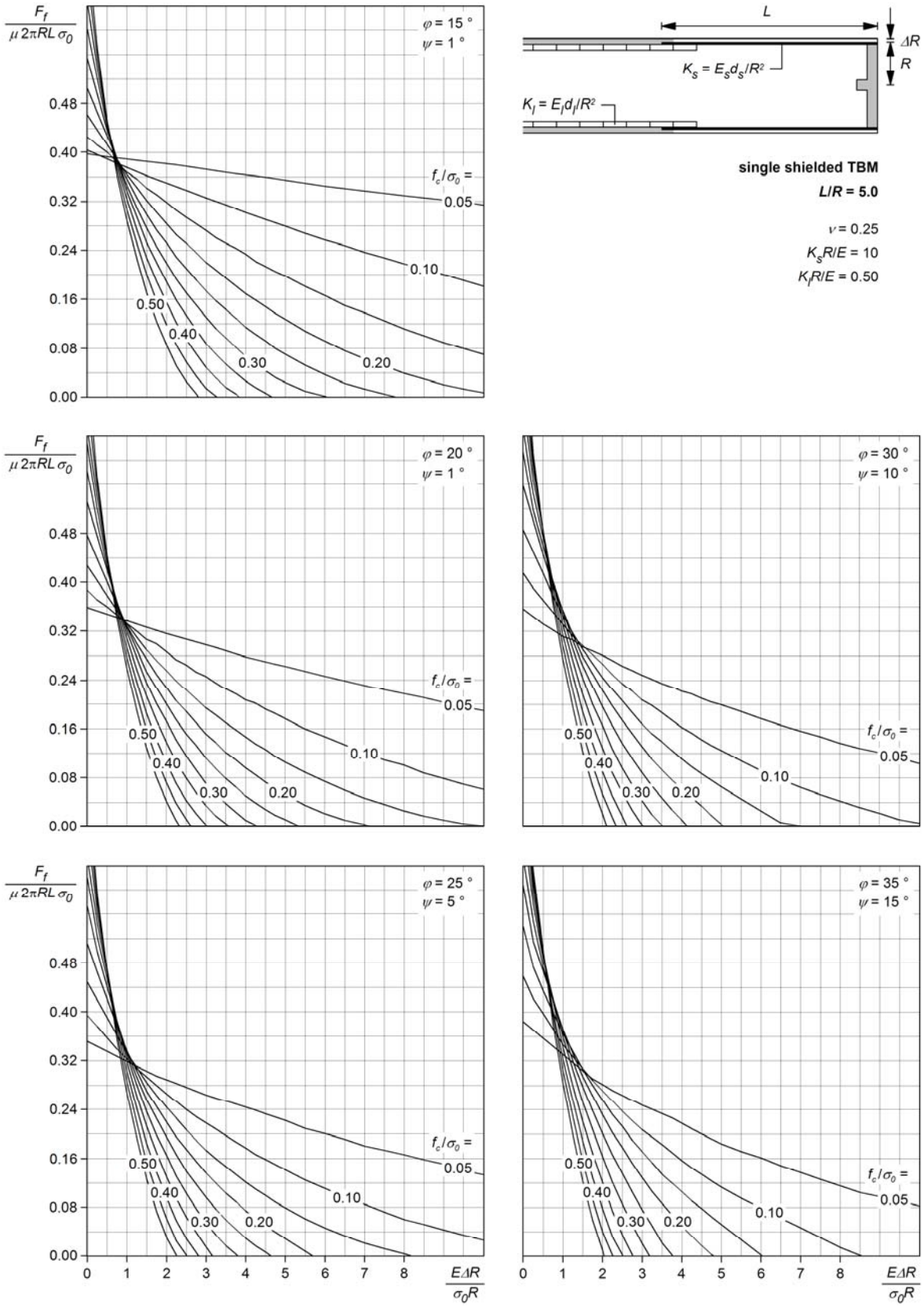

Figure II.3. Single shielded TBM: nomograms for L/R = 5.0.

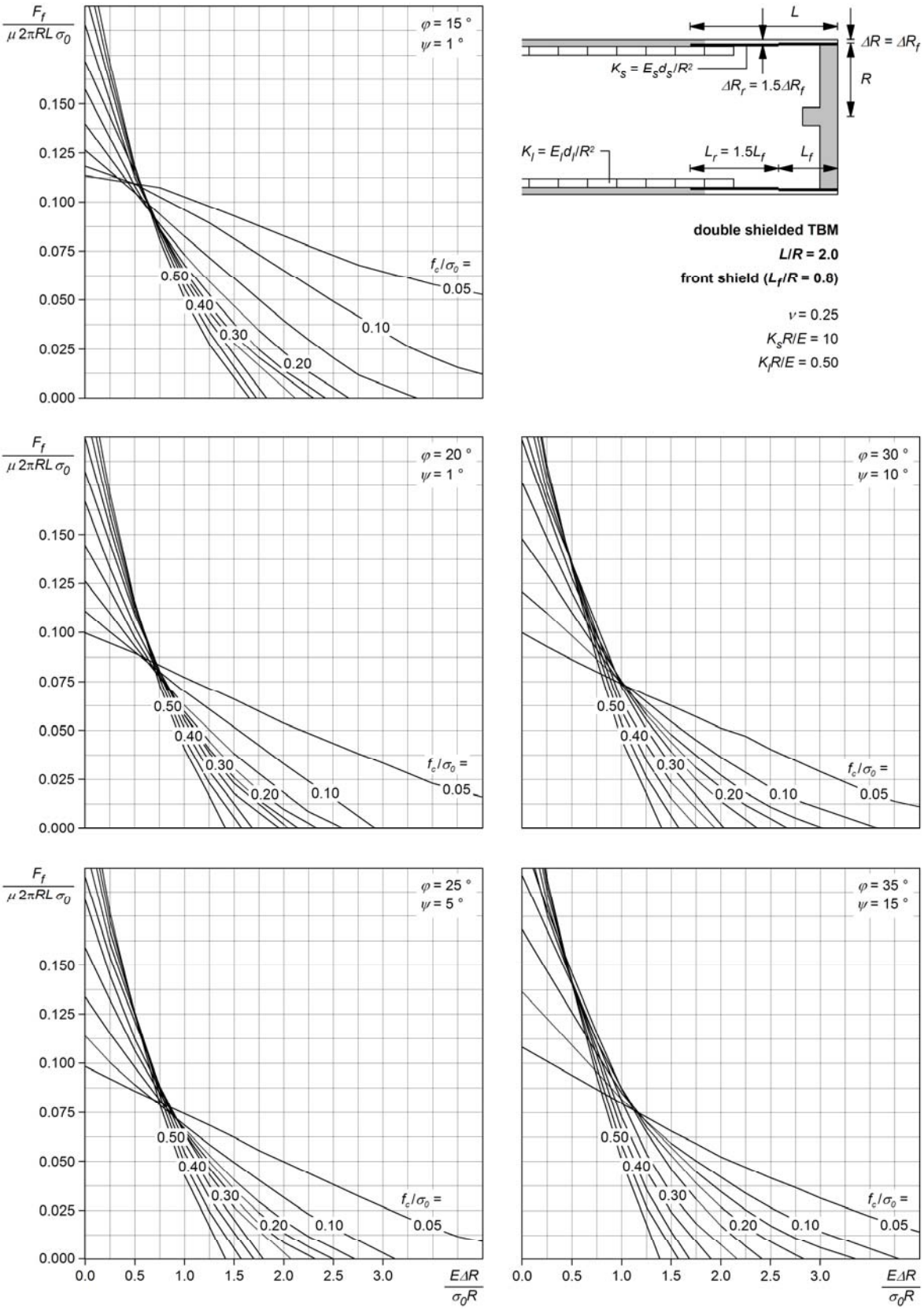

Figure II.4. Double shielded TBM: nomograms for L/R = 2.0 – front shield.

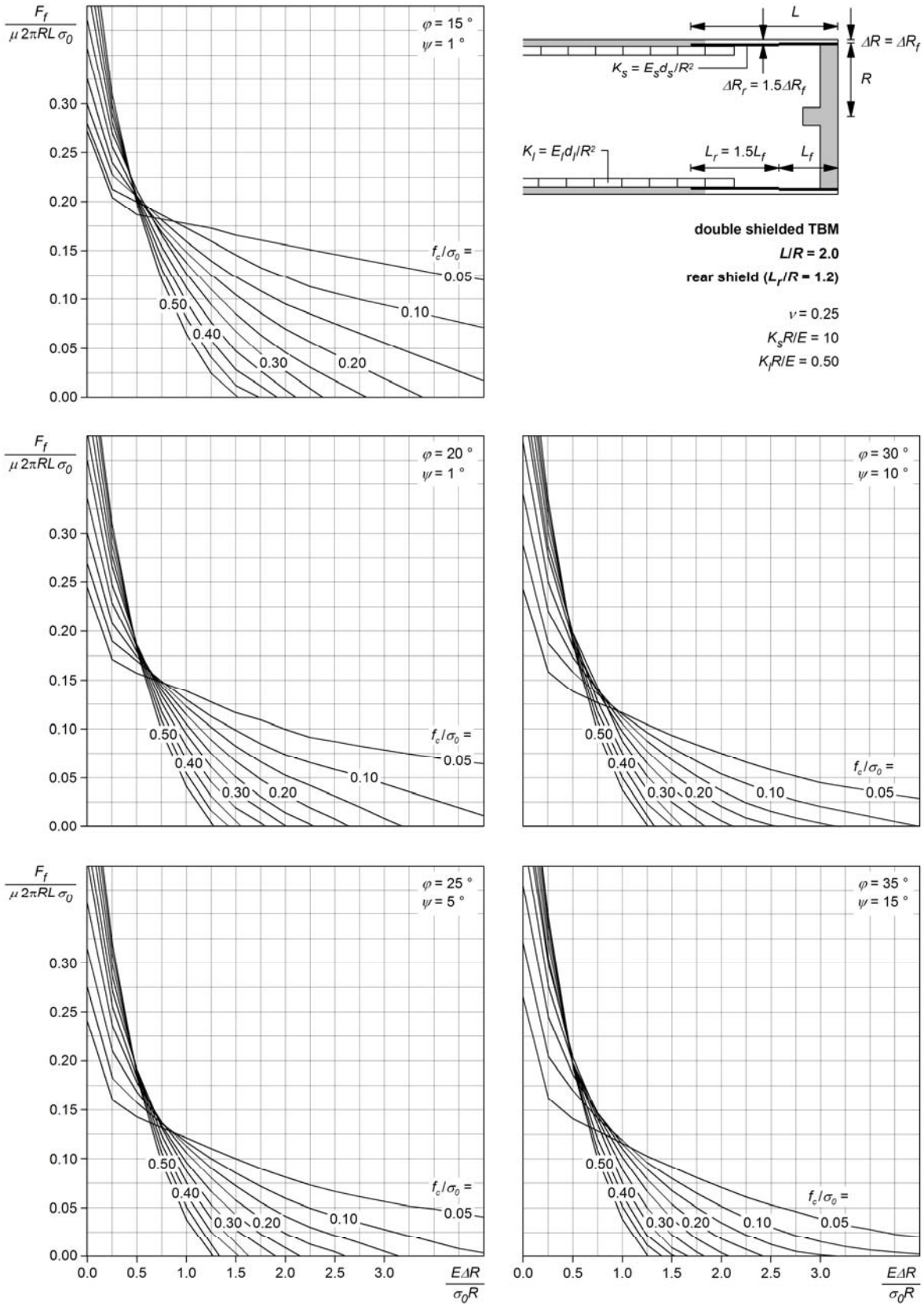

Figure II.5. Double shielded TBM: nomograms for L/R = 2.0 – rear shield.

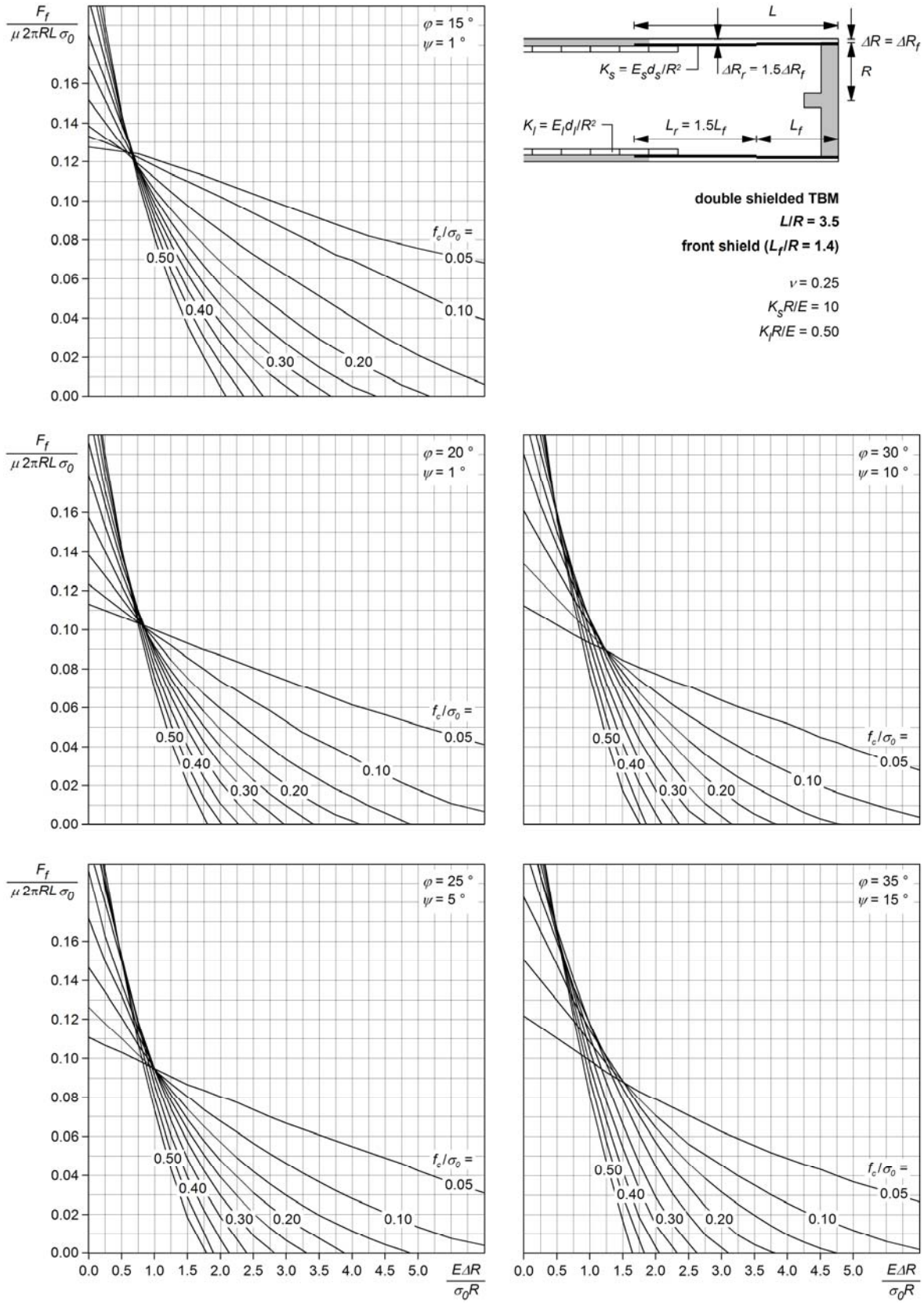

Figure II.6. Double shielded TBM: nomograms for L/R = 3.5 – front shield.

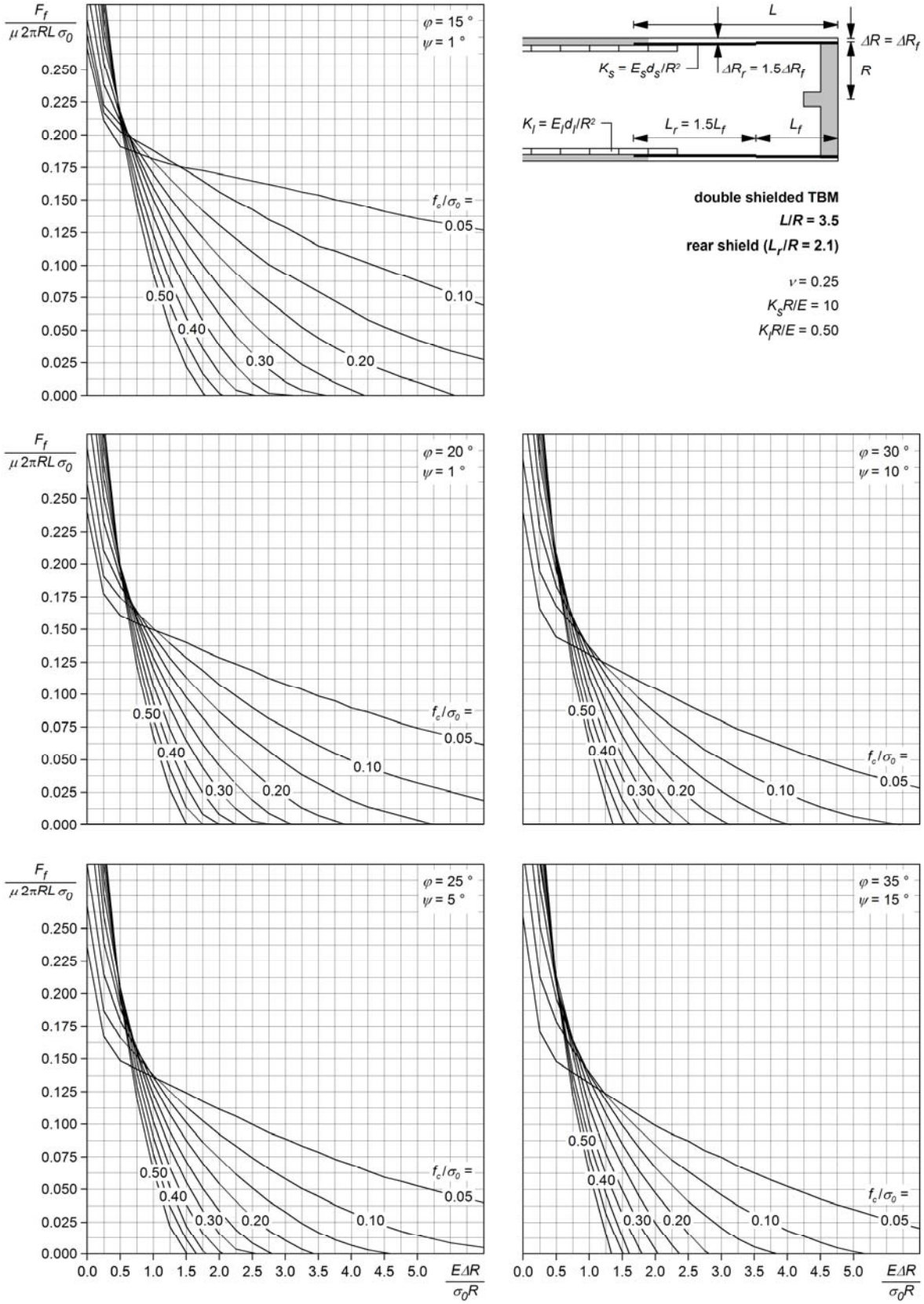

Figure II.7. Double shielded TBM: nomograms for L/R = 3.5 – rear shield.

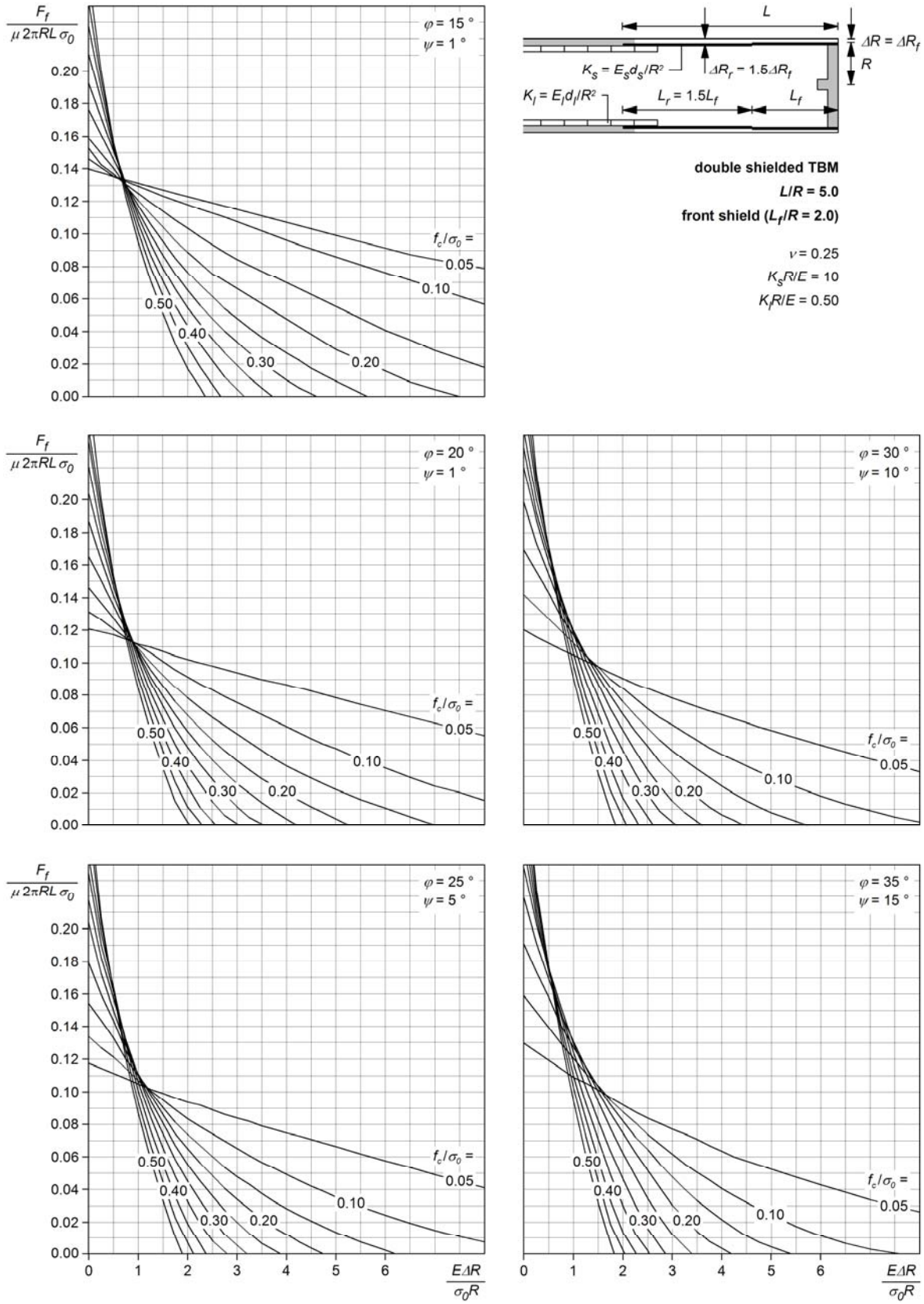

Figure II.8. Double shielded TBM: nomograms for L/R = 5.0 – front shield.

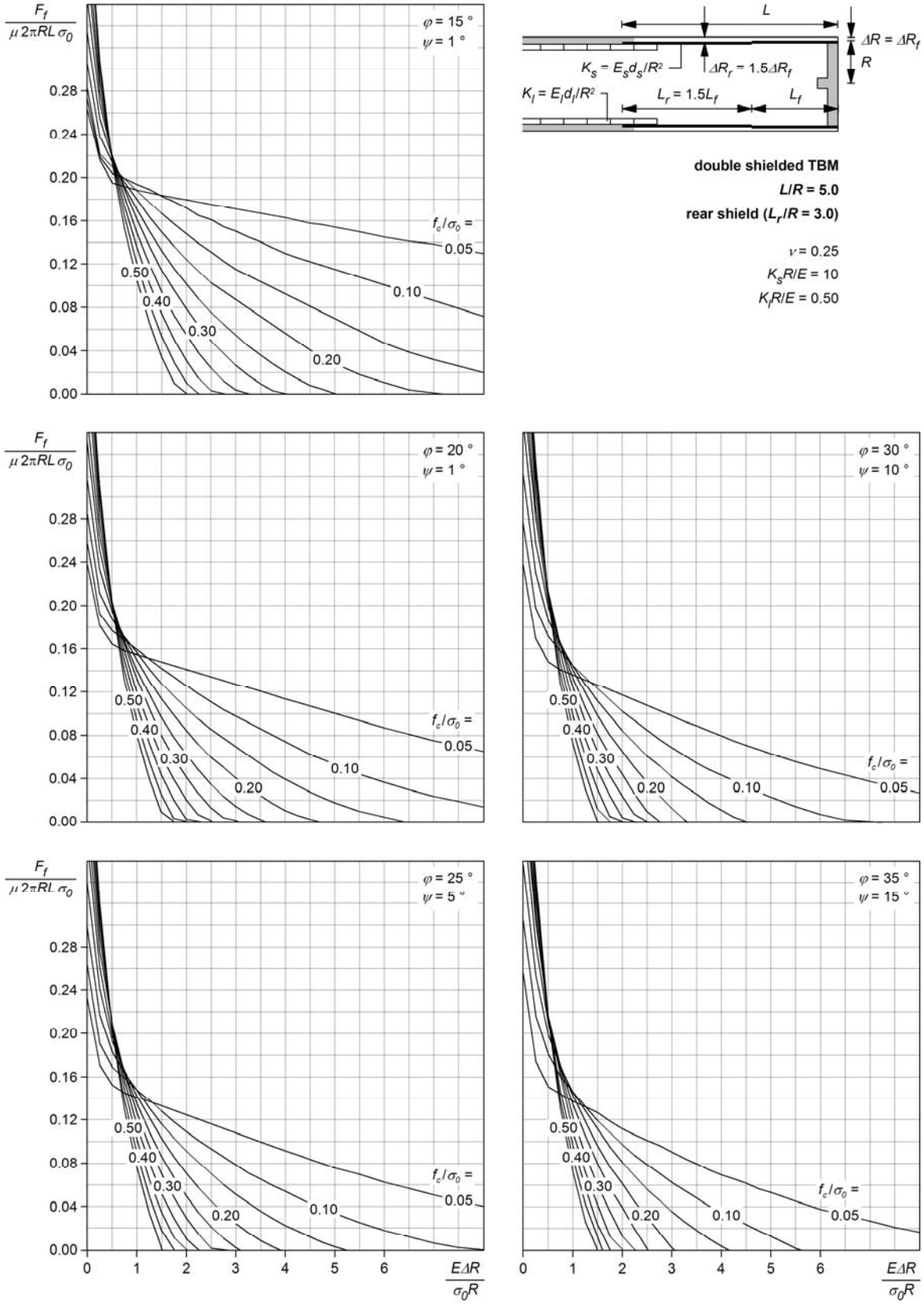

Figure II.9. Double shielded TBM: nomograms for L/R = 5.0 – rear shield.

III Nomograms for the assessment of the loading of segmental linings

Overview of the nomograms

Backfilling type	Normalized location of backfilling	Normalized lining stiffness	Nomogram
Pea gravel and mortar	$\lambda/R = 2$	$K_l R/E = 1$	Figure III.1
		$K_l R/E = 3$	Figure III.2
		$K_l R/E = 10$	Figure III.3
	$\lambda/R = 1$	$K_l R/E = 1$	Figure III.4
		$K_l R/E = 3$	Figure III.5
		$K_l R/E = 10$	Figure III.6
Grouting via shield tail	$\lambda/R = 0$	$K_l R/E = 1$	Figure III.7
		$K_l R/E = 3$	Figure III.8
		$K_l R/E = 10$	Figure III.9

Considered parameter ranges

Ground			
Poisson's ratio	ν	[-]	0.25
Angle of internal friction	φ	[°]	15–35
Dilatancy angle	ψ	[°]	max(1, $\varphi - 20$)
Normalized compressive strength	f_c/σ_0	[-]	0.10–0.50
TBM			
Normalized shield stiffness	$K_s R/E$	[-]	10
Normalized shield length	L/R	[-]	1
Backfilled segmental lining			
Normalized stiffness	$K_l R/E$	[-]	1, 3 or 10 (see above)
Normalized radial gap size	$\Delta R_l/\Delta R$	[-]	3
Normalized location of backfilling	λ/R	[-]	0, 1 or 2 (see above)

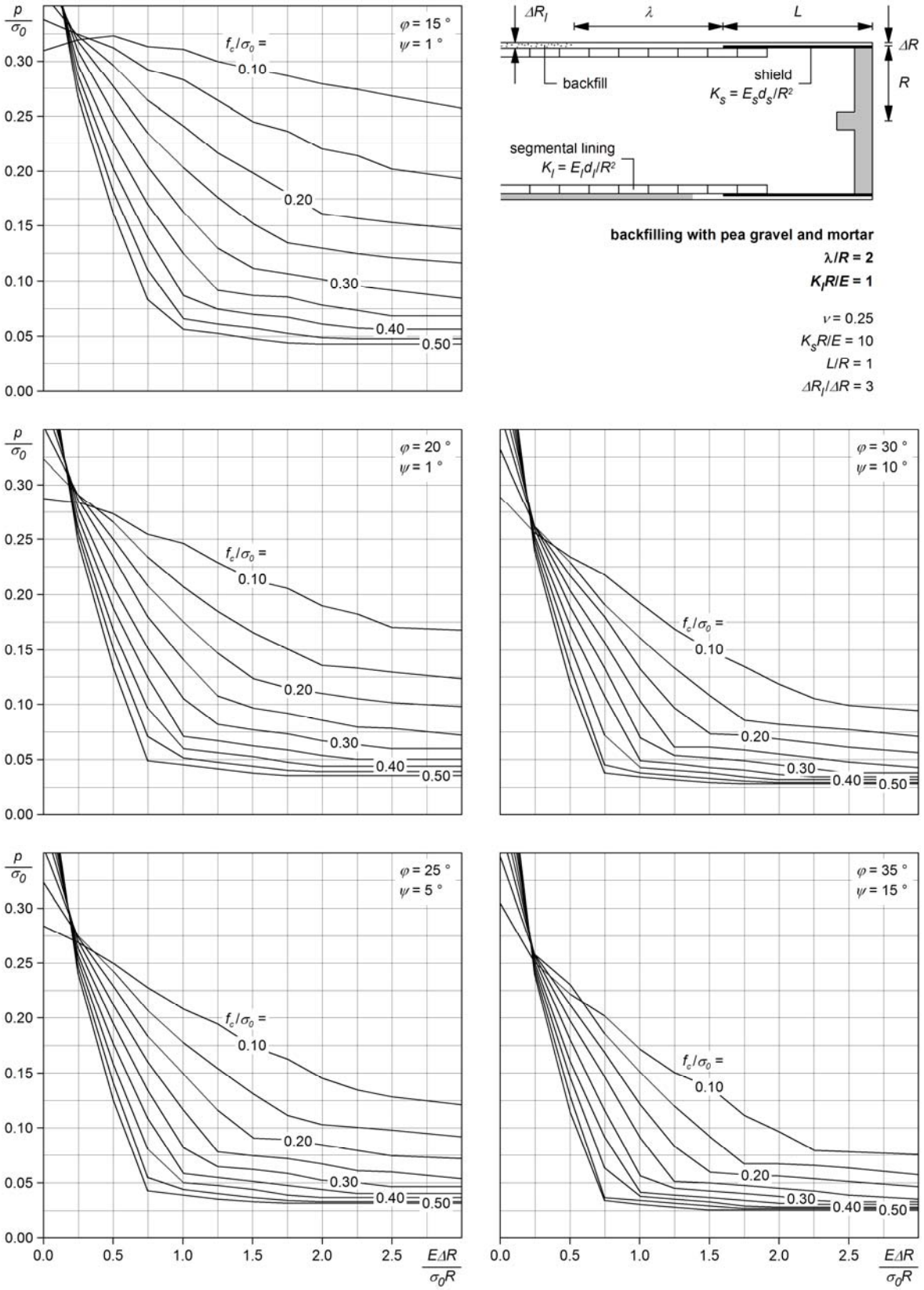

Figure III.1. Backfilling with pea gravel and mortar: nomograms for $\lambda/R = 2$ and $K_lR/E = 1$.

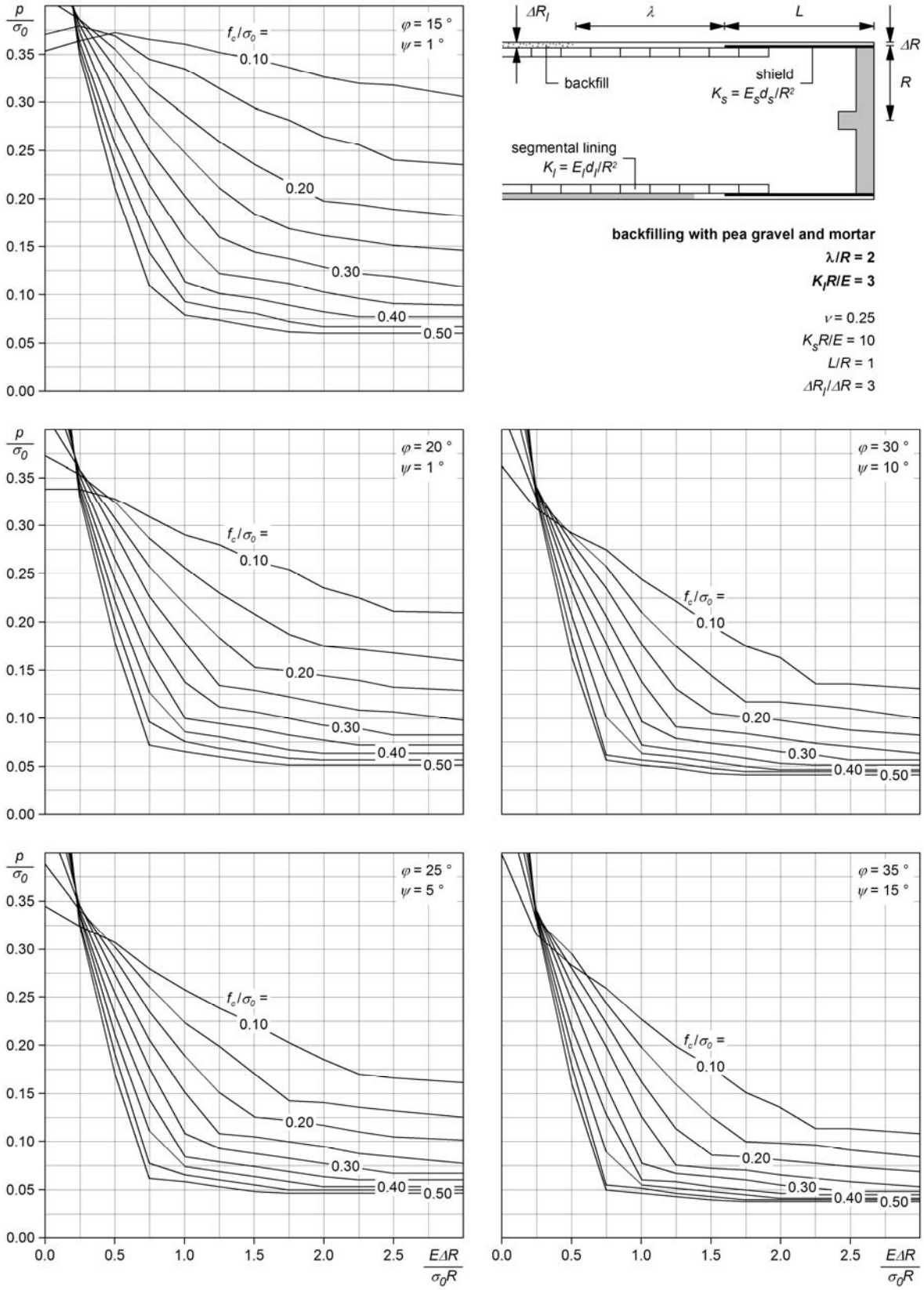

Figure III.2. Backfilling with pea gravel and mortar: nomograms for $\lambda/R = 2$ and $K_l R/E = 3$.

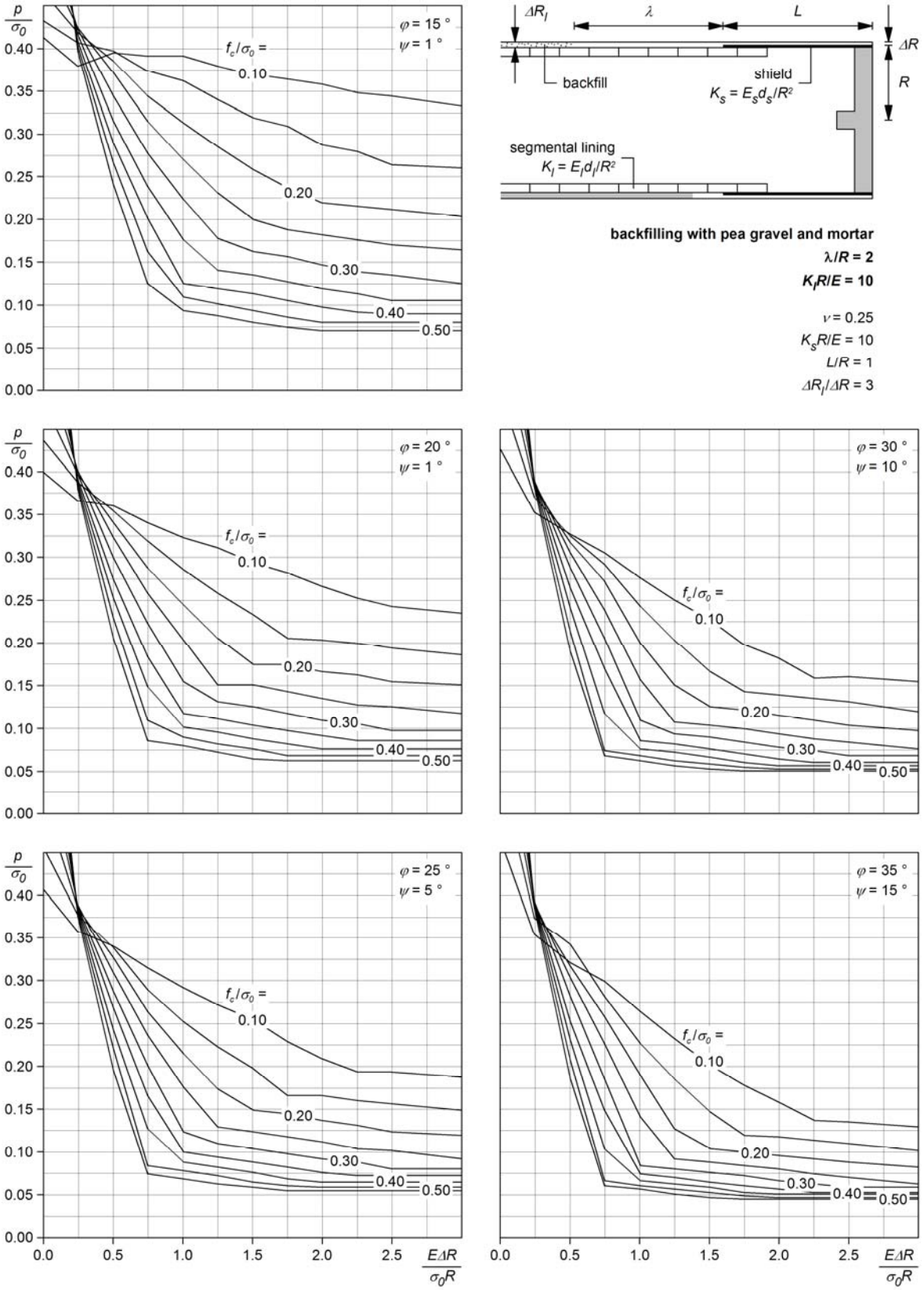

Figure III.3. Backfilling with pea gravel and mortar: nomograms for $\lambda/R = 2$ and $K_lR/E = 10$.

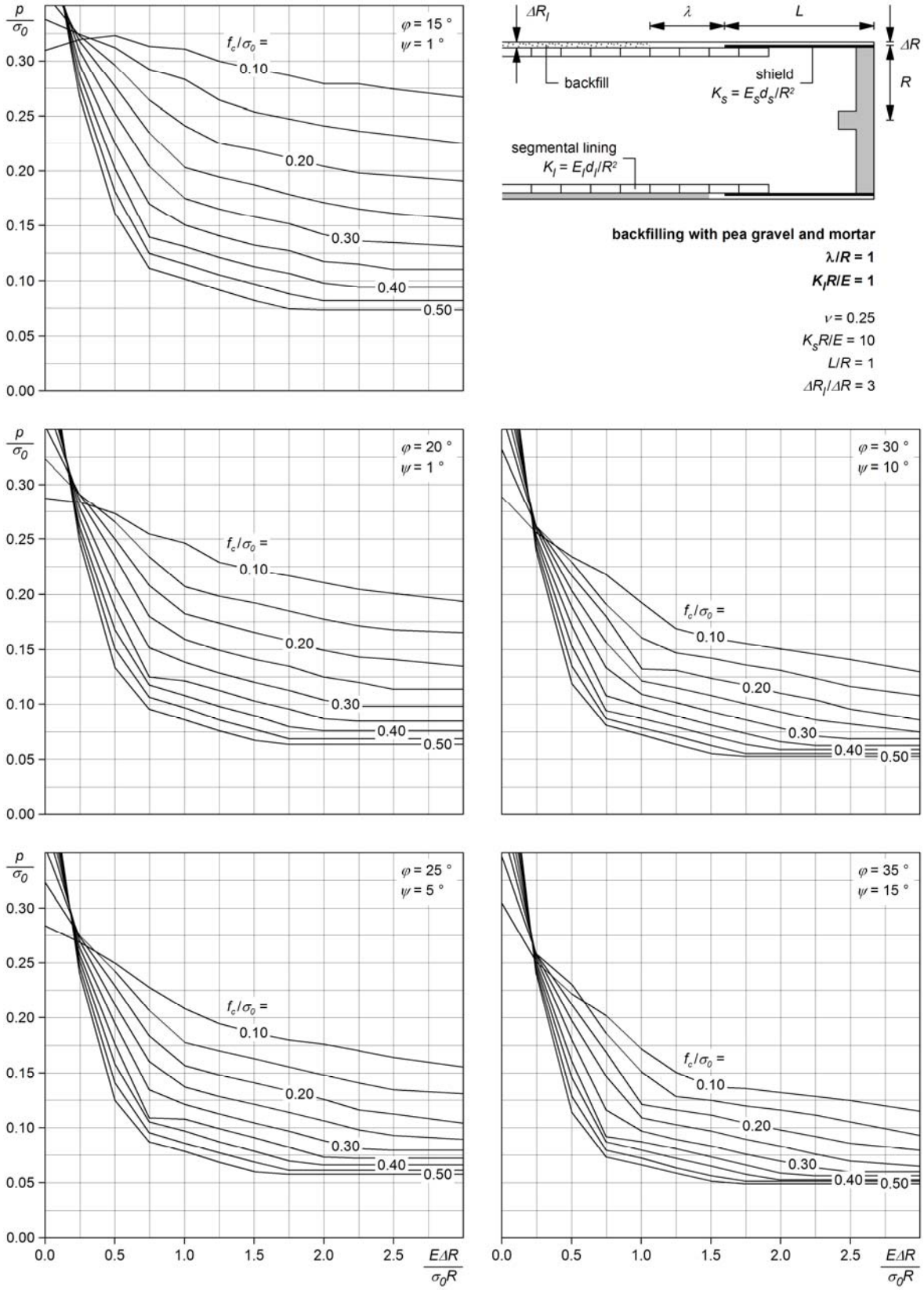

Figure III.4. Backfilling with pea gravel and mortar: nomograms for $\lambda/R = 1$ and $K_l R/E = 1$.

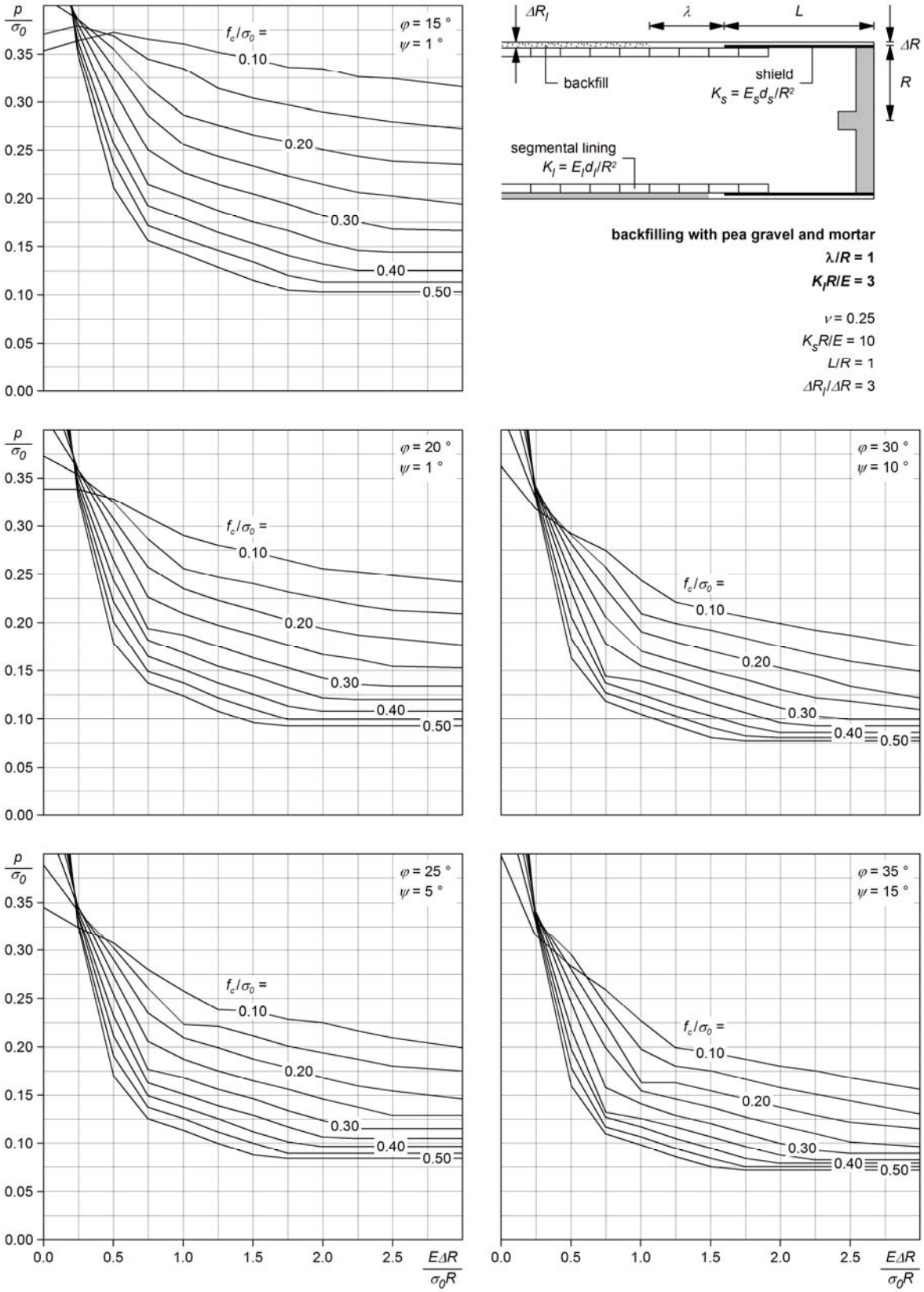

Figure III.5. Backfilling with pea gravel and mortar: nomograms for $\lambda/R = 1$ and $K_lR/E = 3$.

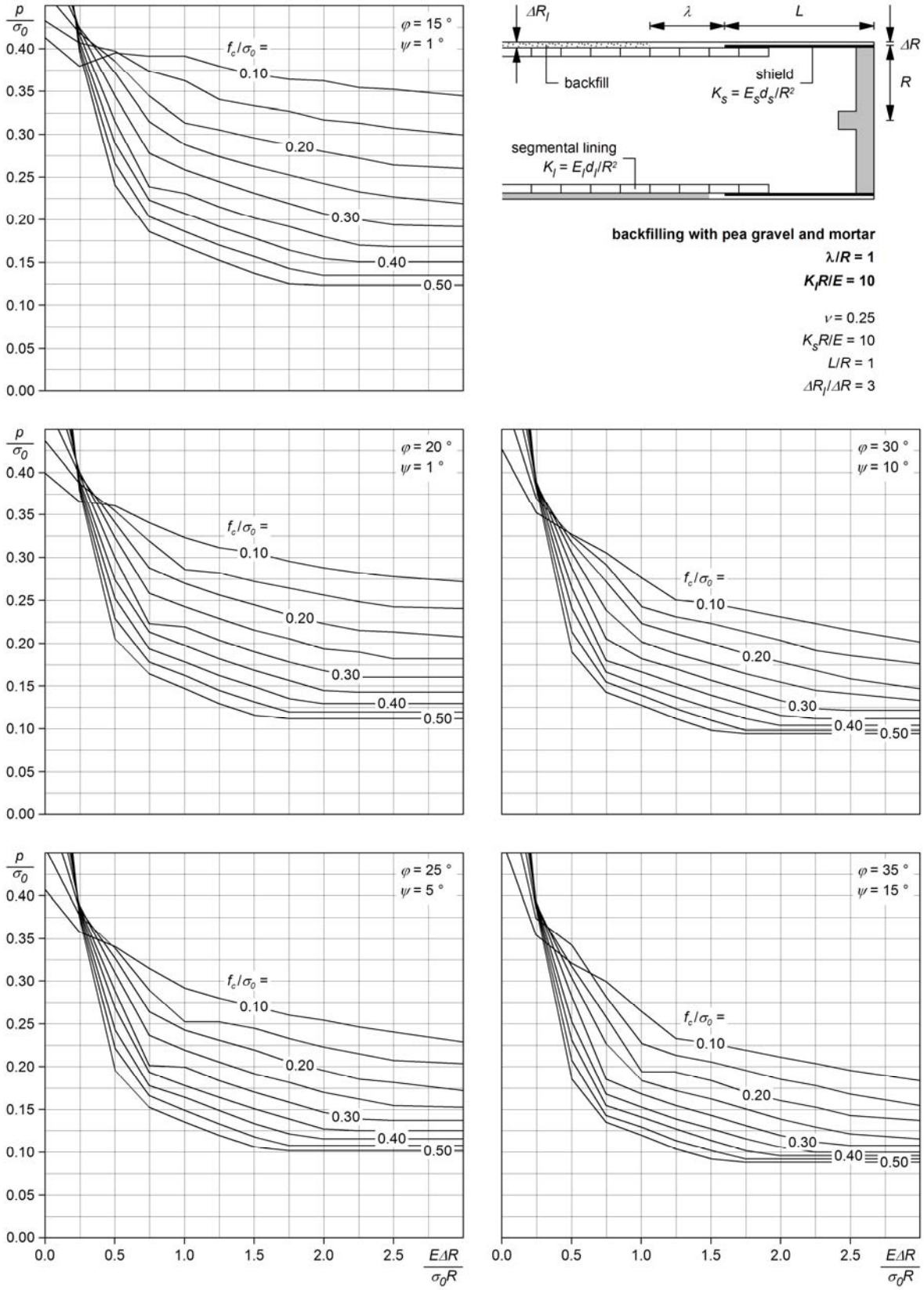

Figure III.6. Backfilling with pea gravel and mortar: nomograms for $\lambda/R = 1$ and $K_lR/E = 10$.

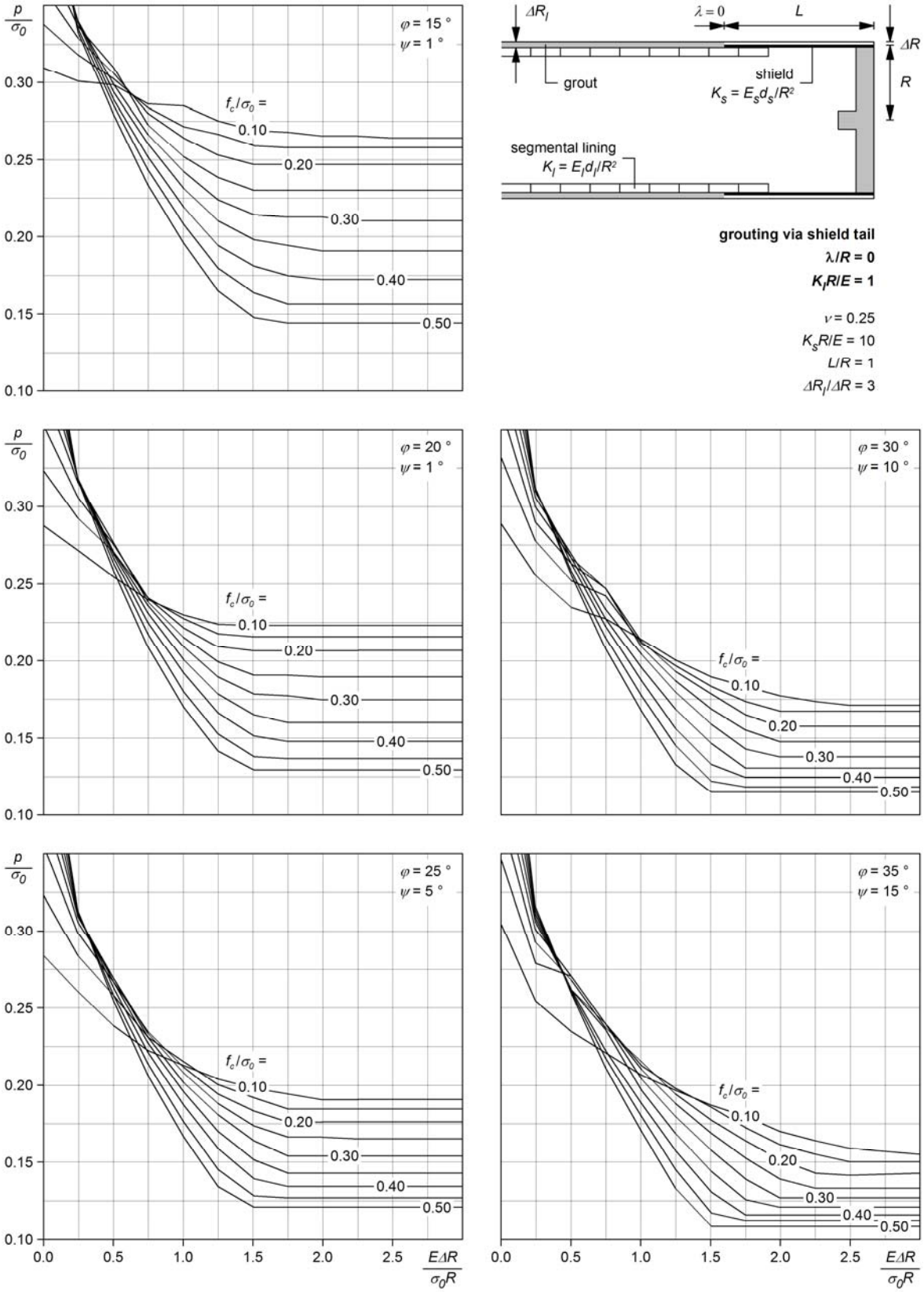

Figure III.7. Backfilling with grouting via the shield tail: nomograms for $\lambda/R = 0$ and $K_lR/E = 1$.

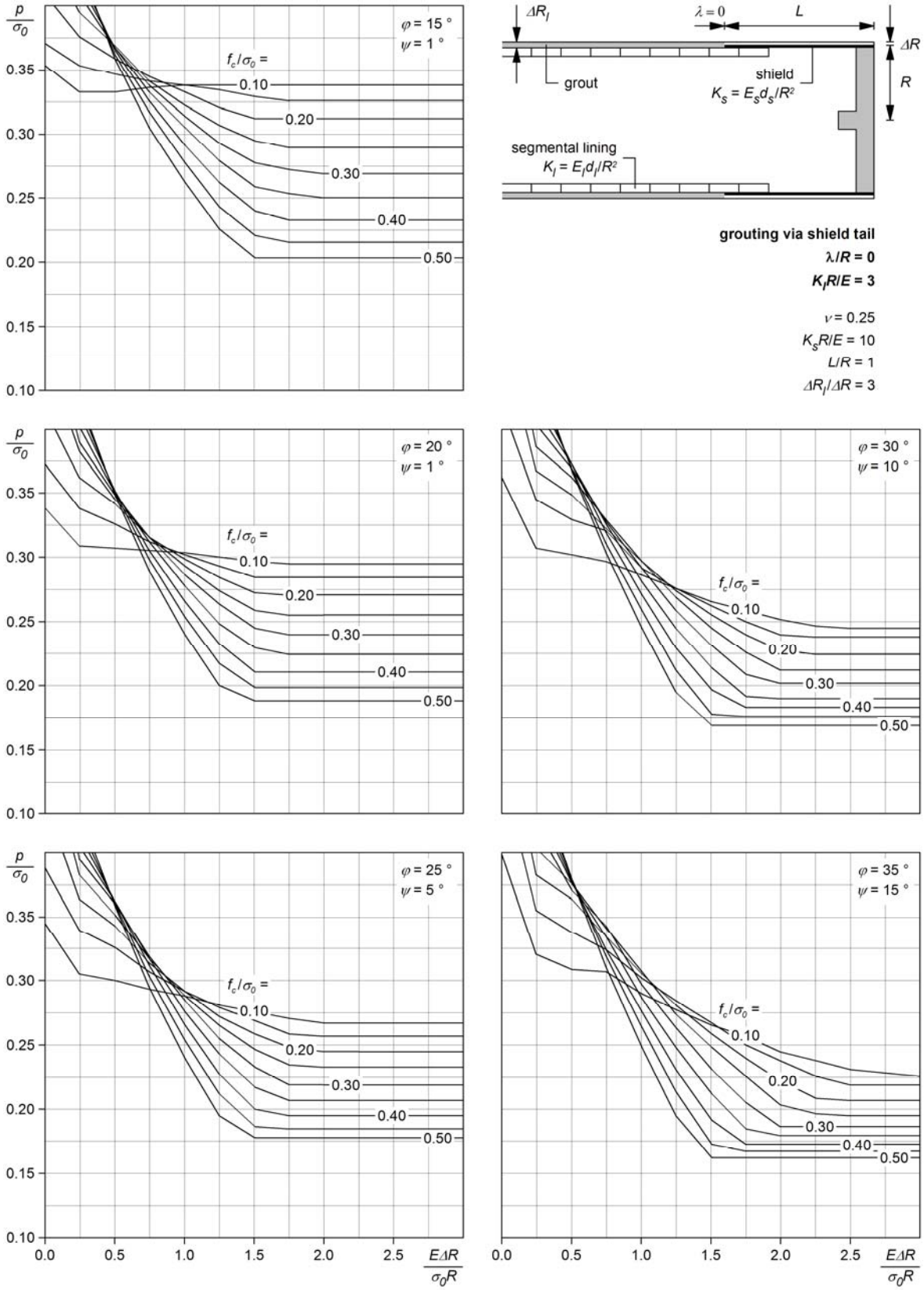

Figure III.8. Backfilling with grouting via the shield tail: nomograms for $\lambda/R = 0$ and $K_l R/E = 3$.

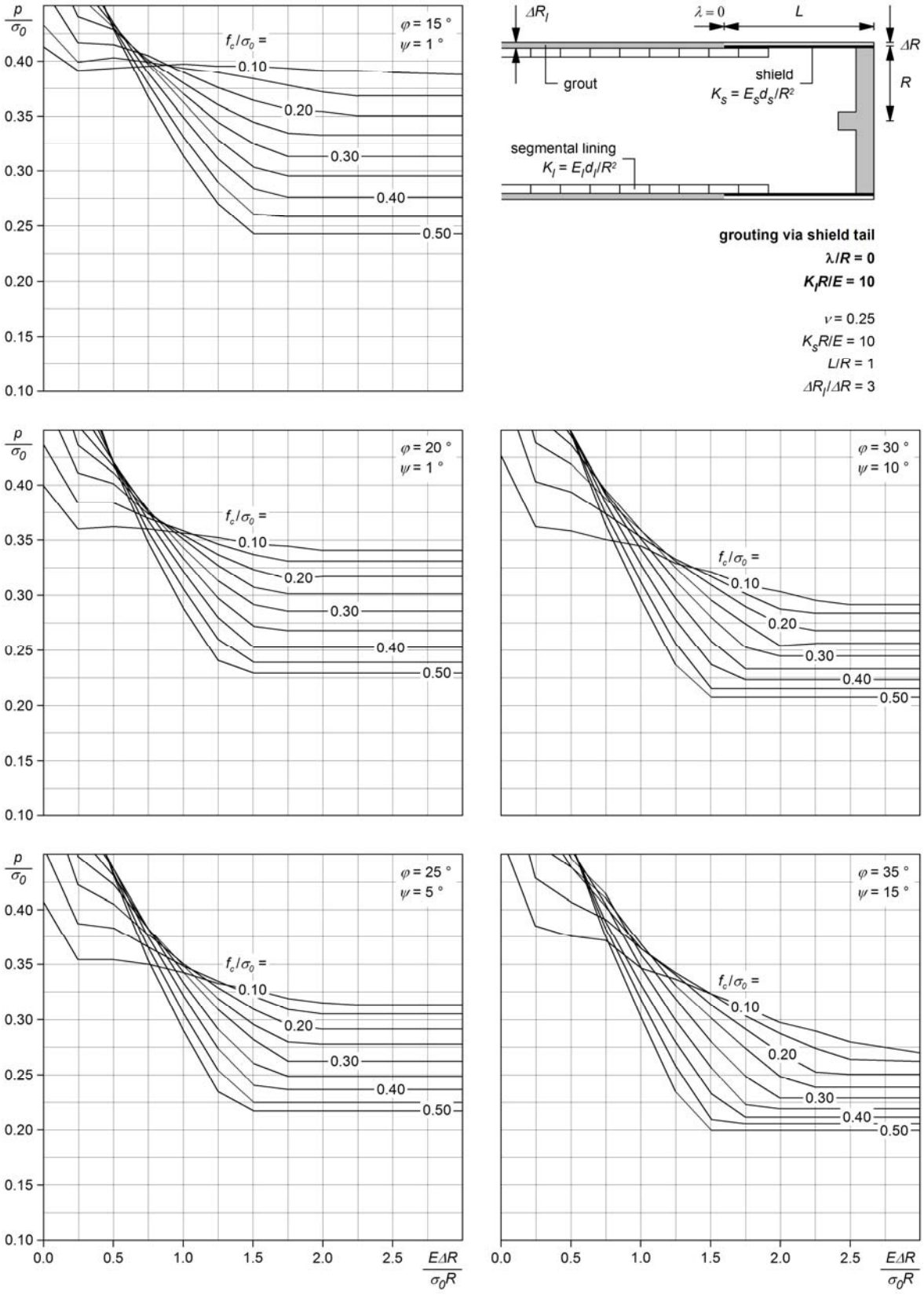

Figure III.9. Backfilling with grouting via the shield tail: nomograms for $\lambda/R = 0$ and $K_lR/E = 10$.

Notation

c	cohesion of the ground
c_g	compressibility of the rock or soil grains
c_w	compressibility of the water
D	boring diameter
d_1	thickness of the shotcrete layer
d_2	height of the deformable elements (yielding support)
d_b	thickness of the backfilling
d_l	thickness of the lining
d_s	thickness of the shield
e	extrusion rate of the core
E	Young's modulus of the ground
E_b	Young's modulus of the backfilling
E_k	entity of N^2 chart (the subscript k refers to the entity numbering)
E_l	Young's modulus of the lining
E_s	Young's modulus of the shield
E_{sc}	Young's modulus of the shotcrete
F	thrust force
F_b	boring thrust force
F_c	maximum cutter force
f_c	uniaxial compressive strength of the ground
$f_{c,l}$	uniaxial compressive strength of the lining
$f_{c,sc}$	uniaxial compressive strength of the shotcrete
F_f	thrust force needed for overcoming friction
F_f^*	normalized required thrust force (for overcoming friction)
F_g	thrust force that can be reacted by the grippers
$F_{g,i}$	installed gripper force
F_i	installed thrust force
F_r	required thrust force
G	ground
H	depth of cover
h	hydraulic head
h_0	initial hydraulic head
h_0^*	reduced initial hydraulic head
k	permeability of the ground
K_b	stiffness of the backfilling
K_c	composite stiffness (segmental lining and backfilling)
K_l	stiffness of the lining
K_s	stiffness of the shield
l	length of a critical geological zone
L	length of the shield
L_f	length of the front shield (double shielded TBM)
L_r	length of the rear shield (double shielded TBM)
N	number of physical and functional entities of a N^2 chart
n_c	number of cutters
p	ground pressure
P	penetration
p^*	normalized ground pressure
P_A, P_B	problems in the back-up area (zone A and zone B, respectively)
p_{max}	bearing capacity of the segmental lining
p_s	average ground pressure acting upon the shield
p_w	pore water pressure
Q	water flow
r	cutter head rotational speed
R	tunnel radius
$R_{F,T}$	reaction force
$R_{l,o}$	outer radius of the segmental lining
r_{max}	maximum possible cutter head rotational speed (TBM design)
r_{max}^*	maximum possible cutter head rotational speed (operational conditions)
$R_{s,i}$	inner radius of the shield

$R_{s,o}$	outer radius of the shield
s	step length (step-by-step calculations)
S_1, S_2	tunnel support (type, quantity, parameters, distance behind face) in the machine area and in the back-up area, respectively
SF	safety factor
t	time
T	torque
t_1	operational standstill time
t_2	standstill time due to jamming of the TBM
t_3	standstill time due to other problems
TBM	tunnel boring machine
t_{crit}	critical duration of a standstill
T_f	required torque for overcoming friction
T_g	torque that can be reacted by the grippers
T_i	installed torque
T_r	rolling resistance of the cutter head
t_s	difference between radius of the shield intrados and radius of the segmental lining extrados
u	radial displacement of the ground (at the tunnel boundary)
u_b	radial displacement of the bored profile before completion of the backfilling
u_e	extrusion of the core
u_l	radial displacement of the lining
v	advance rate
v_g	gross advance rate
v_n	net advance rate
x	radial co-ordinate (distance from the tunnel axis)
y	axial co-ordinate (distance behind the tunnel face)
y'	position of the tunnel face
#	number
{x-y}	interactions between the entities E_x and E_y of a N^2 chart
ΔD	overboring (facility, amount of the increase of the boring diameter D)
ΔD_l	annular gap (in diameter)
ΔD_s	overcut (in diameter)
ΔR	difference between boring radius and radius of the shield extrados
ΔR_f	difference between boring radius and radius of the front shield extrados (double shielded TBM)
ΔR_l	difference between boring radius and radius of the lining extrados
ΔR_r	difference between boring radius and radius of the rear shield extrados (double shielded TBM)
α	utilization degree of the TBM
δ	ground deformation
γ	unit weight of the ground
γ_w	unit weight of the water
φ	angle of internal friction of the ground
λ	location (distance behind the shield) where backfilling is completed
λ^*	location (distance behind the shield) where the ground closes the gap around the segmental lining
μ	shield skin friction coefficient
ν	Poisson's ratio of the ground
σ	stress
σ_0	initial stress
σ_l	ground pressure acting upon the tunnel support
$\sigma_{l,max}$	maximum possible ground pressure acting upon the tunnel support (bearing capacity)
σ_{TBM}	ground pressure acting upon the TBM (cutter head or shield)
τ_{TBM}	shear stress acting upon the TBM (cutter head or shield)
ψ	dilatancy angle of the ground

References

Amberg, F., 2008. Personal communication. Amberg Engineering AG, February 2008.

Amberg, R., 1992. Economic aspects when building tunnels with major overburden. Tunnel 92 (3), 120–124.

Anagnostou, G., 1992. Untersuchungen zur Statik des Tunnelbaus in quellfähigem Gebirge. Veröffentlichungen des Instituts für Geotechnik (IGT) der ETH Zürich, Band 201 – ETH-Dissertation Nr. 9553, vdf Verlag der Fachvereine an den schweizerischen Hochschulen und Techniken AG Zürich.

Anagnostou, G., 1993. Modelling seepage flow during tunnel excavation. Safety and environmental issues in rock engineering, Eurock '93, Lisbon, Volume 1, 3–9, A.A.Balkema Rotterdam Brookfield.

Anagnostou, G., 1995. The influence of tunnel excavation on the hydraulic head. International Journal for Numerical and Analytical Methods in Geomechanics 19 (10), 725–746.

Anagnostou, G., 2007a. Continuous tunnel excavation in a poro-elastoplastic medium. Tenth international symposium on numerical models in geomechanics, NUMOG X, Rhodes, 183–188, Taylor & Francis Group London.

Anagnostou, G., 2007b. The one-step solution of the advancing tunnel heading problem. ECCOMAS Thematic conference on computational methods in tunnelling, EURO:TUN 2007, Vienna, 90, Vienna University of Technology.

Anagnostou, G., 2007c. Practical consequences of the time-dependency of ground behaviour in tunnelling. Rapid Excavation and Tunnelling Conference, Toronto, 225–265, SME Inc. Littleton.

Anagnostou, G., 2009a. The effect of advance-drainage on the short-term behaviour of squeezing rocks in tunnelling. International symposium on computational geomechanics (COMGEO I), Juan-les-Pins, 668–679, International Centre for Computational Engineering Rhodes.

Anagnostou, G., 2009b. Pore pressure effects in tunnelling through squeezing ground. ECCOMAS Thematic conference on computational methods in tunnelling, EURO:TUN 2009, Bochum, 361–368, Aedificatio Publishers Freiburg.

Anagnostou, G., Cantieni, L., 2007. Design and analysis of yielding support in squeezing ground. The second half century of rock mechanics, 11th Congress of the International Society for Rock Mechanics (ISRM), Lisbon, Volume 2, 829–832, Taylor & Francis Group London.

Anagnostou, G., Cantieni, L., Nicola, A., Ramoni, M., 2010a. Face stability assessment for the Lake Mead No 3 Intake Tunnel. Tunnel vision towards 2020, ITA World Tunnel Congress 2010, Vancouver, TAC Vancouver.

Anagnostou, G., Cantieni, L., Nicola, A., Ramoni, M., 2010b. Lake Mead No 3 Intake Tunnel – geotechnical aspects of TBM operation. Tunnelling: sustainable infrastructure, North American Tunnelling Conference, Portland, 125–135, SME Inc. Littleton.

Anagnostou, G., Kovári, K., 1993. Significant parameters in elastoplastic analysis of underground openings. Journal of Geotechnical Engineering 119 (3), 401–419.

Anagnostou, G., Kovári, K., 2005. Tunnelling through geological fault zones. International symposium on design, construction and operation of long tunnels, Taipei, Volume 1, 509–520, Chinese Taipei Tunnelling Association.

Anagnostou, G., Pimentel, E., Ramoni, M., Schürch, R., 2010c. Assessment of the major geotechnical risks. El Teniente New Access Tunnels, Report 102401 – February 1, 2010, unpublished.

Anagnostou, G., Ramoni, M., 2007. Untersuchungen zum TBM-Vortrieb südlich der Chiera Synform. AlpTransit Gotthard, Gotthard Basistunnel, Teilabschnitt Faido, Bericht 071101 – 20. Dezember 2007, Professur für Untertagbau, Institut für Geotechnik (IGT), ETH Zürich, unveröffentlicht.

Anagnostou, G., Ramoni, M., 2009. Untersuchungen zum Gefährdungsbild "Verklemmen des Schildes in druckhaftem Gebirge" (NBS km 42+000–43+500). Bosslertunnel, Neubaustrecke Wendlingen – Ulm, Deutsche Bahn AG, Bericht 091901 – 15. September 2009 (herstellt im Auftrag der Herrenknecht AG, Schwanau), Professur für Untertagbau, Institut für Geotechnik (IGT), ETH Zürich, unveröffentlicht.

Andraskay, E., 1986. The significance of geological data for mechanical drivage and selection of the drilling diameter. Tunnel 86 (2), 122–130.

Anonymus, 1993. Streckenvortriebsmaschine hinterschneidet das Gestein. Glückauf 129 (10), 753.

Babendererde, S., 1986. Extruded concrete lining. International congress on large underground openings, Florence, Volume 1, 607–611, SIG Milan.

Babendererde, S., 1989. Fortschritte beim mechanischen Vortrieb grosser Tunnelquerschnitte. Eisenbahntechnische Rundschau 38 (10), 619–623.

Babendererde, S., Babendererde, J.O., 2001. Extruded concrete lining – the future lining technology for industrialized tunnelling. Rapid Excavation and Tunnelling Conference, San Diego, 679–685, SME Inc. Littleton.

Barla, G., 2001. Tunnelling under squeezing rock conditions. Eurosummer-School in Tunnel Mechanics, Innsbruck, 169–268, Logos Verlag Berlin.

Barla, G., 2004. Corso di meccanica delle rocce 2. Materiale per le lezioni, Dipartimento di ingegneria strutturale e geotecnica, Politecnico di Torino.

Barla, G., Pelizza, S., 2000. TBM tunnelling in difficult ground conditions. GeoEng2000 – International conference on geotechnical & geological engineering, Melbourne, Volume 1, 1471–1489, Technomic Publishing Company Inc. Lancaster.

Baumann, L., Zischinsky, U., 1993. Neue Löse- und Ausbautechniken zur maschinellen "Fertigung" von Tunneln in druckhaftem Fels. Innovationen im unterirdischen Bauen, STUVA-Tagung '93, Hamburg, Forschung+Praxis 35, 64–69, Alba Fachverlag GmbH + Co. KG Düsseldorf.

Beckmann, U., 1984. Tunnelbau im Untertagebau – Tunnelbohrmaschinen und ihr Einsatz im Festgestein. Taschenbuch für den Tunnelbau 1985, 57–101, VGE Verlag Glückauf GmbH Essen.

Bergmeister, K., 2007. Brenner Base Tunnel: link between Munich and Verona. Tunnel 2007 (1), 9–20.

Billig, B., Ebsen, B., Gipperich, C., Schaab, A., Wulff, M., 2007a. DeCo Grout – innovative grout to cope with rock deformations in TBM tunnelling. Underground space – the 4th dimension of metropolises, ITA World Tunnel Congress 2007, Prague, Volume 2, 1487–1492, Taylor & Francis Group London.

Billig, B., Gipperich, C., Wulff, M., Schaab, A., 2007b. Ausbausysteme für den maschinellen Tunnelbau in druckhaftem Gebirge. Taschenbuch für den Tunnelbau 2008, 223–262, VGE Verlag GmbH Essen.

Böckli, O., 2008. Teilabschnitt Faido – bisherige Erfahrungen mit dem TBM-Vortrieb. FGU-Fachtagung für Untertagbau, Swiss Tunnel Congress 2008, Luzern, D0229, 49–58, SIA Zürich.

Boissonnas, Y., 2008. Gotthard Base Tunnel – experience of a TBM excavation with large overburden. Building underground for the future, AFTES International Congress Monaco, Montecarlo, 247–250, Edition specifique Limonest.

Brunar, G., Powondra, F., 1985. Nachgiebiger Tübbingausbau mit Meypo-Stauchelementen. Felsbau 3 (4), 225–229.

Burger, W., 2009. Personal communication. Herrenknecht AG, March 2009.

Caldarella, A., 1986. La galleria "Santomarco" della nuova linea Paola – Cosenza. Congresso internazionale su grandi opere sotterranee, Firenze, Volume 1, 93–107, Dipartimento di ingegneria civile, Università di Firenze.

Cantieni, L., Anagnostou, G., 2007. On the variability of squeezing in tunnelling. The second half century of rock mechanics, 11th Congress of the International Society for Rock Mechanics (ISRM), Lisbon, Volume 2, 983–986, Taylor & Francis Group London.

Cantieni, L., Anagnostou, G., 2009a. The effect of the stress path on squeezing behaviour in tunnelling. Rock Mechanics and Rock Engineering 42 (2), 289–318.

Cantieni, L., Anagnostou, G., 2009b. The interaction between yielding supports and squeezing ground. Tunnelling and Underground Space Technology 24 (3), 309–322.

Cantieni, L., Anagnostou, G., 2010. On a paradox of elasto-plastic tunnel analysis. Rock Mechanics and Rock Engineering, doi: 10.1007/s00603-010-0126-1 (available online).

Concilia, M., Grandori, R., 2004. New Viola Water Transfer Tunnel. Mechanized tunnelling: challenging case histories, International congress, Turin, 27–34, GEAM Turin.

Croci, G., 1986. Progettazione, costruzione e sperimentazione del rivestimento prefabbricato della galleria Santomarco nella zona interessata da terreni estremamente spingenti con ricoprimento di circa 1000 metri. Congresso internazionale su grandi opere sotterranee, Firenze, Volume 1, 137–146, Dipartimento di ingegneria civile, Università di Firenze.

Dowden, P.B., Cass, D.T., 1991. Shielded TBM's – matching the machine to the job. Rapid Excavation and Tunnelling Conference, Seattle, 787–805, SME Inc. Littleton.

Downing, B., Carter, T., Beddoes, R., Moss, A., Dowden, P., 2007. Use of tunnel boring machines at depth: extending the limits. Rapid Excavation and Tunnelling Conference, Toronto, 1131–1142, SME Inc. Littleton.

Einstein, H.H., Bobet, A., 1997. Mechanized tunnelling in squeezing rock – from basic thoughts to continuous tunnelling. Tunnels for people, ITA World Tunnel Congress '97, Vienna, Volume 2, 619–632, A.A.Balkema Rotterdam Brookfield.

Eistert, M., 1982. Maschinelles Auffahren von horizontalen Tunnelstrecken grösseren Durchmessers mit Tunnelbohrmaschinen an Beispielen in Frankreich, Guatemala und der Schweiz. Felsmechanik: Kavernen und Druckschächte, ISRM Symposium, Aachen, Band 2, 779–787, A.A.Balkema Rotterdam.

Farrokh, E., Rostami, J., 2009. Effect of adverse geological condition on TBM operation in Ghomroud Tunnel Conveyance Project. Tunnelling and Underground Space Technology 24 (4), 436–446.

Floria, V., Fidelibus, C., Repetto, L., Russo, G., 2008. Drainage and related increase of short-term strength of low permeability rock mass. Building underground for the future, AFTES International Congress Monaco, Montecarlo, 281–284, Edition specifique Limonest.

Flury, S., Priller, A., 2008. Gotthard Base Tunnel – Part-Section Faido. Tunnel 2008 (4), 47–51.

Foster, J.R., 1997. Characterisation of tunnel boring machines. Workshop "The Gibraltar Crossing", Tarifa, ITA Bron Cedex.

Gamper, C., Knapp, M., Fiest, T., 2009. Jenbach Tunnel – a shallow hydroshield drive. Geomechanics and Tunnelling 2 (5), 494–501.

Gehring, K., Kogler, P., 1997. Mechanized tunnelling: where it stands and where it has to proceed from a manufacturers view point. Tunnels for people, ITA World Tunnel Congress '97, Vienna, Volume 2, 651–664, A.A.Balkema Rotterdam Brookfield.

Gehring, K.H., 1996. Design criteria for TBM's with respect to real rock pressure. Tunnel boring machines – trends in design & construction of mechanized tunnelling, International lecture series TBM tunnelling trends, Hagenberg, 43–53, A.A.Balkema Rotterdam Brookfield.

Gerstner, R., Vigl, A., 1996. Geologe und Bautechniker im Umgang mit dem geologisch bedingten Baurisiko. Felsbau 14 (6), 337–341.

Gollegger, J., Priller, A., Rausch, M., 2009. The use of open tunnel boring machines in squeezing rock in the Gotthard Base Tunnel. Geomechanics and Tunnelling 2 (5), 591–600.

Grandori, R., 1993. Scavo meccanizzato a piena sezione di gallerie di grande diametro. Opere in sotterraneo, XVIII Convegno nazionale di geotecnica, Rimini, Volume 2, 243–252, Associazione Geotecnica Italiana Roma.

Grandori, R., 1996. La TBM universale alle soglie del 2000 – aspetti tecnici ed imprenditoriali. Gallerie e grandi opere sotterranee 23 (50), 38–48.

Grandori, R., 2001. Manila Aqueduct (Philippines) – the construction of the Umiray – Angat Tunnel Project – a success of organisation and technology against a unique combination of the most adverse conditions ever encountered in tunnelling. Rapid Excavation and Tunnelling Conference, San Diego, 777–790, SME Inc. Littleton.

Grandori, R., Antonini, F., 1994. Double shield TBM excavation technique – recent experiences and future development. Felsbau 12 (6), 490–494.

Grandori, R., Jäger, M., Antonini, F., Vigl, L., 1995. Evinos – Mornos Tunnel (Greece) – Construction of a 30 km long hydraulic tunnel in less than three years under the most adverse geological conditions. Rapid Excavation and Tunnelling Conference, San Francisco, 747–767, SME Inc. Littleton.

Graziani, A., Capata, A., Romualdi, P., 2007. Analysis of rock-TBM-lining interaction in squeezing rock. Felsbau magazin 25 (6), 23–31.

Gütter, W., 2007. Weiterentwicklung einer 10-m-Doppelschild-TBM für stark druckhaftes Gebirge. Felsbau magazin 25 (6), 32–37.

Hartwig, S., 1995. TBM-Konstruktionsüberlegungen zum NEAT-Projekt. TBM know-how zum Projekt NEAT, The Robbins Company Symposium, Luzern, The Robbins Company Kent.

Hentschel, H., 1997. Breakthrough at the Vereina Tunnel. Tunnel 97 (4), 10–22.

Hentschel, H., 2000. TBM with innovative support concept. Tunnel 2000 (2), 20–28.

Herrenknecht, 2003. Technical documentation. Herrenknecht AG, Schwanau (Germany).

Herrenknecht, M., 2010. Tunnelling through squeezing rock with TBM. Brenner Base Tunnel and Access Routes, BrennerCongress 2010, Innsbruck, 45–54, Ernst & Sohn Verlag für Architektur und technische Wissenschaften GmbH Berlin.

Herrenknecht, M., Böckli, O., Bäppler, K., 2009. Gotthard Base Tunnel, Section Faido, Previous experience with the use of the TBM. Rapid Excavation and Tunnelling Conference, Las Vegas, 1182–1205, SME Inc. Littleton.

Herrenknecht, M., Rehm, U., 2007. Mechanized tunnelling for long distance tunnels under heterogeneous rock conditions. Brenner Basistunnel und Zulaufstrecken, Internationales Symposium BBT 2007, Innsbruck, 175–182, Innsbruck University Press.

Herzog, M., 1985. Die Pressenkräfte bei Schildvortrieb und Rohrverpressung im Lockergestein. Baumaschine + Bautechnik 32 (6), 236–238.

Hoek, E., 2001. Big tunnels in bad rock. Journal of Geotechnical and Geoenvironmental Engineering 127 (9), 726–740.

Hoek, E., Marinos, P., 2000a. Predicting squeeze – Part one: estimating rock mass strength. Tunnels & Tunnelling International 32 (11), 45–51.

Hoek, E., Marinos, P., 2000b. Predicting squeeze – Part two: estimating tunnel squeezing problems. Tunnels & Tunnelling International 32 (12), 33–36.

ITA, 2003. Long traffic tunnels at great depth. ITA Working group N° 17 "Long tunnels at great depth", ITA Lausanne.

Iwasaki, T., Miura, K., Kawakita, M., Yamada, T., Sano, N., 1999. A long tunnel project by TBM method. Challenges for the 21st century, ITA World Tunnel Congress '99, Oslo, Volume 2, 857–863, A.A.Balkema Rotterdam Brookfield.

John, M., Schneider, E., 2007. TBM tunnelling in squeezing rock. Felsbau magazin 25 (6), 12.

Klonsdorf, G., Schaser, F., 1991. Baudurchführung des Freudensteintunnels – bergmännische und offene Bauweisen. Der Freudensteintunnel, DB Neubaustrecke Mannheim – Stuttgart, Ingenieurbauwerke ibw Nr. 7 12/91, 119–171, Elite Trust Vaduz.

Korbin, G.E., 1998. Claims and tunnel boring machines: contributing factors and lessons learned. Engineering Geology – a global view from the Pacific Rim, 8th International congress of the International Association for Engineering Geology and the Environment (IAEG), Vancouver, Volume 5, 3523–3528, A.A.Balkema Rotterdam Brookfield.

Kovári, K., 1977. The elasto-plastic analysis in the design practice of underground openings. Finite elements in geomechanics, 377–412, John Wiley & Sons Ltd London.

Kovári, K., 1986a. Rock deformation problems when using full-facing cutting equipment in rock, Part 1. Tunnel 86 (3), 236–244.

Kovári, K., 1986b. Rock deformation problems when using full-facing cutting equipment in rock, Part 2. Tunnel 86 (4), 289–298.

Kovári, K., 1994. On the existence of the NATM: erroneous concepts behind the New Austrian Tunnelling Method. Tunnel 94 (1), 16–25.

Kovári, K., 1995. The two Base Tunnels of the Alptransit Project: Lötschberg and Gotthard. Worldwide innovations in tunnelling, STUVA-Tagung '95, Stuttgart, Forschung+Praxis 36, 23–29, Alba Fachverlag GmbH + Co. KG Düsseldorf.

Kovári, K., 1998. Tunnelling in squeezing rock. Tunnel 98 (5), 12–31.

Kovári, K., 2005. Method and device for stabilizing a cavity excavated in underground construction. US Patent 20050191138.

Kovári, K., Anagnostou, G., 1995. The ground response curve in tunnelling through short fault zones. 8th Congress of the International Society for Rock Mechanics (ISRM), Tokyo, Volume 2, 611–614, A.A. Balkema Rotterdam.

Kovári, K., Ramoni, M., 2008. Jamming of shield – numerical investigations. Uluabat Power Tunnel (Turkey) – TBM drive, Report – January 25, 2008, unpublished.

Kovári, K., Staus, J., 1996. Basic considerations on tunnelling in squeezing ground. Rock Mechanics and Rock Engineering 29 (4), 203–210.

Lano, R.J., 1990. The N2 Chart. System and software requirements engineering, 244–271, IEEE Computer Society Press Washington.

Lavdas, N., 2010. Einsatzgrenzen vom Tübbingausbau beim TBM-Vortrieb in druckhaftem Gebirge. Master thesis, ETH Zurich.

Lenk, K., 1931. Der Ausgleich des Gebirgsdruckes in grossen Teufen beim Berg- und Tunnelbau. Springer-Verlag Berlin.

Lombardi, G., 1973. Dimensioning of tunnel linings with regard to constructional procedure. Tunnels and Tunnelling 5 (4), 340–351.

Lombardi, G., 1981. Bau von Tunneln bei grossen Verformungen des Gebirges. Tunnel 81, Internationaler Kongress, Düsseldorf, Band 2, 351–384, Messegesellschaft mbH NOEWA Düsseldorf und Deutsche Gesellschaft für Erd- und Grundbau e.V. Essen.

Lovat, 1997. Questionnaire on the TBM design for the experimental tunnel under the Gibraltar Straits (TBM manufacturers inquiry). Workshop "The Gibraltar Crossing", Tarifa, ITA Bron Cedex.

Lunardi, P., Focaracci, A., 2000. Impostazione progettuale e costruttiva delle opere in sotterraneo della Variante Sud della tratta A. V. Bologna – Firenze. Quarry & Construction 37 (2), 93–98.

Maidl, B., Herrenknecht, M., Anheuser, L., 1995. Maschineller Tunnelbau im Schildvortrieb. Ernst & Sohn Verlag für Architektur und technische Wissenschaften GmbH Berlin.

Maidl, B., Schmid, L.R., Ritz, W., Herrenknecht, M., 2001. Tunnelbohrmaschinen im Hartgestein. Ernst & Sohn Verlag für Architektur und technische Wissenschaften GmbH Berlin.

Matter, J., Stauber, A., Bauer, F., Daller, J., 2007. ÖBB Wienerwaldtunnel – Erfahrungen aus dem Vortrieb. FGU-Fachtagung für Untertagbau, Swiss Tunnel Congress 2007, Luzern, D0222, 101–112, SIA Zürich.

McCusker, T.G., 1996. Tunnelling in difficult ground. Tunnel engineering handbook, Second edition, 153–176, Chapman & Hall New York.

Mendaña, F., 2007. Guadarrama Tunnel construction with double shield TBMs. Rapid Excavation and Tunnelling Conference, Toronto, 1079–1093, SME Inc. Littleton.

Moulton, B.G., Cass, D.T., Nowak, D.E., Poulin, R.M., 1995. Tunnel boring machine concept for converging ground. Rapid Excavation and Tunnelling Conference, San Francisco, 509–523, SME Inc. Littleton.

NASA, 2007. Systems engineering handbook. NASA/SP-2007-6105 Rev1, National Aeronautics and Space Administration Washington.

Nasri, V., Fauvel, P., 2005. Lyon – Turin long and deep railway tunnel project. Rapid Excavation and Tunnelling Conference, Seattle, 531–543, SME Inc. Littleton.

Nelson, P.P., Peterson, C.R., Einstein, H.H., Hood, M., 1992. Manufacturing underground space. Towards new worlds in tunnelling, International congress, Acapulco, Volume 1, 29–36, A.A.Balkema Rotterdam Brookfield.

Nguyen Minh, D., Corbetta, F., 1991. Nouvelle méthodes de calcul des tunnels revêtus incluant l'effet du front de taille. 7th Congress of the International Society for Rock Mechanics (ISRM), Aachen, Volume 2, 1335–1338, A.A.Balkema Rotterdam Brookfield.

Oreste, P.P., Peila, D., 2000. I consolidamenti come mezzo per permettere lo scavo meccanizzato di gallerie. Lo scavo meccanizzato delle gallerie, mir2000 – VIII ciclo di conferenze di meccanica e ingegneria delle rocce, Torino, 217–274, Pàtron Editore Bologna.

Peila, D., Pelizza, S., 2009. Ground probing and treatments in rock TBM tunnel to overcome limiting conditions. Journal of Mining Science 45 (6), 602–619.

Pelizza, S., Peila, D., Borio, L., Dal Negro, E., Schulkins, R., Boscaro, A., 2010. Analysis of the performance of two component backfilling grout in tunnel boring machines operating under face pressure. Tunnel vision towards 2020, ITA World Tunnel Congress 2010, Vancouver, TAC Vancouver.

Pliego, J.M., 2005. Open session – the Gibraltar Strait Tunnel. An overview of the study process. Tunnelling and Underground Space Technology 20 (6), 558–569.

Podjadtke, R., Weidig, G., 2010. Adjustable flexible segment lining. Tunnel 2010 (7), 37–42.

Pohl, R., 1979. Untersuchungen zu technischen Lösungen für die Herstellung von Abwasserleitungen unter der Bedingungen städtischer Rekonstruktionsgebiete mit Hilfe des Durchörterungsverfahrens. Dissertation, Technische Hochschule Leipzig.

Prader, D., 1972. Beispiele von Druckerscheinungen im Tunnelbau. Internationales Symposium für Untertagbau, Luzern, 82–98, Schweizerische Gesellschaft für Boden- und Felsmechanik Zürich.

Ramoni, M., 2010. On the feasibility of TBM drives in squeezing ground and the risk of shield jamming. Veröffentlichungen des Instituts für Geotechnik (IGT) der ETH Zürich, Band 236 – ETH Dissertation Nr. 18965, vdf Hochschulverlag AG Zürich.

Ramoni, M., Anagnostou, G., 2008. TBM drives in squeezing rock – shield-rock interaction. Building underground for the future, AFTES International Congress Monaco, Montecarlo, 163–172, Edition specifique Limonest.

Ramoni, M., Anagnostou, G., 2010a. Thrust force requirements for TBMs in squeezing ground. Tunnelling and Underground Space Technology 25 (4), 433–455.

Ramoni, M., Anagnostou, G., 2010b. Tunnel boring machines under squeezing conditions. Tunnelling and Underground Space Technology 25 (2), 139–157.

Ramoni, M., Anagnostou, G., 2011a. The effect of consolidation on TBM shield loading in water-bearing squeezing ground. Rock Mechanics and Rock Engineering 44 (1), 63–83.

Ramoni, M., Anagnostou, G., 2011b. The interaction between TBM, ground and tunnel support in TBM tunnelling through squeezing ground. Rock Mechanics and Rock Engineering 44 (1), 37–61.

Ramoni, M., Lavdas, N., Anagnostou, G., 2011. Squeezing pressure on segmental linings. Tunnelling and Underground Space Technology, doi: 10.1016/j.tust.2011.05.007 (available online).

Rehm, U., 2005. Personal communication. Herrenknecht AG, May 2005.

Robbins, R.J., 1982. The application of tunnel boring machines to bad rock conditions. Rock mechanics: caverns and pressure shafts, ISRM Symposium, Aachen, Volume 2, 827–836, A.A. Balkema Rotterdam.

Robbins, R.J., 1992. Large diameter hard rock boring machines: state of the art and development in view of Alpine base tunnels. Felsbau 10 (2), 56–62.

Robbins, R.J., 1997. Hard rock tunnelling machines for squeezing rock conditions: three machine concepts. Tunnels for people, ITA World Tunnel Congress '97, Vienna, Volume 2, 633–638, A.A.Balkema Rotterdam Brookfield.

Sänger, B., 2006. Disc cutters for hardrock TBM 1986–2006 – history and tendencies of development. Felsbau 24 (6), 46–51.

Schmid, L.R., 2006. TBM-Vortrieb im Fels – Möglichkeiten und Grenzen. geotechnik 29 (2), 194–198.

Schmid, L.R., 2008. Personal communication. SMH Tunnelbau AG, March 2008.

Schneider, E., Home, L., Sänger, B., Kolb, S., 2007. Innovative concept for constructing the Brenner Base Tunnel with previously produced exploratory tunnel. Tunnel 2007 (1), 21–33.

Schneider, E., Rotter, K., Saxer, A., Röck, R., 2005. Compex Support System. Felsbau 23 (5), 95–101.

Schneider, E., Spiegl, M., 2008. Convergency compatible support systems. Tunnels & Tunnelling International 40 (6), 40–43.

Schneider, E., Spiegl, M., 2009. Personal communication. SSP BauConsult GmbH, May 2009.

Schneider, W., Kapeller, E., 1995. Überbohrsystem – praktische Erfahrungen. TBM know-how zum Projekt NEAT, The Robbins Company Symposium, Luzern, The Robbins Company Kent.

Schubert, W., 2000. TBM excavation of tunnels in squeezing rock. Lo scavo meccanizzato delle gallerie, mir2000 – VIII ciclo di conferenze di meccanica e ingegneria delle rocce, Torino, 355–364, Pàtron Editore Bologna.

Shimaya, S., 2005. 12.84m-diameter TBM bores a 10.7 km-long tunnel at great depth. International symposium on design, construction and operation of long tunnels, Taipei, Volume 1, 159–166, Chinese Taipei Tunnelling Association.

Solexperts, 2007. HIDCON-Elemente im Tunnelbau. Solexperts AG, Mönchaltorf (Schweiz).

Stahn, C., Grimm, K., 2006. Der Wienerwaldtunnel – eine tunnelbautechnische Herausforderung. geotechnik 29 (2), 167–172.

Steiner, W., 2000. TBM tunnelling – geotechnics influencing mechanics. Felsbau 18 (2), 28–34.

Sterpi, D., Gioda, G., 2007. Ground pressure and convergence for TBM driven tunnels in visco-plastic rocks. ECCOMAS Thematic conference on computational methods in tunnelling, EURO:TUN 2007, Vienna, 89, Vienna University of Technology.

Strohhäusl, S., 1996. TBM tunnelling under high overburden with yielding segmental linings; Eureka Project EU 1979 – "Contun". Tunnel boring machines – trends in design & construction of mechanized tunnelling, International lecture series TBM tunnelling trends, Hagenberg, 61–68, A.A.Balkema Rotterdam Brookfield.

Terada, M., Moriyama, M., Yamazaki, T., 2008. 12.84 m diameter TBM excavated the long expressway tunnel with 1000 m overburden. Underground facilities for better environment & safety, ITA World Tunnel Congress 2008, Agra, Volume 2, 1098–1106, Central Board of Irrigation & Power New Delhi.

Toolanen, B., Hartwig, S., Janzon, H., 1993. Design considerations for large hard rock TBMs when used in bad ground. Rapid Excavation and Tunnelling Conference, Boston, 853–868, SME Inc. Littleton.

Tusch, K.N., Thompson, J.F.K., 1996. Method of connection. US Patent 5489164.

Vermeer, P.A., de Borst, R., 1984. Non-associated plasticity for soils, concrete and rock. HERON 29 (3), 1–64.

Vicenzi, I., Pedrazzini, S., Ferrari, A., Gubler, G., Böckli, O., 2007. Deep tunnelling in hardrock with large diameter TBM: what's up? An experience from the Gotthard Base Tunnel. Underground space – the 4th dimension of metropolises, ITA World Tunnel Congress 2007, Prague, Volume 1, 267–272, Taylor & Francis Group London.

Vigl, A., 2003. TBM support in squeezing rock – a convergence-compatible segmental lining system. Felsbau 21 (6), 14–18.

Vigl, L., Gütter, W., Jäger, M., 1999. Doppelschild-TBM – Stand der Technik und Perspektiven. Felsbau 17 (5), 475–485.

Vigl, L., Jäger, M., 1997. Double shield TBM and open TBM in squeezing rock – a comparison. Tunnels for people, ITA World Tunnel Congress '97, Vienna, Volume 2, 639–643, A.A.Balkema Rotterdam Brookfield.

Voerckel, M., 2001. Tunnelling with TBM – state of the art and future development. Progress in tunnelling after 2000, ITA World Tunnel Congress 2001, Milan, Volume II, 493–500, Pàtron Editore Bologna.

Vogelhuber, M., 2007. Der Einfluss des Porenwasserdrucks auf das mechanische Verhalten kakiritisierter Gesteine. Veröffentlichungen des Instituts für Geotechnik (IGT) der ETH Zürich, Band 230 – ETH Dissertation Nr. 17079, vdf Hochschulverlag AG Zürich.

Vogelhuber, M., Anagnostou, G., Kovári, K., 2004. Pore water pressure and sepage flow effects in squeezing ground. Caratterizzazione degli ammassi rocciosi nella progettazione geotecnica, mir2004 – X ciclo di conferenze di meccanica e ingegneria delle rocce, Torino, 495–509, Pàtron Editore Bologna.

Wirth, 2003. Technical documentation. Wirth GmbH, Erkelenz (Germany).

Wittke-Schmitt, B., Gattermann, J., Wittke, W., 2005. Risiken bei konventionellen und maschinellen Vortrieben sowie Massnahmen zur Minimierung. Taschenbuch für den Tunnelbau 2006, 49–92, VGE Verlag Glückauf GmbH Essen.

Wolff, W., Goliasch, R., 2003. Überschneideinrichtungen auf Hartgesteins-TBM – kritische Betrachtungen anhand der Erfahrungen vom Lötschberg Basistunnel. Felsbau 21 (5), 147–154.

Projektabschluss

Schweizerische Eidgenossenschaft
Confédération suisse
Confederazione Svizzera
Confederaziun svizra

Eidgenössisches Departement für
Umwelt, Verkehr, Energie und Kommunikation UVEK
Bundesamt für Strassen ASTRA

FORSCHUNG IM STRASSENWESEN DES UVEK **ARAMIS SBT**

Formular Nr. 3: Projektabschluss

erstellt / geändert am:	20.12.2010

Grunddaten

Projekt-Nr.:	**FGU 2007/005**
Projekttitel:	Entscheidungsgrundlagen und Hilfsmittel für die Planung von TBM-Vortrieben in druckhaftem Gebirge
Enddatum:	31.12.2010

Projektleiter

Texte:

Zusammenfassung der Projektresultate:

(i) Strukturierte qualitative Untersuchung der spezifischen Probleme sowie der vielfältigen Schnittstellen und Wechselwirkungen zwischen Gebirge, Vortriebseinrichtung (TBM und Nachläufer) und Ausbau mit Einbezug von Erfahrungen aus ausgeführten Projekten.

(ii) Kritischer Überblick über die technischen Optionen (TBM-Technologie und Ausbau) für das Überwinden von druckhaften Verhältnissen bei einem TBM-Vortrieb.

(iii) Quantitative Untersuchung der Interaktion zwischen Gebirge, Schild und Ausbau.

(iv) Quantitative Untersuchung des Einflusses der Bruttovortriebsleistung und der Stillstandsdauer auf die Schildbelastung unter Berücksichtigung der Zeitabhängigkeit des Gebirgsverhaltens.

(v) Qualitative und quantitative Untersuchung des Einflusses der Art, Ort und Dicke der Hinterfüllung auf die Belastung eines Tübbingausbaus.

(vi) Aufzeigen möglicher Vorgehensweisen (Leitfaden) für die Beurteilung eines TBM-Vortriebs in druckhaftem Gebirge anhand konkreter Fallbeispiele.

(vii) Herstellung von Hilfsmitteln für die Planung: Nomogramme für die Ermittlung der erforderlichen Vorschubkraft und der Belastung eines Tübbingausbaus (welche die für die für die praktische Anwendung relevante Bandbreite der Gebirgsparameter, des primären Spannungszustandes, der TBM- und Ausbau-Charakteristiken abdecken) sowie Zusammenstellung von technischer Daten. Die Nomogramme und die technischen Daten erlauben die Einschätzung der Machbarkeit eines TBM-Vortriebs in einer gegebenen

Schweizerische Eidgenossenschaft
Confédération suisse
Confederazione Svizzera
Confederaziun svizra

Eidgenössisches Departement für
Umwelt, Verkehr, Energie und Kommunikation UVEK
Bundesamt für Strassen ASTRA

	geotechnischen Situation sowie die Beurteilung verschiedener technischer oder baubetrieblicher Massnahmen.
Zielerreichung:	Die gestellten Ziele wurden erreicht. Die erfolgreiche Anwendung der methodischen Ansätze sowie der erarbeiteten Entscheidungshilfen im Rahmen konkreter Projekte bestätigt deren Praxistauglichkeit.
Folgerungen und Empfehlungen:	Die Beurteilung eines TBM-Vortriebs in druckhaftem Gebirge erfordert eine systematische Vorgehensweise. Letztere soll sowohl die Eigenschaften des Gebirges als auch diejenige des Ausbaus und der TBM einbeziehen. Dasselbe gilt auch für die spezifische Fragestellung der Wahl des Ausbausystems. Zum Beispiel führt die Anwendung eines nachgiebigen Ausbaus zu einer kleineren Belastung desselben aber zu einer erhöhten Schildbelastung. Hingegen ist ein steifer Ausbau vorteilhafter in Bezug auf die erforderliche Vorschubkraft, bedingt aber, dass der Ausbau einen höheren Gebirgsdruck aufnehmen muss. In letzter Zeit sind verschiedene, vielversprechende technologische Entwicklungen vorgeschlagen worden, die das Erweitern des Einsatzbereiches von Tübbingen ermöglichen sollen. Nachgiebige Tübbingringe sowie komprimierbare Hinterfüllmaterialen erzielen den Einsatz von Tübbingen als nachgiebiger Ausbau. Der Einsatz von Hochleistungsbeton soll die Aufnahme von noch höheren Gebirgsdrücken ermöglichen. Die Anwendbarkeit dieser neusten Entwicklungen sollte im Rahmen weiterführender Untersuchungen – die betontechnologische, logistische, statische sowie TBM-spezifische Aspekte zu berücksichtigen haben – analysiert werden.
Publikationen:	Hauptpublikationen: Ramoni, M., Anagnostou, G., 2010d. Tunnel boring machines under squeezing conditions. Tunnelling and Underground Space Technology 25 (2), 139–157. Ramoni, M., Anagnostou, G., 2010b. The interaction between TBM, ground and tunnel support in TBM tunnelling through squeezing ground. Rock Mechanics and Rock Engineering, doi: 10.1007/s00603-010-0103-8 (available online). Ramoni, M., Anagnostou, G., 2010a. The effect of consolidation on TBM shield loading in water-bearing squeezing ground. Rock Mechanics and Rock Engineering, doi:10.1007/s00603-010-0107-4 (available online). Ramoni, M., Anagnostou, G., 2010c. Thrust force requirements for TBMs in squeezing ground. Tunnelling and Underground Space Technology 25 (4), 433–455. Ramoni, M., Lavdas, N., Anagnostou, G., 2010. Squeezing pressure on segmental linings. Tunnelling and Underground Space Technology (accepted for publication).

Beurteilung der Begleitkommission:
Diese Beurteilung der Begleitkommission ersetzt die bisherige separate fachliche Auswertung.

Beurteilung:	Die Arbeit adressiert eine grundsätzliche Fragestellung im mechanischen Tunnelvortrieb. Die Problematik ist vielschichtig und von einer nicht unerheblichen Anzahl von Parametern beeinflusst. Eine konsistente Analyse dieser Parameter und ihre gegenseitige Beeinflussung war Ziel der Arbeit, verbunden mit der Darstellung der Ergebnisse in der leicht les- und anwendbaren Form von Nomogrammen, mit dem Ziel diese Ergebnisse so praxisnah wie möglich zu präsentieren.
Umsetzung:	Die Forschungsarbeit setzt sich mit den Fragen detailliert auseinander und analysiert die massgebenden Einflussgrössen. Daher gelingt es auch, daran anschliessend diese Einflussgrössen in einer N-N-Matrix darzustellen und die gegenseitigen Abhängigkeiten einzubringen. Auf diese Weise ist eine rasche Analyse der massgebenden Parameter und ihrer Auswirkungen möglich. Die Qualität der Arbeit ist hoch: einerseits aufgrund der Tiefe und Breite der Analyse, andererseits auch aufgrund der Kondensation der gegenseitigen Abhängigkeiten der Parameter in der Form von Nomogrammen. Dieser Ansatz ist auch neuartig im Bereich des Untertagebaus, er ermöglicht aber auch in einer frühen Phase von Projekten eine effektive Beurteilung des Problems des Einklemmens der Tunnelbohrmaschine.

Schweizerische Eidgenossenschaft
Confédération suisse
Confederazione Svizzera
Confederaziun svizra

Eidgenössisches Departement für
Umwelt, Verkehr, Energie und Kommunikation UVEK
Bundesamt für Strassen ASTRA

weitergehender Forschungsbedarf:	Die Interaktion zwischen Vortrieb, Ausbau und umgebendes Gebirge ist die zentrale Grösse in der Analyse des Problems. In der vorliegenden Arbeit konnten die Aspekte der Tragfähigkeit respektive der Deformierbarkeit des Ausbaus nur ungenügend bearbeitet werden (was aber für die vorliegende Fragestellung irrelevant ist). Hier wäre ein weitergehender Forschungsbedarf gegeben.
Einfluss auf Normenwerk:	Es besteht kein Einfluss auf das Normenwerk.

Präsident Begleitkommission:

Name:	Amberg	Vorname:	Felix
Amt, Firma, Institut:	Amberg Engineering AG		
Strasse, Nr.:	Trockenloostrasse 21, Postfach 27		
PLZ:	CH-8105	Email:	famberg@amberg.ch
Ort:	Regensdorf-Watt	Telefon:	+41 44 870 91 11
Kanton, Land:	Zürich, Schweiz	Fax:	+41 44 870 06 20

Unterschrift Präsident Begleitkommission:

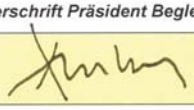

Verzeichnis der Berichte der Forschung im Strassenwesen

Bericht-Nr.	Projekt-Nr.	Titel	Jahr
616	AGB 2002/020	Beurteilung von Risiken und Kriterien zur Festlegung akzeptierter Risiken in Folge aussergewöhnlicher Einwirkungen bei Kunstbauten *Appréciation et critères d'acceptation des risques dus aux actions extraordinaires pour les ouvrages d'art* *Assessment of residual risks and acceptance criteria for accidental loading for infrastructural facilities*	2009
618	AGB 2005/102	Sicherheit des Verkehrssystems Strasse und dessen Kunstbauten: Methodik zur vergleichenden Risikobeurteilung *Bases d'une méthode pour une appréciation comparative des risques* *Methodological basis for comparative risk assessment*	2009
620	AGB 2005/104	Sicherheit des Verkehrssystems Strasse und dessen Kunstbauten: Effektivität und Effizienz von Massnahmen *Efficacité et efficience des interventions* *Effectiveness and efficiency of interventions*	2009
623	AGB 2005/107	Sicherheit des Verkehrssystems Strasse und dessen Kunstbauten: Tragsicherheit der bestehenden Kunstbauten *Sécurité structurale des ouvrages d'art existants* *Structural safety of existing highway structures*	2009
625	AGB 2005/109	Sicherheit des Verkehrssystems Strasse und dessen Kunstbauten: Effektivität und Effizienz von Massnahmen bei Kunstbauten *Efficacité et efficience des interventions sur les ouvrages d'art* *Effectiveness and efficiency of interventions on highway structures*	2009
626	AGB 2005/110	Sicherheit des Verkehrssystems Strasse und dessen Kunstbauten: Baustellensicherheit bei Kunstbauten *Sécurité sur les chantiers d'ouvrages d'art* *Safety on constructions sites off highway structures*	2009
636	AGB 2002/028	Dimensionnement et vérification des dalles de roulement de ponts routiers *Bemessung und Nachweis der Fahrbahnplatten von Strassenbrücken* *Design and verification of bridge deck slabs for highway bridges*	2009
637	AGB 2005/009	Détermination de la présence de chlorures à l'aide du Géoradar *Georadar zur Auffindung von Chloriden* *Detection of chlorides using ground penetrating radar*	2009
1233	ASTRA 2000/420	Unterhalt 2000 / Forschungsprojekt FP2 Dauerhafte Komponenten bitumenhaltiger Belagsschichten *Components durables des couches bitumineux* *Durable components in bituminous layers*	2009
1237	VSS 2007/903	Grundlagen für eCall in der Schweiz *Bases pour eCall en Suisse* *Technical and organisational basis for eCall in Switzerland*	2009
1239	VSS 2000/450	Bemessungsgrundlagen für das Bewehren mit Geokunststofffen *Bases de dimensionnement pour le renforcement par géosynthétiques* *Design of reinforcement with geosynthetics*	2009
1240	ASTRA 2002/010	L'acceptabilité du péage de congestion: Résultats et analyse de l'enquête en Suisse *Stau auf Strassen: Resultate und Analysen von Untersuchungen in der Schweiz* *Acceptance of road pricing: results and analysis of surveys carried out in Switzerland*	2009
1241	ASTRA 2001/052	Erhöhung der Aussagekraft des LCPC Spurbildungstests *Amélioration des informations fournies par l'essai d'orniérage LCPC* *Improving information on materials behaviour obtained from the LCPC wheel tracking test*	2009
1246	VSS 2004/713	Massnahmenplanung im Erhaltungsmanagement von Fahrbahnen: Bedeutung Oberflächenzustand und Tragfähigkeit sowie gegenseitige Beziehung für Gebrauchs- und Substanzwert *Influences et interactions de l'état de surface et de la portance sur la valeur intrinsèque et la valeur d'usage* *Influences and interactions of the surface quality and the bearing capacity on the intrinsic value and the user value*	2009
1247	VSS 2000/348	Anforderungen an die strassenseitige Ausrüstung bei der Umwidmung von Standstreifen *Exigences à l'équipement routier pour l'utilisation de la bande d'arrêt d'urgence* *Requirements for road side equipment by hard shoulder usage*	2009
1249	FGU 2003/004	Einflussfaktoren auf den Brandwiderstand von Betonkonstruktionen *Facteurs d'influence sur la résistance au feu de structures en béton* *Influences on the fire resistance of concrete structures*	2009
1252	SVI 2003/001	Nettoverkehr von verkehrsintensiven Einrichtungen (VE) *Trafic net des installations générant un trafic important (IGT)* *Net traffic induction of installations producing high traffic volumes (VE)*	2009

Bericht-Nr.	Projekt-Nr.	Titel	Jahr
1253	VSS 2001/203	Rétention des polluants des eaux de chausées selon le système "infilitrations sur les talus" – vérification in situ et optimisation *Retention der Schadstoffe des Strassenabwassers durch das "über die Schulter Versickerungs-System" – in situ Verifikation und Optimierung* *Road runoff pollutant retention by infiltration through the roadside slopes – in situ verification and optimization*	2009
1254	VSS 2006/502	Drains verticaux préfabriqués thermiques pour la consolidation in situ des sols *Vorfabrizierte, vertikale, thermische Entwässerungsleitungen für die in situ Konsolidierung von Böden* *Prefabricated thermal vertical drains for in situ consolidation of soils*	2009
1255	VSS 2006/901	Neue Methoden zur Erkennung und Durchsetzung der zulässigen Höchstgeschwindigkeit *Nouvelles méthodes pour reconnaitre et faire respecter la vitesse maximale autorisée* *New methods to identify and enforce the authorized speed limit*	2009
1256	VSS 2006/903	Qualitätsanforderungen an die digitale Videobild-Bearbeitung zur Verkehrsüberwachung *Exigences de qualité posées au traitement vidéo numérique pour la surveillance du trafic routier* *Quality requirements for digital video-analysis in traffic surveillance*	2009
1257	SVI 2004/057	Wie Strassenraumbilder den Verkehr beeinflussen – der Durchfahrtswiderstand als Arbeitsinstrument bei der städtebaulichen Gestaltung von Strassenräumen *L'influence de l'aménagement de l'espace de la route sur le trafic* *La résistance de passage du trafic comme instrument de travail pour la conception urbaine de zone routière*	2009
1258	VSS 2005/802	Kaphaltestellen – Anforderungen und Auswirkungen *Arrêt en cap – exigences et effets* *Cape stops – requirements and impacts*	2009
1260	FGU 2005/001	Testeinsatz der Methodik "Indirekte Vorauserkundung von wasserführenden Zonen mittels Temperaturdaten anhand der messdaten des Lötschberg Basistunnels *Test de la méthode "Prédiction indirecte de zones de venue d'eau au moyen de données thermiques" à l'aide des données du tunnel de base du Lötschberg* *Test of the method "Indirect prediction ahead of water bearing zones with temperatures data" with the measured data from the Lötschberg Base Tunnel*	2009
1261	ASTRA 2004/018	Pilotstudie zur Evaluation einer mobilen Grossversuchsanlage für beschleunigte Verkehrslastsimulation auf Strassenbelägen *Etude de pilote pour l'évaluation d'une machine mobile à vrai grandeur qui permet de simuler le trafic sur les routes dans une manière accélérée* *Pilot-study for the evaluation of a mobile full-scale accelerated pavement testing equipment*	2009
1262	VSS 2003/503	Lärmverhalten von Deckschichten im Vergleich zu Gussasphalt mit strukturierter Oberfläche *Caractéristiques de bruit de couches de roulement en comparaison avec des couches d'asphalte coulé (Gussasphalt) avec surface construite* *Comparison of noise characteristics of wearing courses with mastic asphalt (Gussasphalt) with designed surface*	2009
1264	SVI 2004/004	Verkehrspolitische Entscheidfindung in der Verkehrsplanung *Politique de transport: la prise de décision dans la planification des transports* *Transport-policy decision-talking in transport planning*	2009
1265	VSS 2005/701	Zusammenhang zwischen dielektrischen Eigenschaften und Zustandsmerkmalen von bitumenhaltigen Fahrbahnbelägen (Pilotuntersuchung) *Relation entre les propriétés diélectriques des revêtements routiers et leur condition* *A relationship between the dielectric properties of asphalt pavements and the present condition of the road*	2009
1267	VSS 2007/902	Einsatz modellbasierter Datentransfernormen (INTERLIS) in der Strassenverkehrstelematik *Utilisation des standards d'échange de données basés modélisation pour la télématique des transports routiers à l'exemple des données de traffic* *Use of modal driven data transfer standards in the road transport telematic exemplified by traffic data*	2009
1268	ASTRA 2005/007	PM10-Emissionsfaktoren von Abriedspartikeln des Strassenverkehrs (APART) *PM10 emission factors of abrasion particles from road traffic* *Facteurs d'émission des particules d'abrasion dues au trafic routiers*	2009
1269	VSS 2005/201	Evaluation von Fahrzeugrückhaltesystemen im Mittelstreifen von Autobahnen *Evaluation of road restraint systems in central reserves of motorways* *Évaluation de dispositifs de retenue de véhicule sur le terre-plein central des autoroutes*	2009
1270	VSS 2005/502	Interaktion Strasse – Hangstabilität: Monitoring und Rückwärtsrechnung *Interaction route – stabilité des versants: Monitoring et calcul à rebours* *Road-landslide interactions: Monitoring and inverse stability analysis*	2009
1271	VSS 2004/201	Unterhalt von Lärmschirmen *Entretien des écrans antibruit* *Maintenance of noise reducing devices*	2009
1274	SVI 2004/088	Einsatz von Simulationswerkzeugen in der Güterverkehrs- und Transportplanung *Applications des modèles simulations dans le domaine de planification en transport marchandises* *Application of simulation tools in freight traffic and transport planning*	2009

Bericht-Nr.	Projekt-Nr.	Titel	Jahr
1275	ASTRA 2006/016	Dynamic urban origin – destination matrix – estimation methodology *Méthodologie pour l'estimation de matrices origine-destination dynamiques en réseau urbain* *Methode zur Ermittlung dynamischer Quell-Ziel-Matrizen für städtische Netzwerke*	2009
1278	ASTRA 2004/016	Auswirkungen von fahrzeuginternen Informationssystemen auf das Fahrverhalten und die Verkehrssicherheit – verkehrstechnischer Teilbericht *Influence des systèmes d'information embarqués sur le comportement de conduite et la sécurité routière – rapport partiel d'ingénierie de la circulation* *Influence of In-Vehicle Information Systems on driver behaviour and road safety – report part of traffic engineering*	2009
1279	VSS 2005/301	Leistungsfähigkeit zweistreifiger Kreisel *Capacité des giratoires à deux voies de circulation* *Capacity of two-lane roundabouts*	2009
1285	VSS 2002/202	In situ Messung der akustischen Leistungsfähigkeit von Schallschirmen *Mesures in situ des propriétés acoustiques des écrans antibruit* *In situ measurement of the acoustical properties of noise barriers*	2009
1287	VSS 2008/301	Verkehrsqualität und Leistungsfähigkeit von komplexen ungesteuerten Knoten: Analytisches Schätzverfahren *Procédure analytique d'estimation de la capacité et du niveau de service de carrefours sans feux complexes* *Analytic procedure to estimate capacity and level of service at complex uncontrolled intersections*	2009
1299	VSS 2008/502	Projet initial – Enrobés bitumineux à faibles impacts énergétiques et écologiques *Initial Projekt – Asphalt-Mischgut mit geringer ernergetischer und ökologischer Belastung* *Initial Project – Bituminous mixture with low energy and ecological impacts*	2009
1301	SVI 2007/006	Optimierung der Strassenverkehrsunfallstatistik durch Berücksichtigung von Daten aus dem Gesundheitswesen *Affinement des statistiques des accidents de la route par la prise en compte des données de la santé publique* *Optimization of road traffic accident statistics by consideration of public health care data*	2009
617	AGB 2005/100	Sicherheit des Verkehrssystems Strasse und dessen Kunstbauten: Synthesebericht *Rapport de synthèse* *Synthesis report*	2010
619	AGB 2005/103	Sicherheit des Verkehrssystems / Strasse und dessen Kunstbauten / Ermittlung des Netzrisikos *Estimation du risque pour le réseau* *Estimation of the network risk*	2010
624	AGB 2005/108	Sicherheit des Verkehrssystems / Strasse und dessen Kunstbauten / Risikobeurteilung für Kunstbauten *Appréciation des risques pour les ouvrages d'art* *Risk assessment for highway structures*	2010
630	AGB 2002/016	Korrosionsinhibitoren für die Instandsetzung chloridverseuchter Stahlbetonbauten *Inhibiteurs de corrosion pour la remise en état des ouvrages en béton armé, contaminés par des chlorures* *Corrosion inhibitors for the rehabilitation of chloride contaminated reinforced concrete structures*	2010
632	AGB 2008/201	Sicherheit des Verkehrssystems Strasse und dessen Kunstbauten: Testregion – Methoden zur Risikobeurteilung *Région test – Méthodes pour l'appréciation des risques* *Test region – Methods of risk assessment*	2010
640	AGB 2003/011	*Nouvelle méthode de vérification des ponts mixtes à âme pleine* *Neue Bemessungsmethode für Stahlbetonverbundbrücken mit Vollwandträger* *New method for design of steel-concrete composite plate girder bridges*	2010
645	AGB 2005/021	Grundlagen für die Verwendung von Recyclingbeton aus Betongranulat *Bases pour l'utilisation du béton de recyclage en granulats de béton* *Fundamentals for the use of recycled concrete comprised of concrete material*	2010
945	AGB 2005/021	Grundlagen für die Verwendung von Recyclingbeton aus Betongranulat *Bases pour l'utilisation du béton de recyclage en granulats de béton* *Fundamentals for the use of recycled concrete comprised of concrete material*	2010
1272	VSS 2007/304	Verkehrsregelungssysteme – behinderte und ältere Menschen an Lichtsignalanlegen *Aménagement des feux de signalisation pour les personnes a mobilité réduite ou âgées* *Traffic control systems – handicapped and older people at signalized intersections*	2010
1277	SVI 2007/005	Multimodale Verkehrsqualitätsstufen für den Strassenverkehr – Vorstudie *Niveaux de service multimodales de la circulation routière – études préliminaires* *Multimodal level of service of road traffic – preliminary study*	2010
1282	VSS 2004/715	Massnahmenplanung im Erhaltungsmanagement von Fahrbahnen: Zusatzkosten infolge Vor- und Aufschub von Erhaltungsmassnahmen *Coûts supplémentaires engendrés par l'exécution anticipée ou retardée des mesures d'entretien* *Additional costs caused by bringing forward or delaying of standard interventions for road maintenance*	2010

Bericht-Nr.	Projekt-Nr.	Titel	Jahr
1284	VSS 2004/203	Evacuation des eaux de chaussée par les bas-cotés *Entwässerung über das Bankett* *Road runoff on road sides*	2010
1288	ASTRA 2006/020	Footprint II – long term pavement: performance and environmental monitoring on A1 *Footprint II – Langzeit-Belag-Performance und Umwelt Monitoring an der A1* *Footprint II – Long terme performance des chaussées et surveillance de l'environnement à la A1*	2010
1289	VSS 2005/505	Affinität von Gesteinskörnungen und Bitumen, nationale Umsetzung der EN *Affinité entre granulat et bitume, mise en application nationale de la EN* *Affinity between aggregate and bitumen, national implementation of the EN*	2010
1291	ASTRA 2009/005	Fahrmuster auf überlasteten Autobahnen: Simultanes Berechnungsmodell für das Fahrverhalten auf Autobahnen als Grundlage für die Berechnung von Schadstoffemissionen und Fahrzeitgewinnen *Modèles de conduite sur autoroutes surchargées* *Speed patterns on congested highways*	2010
1293	VSS 2005/402	Détermination de la présence et de l'efficacité de dope dans les bétons bitumineux *Bestimmung der Anwesenheit und Wirksamkeit von Haftmittel im Asphaltbeton* *Determination of the presence and efficiency of adhesion agent in asphalt concrete*	2010
1294	VSS 2007/405	Wiederhol- und Vergleichspräzision der Druckfestigkeit von Gesteinkörnungen am Haufwerk *Répétabilité et reproductibilité de la résistance à la compression des granulats en vrac* *Repeatability and reproductibility of the compressive strength on the stack*	2010
1295	VSS 2005/305	Entwurfsgrundlagen für Lichtsignalanlagen und Leitfaden *Base de projet pour installations de feux de circulation et guide* *Design basics for traffic light systems and guidelines*	2010
1298	ASTRA 2007/012	Griffigkeit auf winterlichen Fahrbahnen *Adhérence sur les chaussées hivernales* *Skid resistance of winter road surfaces*	2010
1303	ASTRA 2009/010	Geschwindigkeiten in Steigungen und Gefällen; Überprüfung *Speed on upgrades and downgrades; revision* *Les vitesses dans les rampes et les pentes; vérification*	2010